Application of Wireless Signal Scanning in Traffic Studies

by

Shahriar Mohammadi

A thesis submitted to the Faculty of Graduate and Postdoctoral Affairs in partial fulfillment of the requirements for the degree of

Doctor of Philosophy

in

Civil Engineering

Carleton University
Ottawa, Ontario

Abstract

With advances in communication technologies, innovative traffic data collection approaches have been developed. A means for this purpose is wireless technology which is sufficiently widespread among road users. Traffic data may be collected using signal scanners detecting wireless signals in the vicinity of them. As the data provided by signal scanners involve no direct information about the position of the signal source, the applications of this technology in traffic studies have been limited to finding some parameters in certain situations. The purpose is developing the applications of wireless signal scanning in traffic studies which require positional data of road users. This is achieved utilizing the potentials of received signal strength indicator (RSSI) of wireless signals transmitted by personal smart devices.

Wi-Fi, Bluetooth Classic and Bluetooth Low Energy are three widespread signal modes, transmitted by popular beacons used in daily life. A comparative study of the field performance of these signal modes is conducted, investigating their characteristics important in gathering traffic flow parameters whenever positional data of road users are required. This provides the possibility of selecting the most suitable signal mode for the intended applications of the technology based on the requirements of the methods.

A technique for positioning of beacons based on their transmitted signals, applicable in transportation studies is developed. This technique provides the possibility of positioning in intersections and their surrounding areas as well as congested road segments. The technique is based on the strength of signals transmitted by beacons, creating radio maps, and applying an algorithm called k-nearest neighbors. The procedure is optimized,

and the accuracy and functionality of the technique is improved via modification of the system arrangement and application of proper filtering algorithms.

A method for detection and classification of turning movements applicable in small urban intersections is developed based on wireless signals. The method utilizes the time profiles of the RSSI values of the signals emitted by beacons carried by turning vehicles. The signals are collected by an array of signal scanners carefully located on the intersection approaches. Turning movements are classified comparing signature points of the RSSI-time profiles and their occurrence moments.

Acknowledgements

I could not have completed this research work without the cooperation and support of several individuals and organizations. I would like to deeply appreciate:

Prof. Karim Ismail, my supervisor for his kind encouragement and support, and generous, precise, and valuable guidance throughout all the stages of the research.

Prof. Stephen Fai, Prof. Bilal Farooq, Prof. Ahmad Jrade and Prof. Adam Weiss, the examination committee members, for their insight and constructive comments.

Prof. Mario Santana-Quintero, faculty member of the Civil and Environmental Engineering Department and Prof. Mohamed Atia, faculty member of the Systems and Computer Engineering Department at Carleton University for their valuable technical advice.

Dr. Amir H. Ghods, PhD in transportation engineering, for providing the utilized wireless signal scanners and his worthwhile technical support.

Stephen Vickers, civil engineering laboratory technician at Carleton University for his enthusiastic technical solutions and support.

Mohanad Albatta, Junshen Feng, Luckson Kamisa and Asfandyar Khan, Carleton University students for their assistance in the extensive field experiments of the research.

The managers and personnel of National Capital Commission (NCC) for their cooperation in providing the possibility to conduct the experiments in the Ottawa test tracks center for autonomous vehicle technologies.

Thank you

Dedicated to my beloved wife Yasaman, my father, mother, mother-in-law, brothers, and sister

Thank you for your patience and support

Table of Contents

List of Tables

List of Illustrations

List of Abbreviations

Angle of Arrival (AOA)

Average Absolute Speed Error (AASE)

Bluetooth Low Energy (BLE)

Class of Device (COD)

Dilution of Precision (DOP)

Geoff E. Havers (GEH)

Industrial, Scientific, and Medical (ISM)

Intelligent Transportation Systems (ITS)

Internet Protocol (IP)

Institute of Electrical and Electronics Engineers (IEEE)

K-Nearest Neighbors (KNN)

Level of Service (LOS)

Line of Sight (LOS)

Local Area Networks (LAN)

Media Access Control (MAC)

Median Absolute Deviation (MAD)

Multiple-Input and Multiple-Output (MIMO)

National Capital Commission (NCC)

Non-Line of Sight (NLOS)

Origin-Destination (OD)

Post Processed Kinematic (PPK)

Radio Technical Commission for Maritime (RTCM)

Real-Time Kinematic (RTK)

Received Signal Strength Indicator (RSSI)

Single Hidden Layer Feed-Forward Neural Network (SHLFFNN)

Speed Error Bias (SEB)

Support Vector Machine (SVM)

Support Vector Regression (SVR)

Time of Arrival (TOA)

Time Difference of Arrival (TDOA)

Time Laps Aerial Photography (TLAP)

Wireless Local Area Network (WLAN)

Chapter 1: Introduction

1.1 Background

The operation, condition, and safety performance of transportation assets depend on the quality of traffic data. These data should be collected by transportation agencies in an objective and unbiased manner leading to proper decisions (Pande & Wolshon, 2016). Travel time, delay, origin-destination (OD), and intersection turning movement counts are among the most important pieces of data required. Collecting these data comes with considerable challenges as they consume large resources. With advances in communication and wireless technologies, innovative data collection methods in traffic studies are emerging. An overview of the most common types of traffic data collection which can be supported by wireless technology is presented hereafter.

A key determinant of many traffic planning and analysis decisions is traffic volume. Traffic volume studies quantify the number of road users in areas of interest within a specified period of time. Knowledge of traffic volume widely helps in determining various traffic parameters, *e.g.*, flow, density, turning movement counts, safety analysis, traffic signal design, and traffic control warrants. Flow and density predict speed and travel time on road segments. Travel time and delay studies are conducted to evaluate the quality of traffic in a route. The effectiveness of improvement actions may be assessed comparing the results of these studies before as well as after the improvements. The priority of projects may be determined comparing the severity of situations in different segments. The results may be used by transportation planners in supporting various decisions and policies (Garger & Hoel, 2018).

Origin-Destination (OD) studies specify movement patterns of road users between different regions of a certain area. Particularly, turning movement counts quantify the number of vehicle movements between the origins and destinations in an intersection during a period of time. Turning movement data may be used in planning and operational analysis levels. Traffic impact analysis, signal timing, capacity analysis, and geometric design are among the important applications of them. Intersection delay studies may be conducted to specify the traffic level of service and assess the efficacy of traffic control strategies. These data may be used to assess the performance of the intersections and to conclude if the vehicles should be guided to the other routes (Florida Department of Transportation, 2021). Intersection studies are routinely conducted by many transportation agencies, counting turning movements and measuring intersection delays (Pande & Wolshon, 2016).

There are two main data collection approaches: fixed point observations and probe (floating) vehicle observations. In the fixed point approach, traffic data are collected non-intrusively. Data are collected using stationary sensors such as loop detectors, video cameras, radar detectors, and wireless signal scanners or using traditional techniques such as license plate surveys and interviews (Schroeder, et al., 2010), (Seo, et al., 2015). Fixed point approach is used for collecting a wide range of data such as speed, travel time, vehicle counts and OD matrices depending on the selected tools (Emami, et al., 2020).

The probe vehicle approach is mostly common in travel time and delay studies. In this approach, a vehicle moves with traffic streams to collect the floating data between specified points (Emami, et al., 2020). The technique may be conducted in several ways depending on the instrumentation used in the study. It may be conducted manually by an

observer inside the vehicle, recording time and distance at predefined checkpoints or using equipment like GPS systems (Turner, et al., 1998).

As another classification, traffic data collection may be conducted using either manual or automatic approaches. Manual approaches are referred to the studies in which data are collected by observers in the field or from video recordings in the office. The observers manually tally the road users passing an intended point in a road segment or an intersection. In automated approaches effort is made to reduce the observer workload using the technology (Florida Department of Transportation, 2021).

On-road and roadside equipment are two types of technologies used in automatic counts. Pneumatic tubes and inductive loops are the common on-road equipment. Video image processing is an important example of roadside technologies. Infrared, radar, and laser technologies are other examples of roadside technologies applicable in intersection counts (Pande & Wolshon, 2016). Different types of automatic data collectors generally involve two principal components: sensors for detecting the presence of road users and a data recorder (Schneider, et al., 2005). Technologies based on intelligent transportation systems (ITS) can be utilized for real-time traffic data collection as well. Although their primary applications may be related to specific purposes other than travel time data collection, such as real-time route guidance or traffic monitoring, they may also be used in travel time and delay measurement. Signpost-based technique, ground-based radio navigation, automatic vehicle identification transponders, and cellular probes are examples of ITS vehicle probe techniques (Turner, et al., 1998).

Pneumatic tubes are rubber tubes laid perpendicular to the road direction and connected to an electronic counter. These tubes are generally used for short-term traffic

studies because they may become conspicuous if exposed to traffic for long time periods or if high volumes of heavy trucks exist. Inductive loops involve one or several loops of electric circuits, usually insulated and embedded below the surface of the road and connected to a controller unit by a cable. They are generally installed permanently because they should be buried below the roadway surface (Garger & Hoel, 2018). On-road technologies generally specify volumes on the roads and intersection legs, although information such as speed, length, and classification of passing vehicles may also be obtained from them (Pande & Wolshon, 2016). This equipment cannot detect and count turning movements directly. Because setting this equipment up is generally time-consuming and costly, they are not efficient for short-term studies (Florida Department of Transportation, 2021).

Video image processing systems involve one or several cameras, a computer for digitizing and processing images, and a software for extracting traffic data such as volume and speed from the images (Garger & Hoel, 2018). Video image processing can directly determine turning movements. A disadvantage of these systems is that their function may be affected by lighting conditions, movement, weather, and blockage by objects (Florida Department of Transportation, 2021). Fog can disrupt the performance of video detection systems (Garger & Hoel, 2018).

Traffic data collection generally requires several people in different locations. It may be required to coordinate with municipalities for installation of the equipment (Pande & Wolshon, 2016). While in manual approaches, equipment costs and set-up time are minimized, they require more labour forces. These labour forces should be trained and periodic relief time should be considered for them. The main disadvantages of manual

approaches are that they are labour-intensive and costly as a result, subject to human limitations and can only be conducted in short time periods. These factors cause the inefficiency of manual approaches as the duration of data collection increases in the field (Garger & Hoel, 2018).

Automatic approaches of data collection provide the possibility of gathering large amounts of data faster and with less resources (Pande & Wolshon, 2016). These approaches require less personnel for data collection, but more equipment and longer set-up time. Installation of the equipment may require temporary closure of some parts of the roads or intersections; therefore, they have their highest efficiency, when long study time periods or large amounts of data are required (Garger & Hoel, 2018). Reliability of the equipment in these approaches has always been a disadvantage for them and the probability of equipment failure should be considered in data collection planning. Automatic approaches often require post-processing.

In general, the selection of the study approach depends on the purpose of the study, route length and characteristics, required duration of data collection and available resources (Florida Department of Transportation, 2021). Although manual data collection techniques were historically the only option for traffic studies, automated approaches are becoming more popular and cost-effective. Automated vehicle count stations are found along arterials and freeways as standard features (Pande & Wolshon, 2016).

An innovative and efficient means for traffic data collection is wireless technology which is sufficiently widespread among road users. Nowadays, most of electronic consumer devices are manufactured equipped with wireless modules for communication with devices in their proximity (Bachmann, et al., 2013). Growth of these devices is the

stimulator for development of alternative traffic sensing tools to supplement the existing traffic monitoring and management systems (Friesen & McLeod, 2015). Data collection approaches based on wireless technology have been developed in recent years. These methods perform based on detection of Wi-Fi and Bluetooth signals transmitted by signal transmitters (beacons) present in the study area. (Yang & Wu, 2018) emphasized that significant growth in popularity of wireless enabled devices among road users increases penetration rate of this technology and size of data samples.

1.2 Technology Introduction

A promising platform for traffic data collection is utilizing wireless signal scanning and localization technology. Signal scanners are devices for detecting wireless signals in the vicinity of them. They are commercially available and widely used by traffic agencies.

These devices may function in different modes and based on various signal attributes. Wi-Fi, Bluetooth Classic and Bluetooth Low Energy (BLE) are three widespread wireless signal modes, transmitted by popular beacons used in daily life. BLE is a variation of Bluetooth, operating similarly in 2.4 GHz frequency band (Bluetooth SIG, 2021).

As wireless beacons are sufficiently widespread among road users, thanks to the popularity of Wi-Fi and Bluetooth activated communication and smart devices, the transmitted signals by them may be collected by signal scanners and used in determining some traffic parameters. Media access control (MAC) address, signal mode, detection timestamp and received signal strength indicator (RSSI) are the only data the currently available models of signal scanners that are used by traffic agencies provide (Figure 1.1). A MAC address is a globally unique ID assigned to each network module. RSSI in telecommunication indicates the power present in a received radio signal (Sauter, 2011).

As none of these provide direct information about the position of the beacon, the applications of this technology in traffic studies have been limited to finding some parameters in certain situations.

mac	type	rssi	create_time
7921f90ab005	1	-46	1600543916
73ce825d0610	1	-89	1600543916
122b82e73d79	1	-79	1600543916
fc4aac8fa25f	1	-62	1600543916
122b82e73d79	1	-79	1600543916
14dc7a8cf387	1	-91	1600543916
14dc7a8cf387	1	-89	1600543916
73ce825d0610	1	-89	1600543916
122b82e73d79	1	-79	1600543917
7921f90ab005	1	-47	1600543917
73ce825d0610	1	-88	1600543917
122b82e73d79	1	-79	1600543917
122b82e73d79	1	-78	1600543917
122b82e73d79	1	-79	1600543917
14dc7a8cf387	1	-89	1600543917
7921f90ab005	1	-48	1600543917
73ce825d0610	1	-88	1600543917

Figure 1.1 Sample row data provided by a wireless signal scanner.

(Quayle, et al., 2010) mentioned the advantages and disadvantages of wireless signal scanning technique in traffic studies as follows:

Advantages

- The technique may be applied in travel time and space mean speed measurement as well as OD classification.
- No vehicles are added to the system during the measurements.
- The collected data may be used in real or near real time.
- Data collection costs are low in comparison with manual approaches. The technology is commercially available with low equipment costs.

- Traffic data may be collected in larger volumes, longer time periods and with lower incremental costs compared with traditional techniques.

Disadvantages

- The technique may not be applied for measurement of point speeds.
- Data analysis is required to filter outliers.
- The equipment in this technique needs a power source.

1.2.1 Wireless Communication

Wireless communication refers to data transfer between different points not physically connected. Currently, people are surrounded by wireless enabled devices and wireless communicators which may be found almost everywhere. Wireless communication is globally widespread through ubiquitous devices such as cellphones, laptops, cordless phones, headsets, GPS units and devices which use this technology to exchange data (Gupta, 2016). Wi-Fi, Bluetooth Classic and BLE are three wireless technologies normally used in smart personal communication devices with the potential to be used in transportation studies.

1.2.1.1 Wi-Fi

Wireless local area network (WLAN) is a data transmission system, providing short-range connection using wireless links instead of fixed infrastructure and cables. The institute of electrical and electronics engineers (IEEE) 802 committee is the accepted authority for local area networks (LAN) and is responsible for determining LAN standards. IEEE 802.11 standard is specifically allocated to WLANs by this committee and defines the structures and formats of these systems. Wi-Fi is a trademark used for most modern WLANs. Wi-Fi devices provide local area networking and use radio waves for data

exchange. They provide internet access for the devices located in the range of routers connected to the internet (Labiod, et al., 2007). IEEE 802.11 stablishes different versions of Wi-Fi standards. These versions use various radio technologies, support different ranges, and may achieve different speeds. IEEE 802.11b, 802.11g and 802.11n are among these versions, allowing for higher data rates compared with the original 802.11 standard. Most Wi-Fi networks operate in 2.4 GHz industrial, scientific, and medical (ISM) frequency band. This frequency band is globally license free and is broken up into 11 channels, spaced 5 MHz apart in North America (Alan & Chi-Yu, 2010) , (Walrand & Parekh, 2018). Today, 802.11 built in chipsets are globally used in portable devices such as cellphones, laptops, and tablets.

1.2.1.2 Bluetooth Classic

Bluetooth is a standard aiming at short range, low power, low cost, and wireless communication between devices over radio links. Originally developed in Sweden in 1994, Bluetooth is a technology for cable replacement when connecting devices. Bluetooth standards are globally specified by IEEE 802.15 as a working group of IEEE 802 committee. The adoption of Bluetooth in smart mobile phones, laptops and tablets is almost exhaustive. It is broadly used in car kits, wireless headsets, speakers, and keyboards. Bluetooth Classic uses 2.4 GHz frequency band. It shares this band with several other systems such as Wi-Fi devices, cordless phones, near-field communication, and remote-control toys, which is a cause of interference. This frequency band uses a hopping mechanism with 79 channels, spaced 1 MHz apart to battle interference. Bluetooth supports ad hoc connections, *i.e.*, it does not require pre-existing infrastructure like routers or access points. A maximum distance of 100 m may be supported by Bluetooth, although it is

generally used in shorter distances. In order to detect a Bluetooth device, it needs to be in discoverable mode. A second device must search in its vicinity to find a Bluetooth enabled device. This process is called inquiry and results in identification of the discoverable devices located in the vicinity. In non-discoverable mode, the beacon does not respond to inquiries, therefore it may not be detected (Gupta, 2016).

1.2.1.3 Bluetooth Low Energy (BLE)

Bluetooth systems have two broad classifications: Bluetooth Classic and Bluetooth low energy (BLE). Starting from Version 4.0, BLE protocol was introduced as a subset of Bluetooth in addition to Bluetooth Classic. BLE was designed for lower power consumption as well as lower complexity and cost in comparison with Bluetooth Classic. Bluetooth Classic devices need to be recharged in a few days or weeks, but BLE devices can operate for months and even years using small batteries such as coin cells without the need for recharging or replacing. These come at the expense of reductions in some functionalities such as throughput and support of voice channels in order to reduce the required memory. BLE technology is compatible with the existing Bluetooth infrastructure. This means that the upgraded devices will be able to communicate through BLE in addition to Bluetooth Classic. BLE operates in 2.4 GHz frequency band similar to Bluetooth Classic and Wi-Fi. It has a frequency hopping mechanism and uses 40 channels spaced 2 MHz apart. Creating a connection in BLE mode takes much less time compared with Bluetooth Classic. This is because the number of advertising channels dedicated to creating a connection is lower in BLE mode. Bluetooth devices may support either Bluetooth Classic, BLE or both. Smart watches, key fobs, and fitness equipment are examples of the devices

only supporting BLE. Smartphones, laptops, and tablets may support both Bluetooth Classic and BLE modes (Gupta, 2016).

Bluetooth Special Interest Group (Bluetooth SIG) introduced Bluetooth 5.0 in 2016. The main focus of the new features in this version is on Internet of Things technology. Similar to Bluetooth 4.0, both classic and low energy protocols are supported in this version. The latest version up to this date is Bluetooth 5.3 released in 2021 (Bluetooth SIG, 2021). Enhanced speed, LE advertising extensions (Bluetooth SIG, 2016), angle of arrival and angle of departure (Bluetooth SIG, 2019) are among the main improvements through Version 5.0 and its updates.

1.2.2 MAC Address

Media access control (MAC) address, also known as physical address, is a globally unique ID, assigned to each network module in order to identify the device (Figure 1.2).

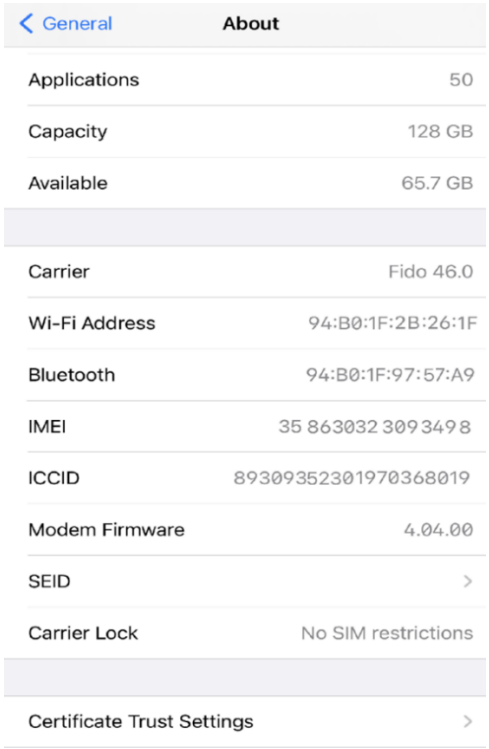

Figure 1.2 Wi-Fi and Bluetooth MAC addresses of a smart phone.

Each MAC address corresponding to an IEEE 802 module has a 48-bit (6-byte) structure and involves 12 hexadecimal characters. Hexadecimal system is a numeral system composed of 16 symbols in contrary to the common decimal system in which numbers are represented using 10 symbols. Hexadecimal system represents numbers using digits 0–9 indicating the values 0 to 9 and A–F indicating 10 to 15. A 48-bit MAC address generally follows one of the below formats, although other formats may also be used (Gupta, 2016):

AB:CD:EF:GH:IJ:KL

ABC-DEF-GHI-JKL

The 48-bit structure makes generation of 2^{48} potential MAC addresses possible. The first 24-bit half (prefix) contains the manufacturer ID and is allocated by IEEE registration authority. This part of the MAC address is called organizationally unique identifier (OUI) (Gupta, 2016). For instance, the prefix 98:FE:94 indicates that the manufacturer is Apple Inc., or the prefix 00:13:E8 indicates that the manufacturer is Intel Corporation. Each vendor often possesses many OUIs to assign to its products (Maclookup.app, 2021). The second half of the MAC address is uniquely assigned by the manufacturer to the network module to ensure that no two modules have identical MAC addresses (Gupta, 2016).

MAC addresses are different from internet protocol (IP) addresses. MAC is the physical address of the device, whereas an IP address is the logical address assigned to a device and is used to uniquely locate that device when there is a connection to a specific network (Walrand & Parekh, 2018). MAC addresses are innately secure. To identify the owner of a certain MAC address, it is required to view this address on the device which is not possible for the others in normal conditions. This provides a higher level of privacy for

traffic data collection in comparison with traditional techniques like license plate survey or video recording in which the license plates of vehicles are recorded or road users are filmed.

1.3 MAC Re-identification

Most of the applications of wireless technology in traffic studies are based on a technique called MAC re-identification. In this technique, wireless signal scanners are installed in different sections of the roads in the study area. The signal scanners detect the beacons located in their detection zones and collect their data. These data include signal mode, MAC address and detection timestamps of the detected beacons. In addition, RSSI values of the detected signals may also be provided by more advanced models of signal scanners used by traffic agencies. Traffic parameters may be determined if identical MAC addresses are detected at different timestamps by the signal scanners located in different sections.

Travel time, space mean speed and OD are three major traffic parameters determinable by MAC re-identification technique. Moreover, this technique can provide detailed information about occurrence time of peak-hour traffic and its duration as well as statistical variations in reliability of travel time measurements over time. The data collected using this technique are applicable in measurement of fluctuations in traffic patterns. They may be used in studying the efficacy of transportation system improvements, *e.g.*, adding new lanes or signal timing optimization. Traffic data collection may be propelled by MAC re-identification technique due to its automated nature and low cost (Quayle, et al., 2010).

Travel time is a vital parameter which captures mobility and helps in travel demand modelling. In terms of accuracy, a maximum relative error of 5% may be considered a desired accuracy in travel time estimation. A common technique is the use of probe

vehicles. To achieve this accuracy, probe vehicle sample size should at least be 3% of the vehicles population (Chen & Chien, 2001). Road traffic characteristics may be determined more effectively with larger amounts of raw data (Quayle, et al., 2010). A minimum of 3 to 5% of the vehicles on the roads can be captured using MAC re-identification technique. The popularity of this technique is becoming more in the US, because the sample sizes collected using MAC re-identification are comparable to probe vehicle approach (Garger & Hoel, 2018).

Researchers identified a few factors challenging MAC re-identification technique (Quayle, et al., 2010). These factors can compromise the accuracy of measurement process of traffic parameters. A beacon may be detected by a signal scanner several times or not detected at all depending on its proximity to the signal scanner, on its speed, and on the time-interval located inside the detection zone of the signal scanner. Using multiple signal scanners at a point may increase the likelihood of detecting beacons passing that point. Another challenge occurs when there are alternative routes or when some road users have discontinuous trips, excessively low or high speeds. The durations of these trips tend to be different from normal trips, causing occurrence of outlier data. Existence of different modes of transportation and different types of road users may also produce outliers. Although some types of outliers provide valuable information about the road users and trip types, they may be refined from the data according to the purpose of the study. Some researchers argued that travel time and speed measurements by MAC re-identification technique may be inaccurate because of the uncertainty about the actual location of the detected beacons which may be in the omnidirectional range of around 50 m (Friesen, et al., 2014).

Finally, due to the limitations of the data provided by wireless signals, some doubt was expressed regarding the ability of this technique in finding several important traffic parameters including traffic volumes, turning movements, travel modes as well as lane by lane information which may be used in studying driving behaviors and lane change maneuvers (Yang & Wu, 2018).

1.4 Problem Definition

Wireless technology has garnered a growing appeal in traffic data collection in recent years. Currently, the most common applications of the technology are travel time measurement and OD classification in long road segments (around 1.5 km or more) using MAC re-identification technique. This is done determining the presence of a beacon carried by a road user in an origin and a destination by signal scanners. These studies are limited to long road segments due to the limitations of this technology in accurate determination of positional data of road users.

The data signal scanners provide, do not include any direct information about the exact location of the detected beacons. Detection range of a signal scanner varies from several tens to several hundreds of meters, mostly depending on the signal mode and hardware. Detection of a beacon by a signal scanner only specifies that the detected beacon is located within a circle centred around the scanner with a radius equal to the detection range.

MAC re-identification works based on detection of a beacon or its presence in two different areas. In order to find travel time or speed, two signal scanners are installed at two points along a road. If a certain beacon is detected by these two signal scanners, its detection information may be used for calculating its travel time. The difference between

the detection timestamps of the two signal scanners specifies the travel time in the road segment. Knowing the travel time as well as the distance between the two signal scanners, the average speed of the vehicle may also be calculated.

In classic technique, the distance between the two signal scanners should be selected relatively long. The first reason is that if the two detection areas overlap, calculating travel time or speed will not be possible. The other reason is that the measured travel time in this technique has some inaccuracy, due to the relatively large detection zone of the signal scanners; therefore, the distance between the two scanners should be long enough to have negligible inaccuracies. Due to these reasons, MAC re-identification technique for travel time and speed measurement in short road segments and for finding intersection delays; or in general for the purpose of finding microscopic traffic flow characteristics is not applicable.

MAC re-identification technique may also be applied in OD studies, installing a signal scanner at each possible origin and destination. If it is used in these studies, the distance between the signal scanners installed on the origins and destinations should be long enough not to have any common detection areas.

The deficiency of state-of-the-art MAC re-identification techniques can be apparent in applications involving turning movements in intersections located in dense urban areas such as central business districts in which the distances between the adjacent intersections are normally short. For finding origins and destinations in these intersections, there must be at least one signal scanner located in each of the intersection legs. In such areas, the signal scanners installed around the intended intersection may detect beacons located in the adjacent intersection areas (intersections and their legs); or a beacon located in the

intended intersection area may be detected by more than one or even all the scanners at a moment. These occur because of the short distances between the intersections and subsequently the signal scanners.

For instance, in a four-legged intersection, four signal scanners are required to find turning movements and each of them should be installed on one of the intersection legs. In downtown areas, the distances between the adjacent intersections are generally short; around 50 m. Considering the detection range of wireless signal scanners which is typically longer than 50 m, installing the scanners on the legs, but far from the intended intersection, will not guarantee that the detected beacons are in that intersection area (Figure 1.3a). Hence, the signal scanners should be installed on the legs, but close to the intended intersection. If the signal scanners are installed close to the intersection, each scanner will cover more than one intersection leg (Figure 1.3b); therefore, a certain beacon, passing the intersection may be detected by more than one scanner or even four of them at a moment. However, in determination of a turning movement using MAC re-identification technique, the beacon should only be detected by the signal scanners located on the origin and destination legs at different moments. Due to this issue, classifying turning movements of road users based on MAC re-identification or presence of beacons in the detection range of signal scanners solely is currently not possible.

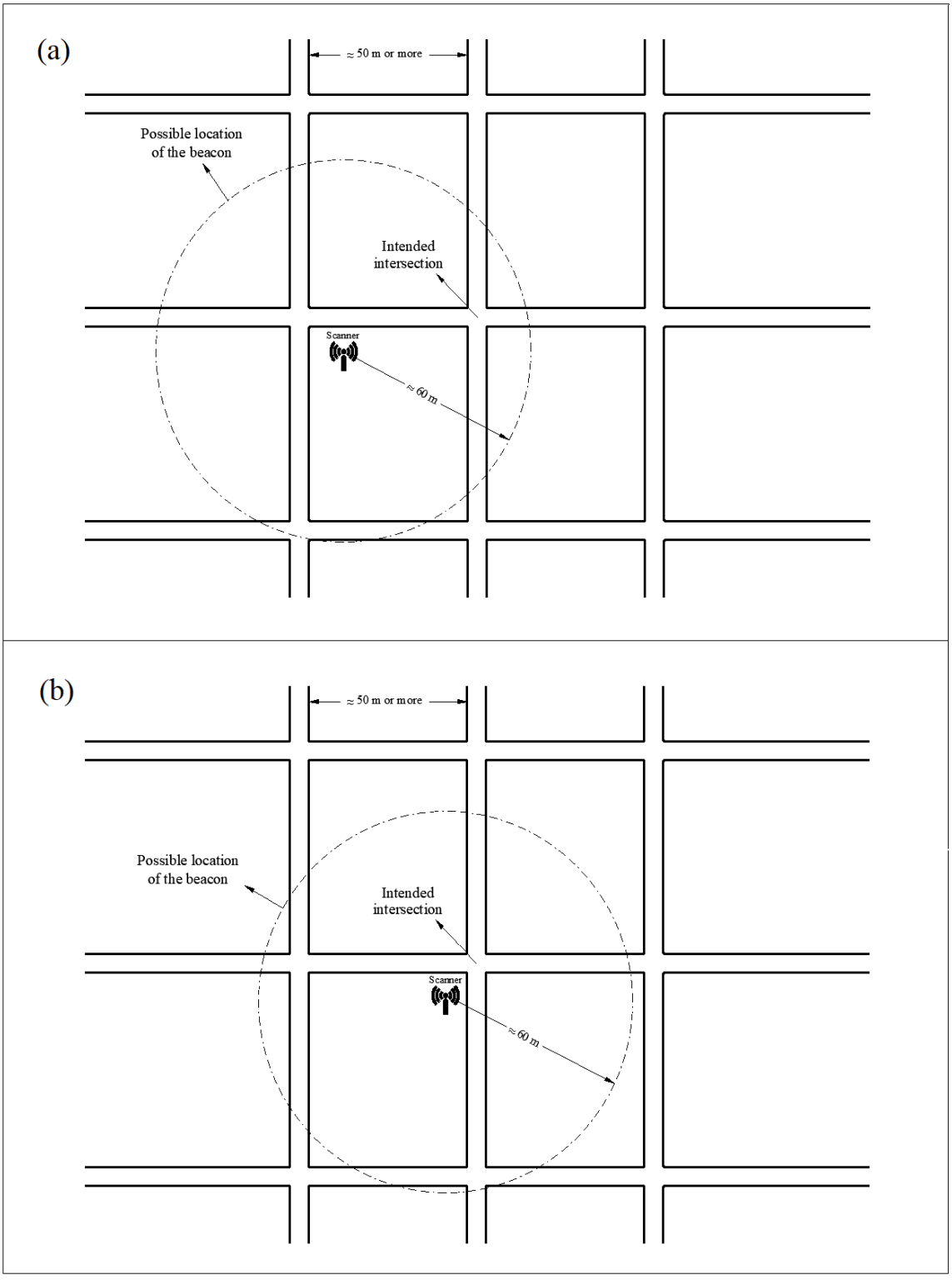

Figure 1.3 The coverage area of a signal scanner with a detection range of around 60 m: (a) installed far from the intended intersection; (b) installed close to the intended intersection.

To the author's knowledge, this technology has not been applied for determining travel time and speed in short road segments and also for determination of turning movements and delay in intersections located in dense urban areas. This is because the positional accuracy required in determination of these parameters in the mentioned situations is much more than only presence in a circle with a radius of several tens to several hundreds of meters.

Positioning of beacons based on their transmitted signals is a challenging task. RSSI is a measurement available in signal scanning which has the potential to be used in beacon positioning, since its values normally decrease as the distance between the beacon and signal scanner increases. RSSI may be used for finding the approximate distance between the beacon and signal scanner, but it may require extensive refinement to overcome accuracy issues, as RSSI values normally have fluctuations and include outliers. Moreover, the RSSI values contain no inherent information about the direction and the relative position of the beacon.

1.5 Research Objectives

1. Having a relatively accurate estimate of position based on wireless signals is a significant step toward improving the accuracy of traffic data using this technology. It will provide the possibility of travel time and delay measurement in situations where the classic MAC re-identifications technique is not applicable, *e.g.,* measuring travel time in short road segments suffering from heavy traffic and finding intersection delays. More importantly, the developed and enriched data will open the door for more advanced applications and solutions in collision warning systems, safety analysis, and data analytics with the ability to distinguish different modes of

traffic. It can be very useful for monitoring different traffic modes, *e.g.*, pedestrians or cyclists, and contribute to a safer and more efficient mobility. Thus, a goal with a significant practical value is to find a solution for locating beacons applicable in transportation data collection. The solution may be based on the RSSI values of the signals transmitted by road users' beacons, collected by wireless signal scanners.

2. Design and optimization of signalized intersections are among the important tasks of traffic agencies. The first step through this task is collecting turning movement data. Traditional approaches for collecting these data require a lot of resources and may not be applicable everywhere and in all conditions. An efficient approach may be applying wireless technology and developing an innovative data collection technique based on that. Unlike the common MAC re-identification approach for OD determination, this technique should be applicable in areas like central business districts in which the distances between the adjacent intersections are generally short.
3. The strength of Wi-Fi, Bluetooth Classic and BLE signal modes, received by signal scanners is measured by RSSI; therefore, the three modes may potentially be applied in traffic studies which need the positional data of the beacons. While the three signal modes may be utilized in these studies, the question which arises is that which signal mode leads to higher quality and accuracy as well as more convenience of data collection. To address this, it is required to investigate the important factors which may affect the mentioned measures. These factors should be selected considering the characteristics of traffic studies. They should be investigated in an outdoor environment and the general nature of traffic streams needs to be considered. To

propose the most suitable mode for each of the intended applications, it is required to investigate the characteristics and differences of the three mentioned signal modes.

1.6 Research Contributions

1. A comparative study of the field performance of Wi-Fi, Bluetooth Classic and BLE signal modes is conducted, investigating their characteristics important in gathering traffic flow parameters whenever accurate positional data of road users are required. This study provides the possibility of selecting the most suitable signal mode for the intended applications of the technology based on the requirements of the methods. Extensive field work is required to gauge the applicability in real-life.
2. The integration of wireless technology in vehicle-pedestrian collision warning systems will be investigated. This is a potential application of the aforementioned comparative study. The most suitable signal mode for integration in these systems will be introduced based on their requirements.
3. A technique for positioning of beacons transmitting wireless signals in outdoor areas applicable in transportation data collection will be proposed. The proposed technique will be based on the strength of wireless signals transmitted by beacons, creating radio maps, and applying an algorithm called k-nearest neighbors (KNN). KNN algorithm will be integrated in a wireless positioning technique to determine the location of the beacons in an intersection. The accuracy and functionality of the algorithm will be improved through modifications in the scanners set-up and stations arrangement.
4. A technique for determination of turning movements, using wireless signals applicable in dense urban areas will be developed. The technique will use RSSI-time

profiles of beacons, created based on the signals collected by the signal scanners, located on the intersection legs.

1.7 Organization of the Thesis

This thesis is presented in six chapters according to the following order:

1. The present chapter provided an overview of the most common types of traffic data collection with the potential to be supported by wireless technology. The utilized technologies in the thesis were introduced and the motivation for the research was discussed. The thesis objectives and contributions were also presented in this chapter.
2. The second chapter reviews the literature. This chapter may broadly be divided into two parts. The first part covers the previous studies on the characteristics of wireless signals as well as the progress made in wireless signal-based positioning. The second part overviews the studies on the applications of wireless signal scanning technology in the field of transportation.
3. The third chapter investigates Wi-Fi, Bluetooth Classic and BLE signal characteristics important in traffic studies which require the positional data of road users in the form of a comparative study. The special case of vehicle-pedestrian collision warning systems is also investigated as an example of the applications of the results of this chapter.
4. The fourth chapter presents a technique for positioning of beacons based on their transmitted signals applicable in transportation studies. Effort is made to find solutions for improving the functionality and accuracy of the developed technique. The performance of numerous filtering algorithms in enhancing the accuracy of the results is also examined in this chapter.

5. The fifth chapter aims at turning movement classification. A technique for finding intersection turning movements based on wireless signals is developed and its performance in different situations is examined.
6. The thesis will be summarized in the sixth chapter, its conclusions will be presented, and the research limitations will be mentioned. In addition, several recommendations for the future studies are provided in this chapter.

Chapter 2: Literature Review

2.1 Wireless Signal-Based Positioning

Received signal strength indicator (RSSI), time of arrival (TOA), time difference of arrival (TDOA) and angle of arrival (AOA) are among the attributes of wireless signals applied in wireless signal-based positioning methods. An overview of the previous studies on development of positioning methods based on them is presented hereafter with more focus on RSSI-based techniques.

2.1.1 Received Signal Strength Indicator

2.1.1.1 RSSI-Distance Models

The relationship between RSSI and distance is the foundation for RSSI-based wireless signal positioning (Xu, et al., 2010). Extensive effort has been made to use the received strength of radio frequency signals transmitted by beacons for estimation of the distance from wireless signal scanners. The distance between a beacon and a certain signal scanner is estimated by the models that relate this distance to the reduction in the strength of the signals received by the scanner.

Transmission path between a beacon and a signal scanner may be free or obstructed by obstacles. Unlike wired channels which are predictable, radio channels are random and analyzing them is not easy. Cellular radio systems generally operate in urban areas with non-line of sight (NLOS) paths between beacons and signal scanners. Propagation of electromagnetic waves has a complicated mechanism, generally affected by diffraction, reflection, and scattering. Signal propagation models generally predict average RSSI values at different distances from beacons. As the distance between a beacon and a signal scanner increases, average RSSI values gradually decrease. Large-scale and small-scale

propagation models have been presented to predict the relationship between RSSI and distance in different conditions (Rappaport, 2002), (Dalal, 2015).

(Rappaport, 2002) and (Dalal, 2015) collected several RSSI-distance models developed by different researchers:

1. A widely used free space propagation model for predicting the received power by a signal scanner in different distances is Friis equation:

$$P_r(d) = \frac{P_t\, G_t\, G_r\, \lambda^2}{(4\,\pi)^2\, d^2\, L} \qquad (2.1)$$

in which:

$P_r(d)$ = received power at a distance of d from the beacon

P_t = transmitted power

G_t = beacon antenna gain

G_r = signal scanner antenna gain

λ = wavelength (m)

d = the distance between the beacon and the signal scanner (m)

L = propagation unrelated loss factor of the system

In this equation, $P_r(d)$ and P_t should have the same units and G_t, G_r and L are dimensionless quantities.

2. The received power in free space at a distance of d may also be predicted knowing the average received power at a distance of d_0. The average received power at d_0 may be determined using Friis equation. It may also be measured in the field taking the average of received powers in several points located at a radial distance of d_0 in the far-field region of the beacon and closer than any practical distance in mobile communication systems. Far-

field distance is the largest dimension of the beacon antenna aperture and the wavelength of the carrier. Far-field region is the region beyond this distance. In free space, the received power at a distance greater than d_0 may be calculated by:

$$P_r(d) = P_r(d_0) \left(\frac{d_0}{d}\right)^2 \qquad (2.2)$$

where $P_r(d)$ is the received power at a distance of d from the beacon and $P_r(d_0)$ is the average received power at d_0.

3. Practical propagation models are often developed using both theoretical and empirical approaches. Empirical approaches are usually based on analysis of measured data or curve fitting. The advantage of empirical approaches is that all known and unknown propagation factors are implicitly considered in the models as they are developed based on field measurements. Nevertheless, due to environmental variations and transmission frequency, these models need to be calibrated for different conditions. In both theoretical and measurement-based models, average RSSI decreases logarithmically as the distance increases. Log-distance path loss model is an example of practical models for predicting path loss, or reciprocally RSSI, as a function of the distance between the beacon and signal scanner:

$$PL\ (d) = PL(d_0) + 10\, n \log\ \left(\frac{d}{d_0}\right) \qquad (2.3)$$

in which

$PL\ (d)$ = average path loss at a distance of d from the beacon (dB)

$PL(d_0)$ = average path loss at a distance of d_0 from the beacon (dB)

n = path loss exponent

d = distance from the beacon (m)

d_0 = distance between the beacon and a reference point close to it (m)

Path loss exponent depends on propagation environment and may be defined as the rate at which path loss increases as the distance increases. The magnitude of path loss exponent for a variety of mobile radio environments may be observed in Table 2.1:

Table 2.1 Path loss exponent in different environments (Rappaport, 2002).

Environment	Path loss exponent (*n*)
Free Space	2.0
Urban area cellular radio	2.7–3.5
Shadowed urban cellular radio	3.0–5.0
In building LOS	1.6–1.8
Obstructed in buildings	4.0–6.0
Obstructed in factories	2.0–3.0

4. In the real word conditions, transmission paths are seldom direct as signals are reflected by the ground and other obstacles; hence, free space propagation models are not accurate. Ground reflection (two-ray) is a propagation model in which both direct and ground reflected propagation paths between the beacon and signal scanner are taken into consideration:

$$P_r = P_t\, G_t\, G_r\, \frac{{h_t}^2\ {h_r}^2}{d^4} \qquad (2.4)$$

in which:

P_r = received power at a distance of *d* from the beacon

P_t = transmitted power

G_t = beacon antenna gain

G_r = signal scanner antenna gain

h_t = beacon antenna height

h_r = signal scanner antenna height

d = distance between the beacon and signal scanner

According to (Park, et al., 2016), even in short distances, reception rate is not expected to be 100% of the transmitted signals due to the existence of interference and disturbance. The reception rate does not vary a lot when the distance is short (around 2 m) and is close to 100%, no matter what the signal strength is. However, in longer distances (8–10 m), this rate may even decline to less than 50%. In addition, as the distance increases, the error in distance estimation increases.

RSSI is the resultant of contributions from different directions; therefore, even small beacon movements cause fluctuations in signal strengths (Rappaport, 2002). (Xu, et al., 2010) analyzed experimental data and observed that variances of RSSI values vary with distance. This led to proposing a relationship between these two parameters. They used dynamic variances to develop a log-normal shadowing model between RSSI variance and distance. They also used least square method to dynamically adjust the model coefficients in different environments.

Multipath components cause RSSI fluctuations in real time whose impacts are not considered in path loss models; Hence, developing a proper propagation model is complicated and even impossible in some situations. Attenuations caused by different objects reduce the accuracy of distance estimation models which may result in erroneous outcomes (Tariq, et al., 2017). Presence of human body in signal transmission path may

affect Wi-Fi and Bluetooth signal RSSI values. The reason is that these signals are attenuated by water due to their operating frequency and more than half of human body is made up of water (Retscher, 2017).

In order to enhance the accuracy of distance estimation using RSSI values, (Sung, 2016) proposed a two-phase distance estimation method. In the preliminary phase, the minimum and maximum RSSI values and their corresponding distances in a pre-specified motion pattern were specified to be used in the next phase. The second phase was done using a log-distance path loss model, a Kalman filter, and relative distances found on the basis of the pre-specified minimum and maximum RSSI values. Kalman Filter estimates the current situation or predicts the short-term status based on the available data measurements of the recent situation of the system. This filter was applied along with the path loss model to eliminate outliers. Sudden changes of the signals were refined considering the preceding signals. This method reduced distance estimation errors by 8% in comparison with only removing impulse noises from RSSI values.

In another study, researchers proposed a distance estimation method using RSSI values and applying a particle filter to improve the accuracy of distance estimation (Svecko, et al., 2015). They assessed different combinations of log-distance path loss model, ground reflection model and particle filter algorithm to increase distance estimation accuracy. Particle filter is an extension of Kalman filter and is based on sequential importance sampling technique. In this filter, particles (weighted samples) are used to represent posterior density function. The process is done in three steps including particle generation, particle weight (importance) determination and resampling. The experiments were conducted in a room using 12 signal scanners in a circular arrangement and 8 signal

scanners in a parallel arrangement. The results indicated that the accuracy of distance estimation using the combination of ground reflection model and particle filter was the best, followed by the combination of log-distance path loss model and particle filter.

2.1.1.2 RSSI-Based Positioning

RSSI-distance models based on the detections of one signal scanner are only able to estimate the distance between the beacon and signal scanner; thus neither the direction nor the position. When information from additional signal scanners is available, it will be possible to find the position of the beacon, using basic geometry. In that regard, it will be important to develop proper approaches to combine the results from multiple signal scanners to find the position of the beacon with adequate accuracy. Triangulation, trilateration and fingerprinting are among the solutions for positioning of beacons based on RSSI values.

A positioning method that is commonly applied in wireless signal positioning is triangulation in which triangle specifications are used to find a beacon position. It works based on angle measurement and estimates an unknown point position, forming triangles which connect it to points with known positions (Park, et al., 2016). The positioning method is called trilateration if three distances from an unknown point to three known points are used instead of angles (Makki, et al., 2015). If both angles and distances are used in positioning, the method is called triangulateration.

Trilateration is a mathematical positioning technique by which the two-dimensional position of an unknown point may be determined if its distances from three other points with known positions are known. Trilateration has the potential to be used in wireless signal positioning. To apply this technique for finding the position of a beacon, three signal

scanners with known positions are required (Figure 2.1). It is necessary to find the distances between the beacon and the three signal scanners at a certain moment. These distances may be found using RSSI-distance models or time of arrival technique. The distance between the beacon and each of the three signal scanners forms a circle with a radius equal to the calculated distance and centred on the location of the signal scanner. The position of the beacon will coincide with the intersection of the three formed circles (Makki, et al., 2015). If the common area of the three circles formed by the three measured distances is large, finding the exact position will be more difficult (Park, et al., 2016). In case the three-dimensional position of the beacon is required, the distances to four signal scanners should be known (Tariq, et al., 2017). This may be called quadrilateration.

Effort was made by (Lee, et al., 2016) to improve the accuracy of wireless distance estimation and trilateration positioning in an indoor study using a BLE beacon and four signal scanners. One-dimensional Gaussian filter (G) was applied on RSSI values using the below formula with standard deviation (σ) as the parameter:

$$G(RSSI) = \frac{1}{\sqrt{2\,\pi\sigma}} e^{\left(-\frac{RSSI^2}{2\sigma^2}\right)} \qquad (2.5)$$

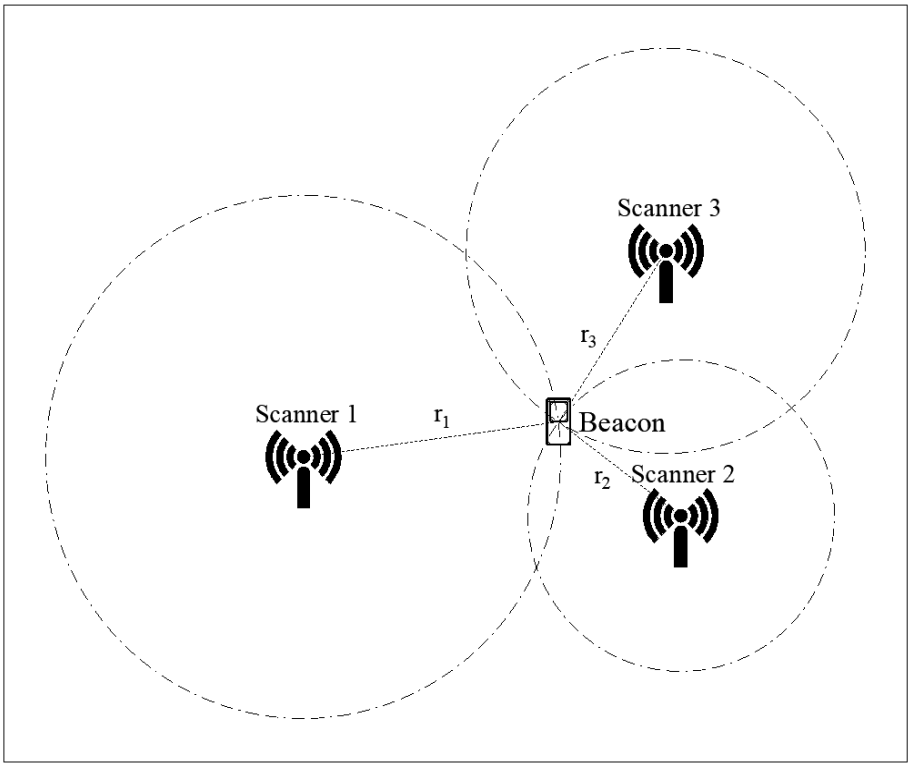

Figure 2.1 Application of trilateration technique in wireless signal positioning (Makki, et al., 2015).

The filter smoothed the RSSI values by convolution with a Gaussian function. It reduced the difference between the minimum and maximum RSSI values as well as the difference between the mode and average of them. A weight algorithm was then applied considering the quality of the filtered RSSI values. The distances between the beacon and signal scanners were found based on Friis equation. Trilateration technique was used for positioning of the beacon. In case there were four simultaneous detections by the four signal scanners, the three shorter distances were used in positioning. Gaussian filter was applied on the estimated locations again for further improvement of the positioning accuracy.

In a simulation-based study, (Lee, et al., 2014) proposed a three-dimensional positioning approach. The simulated location was a 10 m×10 m office. The two-

dimensional position of the beacon was estimated calculating its distances to three signal scanners using trilateration technique. Heron tetrahedron formula was used to find the beacon height and then the two-dimensional position was transformed into a three-dimensional estimation. The approach specified the three-dimensional position of the beacons with less complexity compared with iterative three-dimensional algorithms.

Another three-dimensional positioning approach was proposed by (Park, et al., 2016). Four non-coplanar stationary signal scanners were used to estimate the three-dimensional position of a BLE beacon. The RSSI values of the signals transmitted by the beacon were collected by the four signal scanners and were used to specify the distance between the bacon and each signal scanner by a logarithmic path loss model. A sphere was formed based on these distances and its central point was specified. The (x, y, z) position of the beacon was determined using quadrilateration formulas. The error rate in this approach was 27.3% less than the regular two-dimensional trilateration technique.

Kalman filters as well as mean filters were applied by (Zhou, et al., 2017) in a positioning study conducted in a 140 m^2 indoor area on a stationary Bluetooth beacon. A propagation model was developed and calibrated for Bluetooth signals. Kalman and mean filters were used to smooth the collected RSSI values. Fluctuations were more effectively reduced by Kalman filter; hence, it was selected for filtering the signal strengths. The filtered RSSI values were used to find the distance between the beacon and signal scanner by the propagation model. Weighted least square and quadrilateral techniques were combined for positioning of the beacon. The results indicated that the technique meets the accuracy requirements of indoor positioning if Kalman filter is applied on RSSI values, prior to distance estimation.

Support vector machine (SVM) is a linear machine learning algorithm which classifies input patterns by being trained on labeled data sets. SVM utilizes nonlinear kernel functions which map input data into high-dimensional feature spaces (Chen & Councill, 2003). Support vector regression (SVR) uses SVM algorithm in solving regression problems (Greatlearning, 2020). A wireless positioning technique was proposed based on SVR algorithm involving a training and an online positioning phase (Shi, et al., 2015). A model specifying the relationship between beacon RSSI values and positions was developed in the training phase and the exact positions were determined in the online phase by SVR algorithm. Statistical-based filters and multiple continuous measurement technique were utilized to enhance the quality and consistency of RSSI inputs. The experiments conducted in a building hallway using 17 Wi-Fi signal scanners resulted in an initial average positioning error of 2.25 m whereas filtering the data in addition to using multiple continuous measurement technique reduced the average error to 0.68 m. This was the indicator of the better performance as well as lower computing power demand of the proposed technique in comparison with neural network and probability methods.

K-nearest neighbors (KNN) is a mathematical data classification algorithm for determining the most similar points in a reference set to a test point with certain characteristics (Kuhn & Johnson 2016). (Zhang, et al., 2020) proposed a scalable indoor positioning technique based on distance fitting and fingerprinting approach. The experiments were conducted in a university building using eight Wi-Fi signal scanners. The technique involved two main components: annulus-based localization and local search-based localization. A multinomial RSSI-distance model was used to develop the annulus-based localization component first. To limit the search span for finding the beacon

location, an annulus construction scheme was proposed based on the calculated distances. A subarea division scheme was also proposed to enable the algorithm to select the suitable RSSI-distance model considering the physical characteristics of the environment. Then, the local search-based localization component was developed using the RSSI values collected by the signal scanners and fingerprinting approach. An RSSI distribution probability model was used to set a statistical probability model between the reference points and RSSI values. An algorithm was used to select a set of possible reference points using Bayes theorem and finally, KNN algorithm was applied to find the location of the beacon among the reference points. The results of the experiments indicated an average localization error of 3.48 m and a 76^{th} percentile localization error of 4.02 m.

Considering the inconsistencies observed in the relationship between RSSI and distance, (Wang, et al., 2020) proposed a positioning technique using weighted KNN algorithm. In weighted KNN, higher weights are assigned to the nearer neighbors compared with the farther ones. The experiments were conducted in a university laboratory building using 10 Wi-Fi signal scanners. The technique worked based on signal RSSI similarities and spatial positions. Weighted Euclidean distances were found using a log-distance signal attenuation model and RSSI differences. Approximate positional distances were obtained combining the weighted Euclidean distances and the positional information of the reference points. Applying the weighted KNN algorithm, the nearest reference points were found considering the approximate positional distances between the reference points and the beacon. The lowest mean positioning error and root mean square error achieved in the experiments were 2.32 m and 2.78 m respectively.

(Cao, et al., 2021) proposed a wireless positioning technique using Gaussian process regression and KNN algorithms. The study was based on dual-band Wi-Fi, because it provided more data useful for positioning compared with single-band Wi-Fi. Two experiments were conducted indoors using 5 and 10 dual-band Wi-Fi routers. The RSSI values of the 2.4 and 5.0 GHz signals transmitted from reference points were collected in an offline phase. The RSSI values were normalized to generate dual-band fingerprints. A positioning model was developed for each dual-band fingerprint using Gaussian process regression algorithm. This was done based on the dual-band fingerprint itself as well as the neighborhood fingerprints provided using the distances between the reference points. In online phase, dual-band and 5.0 GHz fingerprints were produced using the Wi-Fi dual-band RSSI values. KNN algorithm was applied on the 5.0 GHz fingerprints to find the initial locations. The 5.0 GHz signals were used in this step, because they were more stable compared with 2.4 GHz signals. The optimal model was developed finding the minimum distances between the initial locations and the reference points. The final positioning estimates were obtained using this model and the dual-band fingerprints. This technique resulted in mean absolute errors of 1.432 and 1.067 m and root mean square errors of 1.712 and 1.331 m in the two experiments.

2.1.2 Time of Arrival

Time-based wireless signal positioning works on the basis of signal travel time between different nodes. The fundamental concept used in this technique is called time of arrival (TOA). TOA is the time it takes for a signal transmitted by a beacon to arrive at a signal scanner. Knowing the velocity of signal propagation, the distance between the beacon and signal scanner may be calculated using time-distance formula. If the distances

between the beacon and three signal scanners are known, trilateration technique may be used for finding the two-dimensional position of the beacon (Tariq, et al., 2017). The main challenge in TOA technique is that it requires extremely precise synchronization of the beacon and all the signal scanners; otherwise, distance estimations will have high inaccuracies (Liu, et al., 2007). This technique is subject to NLOS transmission path, because in NLOS conditions, signals are received from alternative paths due to reflections by the objects present in the area (Spano & Ricciato, 2017).

2.1.3 Time Difference of Arrival

Time difference of arrival (TDOA) is a replacement for TOA. It works based on the differences between travel times of a signal from a beacon to different signal scanners, instead of their absolute values. As the beacon transmits a signal, it may be received by N+1 signal scanners with known positions at different moments, depending on their distances to the beacon. Based on the differences between the arrival timestamps, it will be possible to specify the position of the beacon in N dimensions. The differences between the arrival timestamps are used to form hyperbolas whose foci are the signal scanners positions (Figure 2.2). Hyperbolic multilateration technique may then be used to determine the position of the beacon (Makki, et al., 2015).

In two-dimensional positioning, a minimum of three signal scanners are required. For each TDOA observation by two signal scanners, the possible locations of the beacon form a hyperbola, representing the difference between the distances of the beacon from the two scanners. Selecting Scanner 1 as the reference in Figure 2.2, the two below independent hyperbolic equations may be developed:

$$r_1 - r_2 = \mathrm{c}\,(t_1 - t_2) = \sqrt{(x_1 - x)^2 + (y_1 - y)^2} - \sqrt{(x_2 - x)^2 + (y_2 - y)^2} \qquad (2.6)$$

$$r_1 - r_3 = \mathrm{c}\,(t_1 - t_3) = \sqrt{(x_1 - x)^2 + (y_1 - y)^2} - \sqrt{(x_3 - x)^2 + (y_3 - y)^2} \qquad (2.7)$$

in which t_1, t_2, t_3 are signal travel times from the beacon to Scanners 1,2,3 respectively and c is the velocity of signal propagation. The position of the beacon (x, y) is the intersection of these two non-linear equations. As these two equations may have two intersections, a prior knowledge of the approximate position of the beacon is required in two-dimensional positioning (Makki, et al., 2015), (Tariq, et al., 2017).

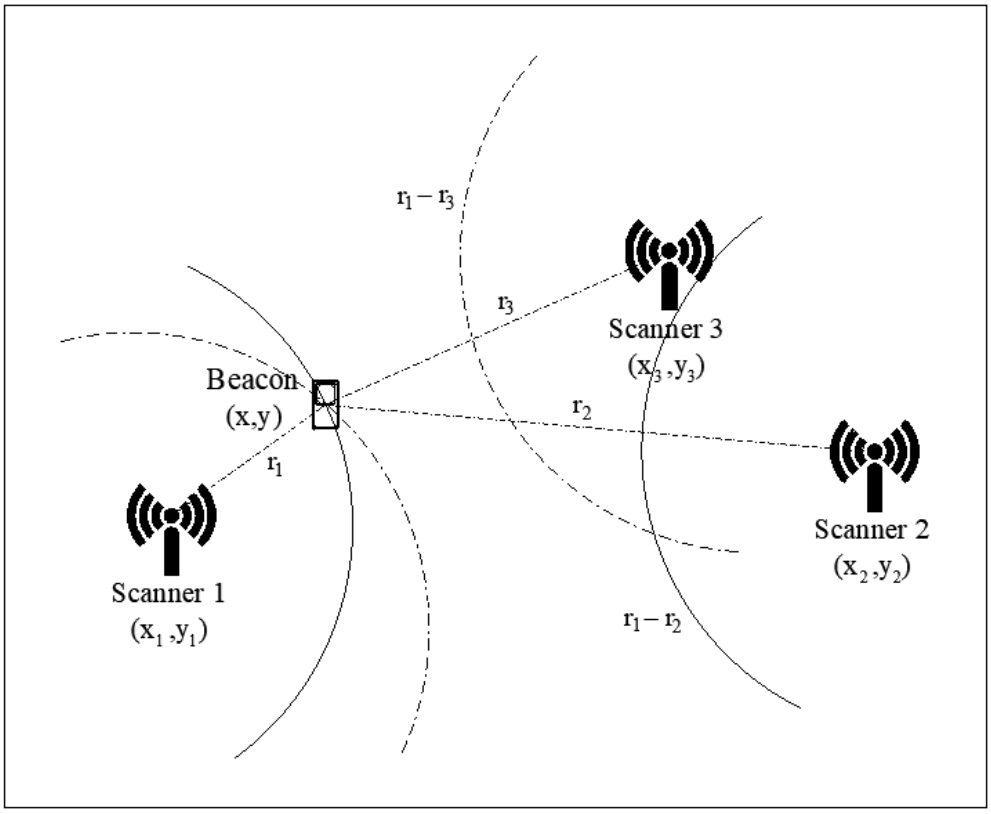

Figure 2.2 TDOA positioning technique (Makki, et al., 2015).

The main challenge in this technique is precise synchronization of the signal scanners (Tariq, et al., 2017). However, its advantage over TOA technique is that synchronization of the beacon is not required (Farid, et al., 2013).

2.1.4 Angle of Arrival

Angle of arrival (AOA) is one of the attributes of wireless signals with the potential to be used in wireless signal positioning. In this technique, angle of arrival of a signal transmitted by the beacon at two signal scanners with known positions are used to find the two-dimensional position of the beacon (Hou, et al., 2018). The accuracy of the technique may be enhanced using more than two signal scanners (Tariq, et al., 2017). For finding three-dimensional position, three scanners are required. According to Figure 2.3, the (x, y) position of the beacon may be determined using the below formulas (Bensky, 2016):

$$x = \frac{d \tan(\alpha_2)}{\tan(\alpha_2) - \tan(\alpha_1)} \qquad (2.8)$$

$$y = \frac{d \tan(\alpha_1) \tan(\alpha_2)}{\tan(\alpha_2) - \tan(\alpha_1)} \qquad (2.9)$$

in which:

d = distance between the two signal scanners

α_1 and α_2 = angles of arrival at the two signal scanners

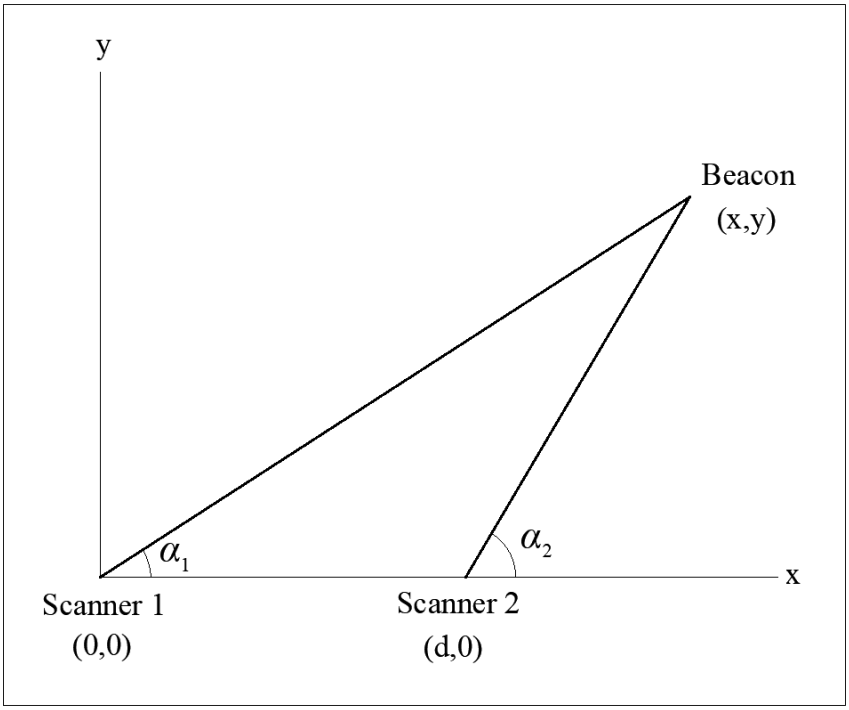

Figure 2.3 AOA positioning technique (Bensky, 2016).

The advantages and disadvantages of each of the wireless signal attributes applicable in positioning was highlighted by (Tariq, et al., 2017) according to Table 2.2. It was emphasized that there is no standard technique meeting all the performance criteria of positioning; therefore, a trade-off between the metrics important in positioning is required for selecting the suitable approach.

Table 2.2 Comparison of the wireless signal attributes applicable in positioning (Tariq, et al., 2017).

Attribute	Advantages	Disadvantages
RSSI	+ Scalable for large areas thanks to the available and low cost required equipment	− Lower accuracy compared with the other attributes − Subject to NLOS and multipath conditions − Time consuming field calibration
TOA	+ Accuracy + Robustness against NLOS and multipath conditions is achievable using proper algorithms.	− extremely precise synchronization of the beacon and signal scanners is required. − Expensive required equipment − High cost of scalability for large areas
TDOA	+ Accuracy + Robust against multipath	− extremely precise synchronization of the signal scanners is required. − Expensive required equipment − High cost of scalability for large areas
AOA	+ Accuracy	− Costly additional antennas are required for angle measurement. − Subject to NLOS conditions − Hardly scalable for large areas due to LOS and hardware requirements

Cellular networks have developed rapidly since their introduction in 1980. The fifth generation of cellular networks (5G) is currently the most recent generation of these systems with prominent improvements in the capabilities. Higher reliability, higher data rates, lower latency, higher connection density, and expanded range of applications are

among the main improvements in this generation. Provision of uninterrupted connections and high data exchange rates for moving users by this generation and its potentials in support of the requirements of internet of things justify utilization of 5G in advanced transportation applications *e.g.*, autonomous vehicles and real time traffic control systems (Devaki, et al., 2019), (Stallings, 2021).

Effort was made by (Han, et al., 2019) to develop a positioning technique for 5G networks. The technique utilized the potentials of multiple-input and multiple-output (MIMO) technology for estimation of AOA. Beamforming antennas were used because they fit the technique requirements. Base stations were divided into near-field and far-field stations. Fourth order cumulants were obtained for the near-field stations whereas adaptive weights were calculated for the far-field stations. Considering the errors oriented from the longitudinal array on the plane angle, linear weights were used to mitigate multi-peak hopping errors. The positioning stage of the technique involved two steps. The first step was coarse positioning in which a search zone for the next step was specified in order to optimize the procedure and limit the non-convex errors. In the second step, exact coordinates were determined using an angle-based formula. The obtained results indicated the adaptability of the technique in the near-field zone and its capability to reduce the errors caused by multipath and NLOS.

2.2 Applications of Wireless Signal Scanning in Traffic Studies

2.2.1 Travel Time and Speed Measurement

Wireless technology is widely applied to measure travel time and space mean speed using MAC re-identification technique. This is because of three main capabilities of wireless signal scanning systems: [*i*] anonymous detection of road users, [*ii*] direct measurement of travel time, [*iii*] cost effectiveness because of the relatively high number of observations and extendable data collection time (Salek Moghaddam & Hellinga, 2013). Measurement of travel time and speed has been the direct subject of a large portion of the studies on the applications of wireless technology in traffic studies, whereas many others have tried to mitigate the issues and challenges arisen during the development of the techniques for measurement of these parameters.

(Quayle, et al., 2010) studied the reliability of Bluetooth MAC address re-identification technique in finding arterial traffic data including travel time, average speed, and OD matrices. Data collection was done during peak hours for 27 days in a 2.5-mile arterial segment located in Portland, Oregon with an average daily traffic of 15000 to 20000 vehicles. Travel time measurements obtained using MAC re-dentification technique were compared with the measurements of a GPS equipped floating car in order to evaluate their accuracy and reliability. Their collected data involved 15 to 45 hourly matching MAC addresses. These were equal to 1.5 to 4.5% of the historical peak volume in the road segment which was approximately 1000 vehicles per hour. They discussed that although these rates may seem to be low, the provided data set is two to three times larger than the results of floating car technique. Although the sample sizes in MAC re-identification technique were larger, the measured travel times were close in the two techniques.

Comparison of the standard deviations of travel time measurements indicated lower values in the data collected by the floating car.

(Barceló, et al., 2010) conducted a study to investigate the quality of short-term travel time forecast and time dependent OD matrix estimation by Bluetooth signal scanners. The study was based on simulation of an 11.5-km section of an urban freeway involving 11 entries and 12 exits. A pilot study was also conducted on a 40-km section of a motorway located in Spain on which five signal scanners were installed at the entries and exits. The proposed method used a Kalman filter approach in which variations of the dynamic system over time were modeled in an iterative process. It predicted the system state based on its current state and the available measurements. The results confirmed the quality of travel time forecasts. The approach also performed well in determination of OD matrices in different traffic conditions, but properly creation of the initial matrices was identified critical for success of the approach.

Researchers also evaluated error magnitudes of arterial travel time measurement in different traffic conditions using Bluetooth MAC re-identification technique in a simulation-based study (Salek Moghaddam & Hellinga, 2013). Characteristics of vehicle trajectories, location of Bluetooth signal scanners, signal controls, different traffic conditions and volumes were taken into consideration. Vehicle trajectories were simulated in Vissim software (Ptvgroup, 2021) for different traffic conditions and different signal controls in an arterial containing two signalized intersections. For each passing vehicle, the location of the first signal detection by each scanner was specified using a Monte Carlo simulation technique. This simulation technique was applied again for finding travel time measurement errors in different conditions. The results indicated that the mean error of

travel time measurement is adequately low for all traffic conditions and negligible for practical purposes. Nevertheless, the variance of measurement errors varies in different traffic conditions.

In MAC re-identification technique, ideal travel time calculated based on posted speed limit may be subtracted from actual travel time to find the delay. Actual travel time is equal to the time difference between the first or last detections of a beacon by two signal scanners. (Abbas, et al., 2013) argued that this approach for intersection delay measurement is inaccurate and underestimates the values. The reason is existence of inherent errors due to random structure of Bluetooth detections in terms of time and space. To address this issue, they proposed a method for intersection delay measurement which worked based on deriving and calibrating equations relating delay to the number of the times a beacon was detected and the time difference between the first and last detections. Nine Bluetooth signal scanners were used in an experiment conducted in an arterial with nine intersections. Bluetooth measurements were synchronized with GPS probe vehicle data including time and location. Comparison of the results with GPS probe vehicle data indicated the superiority of their proposed method over simple MAC re-identification technique in terms of accuracy. Their method also had the potential to be used in near real-time level of service (LOS) estimation of intersection approaches and signal timing optimization.

Although loop detectors can cover almost all passing vehicles, they may only specify the speed at the sensor location, not throughout the road segment. Bluetooth traffic monitoring systems are able to specify space mean speed throughout the road, but their detection rates are lower compared with loop detectors (Bachmann, et al., 2013).

Effort was made by (Bachmann, et al., 2013) to combine the data collected by loop detectors and a Bluetooth traffic monitoring system to enhance the accuracy of traffic speed measurement. The experiments were conducted in Highway 401, Toronto. Several data fusion algorithms were used to combine the data collected by the two techniques, and their performance in accurately determination of traffic speeds along freeways were examined and compared. The fusion algorithms involved Simple Convex, Bar-Shalom/Compo, Measurement Fusion Kalman Filter, Scatt Kalman Filter, Ordered Weighted Averaging, Fuzzy Integral and Neural Network. The results were compared with the measurements of a GPS equipped probe vehicle. It was observed that the results obtained from fused data often had an accuracy equal to or better than the most accurate result, obtained from the Bluetooth system or loop detectors, no matter which one had performed better. All data fusion algorithms improved the accuracy of the results to a similar degree, but Simple Convex, Bar-Shalom/Compo and Measurement Fusion Kalman Filter algorithms performed more consistently. The overall results of the Bluetooth system were more accurate and closer to the GPS equipped probe vehicle measurements in comparison with loop detectors. It was discussed that the existence of even a few measurements by Bluetooth signal scanners can improve the accuracy of speed measurements by loop detectors if fused with each other.

The accuracy and reliability of speed measurement using MAC re-identification and probe vehicle tracking techniques were assessed and compared by (Gong, et al., 2019). Bluetooth data were collected by 12 Bluetooth signal scanners installed along an arterial in Orlando, Florida and Probe vehicle data were provided by a traffic services company. The data collected in the two techniques were compared with high resolution GPS trajectories

for evaluation. Average absolute speed error (AASE) and speed error bias (SEB) were calculated as the two measures selected for comparison of the space mean speeds obtained in the two studied techniques with GPS technique. AASE indicated the absolute difference of the estimated and real speeds and SEB reflected the direction of the difference. The results indicated the better performance of MAC re-identification compared with probe vehicle in terms of accuracy and reliability. The ability of MAC re-identification technique in providing bimodal flow patterns and better compliance with speed limit were introduced as the reasons for its better performance.

An augmentation framework was also presented by (Gong, et al., 2019) for improving the quality of probe vehicle data. The framework used historical data collected by Bluetooth signal scanners. A finite mixture model from Bluetooth data was applied to estimate flow patterns on arterials. This information and a Bayesian inference framework were used to improve space mean speeds. These were effective in most cases and presented a more realistic view of free flow conditions. The framework reduced abnormal data percentage from 13% to less than 4%.

In order to predict the behavior of Bluetooth-based traffic monitoring systems, (Zarinbal Masouleh & Hellinga, 2019) presented a technique to simulate detection of Bluetooth beacons. Vissim software was used to model vehicle motions in a hypothetical road. The effects of the distance between beacons and signal scanners as well as multiple detection of beacons located in the detection range of signal scanners were taken into account in their simulation technique. They proposed application of this technique for evaluation of traffic management projects based on Bluetooth data collection. This was

because of the high accuracy of the technique in simulation of signal detection process, distribution of detection locations and the time difference between successive detections.

2.2.1.1 Outlier Removal from Travel Time Data

Travel time in long freeway segments may be determined accurately in most situations, but in arterials, these measurements are more challenging because of the frequent interruptions in traffic flows. Bluetooth signal detection is subject to outliers (unwanted data) and measurement errors. Existence of entries and exists along the roads, enroute vehicle stops, multiple detection of beacons, non-auto detection, presence of multiple beacons in vehicles, and road users with excessively high or low speeds are examples of the sources of outliers. Inaccurate information about beacons locations due to vast detection zone of signal scanners is another factor reducing the accuracy of travel time measurements in MAC re-identification technique. In practice, the first detections at the origin and destination are usually used for travel time calculation (Salek Moghaddam & Hellinga, 2013). Statistical techniques may be used to clean outliers indicating irrelevant travel times. Setting cut-off percentiles or plausible limits are examples of these techniques. Plausible limits can be defined as median plus/minus appropriate coefficients of standard deviation for travel time and speed measurements. Engineering judgement may be applied and setting static cut-offs should preferably be avoided due to travel time variations throughout the day (Quayle, et al., 2010).

Outliers may not be removed from Bluetooth data collected for travel time and speed measurements by visual observation in real-time; hence, a statistical method for real-time removal of outliers from these data was proposed by (Van Boxel, et al., 2011). Their experiments were conducted in several interstate highways and urban arterials. A

Greenshields traffic flow model was used to relate road segment speed and density. Outliers were identified and removed using standard residuals of the data points in the Greenshields model and setting a 90% confidence threshold. The data were assessed by Shapiro-Wilk normality test before and after outlier removal. The test results indicated that the applied method improved normality of the data from non-normal to normal at the 95% confidence level, implying its effectiveness in removing outliers from travel time data. Although the method was effective in real-time identification of outliers from travel time data in both types of road segments, it performed better in interstate highways compared with urban arterials. One reason was the higher traffic volumes in highways. The other reason was the fact that occurrence of outliers is more likely in arterials because of the vehicles entering or existing the road segments as well as presence of bicycles and pedestrians which artificially impact travel time measurements.

A simulation-based framework was proposed for quantitative evaluation of Bluetooth travel time filtering algorithms (Salek Moghaddam & Hellinga, 2013). The purpose was developing a tool to find out which algorithm is the most proper for a given application with respect to different sources of outliers. Vissim software was used to model a 1.62-km four-lane highway containing three signalized intersections located in Waterloo, Canada in different conditions. Travel times were extracted from the micro-simulation model to be the representative of true data. Monte Carlo simulation technique was used to generate four types of outliers including non-auto detections, enroute stops, presence of multiple beacons in a single vehicle and imprecise detection timestamps. Two different lowpass exponential smoothing algorithms, both developed by (Dion & Rakha, 2006) were selected to apply the evaluation framework on them. The two smoothing algorithms were

used to rectify (clean) the travel time data. Relative travel time improvement, indicating improvement in travel time estimation at a macro level was proposed as the performance measure in the evaluation process. The filtering algorithms were evaluated calibrating a multivariate linear regression model. The dependent variable in this model was relative travel time improvement and the independent variables were binary variables associated with the experiment scenario factors. The framework was able to specify the superior filtering algorithm for each study situation and the range of improvements it might provide. The results of applying the framework on the two examined smoothing algorithms indicated that one of them increased the likelihood of getting worse results by approximately 30% compared with the situations it was not used. In contrary to this algorithm, the relative improvement obtained by the other one was up to 60%.

2.2.1.2 Travel Time in Alternative Routes and Vehicle Trajectories

Wireless signal scanners provide the possibility of gathering road users' data between signal scanning pairs, but they do not specify exact routes (Yildirimoglu, 2021). There may be entries and exits between these scanning pairs providing alternative routes for the road users. If the impacts of these entries and exits are not taken into consideration, they may be the reason for some inaccuracies in the measurements. Effort was made in a few articles to consider alternative routes between the origins and destinations with the purpose of finding vehicle trajectories. These data may be used in traffic assignment analysis as a major step in transportation planning.

In a related study, application of Bluetooth MAC re-identification as a surrogate for traditional license plate matching technique in route selection studies was assessed (Hainen, et al., 2011). The study evaluated the impacts of the closure of a bridge located

in Indiana on four alternative routes. A total of 12 Bluetooth signal scanners were installed along the four routes to collect the MAC addresses and timestamps of the passing beacons. Travel time graphs for different hours of the day were created. Temporary increases in travel times on these graphs helped in identification of congestion points. OD matrices were formed to determine network links with significant traffic volumes. Each cell in a matrix indicated the number of MAC address matchings for the signal scanners located at the beginning and end of the corresponding link. These numbers were used as the indicators of relative volumes on the links. To determine distribution of the trips on the four alternative routes, travel times of the links were combined, and the routes of interest were identified. The 25th and 75th percentile travel times were specified as the limits for filtering the outliers due to irrelevant activity stops and excessive speeds of the vehicles. The results were consistent with travel times estimated based on the links lengths and classification. It was discussed that despite some biases in Bluetooth data such as presence of vehicles carrying multiple Bluetooth enabled devices or other travel modes, the technique is much more cost effective than license plate matching for collecting the data required for trip distribution and route selection.

A method was developed by (Yildirimoglu, 2021) to simultaneously infer vehicle paths and travel times in urban networks. The study was conducted in a road network in Brisbane, Australia using 48 Bluetooth signal scanners for collecting MAC addresses and timestamps of the detected beacons. The method involved a sequential iterative map matching as well as a travel time allocation procedure. An observation score was defined to measure the likelihood of selecting alternative paths based on the number of the observed signal scanners by the vehicles and detection probability. The procedure of determining

road users' trajectories and travel times began with gathering a set of theoretical link travel times representing free flow conditions and historical data. Map matching technique was used to specify the paths consistent with theoretical link travel times and Bluetooth measurements. Travel times were also estimated for the specified paths from the observations. To determine the final travel times, convergences were checked by comparison of the differences between theoretical and path-based estimated travel times using a certain threshold. Mean absolute error and root mean square error of travel times obtained by the developed method and direct MAC re-identification technique were compared with each other. The results indicated the superiority of the developed method in different scenarios. It had more consistent outputs even when the number and distribution of the signal scanners varied significantly. It was emphasized that the method successfully overcomes the limitations of classic MAC re-identification technique when there are alternative paths and missed detections.

In a recent study, (Garrido-Valenzuela, et al., 2022) focused on incompleteness problem of Bluetooth signal detections in determination of vehicle paths. They proposed a solution to infer the path used by a vehicle when there were multiple routes between an origin and destination, even if the beacon was not detected by some of the network signal scanners in the vehicle path. First, a graph of the network and the installed signal scanners was created. Then, based on the Bluetooth data, the distribution of dwell times on each node and travel times on each link were loaded on the graph and the various traffic states during the day were characterized. To determine the probability of using each path and infer the selected one, a Bayesian inference model was applied for pairs of successive detections based on the vehicle travel time and the probable number of missed detections.

The performance of the method was assessed in Aimsun software (Aimsun, 2021) simulating 24 scenarios with different numbers and distributions of signal scanners in the network. The results indicated an accuracy of over 90% in determination of the vehicle paths in some of the scenarios. These scenarios mostly involved higher number of signal scanners in the network and consequently the locations and timestamps of the signal detections were closer in them.

2.2.2 Traffic Flow and Density

A traffic monitoring system was introduced for measuring traffic flow and density using Bluetooth signal scanners (Friesen, et al., 2014). XBee modules were used in the system for communication between the elements. The purpose was presenting a means for data collection on roads and intersections based on detection of consumer Bluetooth devices; statistically representing traffic flow and density. The experiments were conducted on a road in Winnipeg and the results were compared with the counts of a mechanical counter. Approximately 4.5% of the road traffic were counted by the Bluetooth system. This percentage was above the 2–3% statistical requirement proposed by (Herrera, et al., 2010) for accurate traffic flow estimation and may even improve as consumer Bluetooth devices spread more into vehicles. The other advantage of the system was its capability of real time display of the collected data.

A framework for calibration of parameters in traffic flow models applicable in traffic state recognition and its short-term prediction was proposed by (Allström, et al., 2014). The framework was developed using the data collected by Bluetooth signal scanners and radar detectors. The study site was a 5-km highway segment located near Stockholm. Travel time data were collected by Bluetooth signal scanners installed every 500–1000 m

along the highway. Radar detectors mounted over the highway lanes were used for collecting flow and speed data. Compass search optimization algorithm was applied to calibrate parameters defining fundamental traffic diagrams including free flow speed, critical speed and jam density as well as shockwave speeds based on radar data. A gradient-free search optimization algorithm was utilized to calibrate demand, split ratios, and end node capacities.

The data obtained from Bluetooth signal scanners and connected vehicles were fused by (Emami, et al., 2020) to predict short term flows in urban arterials. A connected vehicle is a vehicle equipped with communication devices and able to communicate with other connected vehicles in order to transfer data such as speed, position and motion. Two mid-blocks were selected in Melbourne and two Bluetooth signal scanners were installed at the upstream and downstream of each mid-block. The data collected by these signal scanners were utilized to calculate average speed. This speed was used to find the time at which the beacons passed the specified sections. Counting the number of the beacons passing these sections in each time interval, flow was calculated for the vehicles carrying Bluetooth beacons. These data were used as one source of the measurement data later in Kalman filters whereas the data obtained from connected vehicles were the second source.

The authors used two Kalman filters for predicting the flow: conventional Kalman filter and faded memory Kalman filter (Emami, et al., 2020). The latter was developed to enhance the performance of conventional Kalman filter in noisy conditions, giving more weights to the new measurements. Training data obtained in Vissim software were utilized to calibrate the filters equations for various penetration rates of Bluetooth equipped and connected vehicles. The calibrated filters were used for flow prediction based on the

available real-time measurement data. The performance of the two filters were compared. The results indicated the better performance of faded memory Kalman filter in different situations as it reduced the error rate by 60% in some cases.

2.2.3 Origin-Destination (OD)

Determination of OD matrices using MAC re-identification technique is one of the main applications of wireless signal scanning in traffic studies. This is achieved by installing wireless signal scanners at possible origins and destinations in the study area and matching MAC addresses for the origin and destination pairs.

Unlike license plate matching and driver intercept techniques in which costs increase in proportion to the duration of the study, data collection duration may be extended in MAC re-identification OD studies at a low cost if the equipment is already installed in the study area. Signal scanning equipment may be left in place during data collection. This helps in full day and night-time OD data collection as well as hour-by-hour data collection to be used in dynamic traffic assignment models (Chitturi, et al., 2014).

Traffic counts are generally samples of actual volumes (Pande & Wolshon, 2016). This is true in wireless-based traffic data collection as well. Although long and continuous data collection periods are feasible in this technique, only a percentage of the road users are detected by signal scanners due to various reasons. Some road users may not carry wireless beacons, or their beacons may be off. Moreover, Bluetooth should be in discoverable mode and Wi-Fi should be active to be detectable by Bluetooth or Wi-Fi signal scanners. Due to the incompleteness of the collected data, to find total OD volumes, sample OD matrices should be scaled up to the population. This may be done using appropriate scale (expansion) factors. It is important that the data collection time period is

selected long enough in order to collect sample sizes large enough to be the representative of the population.

A field study was conducted within a 15-mile corridor in Jacksonville, Florida for finding route-specific OD matrices (Carpenter, et al., 2012). Fourteen points along the corridor and its intersecting streets providing a clear view of the OD patterns in the study area were selected for installing the same number of signal scanners. The minimum distance between adjacent signal scanning pairs was 1 mile and the maximum distance was 5 miles. In order to filter unwanted detections from the collected data, several data cleaning measures were determined. MAC addresses detected by only one signal scanner were identified and removed. In case a beacon was detected by a signal scanner multiple times, the last detection was retained, and the other ones were removed, emphasizing that this approach is not proper for travel time measurement and causes underestimation. The maximum acceptable time difference between two detections of a MAC address in a route was considered 30 min. This duration was selected regarding the distance between the signal scanning pairs and traffic conditions. Sequential trip links were specified, and then sample route-specific OD matrices were generated.

Although admitting that scale factors should ideally be found at the time of data collection for the specific corridor, (Carpenter, et al., 2012) compared the detected volumes in the experiments with the historical average annual daily traffic of the corridor. This resulted in a scale factor of 16.29 and detection rate of 6.14%; hence, each cell in the OD matrix was multiplied by 16.29 in order to estimate the total volume for each OD pair.

An advantage of the approach developed by (Carpenter, et al., 2012) was that the detections by the signal scanners located in the middle of the routes were preserved in the

analysis in addition to the detections by the origin and destination signal scanners. The existence of parallel corridors and alternative routes reveals the importance of this type of detections.

A study on the application of Bluetooth MAC re-identification and time laps aerial photography (TLAP) techniques in OD data collection was conducted by (Chitturi, et al., 2014). The purpose was validation and comparison of the functionality of the two techniques in access-controlled networks. Data collection was done in a partial cloverleaf interchange in Madison, Wisconsin during PM peak hours. Nine Bluetooth signal scanners were used to collect Bluetooth data required for MAC re-identification. In TLAP technique, a helicopter was used for aerial photography and then, vehicles were manually tracked frame by frame for generating OD samples. The true volumes on the ramps were counted manually. The other directional volumes were determined using pneumatic tubes and radar counters. The results of the two techniques were compared with the true OD data. Although the results indicated the satisfactory performance of MAC re-identification technique, TLAP results had better fitness to the true data. This was mainly because of higher sampling rate in TLAP technique. Despite these results, it was emphasized that the cost effectiveness and feasibility of MAC re-identification technique in different conditions justifies its application in OD studies.

Uniproportional scaling and biproportional matrix balancing are two approaches for scaling up sample OD matrices to total OD matrices. The first approach is multiplying sample volumes in the matrix by a uniform scale factor equal to the inverse of the average detection rate. In the second approach, scale factors not necessarily identical are assigned to different origins and destinations. Each sample volume is multiplied by the

corresponding scale factors. The volumes are adjusted in an iterative procedure until the total number of trips from each origin and to each destination matches the total observed volume of that zone as far as possible (Chitturi, et al., 2014).

The authors examined the performance of the two aforementioned scaling approaches using Bluetooth data (Chitturi, et al., 2014). Geoff E. Havers (GEH) statistic was used for the comparison of population-scaled Bluetooth OD matrices and true OD matrices. GEH is a measure of goodness of fit in comparison of traffic flows, in which more emphasis is on large flows rather than small flows. This is more representative of the magnitude of error in comparing traffic flows than percentage of the difference between them. According to British highway agency design manual, GEH in travel demand models should be lower than 5 for at least 85% of the observations. Although uniproportional scale factors are widely used in OD estimates, the results of this study indicated the outperformance of biproportional matrix balancing. Only 33% of the movements had GEH values of less than 5 in the first approach with an average of 6.1, which was the indicator of a poor fit; whereas in the second approach, 75% of the movements had GEH values of less than 5 and their average was 3.6. Moreover, in the collected data, the PM peak hour detection rates varied between 2.3 and 7.2% for different OD pairs with an average of 4.4%. The wide range of detection rates was another reason casting doubt on the suitability of applying a uniform scale factor on OD matrices. It was emphasized that OD matrices may be estimated more reliably if the data collected on multiple similar days are combined and biproportional matrix balancing approach is used to scale them up.

2.2.4 Public Transit

In a study in Seattle by (Dunlap, et al., 2016), the authors presented a technique for the determination of origins and destinations of the passengers of public transit system using Wi-Fi and Bluetooth signals. An Android cellphone was used as the signal scanner. An application installed on the cellphone enabled it to detect nearby Wi-Fi and Bluetooth beacons. The cellphone was installed in a bus to collect data along the route. The application collected the MAC addresses and detection timestamps of the detected beacons as well as the GPS location of the cellphone.

To prepare the collected data for generating OD matrices, (Dunlap, et al., 2016) used three filtering criteria. The filters retained the signals of onboard beacons and removed invalid detections corresponding to beacons outside the bus. An onboard beacon should be detected multiple times according to the normal scanning interval which was several seconds. Hence, as the first filter, a threshold was set as the minimum required number of detections for a beacon if onboard. The threshold was selected equal to 4 for Wi-Fi and equal to 2 for Bluetooth mode. The difference between the thresholds in the two modes was because of the longer detection range in Wi-Fi mode compared with Bluetooth. The second filter removed MAC addresses with unreasonable short or long trip durations. The trip duration was calculated deducting the timestamp of the first detection of a MAC address from its last detection timestamp. The acceptable range was set between 60 and 3600 s regarding the time required for travelling between the closest bus stops and travel time between the first and last stops. MAC addresses corresponding to trip durations outside this range were identified and removed. The final filter removed invalid detections based on spatial proximity of the origins and destinations of the rides to the closest bus

stops according to the positional data provided by the GPS. A ride was retained only if the distance between its origin (or destination) and a bus stop was less than a threshold *R*. The distance *R* was set equal to 300 ft for Wi-Fi and 600 ft for Bluetooth mode. The distance was longer for Bluetooth mode to retain an adequately large sample size. The remaining detections were used as reliable data for determining passengers' origins and destinations. OD matrices were formed based on the detection timestamps of MAC addresses and GPS positional data. The results matched the available information about the popularity of the bus stops and field observations.

In another study, authors proposed an approach for filtering the data collected by Wi-Fi and Bluetooth signal scanners in order to accurately find pedestrian counts, flows, and wait times (Kurkcu & Ozbay, 2017). The data were collected in a transit terminal by a total of six Wi-Fi and Bluetooth signal scanners installed at the passenger gates and main entrances. Several filters were applied on the raw data. There were two initial filters which removed the signals corresponding to non-mobile and staff beacons as well as beacons far from the signal scanners. To remove non-mobile and staff beacons, MAC addresses detected more frequently than every 10 minutes for an average of 6 hours were removed. A certain RSSI threshold was determined to remove MAC addresses without any RSSI stronger than the threshold. This filter eliminated beacons located too far from the signal scanners. In order to count the beacons located in the detection zone of the signal scanners, it was required to filter redundant detections of beacons detected multiple times. To address this, 5-min moving blocks were created. Flows between the signal scanners were measured filtering MAC addresses with irregular travel times, considering normal walking speeds for the pedestrians.

Wait times of the individuals at the gates were also determined by (Kurkcu & Ozbay, 2017). This was done calculating the duration between the timestamps of the first and last detections of their beacons. It was noticed that this duration should be shorter than transit headways. Calculated wait times were assigned to different hours of the day according to the first detection moments of the beacons. Comparison of the results with the manually collected data confirmed the accuracy of the proposed approach in estimation of the mentioned parameters as the achieved accuracies were near 90%. It was emphasized that getting accurate volumes are possible provided that the penetration rates of the discoverable devices among the population is known. Having this information, the real volumes may be found multiplying the sample volumes by the proper scale factors calculated based on the penetration rates.

A MAC re-identification technique for determination of spatio-temporal trajectories of passengers in urban rail transit systems using Wi-Fi signals was developed by (Gu, et al., 2021). The data were obtained from a Wi-Fi network installed in Shanghai rail transit stations, platforms and trains and involved the MAC addresses and detection timestamps of the detected beacons present in the transit system. These data were not solely sufficient for determination of the passengers' trajectories due to the incompleteness of the detections in the required time sequences. To overcome the incompleteness problem of the data and provide the possibility of inferring the locations of the missing data, an algorithm was developed to generate the possible spatio-temporal data sets of the passengers. The algorithm considered the Wi-Fi data, train schedules, topology of the transit network and passenger walking times. To determine the next locations in the mobility sequences, an algorithm based on n-gram model was used. N-gram is a probabilistic model, normally

used for predicting the next item in a sequence. The developed technique was able to provide detailed information about the individual passengers' trips such as origins, destinations, selected routes, selected trains and waiting times on the platforms. The accuracy of the technique in determination of the passengers' routes in a four-day data collection period was 93%.

2.2.5 Travel mode

Raw wireless data do not directly provide any information about road users' travel modes. Existence of different modes of travel along the roadways may produce outliers in wireless data which increase the inaccuracies of the estimated parameters (Yang & Wu, 2018). This is not an issue in freeways as the presence of non-motorized modes on them is rare and if present, their speeds are generally quite different from motor vehicles. By contrast, presence of different travel modes on arterials may be considered a problem in travel time calculation; hence, it is required to develop models for classification of beacons according to the mode of transportation.

This problem was analyzed by (Namaki Araghi, et al., 2016). They presented a technique to distinguish between motor vehicles and bicycles prior to travel time calculation using Bluetooth signals. The purpose was reducing the inaccuracies of vehicle travel time measurement in urban arterials due to the presence of different modes of travel. The proposed technique was probabilistic, *i.e.*, the output was the most probable travel mode for a certain beacon carrier.

Different criteria were used by (Namaki Araghi, et al., 2016) to classify travel modes, *e.g.*, [*i*] travel time-based filtering in which an array of the last *n* travel time observations by the signal scanners was created. Each measured travel time was then controlled to be in

the range; [*ii*] class of device (COD) filtering in which the beacons were filtered based on their MAC addresses. COD may be extracted from the beacon MAC address and involves information about the beacon type and class, *e.g.*, mobile phones, headsets, and in-vehicle navigation systems. For instance, if an in-vehicle navigator was detected, it was concluded that it belonged to a motor vehicle, since this type of beacons is almost exclusively utilized in motor vehicles.

They proceeded to use the filtered MAC addresses belonging to motor vehicles to estimate travel times on a bridge in Aalborg, Denmark (Namaki Araghi, et al., 2016). Comparison of the results of the proposed technique and travel times obtained from automated license plate recognition approach using video recordings as the true data indicated similar levels of accuracy. Mean absolute percentage error in their proposed technique was 18% versus 17% in license plate recognition approach. It was emphasized that determination of the criteria for travel mode classification should be dynamic, taking into consideration traffic conditions rather than static.

Similarly, a technique was proposed for determination of different transportation modes using the data collected by Bluetooth signal scanners and applying clustering algorithms (Bathaee, et al., 2018). The reason for using clustering algorithms was their capability in grouping the data. The main experiment was conducted in a road segment containing a four-legged signalized intersection located in Corvallis, Oregon. Time stamped MAC addresses were collected by eight signal scanners installed in the study area. The technique performed based on a parameter defined as the total time a Bluetooth beacon spent in the detection zone of the entire system including all the signal scanners (d_k). This was equal to the difference between the earliest and latest timestamps corresponding to a

certain MAC address in the system. Three clustering algorithms including fuzzy C-means, K-means, and partitioning around medoids were examined for classification of road users. Applying either of the three algorithms on d_k values, transportation modes of the road users were determined by a simple majority vote rule based on to the data collected by each of the signal scanners. The results were checked reviewing the videos recorded by three cameras installed in the study area and visually counting the road users in each mode during the study period. The three algorithms performed well and differentiated the transportation modes with a high accuracy. It was mentioned that closer travel speeds in dense urban environments make the classification procedure more challenging.

In a study in Tucson, Arizona, (Yang & Wu, 2018) developed a mathematical model for travel mode identification using Bluetooth signals. The experiments were conducted in an arterial involving four links and three intersections. One Bluetooth signal scanner was installed at each intersection to collect signals. The model was based on genetic algorithm and a neural network structure called single hidden-layer feed-forward neural network (SHLFFNN). N-fold class validation was applied for statistical assessment of the results. Travel modes were classified into three categories including autos, bicycles, and pedestrians. Speed and travel time of the road users were used as the model inputs and traffic performance measures in travel mode recognition. GPS-enabled devices were used to collect true travel time and speed data for comparison. The results of the experiments indicated the capability of the model in travel mode identification with a low error rate. The model misidentified 6.1% of autos as bicycles and 10.5% of bicycles as autos. Pedestrians were identified correctly with a misidentification rate of zero.

In recent work, authors proposed a technique to estimate the number of pedestrians /bicycles in mixed traffic environments based on BLE signals (Gong & Abdel-Aty, 2021). BLE mode was used because of its high sample detection rate and short but adequate detection range covering the whole intersection area. Eight BLE signal scanners were installed at eight signalized intersections in Orlando, Florida. A two-step framework was developed to distinguish pedestrians/bicycles from permanently present beacons and motorized travel modes. The first step was filtering permanently present beacons, *e.g.*, beacons installed in the area or beacons belonging to police officers. This was done setting a maximum threshold for the difference between the timestamps of the last and first detections of the beacons. For filtering motorized travel modes, it was avoided to use a preset threshold as the minimum speed of these road users, because in congested roadways vehicle speeds are close to pedestrians/bicyclists' speeds. Instead, in the second step, a one-class support vector machine algorithm was used to classify different modes of travel. Historical local samples labeled as motorized were used to train the algorithm. Removing motorized modes from the data sets, the remaining were pedestrians or bicyclists. Comparison of the results with the manual counts of the recorded videos indicated the functionality of the technique as the average absolute error percentage was 6.35%.

2.2.6 Safety Studies

Several researchers have tried to use the data collected by wireless signal scanners in real-time safety analysis. The technology may be applied in design of danger alert systems and for detection of anomalies/incidents along the roadways based on the variations of traffic parameters. Incident detection rate, false alarm rate and mean detection time are three common measures for evaluating the performance of incident detection algorithms.

A powerful algorithm results in high incident detection rates, low false alarm rates and low mean detection times (Yu, et al., 2015).

An automated algorithm for incident detection in arterials by Bluetooth signal scanners was proposed by (Yu, et al., 2015). The algorithm was based on travel time and volume data obtained by a MAC re-identification system as well as a time moving average approach with the capability of recognizing travel time and volume data patterns caused by incidents. Five Bluetooth signal scanners installed approximately 1.6 km apart on a highway in Tigard, Oregon were used for data collection during a 2-month period of time. The signal scanners collected MAC addresses and timestamps of the passing beacons. The detected beacons were estimated to cover approximately 6% of the passing vehicles.

(Yu, et al., 2015) began processing the data filtering outlier travel times. The mean and standard deviation of travel times were dynamically calculated. Mean plus/minus a coefficient of the standard deviation of travel times were set as thresholds, and travel times outside the range were filtered. Ten-period moving averages in which the duration of each period was one minute were calculated for the mean travel time and volume. Indicators were specified for triggering the situations with the probability of incident occurrence. An index was defined to specify the time length the indicators were required to be observed before announcing the occurrence of an incident. The performance was assessed comparing the detections with the reported incident data. The algorithm had the capability to distinguish between normal recurring congestions and congestions due to incidents. The results indicated a detection rate of almost 100% and the number of false alarms was sufficiently low, proving proper functionality of the algorithm.

In a study conducted in Orlando, Florida, (Yuan, et al., 2018) investigated the relationship between incident occurrence on urban arterials and real time characteristics of traffic streams, signal timing as well as weather conditions. The study was conducted in four urban arterials containing 23 intersections. The average distance between the adjacent intersections was approximately 700 m. A total of 23 Bluetooth signal scanners installed at the 23 intersections of the study area were used to collect travel time and space mean speed data. To remove the data highly affected by intersection signal delays, vehicle-level speeds were cleaned using a filtering algorithm. The algorithm removed the data located outside the 75% of the interquartile range of the 15 previous samples on the arterial segment. Traffic volumes and signal timings were obtained from adaptive signal controllers. Weather data were also collected from the nearest weather station. The data were extracted in a 20-min time period divided into four 5-min intervals before the incident occurrence moment. Combining all the collected data, Bayesian conditional logistic models were created to find the parameters with significant impacts on occurrence of incidents. According to the results, average speed, downstream green ratio, upstream left-turn volume, and rain were significant causes of incidents.

An Automated incident detection method for freeways using Bluetooth data was proposed by (Mercader & Haddad, 2020). The method was developed applying isolation forest technique as an unsupervised anomaly detection approach which did not require incident, occupancy, or density information. A set of parameters including time, speed and relative speed variations measured by Bluetooth signal scanners were used as the input data for isolation forest technique. The method worked based on the fact that anomalies are scarce and distinct; hence, input parameters corresponding to these traffic conditions are

distinguishable from normal condition parameters. As anomalies are easier to isolate in comparison with normal instances, anomaly scores were defined considering the isolation level. A historical based threshold for anomaly situations was set and real-time data were isolated to generate anomaly scores. Anomalous situations were determined comparing the anomaly scores with the set threshold. A caveat of the developed method was that it was not able to recognize the mechanisms resulting in anomalous situations, *e.g.*, maintenance operations or occurrence of collisions.

(Raeve, et al., 2020) proposed a technique for blind spot detection based on RSSI values of BLE signals. The purpose was notifying pedestrians and drivers of the possible blind spot accidents. Five BLE signal scanners were installed on three sides of a truck. Two filters were used for cleaning and smoothing the data. First, a threshold was set for the RSSI values in order to filter outliers due to shadowing and fading. RSSIs lower than the threshold were replaced by the set threshold value. A weighted average filter with a sliding window was applied then to smooth the RSSI values. The buffer size and weights of the algorithm were optimized performing several simulations. Being at a distance less than 8 m to the truck was specified as the measure for vulnerability of the pedestrians. The RSSI value corresponding to this distance was considered equal to −70 dBm. The system alerted both the driver and pedestrian if a signal with the RSSI value of higher than −70 dBm as a sign for a potential danger was detected. The results indicated that the system performed well and with a high reliability.

2.2.7 MAC Randomization

As MAC addresses are identifiable by certain devices such as wireless signal scanners, the MAC owners are vulnerable to some privacy breaches, like being trackable,

which are the reason of some concerns (Cunche, 2014). MAC address randomization is a technique in which the MAC address is changed by the network hardware randomly and periodically to temporary addresses different from the true address in order to be anonymous (Martin, et al., 2017).

In MAC re-identification technique, it is required to detect identical MAC addresses by different signal scanners installed at different locations of the study area. This is prevented if MAC address randomization is implemented by a beacon. Therefore, implementation of MAC randomization by smart devices may reduce the number of MAC matchings of signal scanners. This results in longer time periods required to collect adequate sample data for traffic analysis. MAC address randomization is currently implemented by some major mobile phone manufacturers mostly in Wi-Fi mode. A few studies tried to demonstrate the vulnerability of this technique in contrary to its implementation by these manufacturers.

Several algorithms for tracking mobile devices which implement Wi-Fi MAC randomization was presented by (Vanhoef, et al., 2016), claiming that these algorithms can track 50% of mobile devices for more than 20 min. It was shown that tagged parameters in probe requests may be used for device identification and true MAC addresses may be leaked by Wi-Fi protected setup element. Two techniques which could reveal the true MAC addresses even if MAC randomization had been implemented were presented. In the first technique, fake hotspots were created inducing beacons to connect using their true MAC addresses. The second technique was based on 802.11u standard and that Windows and Linux use true MAC addresses to send access network query protocol requests. It was

concluded that none of MAC randomization implementations are solely adequate and successful in providing users' privacy.

Different MAC randomization algorithms applied by manufacturers for various models and operating systems were probed and their effectiveness was evaluated by (Martin, et al., 2017). Several flaws in these algorithms were identified that could be used to defeat the implemented randomization. It was shown that beacons commonly send wireless frames with true MAC addresses even when they are supposed to implement MAC randomization.

The authors, (Martin, et al., 2017), also extended the identification techniques developed by (Vanhoef, et al., 2016). This resulted in defeat of MAC randomization implemented by Android cellphones in 96% of the cases. Moreover, they identified a serious flaw in handling of low-level control frames by wireless chipsets that allowed active attacks to track any wireless device. They proposed using a universal randomization policy for all 802.11 devices, because implementation of exclusive MAC address randomization algorithms by different manufacturers makes tracking of beacons simpler.

2.3 Summary

The previous research relevant to the objectives of the thesis were reviewed in this chapter. The chapter was broadly divided into two parts. In the first part, RSSI, TOA, TDOA and AOA as the attributes of wireless signals with the potential to be used in wireless signal positioning were overviewed. As the techniques proposed in this thesis will be developed based on signal strengths, the focus was mostly on RSSI attribute of the signals. The relationship between RSSI and distance is a foundation for RSSI-based positioning; Hence, several models developed for the relationship between these two

parameters were presented. The previous studies on wireless signal positioning and the progress made in this area were also covered in the first part of this chapter.

In the second part, the studies on the applications of wireless signal scanning in the field of transportation were reviewed. These studies were classified into six major categories: [*i*] travel time and speed measurement, [*ii*] traffic flow and density, [*iii*] origin-destination, [*iv*] travel mode, [*v*] public transit, and [*vi*] safety applications. The first category had two subcategories due to the extent of the relevant studies: [*i*] outlier removal from travel time data and, [*ii*] travel time in alternative routes and vehicle trajectories. These are two important subjects, necessary for enhancing the quality and accuracy of travel time and speed measurements. MAC address randomization as a technique implemented to mitigate the privacy concerns due to detection of MAC addresses and the effort made to demonstrate the breaches of the technique was also overviewed in this chapter.

Chapter 3: Investigating Wi-Fi, Bluetooth, and Bluetooth Low Energy Signal Characteristics for Positioning in Traffic Studies

3.1 Introduction

Using wireless technology for finding microscopic traffic parameters or its successful application in safety systems requires positional information of the beacons. Having an accurate estimate of position is a significant step toward improving the accuracy of traffic data that will open the door to more advanced applications. Thus, an area of significant practical value is to specify the position of the detected beacons. Wi-Fi, Bluetooth Classic (Bluetooth), and BLE are three widespread signal modes, transmitted by popular beacons used in daily life. The strength of the three signal modes received by signal scanners is measured by RSSI. RSSI values have the potential to be used in determining the position of beacons, as the strength of signals normally decreases along with the distance between the beacon and signal scanner. Despite this potential, positioning based on RSSI values generally comes with inaccuracies and many practical complications. This is because RSSI values normally have fluctuations and include outliers.

RSSI is the common metric for measuring signal strength in the three aforementioned wireless signal modes; therefore, all of them may be utilized in traffic studies which need positional data of road users. While positioning methods may be developed for the three signal modes, the question which arises is which signal mode leads to better quality and accuracy as well as more convenience of data collection in traffic studies. To address this, it is necessary to investigate the important factors which may affect the mentioned measures. These factors should be selected considering the characteristics of traffic systems. They should be investigated in an outdoor environment and the general nature of

traffic streams needs to be considered. Concerning these characteristics, five factors including [*i*] RSSI-distance relationship, [*ii*] precipitation effects on the signals, [*iii*] motion effects, [*iv*] non-line of sight effects, and [*v*] signal transmission rates were identified for evaluation. These factors are important in comparing the suitability of the three signal modes for traffic studies in which accurate positional data of road users are required.

3.2 Research Equipment

This research was conducted using wireless signal scanners, manufactured by SMATS Traffic Solutions Inc., and typically used for traffic data collection. The devices functioned in three scanning modes. They could scan the three signal modes in their surrounding area using three separate signal detectors (Figure 3.1). The three scanning modes were Wi-Fi (IEEE 802.11 b/g/n, receiver sensitivity: −92 dBm, transmission power: +18 dBm), Bluetooth (Class 1, receiver sensitivity: −90 dBm, transmission power: +18 dBm), and BLE (receiver sensitivity: −96 dBm, transmission power: +4 dBm). The antennas installed on the signal detectors were long-range, omnidirectional, 2.4 GHz and 2 dBi gain. Figure 3.2 illustrates the block diagram of the signal scanners. There was also a software platform for setting the adjustable parameters and monitoring the collected data including MAC address, signal mode, detection timestamp, and RSSI. The set parameters for each of the three signal modes in the software platform may be observed in Figure 3.3. The beacon in Wi-Fi and Bluetooth modes was an Android operated cell phone and the BLE beacon was a BLE 4.0/4.1 signal transmitter.

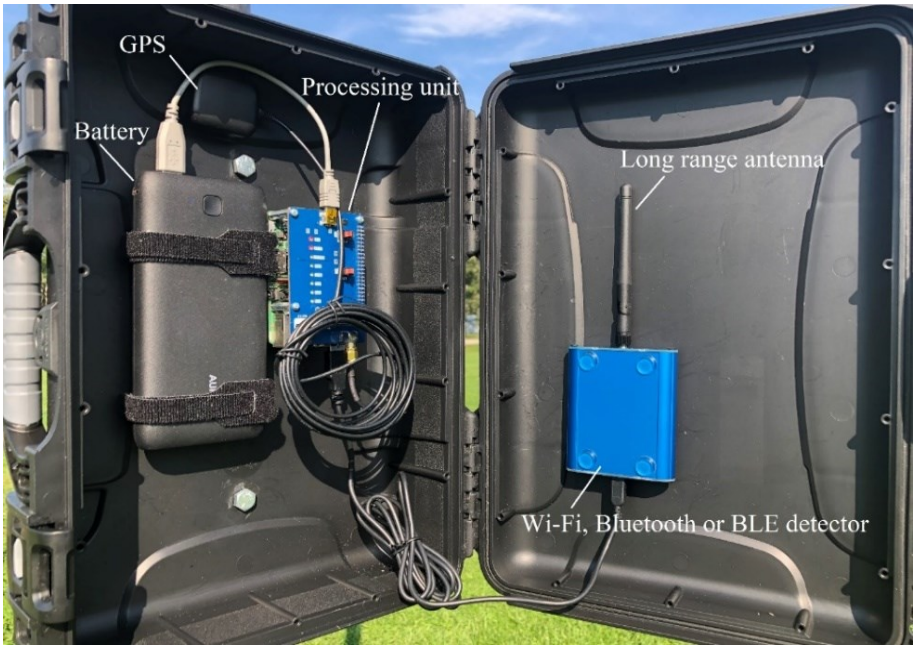

Figure 3.1 A wireless signal scanner, used in the research and its internal components.

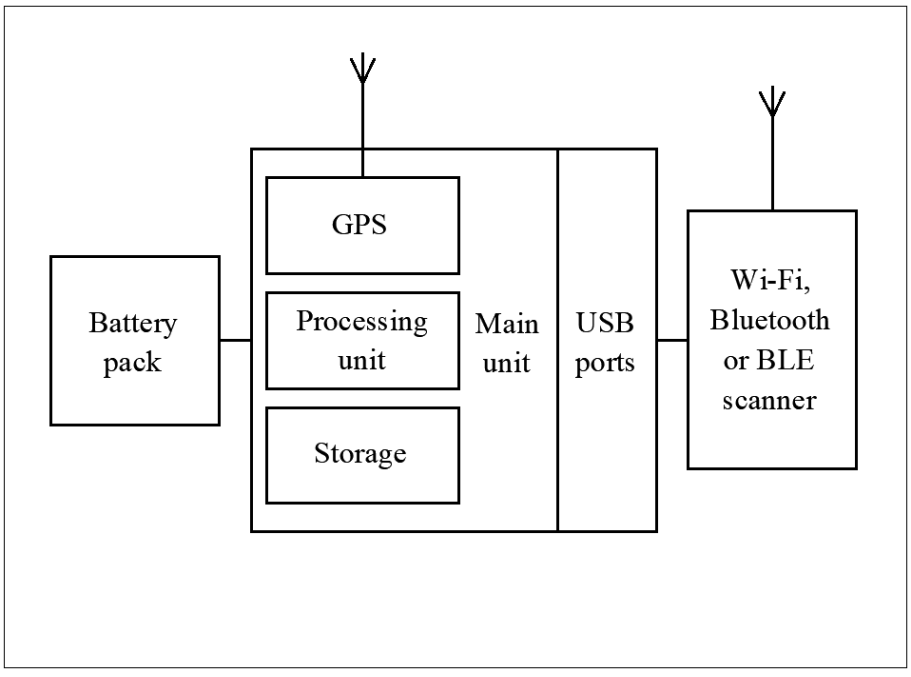

Figure 3.2 Block diagram of the wireless signal scanners.

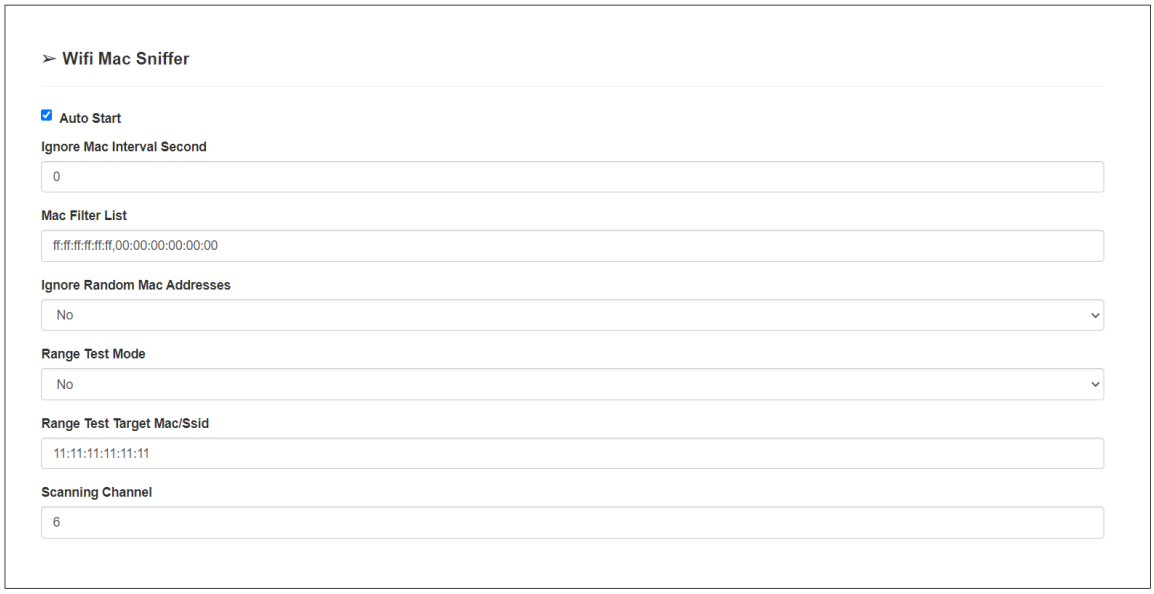

(a)

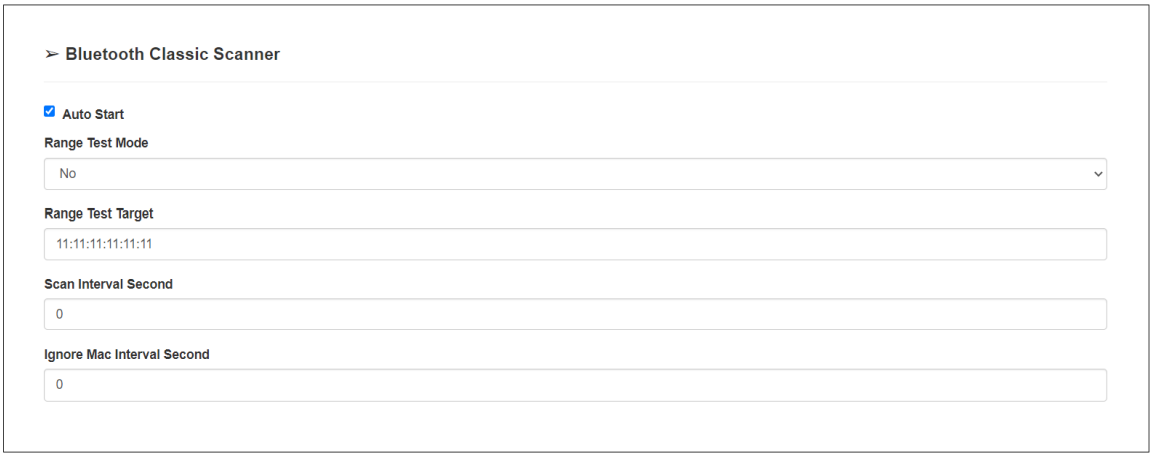

(b)

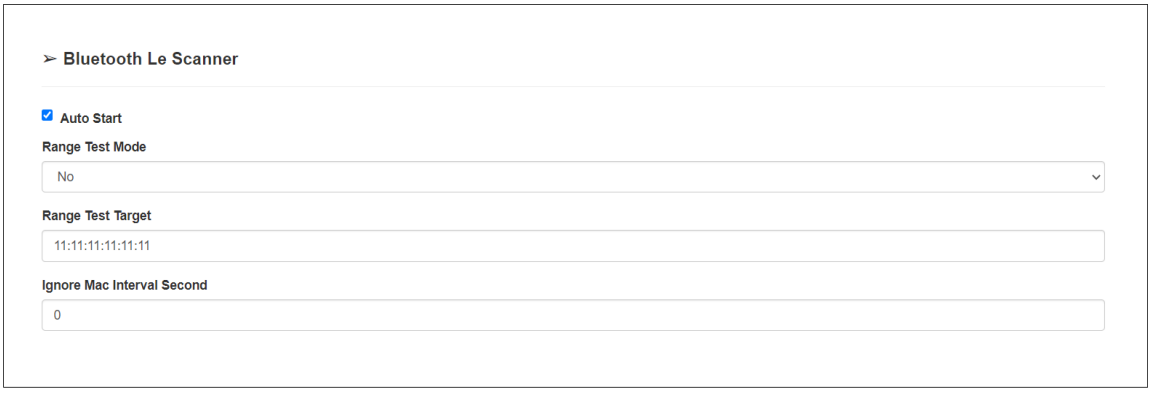

(c)

Figure 3.3 Set parameters in the software platform of the signal scanners in (a) Wi-Fi; (b) Bluetooth; (c) BLE mode.

3.3 Experiments Locations

The five experiments designed for evaluating the five aforementioned factors were conducted in four outdoor sites located in Ottawa, Canada (Figure 3.4): (a) Rideau Canal bike road, a path used by bikes and pedestrians located several meters away from Colonel By Drive near Carleton University campus, both with moderate traffic flows (Site 1), (b) a residential street with a low traffic flow (Site 2), (c) Hunt Club-Riverside Park soccer field next to Paul Anka Drive with a moderate traffic flow (Site 3), and (d) a public parking area next to a high-rise building in which there were a few vehicles on the experiment day (Site 4). As mentioned, the locations were not isolated; there were other beacons in the areas and some activities taking place in the vicinity.

Figure 3.4 Experiments locations: (a) Site 1; (b) Site 2; (c) Site 3; and (d) Site 4.

3.4 Study Method

This chapter investigates the suitability of the three mentioned signal modes considering the characteristics of traffic studies. Effort is made to provide a database enabling traffic practitioners to select the most proper signal mode for different types of traffic applications in which positional data of road users are required. The comparison between the three modes of wireless signals is in the form of five field experiments, described in the next sections. Each experiment was conducted in the three modes separately. The location, weather and environmental conditions were approximately similar for each experiment. As an example of how to use the results of the experiments, the special case of the application of wireless signal scanning in vehicle-pedestrian collision warning systems will be examined at the end of the chapter and the most suitable signal mode for integration in these systems will be determined. The results of this chapter will also be used for selecting the most proper signal modes for development of a wireless signal positioning technique and development of a technique for intersection turning movement classification in Chapters 4 and 5 respectively.

3.4.1 Experiment 1: The Relationship between RSSI and Distance

The distances between a beacon and the signal scanners are important for finding the position of the beacon. RSSI is a parameter obtained in signal scanning which may be used for finding the distance between a beacon and a signal scanner and therefore has the potential to be used in beacon positioning. Hence, a robust relationship between RSSI and distance will lead to more accurate positioning results.

In order to investigate the quality of the relationship between RSSI and distance, a signal scanner was installed on a lighting pole at the height of 1 m and 12 stations were

specified on the ground on a longitudinal path (Site 1). The distance between the first station and the signal scanner was 1 m; this distance was 3 m for the second station, 10 m for the third station and after that the distance between each two stations increased to 10 m. The distance between the last station and the signal scanner was considered equal to 100 m (Figure 3.5a). The beacon was held stationary at each station at the height of 1 m for 1 min, beginning from the nearest station and then was carried to the next stations. The signals transmitted by the beacon from each station were recorded by the signal scanner.

To determine the relationship, the corresponding RSSI-distance chart was created, and its best fit curve was drawn. RSSI values usually involve some fluctuations and outliers which pollute the data. In order to specify the closeness of the data to the fit curve, R-squared value of the fit curve was specified. In addition to the RSSI-distance curve and R-squared value, in order to determine the dispersion of the data at each distance, five stations were selected (3, 10, 40, 70, and 100 m from the signal scanner) and the variance of the RSSI values was calculated for each of them.

3.4.2 Experiment 2: Precipitation Effects

Traffic data collection is generally conducted outdoors; hence, it is important to investigate how variations in weather conditions may impact the quality of signal detection. Rainfall as a probable adverse event during traffic data collection was selected for investigating the effects of weather changes on the data. In order to check if rainfall can have significant impacts on the signals, an experiment was conducted in Site 2.

A beacon was placed at a distance of 20 m from a signal scanner (both at the height of 1 m) on a day for which a moderate rainfall had been forecast and signals were continuously collected (Figure 3.5b).

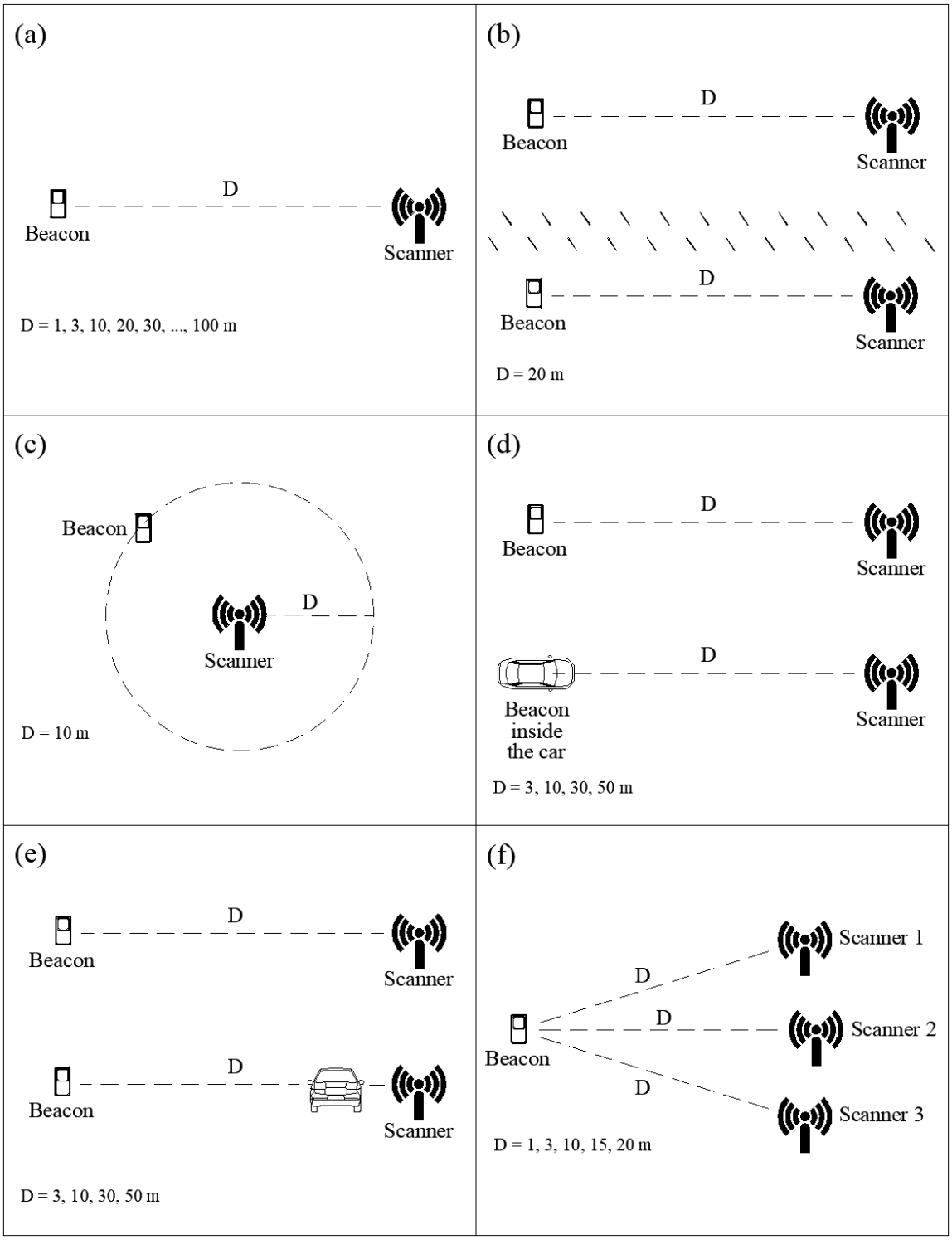

Figure 3.5 Signal scanners and beacon arrangement in (a) Experiment 1; (b) Experiment 2; (c) Experiment 3; (d) Experiment 4-1; (e) Experiment 4-2; (f) Experiment 5.

The moment at which rainfall started was recorded and the signals collected from 15 min before the rainfall to the beginning of it, and the signals collected from the beginning of the rainfall to 15 min after it were separated and compared. In order to compare these two sets of data, the number of the detections, average RSSI values and their variances were considered.

3.4.3 Experiment 3: Effects of Beacon Motion

According to the fact that in general, both signal detection and positioning in traffic studies should be done for moving beacons, investigating the impacts of motion on the quality of signals is important. These impacts were investigated in an experiment conducted on a circular path to keep the other factors, especially the distance between the beacon and the signal scanner constant. A circle with a radius of 10 m was drawn on the ground in Site 3. The signal scanner was placed on the center of the circle at the height of 1 m from the ground. A research assistant carried the beacon at the height of 1 m on the circle perimeter, running at a speed of approximately 10 km/h for two minutes and the transmitted signals were collected by the signal scanner (Figure 3.5c). Then, the beacon was held stationary on a point on the circle perimeter by the research assistant for two more minutes and the data were collected in this position too. The data collected from the moving beacon and the stationary beacon were compared with each other considering the number of the detections, average RSSI values and their variances.

3.4.4 Experiment 4: Non-Line of Sight Effects

In traffic systems, signals are transmitted by beacons belonging to road users in different situations. They may be riding bikes or be the occupants of vehicles; the beacon may be in a pedestrian’s pocket or may be in his/her hand. Existence of obstacles between

a beacon and a signal scanner causes the signals to travel through non-line of sight paths, which may have some impacts on the signals. Therefore, investigating the impacts of existence of obstacles in transmission path on the signals is necessary. Although this may require extensive research and lots of experiments to be thoroughly studied, the impacts of auto glass and vehicle blockage as two examples of the situations causing non-line of sight in traffic systems were investigated in the form of two tests. Each test had two stages. The first stages were conducted in free path or line of sight (LOS), and the second stages were conducted in non-line of sight (NLOS) conditions.

In the first test, a signal scanner was installed on a pole beside a residential street (Site 2) at the height of 1 m and four stations were specified on the ground along the street. The distances between the stations and the signal scanner were 3, 10, 30 and 50 m. The signals transmitted by the beacon from each station were collected in the two stages to examine LOS and NLOS paths. In the first stage in which the path was free, a research assistant stood on each of the stations and held the beacon in his hand at the height of 1 m. In the second stage, the beacon was placed on top of the dashboard in a car with closed windows while stopping on each of the stations to examine NLOS situations (Figure 3.5d). The duration of data collection on each station in each stage was five minutes. For comparison of the data collected from each station, the number of the detections, average RSSI values and their variances in the two situations were considered.

The second test was conducted in a public parking area (Site 4). The first stage of this test was similar to the first stage of the first test. However, in the second stage, the signal transmission path was blocked by a vehicle (Figure 3.5e). In this stage, the beacon was held stationary at each of the four stations by a research assistant for five minutes while

there was a stationary vehicle between the beacon and the signal scanner. The distance between the vehicle and the signal scanner was considered equal to 1 m.

3.4.5 Experiment 5: Signal Transmission Rates

In wireless signal positioning, it is necessary to have signals detected simultaneously by multiple signal scanners in order to determine the position of a moving beacon at a certain moment. Therefore, the higher probability of having such detections increases the chance to have proper signals for positioning.

To investigate signal transmission rates and the opportunity to have simultaneous detections, an experiment was conducted in Site 1 using three signal scanners equipped with the same type of signal detectors. Three signal scanners were used because this is the minimum number of observations required for positioning in trilateration. This is also an acceptable number of signal scanners in radio map technique, developed in the next chapter. The three signal scanners were placed at the height of 1 m above the ground beside each other on a circular sector. Five stations at 1, 3, 10, 15, and 20 m from the signal scanners were specified on the ground. Each station had the same distance from all the three signal scanners (Figure 3.5f). The beacon was placed in a stationary mode at each station at the height of 1 m for 30 min, so that the total experiment duration was 150 min. The signals transmitted by the beacon were recorded by the three signal scanners in order to specify the moments at which the three of them had detected a signal (matching moments). Because of the large number of detections, a MATLAB code was written for finding these moments and the number of them. A time difference of less than 1000 milliseconds, equal to one second was considered as the measure for being simultaneous in the code. The probability of having simultaneous detections by three signal scanners is

equal to the number of matching moments divided by the average number of total detections by a signal scanner during the experiment.

3.5 Results

3.5.1 Experiment 1: The Relationship between RSSI and Distance

RSSI-distance charts and their best fit curves in the three studied modes may be observed in Figure 3.6. It is evident that there is a logarithmic relationship between RSSI values and the distance from the beacon to the signal scanner which is true for the RSSI-distance charts of the three studied modes. In these charts, as the distance increases, the curve slope decreases. The curves have their highest slopes in short distances and then the slopes gradually go to near zero.

The typical equation for the fit curves of the RSSI-distance charts is:

$$RSSI = -\mathrm{a}\ln D - \mathrm{b} \qquad (3.1)$$

where:

RSSI is received signal strength indicator in dBm;

D is the distance from beacon to signal scanner in m;

a and b are positive coefficients;

and the charts for estimating the distance based on RSSI have exponential fit according to the following equation:

$$D = \mathrm{i}e^{-\mathrm{j}(RSSI)} \qquad (3.2)$$

in which:

$$\mathrm{i} = e^{\left(-\frac{\mathrm{b}}{\mathrm{a}}\right)},\ \mathrm{j} = \frac{1}{\mathrm{a}}$$

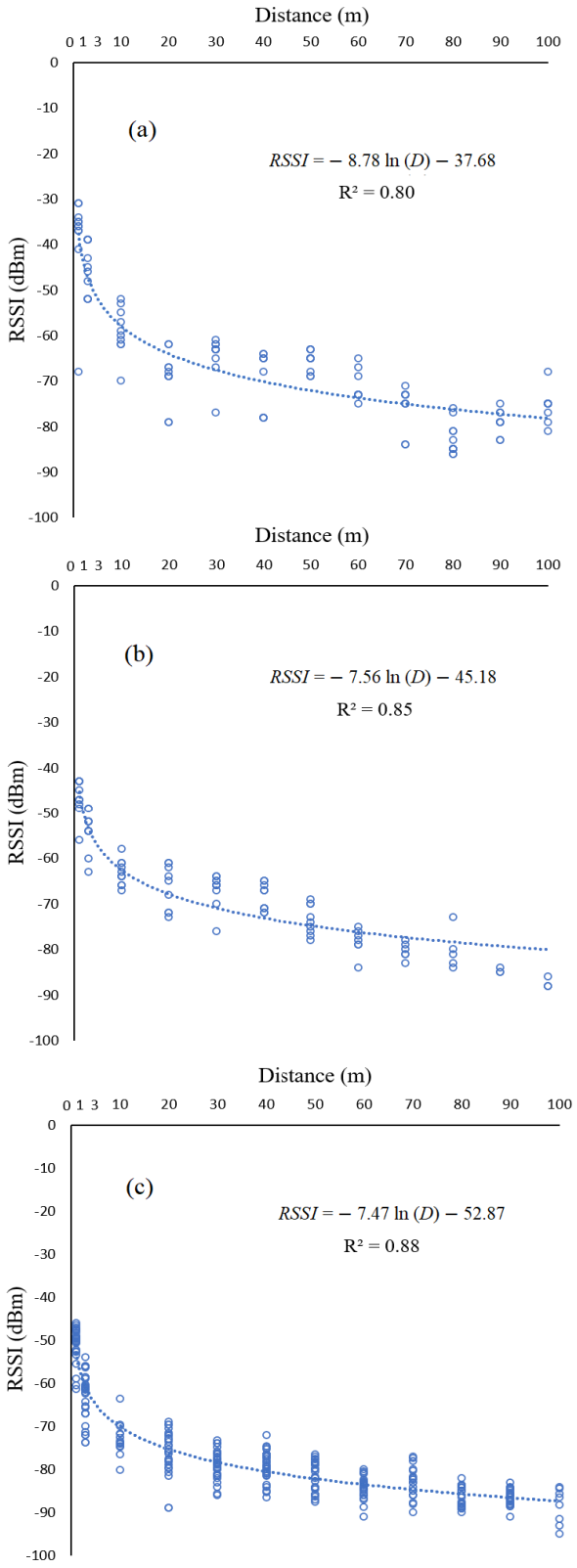

Figure 3.6 RSSI-distance curves for (a) Wi-Fi mode; (b) Bluetooth mode; (c) BLE mode.

According to Figure 3.6, it is observed that R-squared values for Wi-Fi, Bluetooth and BLE equations are 0.80, 0.85 and 0.88 respectively in the conducted experiments. Comparison of these values indicates that in BLE mode, R-squared value is higher than Bluetooth and Wi-Fi modes and its curve is better fit to the data. This value for Wi-Fi mode is the least compared with the other two modes.

The variances of the RSSI values, as another measure for the quality of the signal reception for five stations of the experiments, may be observed in Table 3.1. The histogram of these variances is also provided in Figure 3.7a for better illustration. It is observed that although R-squared value of the BLE curve was the highest among the three modes, RSSI variances generally have their lowest values in Bluetooth mode. The variances are the highest in Wi-Fi mode in most cases.

Repeating the experiments for beacons produced by different manufacturers and in different environments, it was observed that although RSSI-distance curves always follow a logarithmic trend and the findings about ranking of R-squared values and variances are generally true among the three modes, there are some variations in RSSI magnitudes. The manufacturers of network modules are identifiable in MAC addresses (Gupta, 2016), therefore, in order to have more reliable reference data in practice, it is recommended to calibrate the models for different manufacturers and environments.

Table 3.1 Variances of RSSI values.

	Wi-Fi		Bluetooth		BLE	
Distance (m)	Number of detections	RSSI variance $(dBm)^2$	Number of detections	RSSI variance $(dBm)^2$	Number of detections	RSSI variance $(dBm)^2$
3	10	29.6	10	19.9	30	32.0
10	10	27.7	11	7.0	28	15.1
40	9	42.5	10	8.7	31	16.3
70	10	21.2	6	3.1	24	12.9
100	9	12.8	3	1.1	8	17.1

3.5.2 Experiment 2: Precipitation Effects

The results of the experiments conducted to investigate the impacts of precipitation on the signals may be observed in Table 3.2 and Figure 3.7b. The table compares the number of detections, average RSSI values and their variances before and during the rainfall in each mode. Figure 3.7b involves the histogram of the RSSI variances. As observed, none of the parameters were considerably affected by rainfall during a continuous data collection in the three modes. Hence, rainfall does not appear to impact the positioning results given that data are collected without changing other factors.

Table 3.2 Rainfall effects on the signals.

		Number of detections			Average RSSI (dBm) at D = 20 m			RSSI variance $(dBm)^2$ at D = 20 m		
Mode	Rainfall rate (mm/hr)	Total	Cloudy weather	Rainfall	Total	Cloudy weather	Rainfall	Total	Cloudy weather	Rainfall
Wi-Fi	0.5	323	163	160	-59.6	-59.7	-59.5	26.2	25.9	26.6
Bluetooth	0.7	337	171	166	-70.7	-70.5	-70.9	9.7	9.2	10.2
BLE	1.2	873	439	434	-64.6	-64.2	-65.0	11.1	11.8	10.0

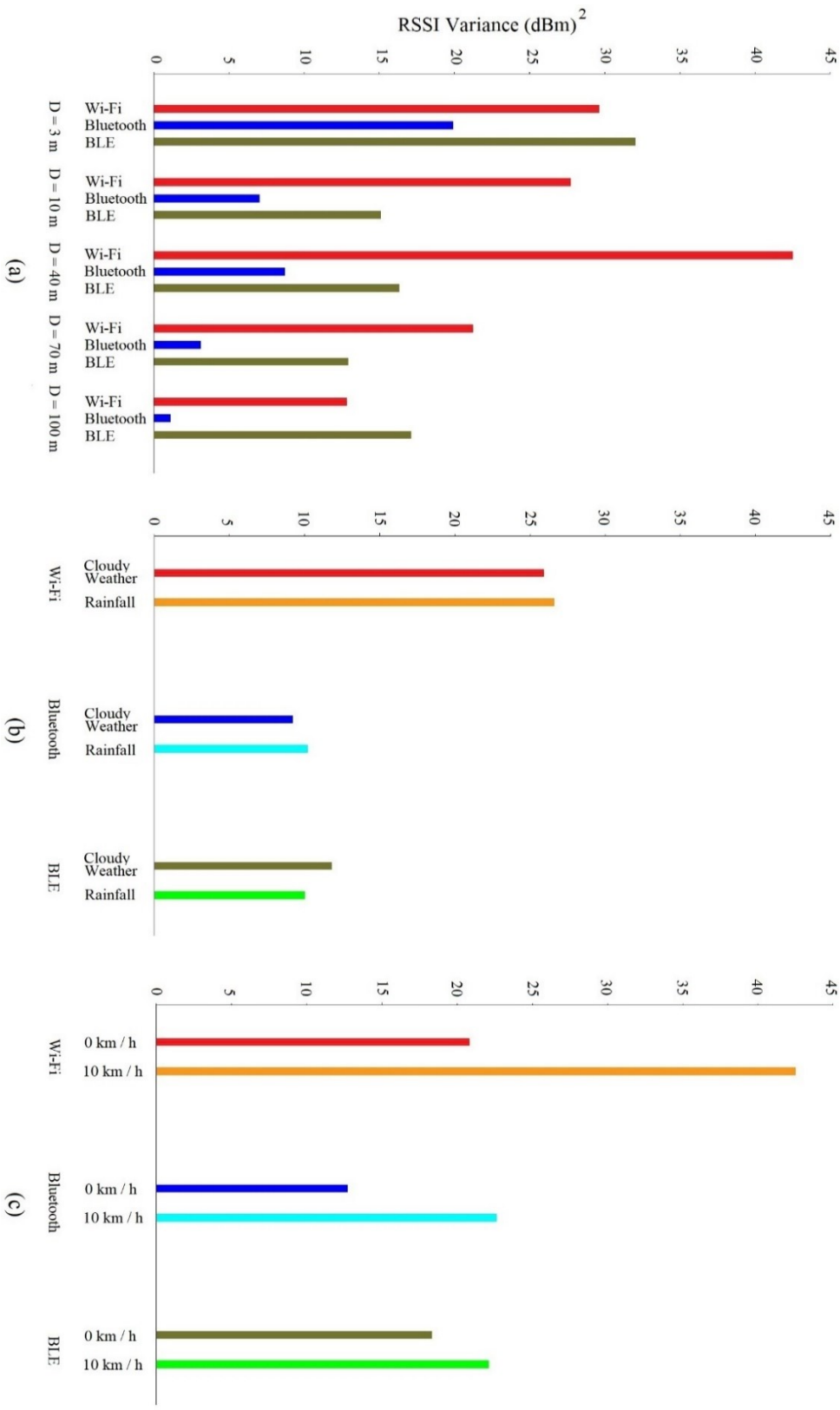
RSSI Variance (dBm)^2
0
5
10
15
20
25
30
35
40
45
(a)
D = 3 m
Wi-Fi
Bluetooth
BLE
D = 10 m
Wi-Fi
Bluetooth
BLE
D = 40 m
Wi-Fi
Bluetooth
BLE
D = 70 m
Wi-Fi
Bluetooth
BLE
D = 100 m
Wi-Fi
Bluetooth
BLE
(b)
Wi-Fi
Cloudy Weather
Rainfall
Bluetooth
Cloudy Weather
Rainfall
BLE
Cloudy Weather
Rainfall
(c)
Wi-Fi
0 km / h
10 km / h
Bluetooth
0 km / h
10 km / h
BLE
0 km / h
10 km / h

(Continued)

(Continued)

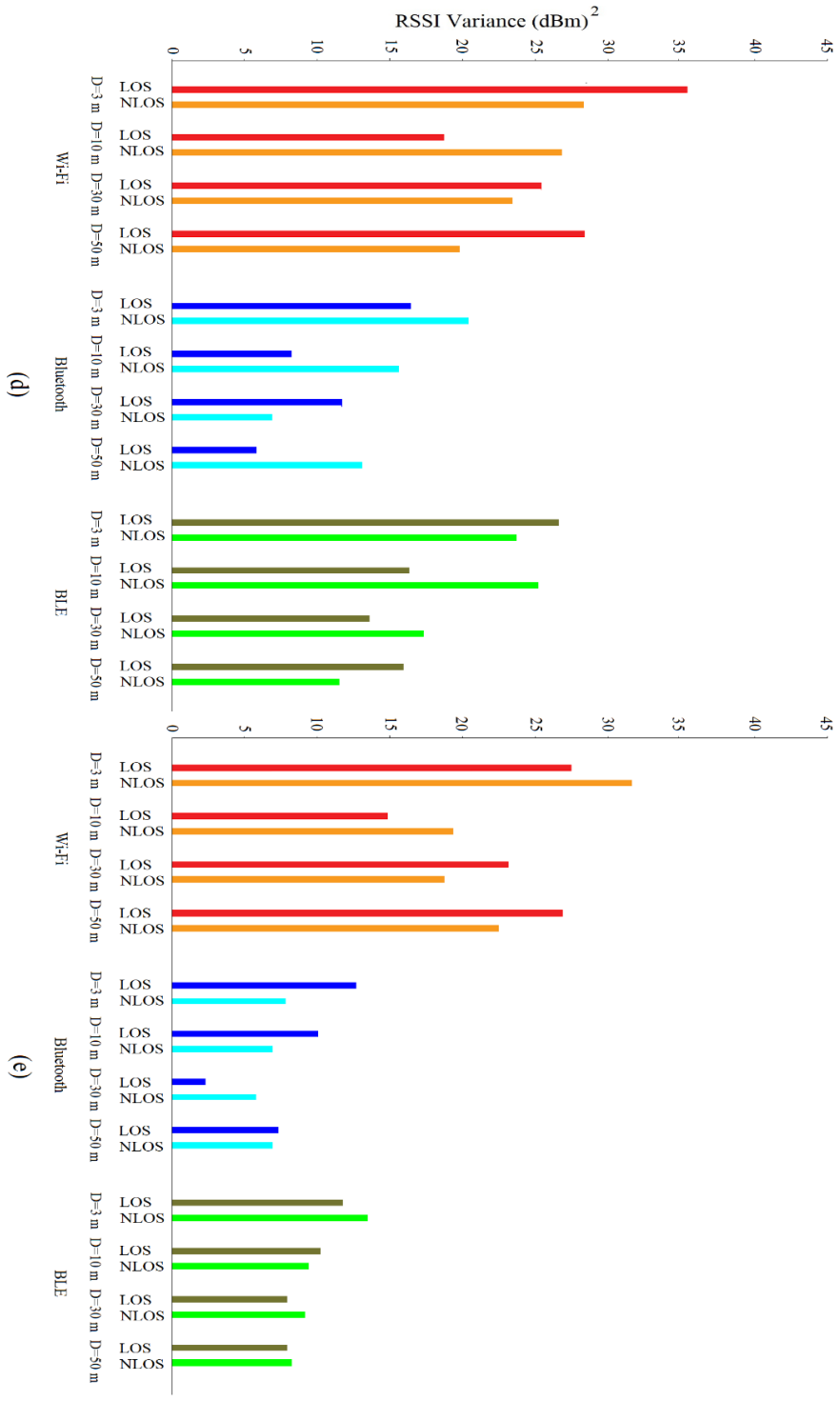

Figure 3.7 Histograms of RSSI variances in (a) Experiment 1; (b) Experiment 2; (c) Experiment 3; (d) Experiment 4-1; (e) Experiment 4-2.

3.5.3 Experiment 3: Effects of Beacon Motion

Table 3.3 and Figure 3.7c summarize the results of the experiments conducted to probe motion impacts on the signals. The number of the signal detections, average RSSI values and their variances during the experiments for both stationary and moving beacons in each scanning mode may be observed in the table. Figure 3.7c involves the histogram of the RSSI variances. Although there seem to be some slight differences in the average RSSI values of stationary and moving beacons in each mode, the differences do not indicate systematic impacts caused by motion as these fluctuations are normal for RSSI values. However, the RSSI variances indicate an overall increase for moving beacons compared with stationary beacons.

Table 3.3 Effects of beacon motion on the signals.

Mode	Distance (m)	Speed (km/h)	Number of detections	Average RSSI (dBm)	RSSI variance $(dBm)^2$
Wi-Fi	10	0	22	-62.4	20.8
		10	21	-60.3	42.5
Bluetooth	10	0	22	-65.4	12.7
		10	24	-63.3	22.6
BLE	10	0	61	-68.7	18.3
		10	54	-69.3	22.1

3.5.4 Experiment 4: Non-Line of Sight Effects

The results of the two tests conducted to investigate the impacts of obstacles on the signals may be observed in Tables 3.4 and 3.5 as well as Figure 3.7d,e. Table 3.4 compares the number of the signals detected by the signal scanner from each station, average RSSI values and their variances when the transmission path was free and when there was an auto glass between the beacon and the signal scanner. Table 3.5 compares the results of free

path situation with the situation in which the path was blocked by a vehicle located between the beacon and the signal scanner. The histograms of the RSSI variances may also be observed in Figure 3.7d,e.

As observed in the two tables, a reduction in the number of the detected signals in NLOS conditions is generally observed compared with LOS conditions. This reduction is slight for the auto glass obstacle in most cases and for vehicle obstacle when the distance between the beacon and the signal scanner is short (3, 10 m). However, for the vehicle obstacle, this reduction tends to be more as the distance increases. In addition, a reduction in the strength of the signals due to the existence of obstacles is generally observable in NLOS conditions, which is again more severe for the vehicle obstacle especially at far distances. The changes in the variances in the two situations do not seem to be systematic.

Table 3.4 Comparison of the signals in LOS path and NLOS path (auto glass obstacle).

		Number of detections		Average RSSI (dBm)		RSSI variance $(dBm)^2$	
Mode	Distance (m)	LOS path	NLOS path	LOS path	NLOS path	LOS path	NLOS path
Wi-Fi	3	54	51	-45.3	-47.4	35.6	28.3
	10	48	46	-58.6	-59.5	18.7	26.8
	30	44	48	-64.8	-65.8	25.4	23.4
	50	47	45	-68.9	-71.6	28.4	19.8
Bluetooth	3	51	50	-53.4	-55.2	16.4	20.4
	10	47	49	-63.1	-61.7	8.2	15.6
	30	45	47	-68.7	-69.4	11.7	6.9
	50	44	41	-75.5	-76.8	5.8	13.1
BLE	3	174	178	-61.7	-61.3	26.6	23.7
	10	169	157	-69.1	-71.0	16.3	25.2
	30	173	165	-75.8	-77.7	13.6	17.3
	50	162	155	-82.3	-83.4	15.9	11.5

Table 3.5 Comparison of the signals in LOS path and NLOS path (vehicle obstacle).

		Number of detections		Average RSSI (dBm)		RSSI variance $(dBm)^2$	
Mode	Distance (m)	LOS path	NLOS path	LOS path	NLOS path	LOS path	NLOS path
Wi-Fi	3	47	49	-46.5	-48.3	27.4	31.5
	10	51	51	-56.7	-56.3	14.8	19.3
	30	43	38	-65.3	-68.0	23.1	18.7
	50	49	41	-69.7	-72.9	26.8	22.4
Bluetooth	3	46	48	-55.6	-57.9	12.6	7.8
	10	50	46	-62.5	-64.8	10.0	6.9
	30	46	43	-68.8	-71.2	2.3	5.8
	50	44	37	-74.3	-78.1	7.3	6.9
BLE	3	183	175	-63.7	-65.8	11.7	13.4
	10	176	163	-71.5	-70.4	10.2	9.4
	30	164	142	-75.3	-78.8	7.9	9.2
	50	167	139	-81.7	-85.4	5.1	8.2

3.5.5 Experiment 5: Signal Transmission Rates

The number of the signals detected by each of the three signal scanners and the moments at which there were simultaneous detections by all of them were specified using the MATLAB code (Table 3.6). The time interval between the consecutive signal detections in Wi-Fi mode was generally between 4 and 7 s, although missing signals were also recognizable, which increased the time between the signals. Each Wi-Fi scanner had 1276 detections on average during the 150-min duration of the experiment. This was equal to 8.5 signal detections per minute on average. The number of the matching moments in this mode was 75, therefore the simultaneous detections by all the three scanners represented 5.9% of total detections. In Bluetooth mode, the time interval between the signals was generally between 5 and 7 s with occasional missing signals. Each Bluetooth

scanner detected 1308 signals on average during the experiment duration which is equal to an average of 8.7 detections per minute. There were 63 matching moments among the detections of the three scanners, which was only 4.8% of the signals. In BLE mode, signals were generally detected every one or two seconds, though there were missing signals recognizable among them. Signal detections were more continuous at short distances and missing signals were mostly at farther distances. The average number of signal detections by the BLE signal scanners in the experiment duration was 4214, equal to 28.1 detections per minute on average. There were 3282 matching moments in this mode, which were 77.9% of the detections.

Table 3.6 Simultaneous detection rates for three signal scanners.

		Number of detections	Simultaneous detections	
Mode	Test duration (min)	Average for each scanner	Number	Percentage (%)
Wi-Fi	150	1276	75	5.9
Bluetooth	150	1308	63	4.8
BLE	150	4214	3282	77.9

3.6 Discussion

It was observed in Experiment 1 that the slopes of RSSI-distance curves gradually go to zero as the distance increases and the functionality of the curves decreases at long distances. This means that RSSI values are more distinct in short distances, and it will be more difficult to have an accurate estimation of the distance based on RSSI at long distances. RSSI values usually involve some fluctuations and outliers which may reduce the accuracy of distance estimation and positioning. The outliers should be removed from the data using appropriate filtering algorithms as far as possible. The R-squared value as

the measure for closeness of the data to the fit curves is an important parameter in RSSI-distance curves. RSSI fluctuations and outliers reduce R-squared value of the fit curves and result in higher inaccuracies in distance estimation. These fluctuations and outliers also cause the variances of the RSSI values to increase which will decrease the accuracy of RSSI-based distance estimation and positioning methods. This is more severe in methods such as trilateration which require the distances of the beacon from multiple signal scanners, because using distances with high inaccuracies will mathematically cause propagation of the errors in calculating the beacon position. Considering these factors in RSSI-distance curves, R-squared values and RSSI variances in the three modes indicated the superiority of Bluetooth and BLE modes. BLE mode had the highest R-squared value, while the variances of Bluetooth RSSI values were lower. Wi-Fi mode had the worst performance concerning these parameters.

Rainfall did not significantly impact the data compared with normal weather conditions in the three modes according to results of the second experiment. This is a promising factor for utilizing wireless technology in traffic studies which require positional data of road users, since the data collection stage may even be conducted in rainy weather conditions. Besides, it should be mentioned that the numerous experiments of this research were conducted in the four seasons, from hot to cold and from clear to snowy weather conditions. No considerable systematic impacts due to the variations in weather conditions were observed during the experiments.

The results of Experiment 3 did not indicate significant differences between the average RSSI values of stationary and moving beacons carried by a running person in any of the three modes, although motion of the beacons generally increased RSSI variances.

This may decrease the positioning accuracy of moving beacons in traffic studies. In this case, no considerable difference in the severity of the motion impacts on moving beacons was observed comparing the three modes with each other; but it should be noted that according to the results of the first experiment, the variances of Wi-Fi RSSI values were generally higher compared with Bluetooth and BLE modes.

The handshakes of a running person may act as an intensifier of the motion impacts on the signals. These shakes may be less severe or not exist when a beacon is carried by a bicycle or a vehicle. Hence, the impacts of motion on a beacon carried by a normal speed bicycle or a relatively low speed vehicle may not be very different with the impacts observed in this experiment, although they may have higher speeds compared with a running person.

Experiment 4, conducted to investigate the impacts of NLOS path situations on the signals, indicated a reduction in the number and strength of the signals caused by the glass and vehicle obstacles without systematic impacts on the variances. The reduction magnitudes in the number and strength of the signals were more for the vehicle obstacle especially at far distances. More severity of the reductions at far distances may be meaningful because of the lower strength of the signals in passing through the obstacles. The changes in these parameters were not considerably different comparing the three modes with each other. Although signals were affected by obstacles, the impacts were not extreme, which is a promising indicator for the possibility of beacon positioning in traffic studies. However, it should be mentioned that different materials exist in the real world and even in vehicles, which may cause more or less attenuation impacts on the signals.

The results of the second experiment, investigating precipitation effects on the signals, may also be justified considering rain drops and snowflakes as obstacles in the transmission paths of the signals. Because of the small dimensions of these particles, their discontinuity and the speed of signals, the insignificancy of precipitation impacts on the signals may be reasonable. As the wavelength of wireless signals is equal to the speed of light divided by the frequency, the wavelength of 2.4 GHz Wi-Fi, Bluetooth and BLE signals is 12.5 cm (Walrand & Parekh, 2018). Therefore, since the rain drops and anow flakes are small relative to the signals wavelength, reflection does not occur, and the attenuation in the strength of signals would not be considerable.

According to the results of Experiment 5, simultaneous detection rates of the three signal scanners were very low in Wi-Fi and Bluetooth modes. In contrast to Wi-Fi and Bluetooth modes, the probability of having simultaneous detections was very high in BLE mode. This is equivalent to a very low probability of having signal detections usable by positioning algorithms in Wi-Fi and Bluetooth modes and a high probability in BLE mode. It is a fact that signal scanners do not detect all the signals transmitted by beacons, but lower simultaneous detection rates in Wi-Fi and Bluetooth modes were mostly because of the lower signal transmission rates of beacons and higher detection intervals of signal scanners in these two modes compared with BLE mode. This finding indicates that if applying Wi-Fi or Bluetooth scanning modes for positioning of road users in traffic studies, the duration of data collection should be considered much longer compared with BLE mode in order to have adequate simultaneous detections. Higher signal transmission rate may also be considered as an advantage for BLE mode over Wi-Fi and Bluetooth modes in

MAC re-identification traffic studies. This factor may increase the probability of beacon detection, especially in case road users have high speeds.

3.7 The Special Case of Vehicle-Pedestrian Collision Warning Systems

The over-representation of pedestrian-involved collisions in fatal outcome is a serious challenge in North America. In 2019, 6519 pedestrians were killed in traffic crashes in the US and Canada. This was equal to one death every 81 min and involved 17.2% of all traffic fatalities during this year (National Highway Traffic Safety Administration , 2020), (Transport Canada, 2021). Extensive effort has been made in recent years to apply advanced onboard technologies to alert drivers when pedestrians are in their close proximity or in hazard zone. Currently, most pedestrian detection sensors are visual or radar-based with significant limitations in certain conditions. They are not always reliable and may only be considered as a backup rather than a self-sufficient system for collision avoidance. Conditions in which pedestrians may not be detected by these systems are often specified in a vehicle owner's manual. Examples are darkness, inclement weather conditions and lateral offset of the vehicle (American Automobile Association Inc., 2019). Detection rates of camera systems significantly decline at nighttime, during precipitations, and in foggy weather conditions. Cameras should be kept relatively clean which may not be observed in many situations (Raeve, et al., 2020). Resolution in radar sensors is relatively low and is not effective in recognizing object details or distinguishing between pedestrians and other objects. Lidar systems are sensitive to precipitation and fog. They may also be blinded by direct sunlight. Ultrasonic detectors do not have the potential to be used for pedestrian detection. They usually have an effective range of 6 m or less and are typically utilized in parking assistance systems (American Automobile Association Inc.,

2019). An application of wireless technology with a significant value may be its integration in vehicle-pedestrian collision warning systems as a supplement for the currently available technologies especially in situations the other systems have inherent limitations. This requires determination of the positional data of pedestrians.

Most pedestrians and cyclists currently, or in the soon future, carry smart devices on their person. The practical context is to utilize the prevalence of beacons and advanced sensing technology in real-time vehicle-pedestrian collision warning systems with the goal of preventing these types of crash. These systems should be able to detect pedestrians if present in the hazard zone of vehicles. The vehicle hazard zone may be considered an area around the vehicle whose edges are several meters away from it. Detection of pedestrians in the hazard zone may be done on account of the potential of RSSI values transmitted by pedestrians' beacons for wireless signal positioning.

The presence of a pedestrian carrying a beacon in the hazard zone of a vehicle may be determined in two approaches. In the first approach, a certain distance from the vehicle is specified as its hazard zone. The RSSI value corresponding to this distance is determined and is set as warning threshold for the system. Detection of RSSI values higher than this threshold by a signal scanner installed on the outer side of the vehicle will be the indicator of the presence of a beacon in its hazard zone (distance-based approach). In the second approach which is more complicated, instead of only determining the presence of a beacon at a distance closer than a threshold around the vehicle, the exact position of the beacon is determined by using multiple signal scanners. Therefore, the position of the pedestrian walking in the vicinity of a vehicle can be dynamically determined and such information is utilized to protect the pedestrian. Specifying a hazard zone around the vehicle, the driver

will be alerted if the position of the beacon is determined to be inside this zone (position-based approach). The advantage of the latter approach may be evident when determination of only the presence of a pedestrian close to the vehicle is not adequate to conclude if it is located in the hazard zone. An example is when the vehicle is moving next to a pedestrian walkway.

Successful application of wireless technology as a collision warning system in motorized vehicles, especially commercial vehicles, may significantly enhance the safety of pedestrians, resulting in reduction of the number of fatalities and injuries due to vehicle-pedestrian crashes. This is dependent on the characteristics of wireless signals as well as the accuracy of wireless signal ranging and positioning methods. In this section, the most appropriate wireless signal mode for integration in collision warning systems in terms of accuracy and functionality will be recommended based on the results of the experiments conducted in this chapter. This is an example of how to use these results to determine the most suitable signal mode for a certain application of wireless signal scanning in transportation systems.

The Relationship between RSSI and Distance: The robustness of the relationship between RSSI and distance is important for distance-based collision warning systems which operate based on a set RSSI threshold corresponding to the beginning of the hazard zone of the vehicles. RSSI-distance relationship is also important for finding the position of the beacons in position-based approach, as it affects the performance of positioning techniques directly or indirectly. A more accurate relationship between RSSI and distance leads to more accurate positioning results. This will increase the accuracy and functionality of collision warning systems.

As observed in Experiment 1, the slopes of RSSI-distance curves gradually go to zero along with the distance between the beacon and signal scanner and the functionality of the curves decreases at long distances. This means that RSSI values are more distinct in short distances. The distinction in short distances is important for the operation of collision warning systems. This is because it enables the system to recognize the beacons located in the hazard zone of the vehicle which may be considered an area around the vehicle whose edges are several meters away from it. Comparison of RSSI-distance curves fitness and RSSI variances in the three modes indicated the better performance of Bluetooth and BLE modes, when the purpose is distance estimation and beacon positioning. The R-squared value was the highest in BLE mode, but Bluetooth RSSI values had lower variances.

Precipitation Effects: Collision warning systems should generally operate outdoors. Rainfall did not significantly impact the data compared with normal weather conditions in any of the three modes according to the results of the second experiment. This is a promising factor for utilizing wireless technology in design of collision warning systems which require positional data of pedestrians, since these systems may operate during precipitation.

Effects of Beacon Motion: Vehicle-pedestrian collision warning systems are designed to detect beacons carried by pedestrians, which may be moving. The results of the third experiment conducted to investigate the impacts of beacon motion on the signals did not indicate significant differences between the average RSSI values of the stationary and moving beacons in any of the three modes. Nevertheless, motion generally increased the variances of RSSI values which may decrease the accuracy of safety systems in moving conditions.

Non-Line of Sight Effects: The results of Experiment 4 may be considered promising for the possibility of beacon detection in collision warning systems under NLOS situations. Collisions usually occur when there are no obstacles between the two involved parties. Hence, non-presence of large obstacles with significant NLOS impacts between the colliding vehicle and pedestrian may be a logical assumption. Blockage may mostly occur by objects whose impacts are minor, e.g., when the beacon is inside the pedestrian's pocket. However, it should be mentioned that reduction in strength of signals due to obstacles in NLOS situations should be taken into consideration in setting RSSI thresholds corresponding to hazard zones. As observed, the impacts were not considerably different among the three modes.

Signal Transmission Rates: This factor is important in the design of position-based collision warning systems because of the nature of safety criteria. To have on time alerts, the system requires to be able to determine the beacon positions in short time intervals. A high probability of having simultaneous detections by multiple signal scanners is necessary to meet this requirement. In the distance-based approach, short time intervals between transmitted signals are important for the system. They reduce the time difference between entrance of the beacon into the hazard zone and alert by the system, which is the indicator of its fast performance.

Intervals of several seconds between the signals in Wi-Fi and Bluetooth modes significantly reduce the functionality of collision warning systems if they are designed to operate in these two modes. Short time intervals between the signals especially in short distances are crucial in safety applications. The capability of continuous signal transmission in BLE mode will enable the system to have fast performance in terms of the

time gap between the entrance of the pedestrians into the hazard zone and the system alert in both distance and position-based approaches. This is equivalent to more time available for drivers to react properly when pedestrians in danger are detected by the system.

Considering the above factors altogether, BLE is recommended as the superior signal mode over Wi-Fi and Bluetooth to be utilized in vehicle-pedestrian collision warning systems. Application of this mode may provide the possibility of fast collision warnings, whereas its capability in accurate distance estimation and positioning is roughly competitive with Bluetooth mode. Wireless technology may improve the functionality of these systems especially in darkness or inclement weather conditions in which the current systems suffer from inherent limitations. The result will be enhancement of the safety level of both drivers and pedestrians and reduction of the number of vehicle-pedestrian collisions.

The potential of wireless signals in providing the possibility of distance estimation and positioning is the motivation for their integration in vehicle-pedestrian collision warning systems by automotive industry. Practical acceptance of these systems by this industry may benefit from the long-lasting and low-cost availability of wireless technology in the market, the economic scalability of mass production and the advances in development of vehicular-specific amendments of wireless standards. The supplement of this economic advantage is that currently, most pedestrians are carriers of different types of wireless signal transmitters thanks to their personal smart devices.

3.8 Summary

The purpose of this chapter was investigating the comparative field performance of Wi-Fi, Bluetooth and BLE signal modes in gathering traffic flow parameters whenever

accurate positions of road users are required. The study compared these wireless signal modes to find out which one provides better results in terms of quality, accuracy, and convenience of data collection. Effort was made to provide a data base to help traffic practitioners select the most suitable signal mode for different applications of wireless signal scanning systems.

Five factors including RSSI-distance relationship, precipitation effects on the signals, motion effects, NLOS effects, and signal transmission rates were selected for evaluation. These factors were selected considering the characteristics of traffic studies and were compared with each other based on the results of the conducted experiments. The comparison between the three modes of wireless signals was in the form of five field experiments. Each experiment was conducted in the three modes separately.

In order to investigate the quality of the relationship between RSSI and distance, RSSI-distance charts were created for the three signal modes in Experiment 1, and their best fit curves were drawn. Comparison of the fitness of the curves and RSSI variances indicated the better performance of Bluetooth and BLE modes, when the purpose is distance estimation and beacon positioning. While the R-squared value was the highest in BLE mode, Bluetooth RSSI values had lower variances which increase the potential for more accurate positioning.

Rainfall as a probable event during traffic data collection was selected for investigating the effects of precipitation and weather changes on the signals. According to the results of the second experiment, rainfall did not significantly affect the data compared with normal weather conditions in the three modes. This indicates that data collection stage in traffic studies may be conducted in rainy conditions.

The third experiment was conducted to investigate the impacts of motion on the quality of signals. Beacon motion did not have severe impacts on the average RSSI values in any of the three modes. However, motion increased RSSI variances, which may decrease the positioning accuracy of moving beacons. No considerable difference in the severity of the impacts of motion on beacons was observed comparing the three modes with each other.

The impacts of the existence of obstacles in the transmission path on the signals were investigated in Experiment 4. This was done probing the impacts of auto glass and vehicle blockage as two examples of the situations causing NLOS in traffic systems. The results indicated a reduction in the number and strength of the signals caused by the glass and vehicle obstacles without systematic impacts on the variances. The reduction magnitudes in the number and strength of the signals were more for the vehicle obstacle especially at far distances. The changes in these parameters were not considerably different among the three modes.

Experiment 5 was conducted to investigate signal transmission rates and the opportunity to have simultaneous detections by multiple signal scanners, necessary for positioning of moving beacons. In Wi-Fi and Bluetooth modes, simultaneous detection rates of multiple signal scanners were very low. In contrast to these two modes, the probability of having simultaneous detections was very high in BLE mode. Lower simultaneous detection rates in Wi-Fi and Bluetooth modes were mostly due to the lower signal transmission rates of beacons and higher detection intervals of signal scanners in these two modes in comparison with BLE. The practical outcome is that if applying Wi-Fi

or Bluetooth scanning modes, the duration of traffic data collection for positioning of road users should be considered much longer compared with BLE mode.

Overall consideration of the five studied factors indicates the superiority of Bluetooth and BLE modes over Wi-Fi mode in traffic studies, especially when accurate positioning of road users is important. In case the accuracy of positioning has the highest priority, Bluetooth mode may be the most proper. However, the time required for data collection in BLE mode is much shorter compared with Bluetooth which makes it a proper option when data collection time is limited. Wi-Fi mode is not recommended for these types of traffic studies.

As an example of the applications of the results of the conducted experiments, the special case of utilizing wireless signal scanning technology in vehicle-pedestrian collision warning systems was probed. BLE mode was recommended as the most suitable signal mode for integration in these systems. The reasons were the potential of BLE mode in accurate positioning as well as providing the possibility of fast collision warnings thanks to the high signal transmission rates in this mode.

Chapter 4: Development of a Positioning Technique for Traffic Data Collection Using Wireless Signals

4.1 Introduction

As presented in Chapter 2, the utilization of wireless sensors in traffic data collection is a well-established topic. However, seldom is the issue of improved localization accuracy addressed. It is hypothesized in this thesis that bringing localization accuracy down to 5 m will break the grounds for new applications and data collection targets not available before. This threshold is a rounded figure and should be sufficient to unambiguously associate road users with a traffic lane and/or intersection approach. This chapter presents a novel and cost-efficient technique which achieves this objective and provides extensive field experiments to develop and validate it.

The practical goal of this work is to find a solution for positioning of beacons transmitting wireless signals in traffic streams. Current models of wireless signal scanners provide limited data when detecting a beacon. These data include MAC address, signal mode, detection timestamp and RSSI without any information about the beacon position. A practical utilization of wireless signals in traffic studies is to locate beacons based on the strength of the transmitted signals. Notably, determining the position of road users at each moment, provides the input for finding numerous traffic parameters even in real time. A relatively accurate estimate of position may significantly enhance the accuracy of traffic data collection such as travel time measurements and turning movements analysis. It provides the possibility of travel time and delay measurement in short road segments in which current MAC re-identification techniques are not applicable. The improved data may

be used in safety analysis, collision warning systems and data analytics with the ability to distinguish and monitor different modes of traffic, *e.g.*, pedestrians or cyclists.

This chapter proposes a solution for wireless signal positioning based on the RSSI values of the signals transmitted by beacons and collected by signal scanners. The technique is developed by creating radio maps and utilizing a k-nearest neighbors (KNN) approach to match signals to calibrated positions. Attempt will be made to improve the accuracy and functionality of the technique via modification of the field deployment set-up and arrangement. The improvement is made through optimization of the number of the stations, along with meeting the minimum positioning accuracy requirements, and making stations and scanners arrangement asymmetric. The minimum required accuracy may be different for various applications. For travel time measurement in short road segments, the required accuracy may be considered equal to or less than 5 m. The procedure will be supplemented by applying numerous filtering algorithms on the data sets in order to mitigate the impacts of signal fluctuations and outliers on the quality of the results.

4.2 Signal Mode

Earlier comparative work in the third chapter revealed that Bluetooth signal mode is the most suitable when the purpose is accurate wireless signal positioning. Although the R-squared values of RSSI-distance curves were the highest in BLE mode, Bluetooth RSSI values had lower variances which increase the potential for more accurate positioning results. Rainfall did not significantly affect the data compared with normal weather conditions in the three modes. The impacts of motion and NLOS signal transmission paths were not considerably different in the three modes. It was also observed that the probability of having simultaneous detections by multiple signal scanners is higher in BLE mode

compared with Wi-Fi and Bluetooth modes. Although using BLE mode may result in higher number of signal detections proper for positioning in a certain time period, accuracy was the first priority in development of the positioning technique in this study. Hence, Bluetooth mode was selected for development of the solution because of its lower signal variances.

4.3 Research Equipment

4.3.1 Wireless Signal Scanners and Beacon

This research was conducted using four wireless signal scanners equipped with Bluetooth detectors. The detectors were Class 1 and had a receiving sensitivity of −90 dBm and a transmission power of +18 dBm. The antennas installed on the signal detectors were omnidirectional, long-range, 2.4 GHz and 2 dBi gain. The beacon used in the experiments was an Android operated cell phone.

4.3.2 RTK System

An approach for measuring the distance between satellites and ground receivers is carrier phase-shift measurement. In this approach, ranges to satellites are measured by observing phase-shifts of the signals from the moment they are transmitted by a satellite until received by a receiver (Ghilani & Wolf, 2012). Determining the number of carrier cycles or wavelengths between the satellite and receiver and then multiplying this number by the carrier wavelength, the range may be calculated. The number of full carrier cycles is determined in a process called ambiguity resolution (Novatel.com, 2021).

Kinematic satellite surveying techniques are based on carrier phase-shift observations and relative positioning methods. In relative positioning, the coordinates of a point are obtained relative to another point in order to remove errors. Kinematic techniques

are able to specify coordinates, while the receiver is stationary or in motion. The accuracy level is good enough for most applications, although it may be lower than static techniques. Kinematic surveying may be post processed or real-time. In post processed kinematic (PPK) technique, the results may be prepared after data collection, but real-time kinematic (RTK) technique provides the results immediately. Two receivers are required in kinematic surveying, a base, and a rover. The base is located on a station with known coordinates and the rover is used to collect the positional data of unknown points. A fundamental objective is to reduce and remove errors common to the base and rover. Both receivers must be lock on a minimum of four satellites during data collection. As an alternative for the base, it is also possible to use local continuously operating reference stations if available near the area. The locations of these stations are known in high accuracy thanks to the receivers located on them (Ghilani & Wolf, 2012).

The rover determines its range to the satellites using ambiguity resolution process and multiplying the number of full carrier cycles by the wavelength. The calculated ranges include errors from sources like satellite clock as well as tropospheric and ionospheric delays. To eliminate these errors the base observations are transmitted to the rover. The rover determines its position using algorithms which merge ambiguity resolution and differential correction (Novatel.com, 2021).

The achievable positioning accuracy of the rover depends on its distance from the base station and the accuracy of the differential corrections. The accuracy of the known position of the base station and the quality of the satellite observations by the base are important for the accuracy of differential corrections (Novatel.com, 2021). Motion of the rover during data processing reduces the accuracy of RTK technique. This may be more

significant if the rover moves fast. Dilution of precision (DOP) spikes, refraction, multipathing and obstructions are other factors reducing the accuracy of kinematic surveying. The obtainable accuracy by RTK is normally within a few centimetres if the distance between the rover and the reference station is less than 30 km (Ghilani & Wolf, 2012).

In one of the experiments of this chapter, it will be required to find the real position of the beacon at certain moments while moving. This will be done using an RTK system. The device selected for this purpose is Leica GS15 receiver (Leica Geosystems, Leica GS15, 2019) along with CS35 interface (Leica Geosystems, Leica CS35, 2019) (Figure 4.1). GS15 will be used as the rover and the active local reference station located in Gatineau, Quebec as the base in the surveying (Radio Technical Commission for Maritime (RTCM) Version 3 IP address: http://142.41.245.88:2107).

Figure 4.1 RTK system used in the research: GS15 receiver and CS35 interface.

4.4 Location of Field Work

The location of the experiments was a four-legged intersection on the test track system of the National Capital Commission (NCC) center for autonomous vehicle technologies; located in Ottawa, Canada (Figure 4.2). The streets leading to this intersection were all two-way, two-lane. There were several buildings in the area and some utility poles around the intersection. Outdoor Wi-Fi internet access was available. The location was not an isolated area and there were other beacons as well as some activities taking place in the vicinity during the experiments. Selection of this site provided the possibility to collect data for forming the calibration vectors required in the positioning technique without the need to block the intersection.

Figure 4.2 Location of the experiments and the wireless signal scanners, installed in the area.

4.5 Study Method

KNN algorithm is utilized in this study, whereas trilateration approach was investigated in the preliminary experiments. In trilateration, if the purpose is finding the location of a beacon on a street, a minimum of three signal scanners are required. Two of the scanners may be located on one side of the street and the third one on the other side (Figure 4.3). An imaginary coordinate system may be drawn; one axis next to and parallel to the street (*x*-axis) and the other one perpendicular to it (*y*-axis). In order to simplify trilateration equations, it is possible to set the origin of the coordinate system (0, 0) on the first signal scanner. The second scanner will be on a point on *x*-axis (*d,* 0), and the third one on a point on the other side of the street (*i*, *j*). The three signal scanners collect the RSSI values transmitted by the beacon located on the street. Calculating the distance between the beacon and each of the three signal scanners based on the RSSI values at a certain moment and using a calibrated RSSI-distance formula, the position of the beacon (*x*, *y*) may be found using the following equations:

$$x = \frac{r_1 2 - \ r_2 2 + \ d^2}{2d} \qquad (4.1)$$

$$y = \frac{r_1 2 - \ r_3 2 + \ i^2 \ + \ j^2}{2j} - \frac{ix}{j} \qquad (4.2)$$

in which r_1 , r_2 and r_3 are the distances between the beacon and Signal Scanners 1, 2, 3 respectively and all the distances should have the same units of length.

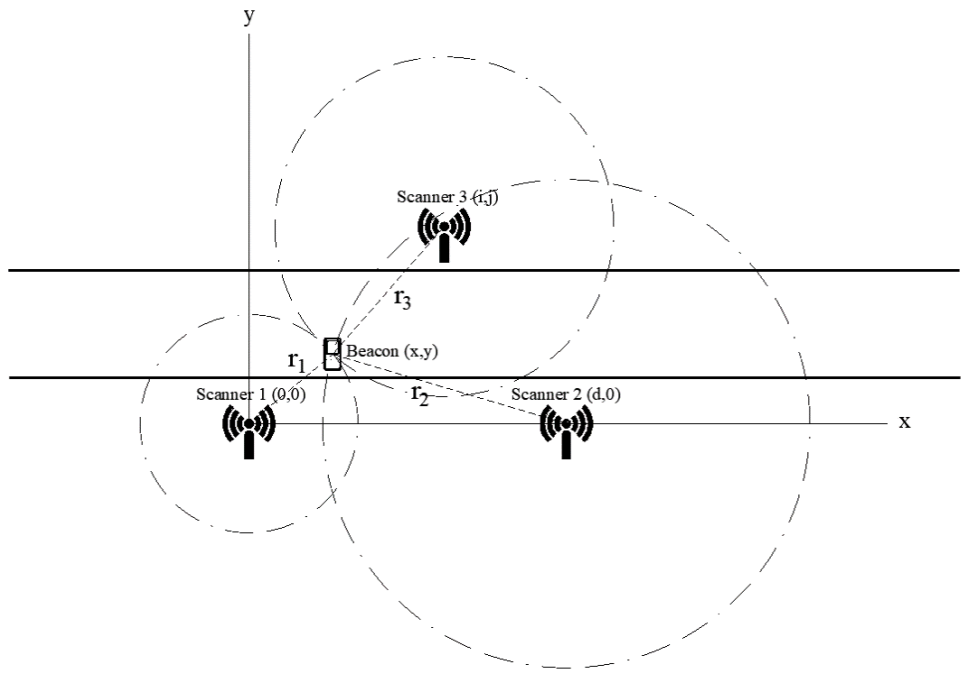

Figure 4.3 Trilateration problem along a street.

The results of the experiments conducted to investigate the performance of trilateration technique were underwhelming. The qualification of this technique for positioning of beacons in traffic studies was found to be inappropriate due to the high inaccuracies, imprecision, and failure of the reliability of the position estimates. The following factors were identified as the root causes of the rejection of this approach: [*i*] RSSI signal packs involve outliers. These outliers may lead to errors in distance estimation based on RSSI-distance formulas; [*ii*] Using multiple distances for finding the beacon position in trilateration formulas will mathematically cause propagation of the errors, as the formulas are based on distances which are not accurate themselves.

4.5.1 K-Nearest Neighbors (KNN) algorithm

KNN is a mathematical data classification algorithm for determining which points in a reference set are similar to a test point with assigned characteristics. The reference set

involves a number of points identified by several known characteristics. Each test point as well as each point in a reference set is identified by a number of known characteristics, forming a vector as its components. For each test point, the algorithm determines *K* points in the reference set as the most similar (nearest) ones to it. This is done comparing the test point vector with each of the reference point vectors. Euclidean distance is a proper metric for determining the nearest reference points to the test point if the components of the vectors are all numeric and addable values. The Euclidean distance in KNN algorithm may be calculated as follows:

$$D_j = \sqrt{\sum_{i=1}^{p} (x_{ai} - x_{bi})^2} \qquad (4.3)$$

where, D_j is the distance between the test point and a reference point, x_{ai} and x_{bi} are the components of the reference and test point vectors and p is the number of the vectors components. If sorted by distance in an incremental order, the *K* reference points with the least distances to the test point may be specified. The algorithm determines these *K* reference points as the nearest neighbors of the test point (Kuhn & Johnson, 2013).

4.5.2 Positioning Technique

The strategy developed in this chapter for positioning of beacons on the basis of the RSSI values of their transmitted signals is creating radio maps and applying KNN algorithm to find out their coordinates. A radio map consists of a database of reference points (stations) in an area and their corresponding RSSI values, collected by a wireless signal scanner when a beacon is located on them. The points may form a grid and their corresponding RSSI values are measured by the signal scanner. For each signal scanner used in the positioning procedure, a radio map is created.

The developed technique includes three stages: calibration, test data collection, and positioning, respectively. The first two stages involve data collection for a beacon and the third stage is determining its position. The calibration stage aims at creating the radio maps; to be used as reference. The test data collection stage aims at collecting data for comparison to be used in the positioning stage along with the radio maps, created in the calibration stage. The positioning stage compares the test data collected in the second stage with the radio maps created in the first stage using KNN algorithm to specify the position of the beacon. The purpose is finding out if the algorithm can correctly specify the beacon position and the probability of correct positioning. In this research, *K* is set to 1 to eliminate the locations with the lower probabilities from contributing to the location estimate.

4.5.3 Experiments

The study involved five field experiments on both stationary and moving beacons. The first four experiments were on stationary beacons with different system arrangements. Based on the results of these four experiments, suitable arrangements for the system were identified. The fifth experiment was conducted on a moving beacon considering the results of the experiments on stationary beacons.

Four Bluetooth signal scanners and a beacon were used in the data collection work. Each of the four signal scanners were used for creating a radio map, based on the signals transmitted by the beacon. The clocks and therefore the timestamps of the four signal scanners were all precisely synchronized by the GPS modules, connected to the processing units of the devices (Figure 4.4).

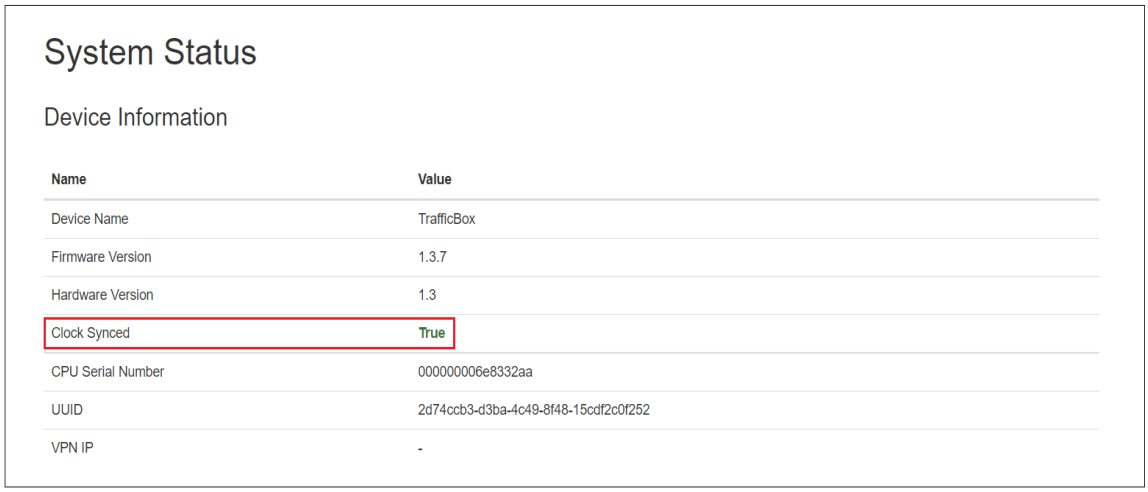

Figure 4.4 Time synchronization of the signal scanners, observable in their software.

4.5.3.1 Part 1: Stationary Beacon

Each of the following experiments involves three stages: calibration, test data collection, and positioning. In order to improve the accuracy, optimize the procedure and find the most proper grid and scanners set-up, four experiments with similar stages, but with different stations and scanners arrangements were conducted and the results were compared with each other. Two types of changes to the initial scanners and stations arrangements (relevant to Experiment 1) were investigated through Experiments 2–4: [*i*] reducing the number of the reference stations along with meeting the accuracy requirements; [*ii*] making the arrangement of the stations and scanners asymmetric. The first change was applied in the second experiment and then in the third and fourth experiments according to the results. The effects of the second change were investigated in the third and fourth experiments.

Experiment 1: In the first experiment, eight stations were specified on each lane of each of the intersection legs with a 3 m distance between each two of them. The first station on each intersection approach was 1.5 m from its beginning. As there were both inbound

and outbound lanes on the intersection approaches, there were 16 stations on each approach. Four stations were also considered in the middle of the intersection; therefore, the total number of the stations in this arrangement was 68. The four signal scanners were located right at the four corners of the intersection, so that the stations and the scanners formed a symmetric arrangement (Figure 4.5). The signal scanners were installed on steel slotted angle posts with concrete bases. The mounting height of the top of the scanners in all the experiments was equal to 1.80 m above the ground surface because of the limited height of the angle posts. However, installing the signal scanners at higher levels may significantly reduce the impacts of NLOS conditions, especially the blockage caused by vehicles if present in the area, as the signals may be received by the scanners in all directions.

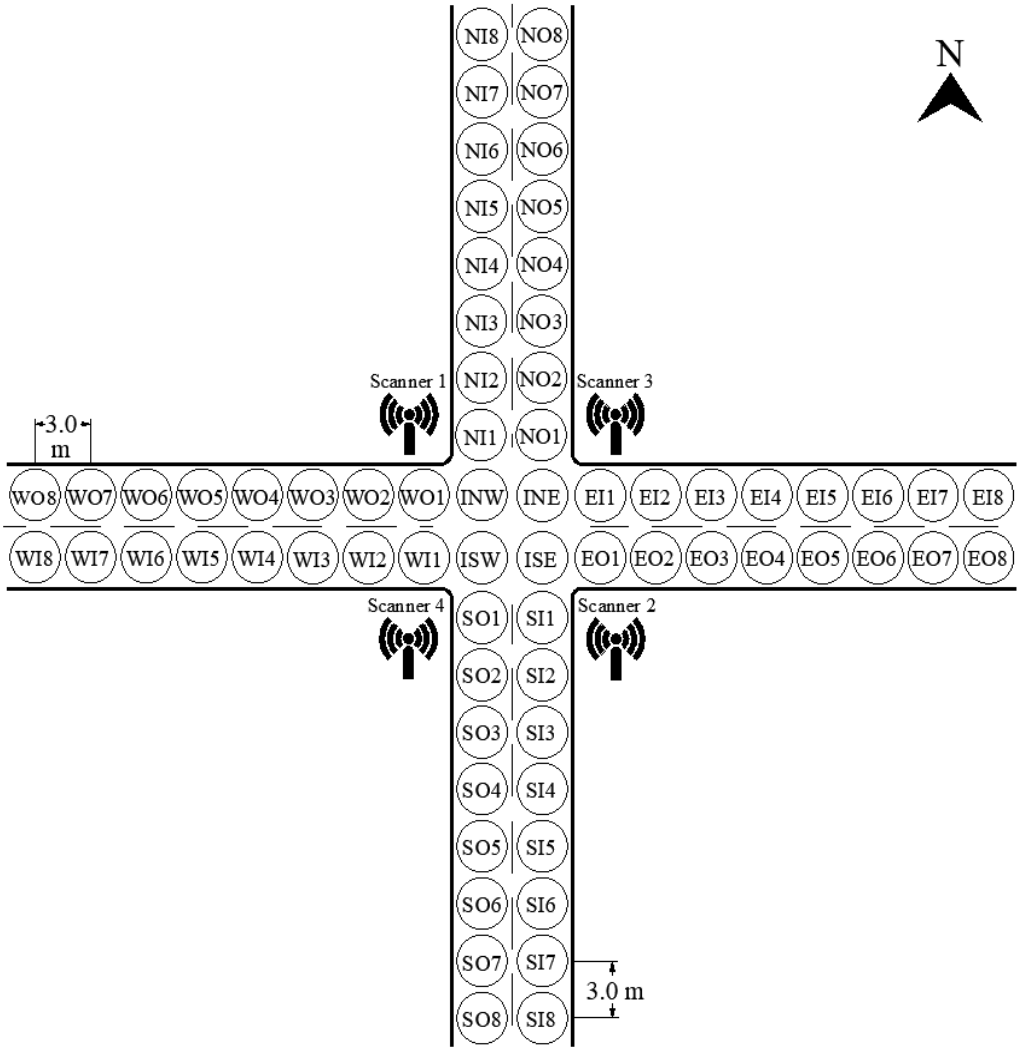

Figure 4.5 Stations and scanners arrangement in Experiment 1 (North direction is approximate.).

In the first stage, to create the required radio maps, the beacon was placed on each of the stations at the height of 1 m for 1 min. In order to eliminate the effects of transmitted signals while moving between the stations, the data associated with moving times were removed; therefore, the beacon was stationary in the whole mentioned time intervals. Signals were collected from all the 68 stations by the four scanners and the average RSSI values for each station collected by each signal scanner were calculated. These average values were used to form the radio maps of the intersection area for each of the signal

scanners. Each set of four average RSSI values, corresponding to each of the stations formed a vector with four components according to the below form. These vectors are hereafter called calibration vectors.

$$\boldsymbol{v}_S = (\overline{RSSI}_1, \overline{RSSI}_2, \overline{RSSI}_3, \overline{RSSI}_4) \qquad (4.4)$$

in which $\boldsymbol{v}_S$ is the RSSI vector for Station S, and $\overline{RSSI}_1$– $\overline{RSSI}_4$ are the average RSSI values of the signals transmitted by the beacon when located on S and received by Scanners 1–4 respectively.

To collect the data required for the second stage, the beacon was held on each of the stations for 30 s and the transmitted signals were collected by the four signal scanners again. The average signal values of the beacon in each station collected by each of the scanners in this stage were also calculated. These data formed other sets of four-component vectors, called test vectors, to be used in the positioning stage along with the calibration vectors.

In the third stage, in order to determine the position of the beacon at each station during the second stage, its corresponding test vector was compared with all the calibration vectors, applying KNN algorithm to find the most probable position, based on the RSSI values. The positioning results were compared with the real locations to specify if the algorithm found the positions correctly and if not, what the positioning errors were.

Experiment 2: The number of the stations in the first experiment was relatively high, resulting in a very time-consuming calibration stage. Hence, to optimize the procedure, effort was made to investigate the impacts of reducing the number of the stations and increasing the distance between them on the accuracy of the results. In the second experiment, half of the stations on each intersection leg were eliminated in a zigzag pattern,

but symmetric with respect to the intersection center. Therefore, the distance between each of the two stations along the street lanes was increased to 6 m. There were still four stations in the middle of the intersection; hence, the total number of the stations in this experiment was 36. The locations of the four signal scanners were like their locations in Experiment 1, at the intersection corners in a symmetric arrangement (Figure 4.6).

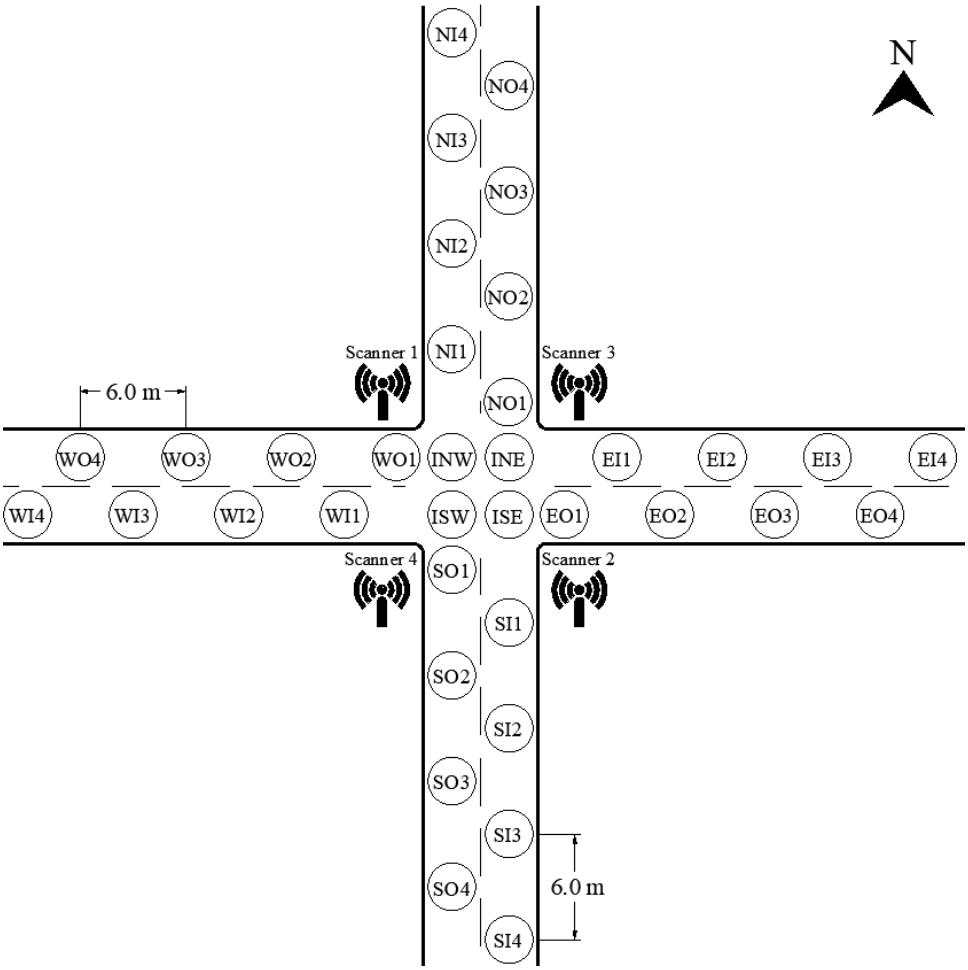

Figure 4.6 Stations and scanners arrangement in Experiment 2.

Experiment 3: In the third experiment, more changes were made in the system arrangement. The purpose was to reduce the positioning error probability via reducing the similarity of the stations' locations relative to the signal scanners on the radio maps. Note that the stations and scanners arrangements in the first two experiments were symmetric.

This may cause the RSSI values of the symmetric stations on the radio maps to be very close to each other, because of the similarity of their distances to the signal scanners. The result is similarity of the components of the calibration vectors for these stations. In positioning, it is necessary that the test vector components of a point be very near to the calibration vector components of the corresponding reference station, so that the positioning can be done correctly. However, other stations with similar calibration vector components may also exist among the reference stations. Such conditions increase the probability of making mistakes by the algorithm because of the signal strength similarities among the calibration vectors.

For this reason, the hypothesis that introducing asymmetry to the stations and scanners arrangement, and consequently the radio maps, would enhance the functionality of the algorithm was investigated. Effort was made to decrease the similarity among the radio maps via changing the stations and scanners locations into an asymmetric set-up. According to this measure and the necessity of optimization of the number of the stations, the following changes were made on the set-up in the third experiment: [*i*] the four scanners were placed at the four corners of the intersection, but not exactly on symmetrical locations. Effort was made to place them at different distances from the intersection corners, but the differences between the distances were low and at most 3.5 m according to Figure 4.7; [*ii*] the distance between the stations in each street lane was changed to 5 m. The stations had a zigzag pattern and the number of the stations in the middle of the intersection was 4. The total number of the stations was 40 as shown in Figure 4.7. In this arrangement, the location of the first signal scanner was chosen to be at the northwest corner; the second scanner was 3.5 m from the beginning of the southern street inbound; the third scanner was 1.5 m from

the beginning of the northern street outbound, and the fourth scanner was 1 m from the beginning of the western street inbound and 2.5 m from the beginning of the southern street outbound.

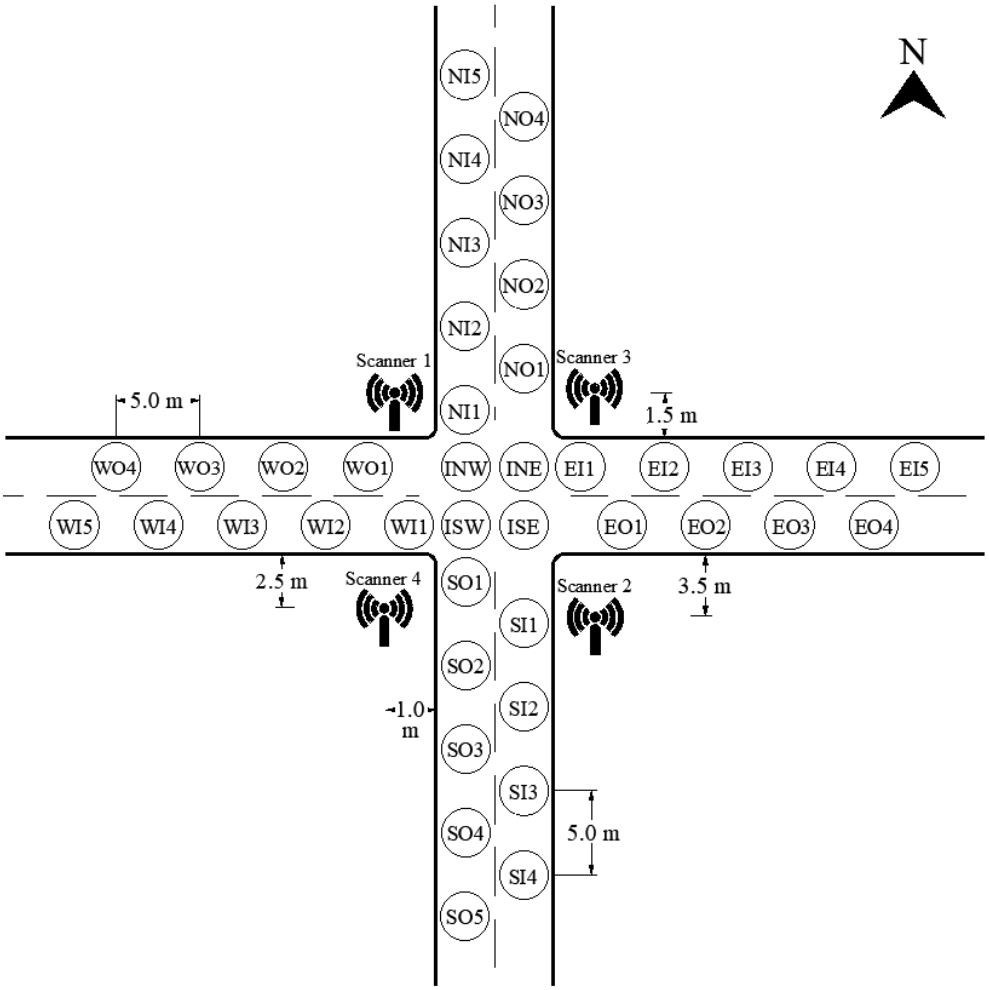

Figure 4.7 Stations and scanners arrangement in Experiment 3.

Experiment 4: The number and the locations of the stations in the fourth experiment were chosen to be the same as Experiment 3, but effort was made to increase the asymmetry level of the system, giving an irregular quadrilateral shape with very different angles to the imaginary lines connecting the four signal scanners. In this experiment, the location of the first scanner was chosen to be 2.5 from the beginning of the western street outbound; the second scanner to be 7.5 m from the beginning of the eastern street outbound; the third

scanner to be 5 m from the beginning of the northern street outbound, and the fourth scanner to be at the southwest corner (Figure 4.8).

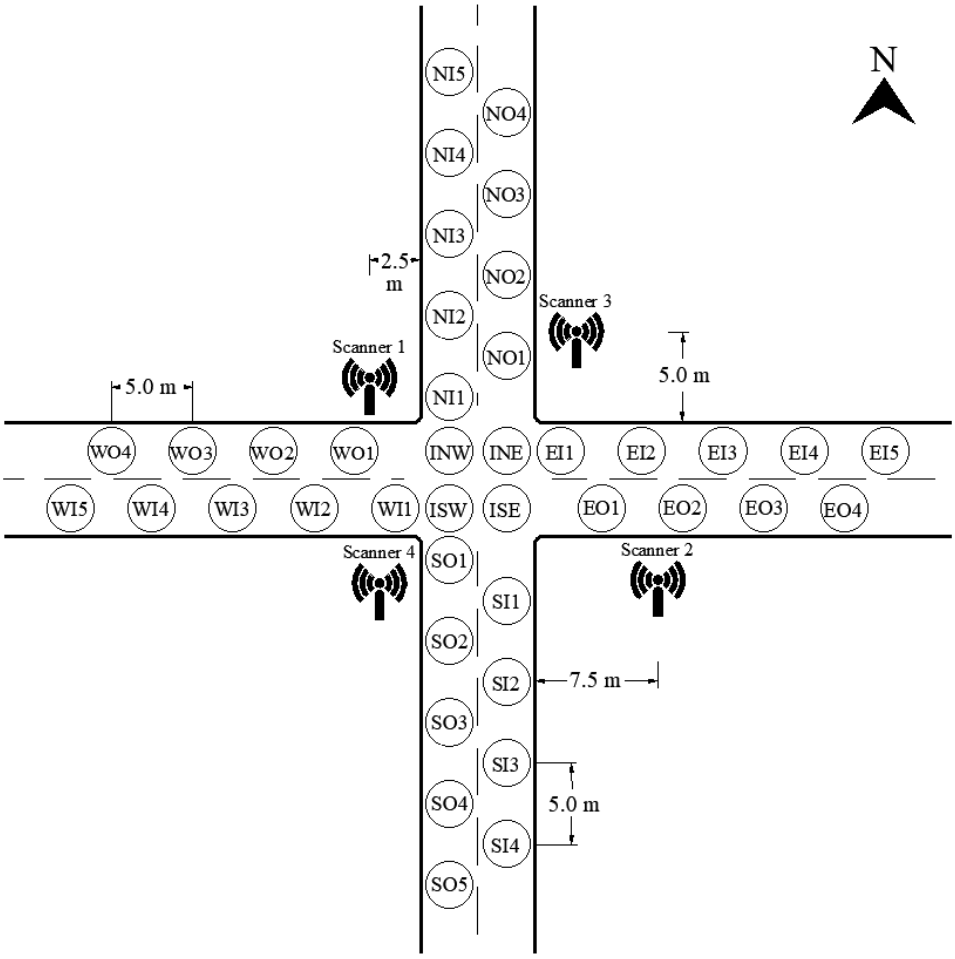

Figure 4.8 Stations and scanners arrangement in Experiment 4.

4.5.3.2 Part 2: Moving Beacon

The foregoing part of this study focused on stationary beacons. As one of the goals of this research is investigating the functionality of wireless signal scanning in transportation studies, the quality of positioning for moving beacons using this technology needs to be considered.

The experiment conducted in this part involved three stages too. The first and the third stages were quite similar to the corresponding stages of the experiments on the

stationary beacon, but in the second stage, the signals of a moving beacon were collected instead of a stationary beacon. Four different stations and scanners arrangements were tested in Part 1 (stationary beacon) to find out which set-up gives more accurate results. As it will be observed in the following sections, the stations and scanners arrangements in Experiments 3 and 4 had the best performance compared with the others. Therefore, it was decided to conduct this experiment, according to the arrangement of Experiment 4 in the first part. The calibration vectors of Experiment 4 were also used in this part because of the similarity of the first stage in the two parts.

For the test data collection stage, two research assistants participated. The first carried the beacon at the height of 1 m, walking on the stations in the grid area in a random manner for 45 min. The motion speed during this stage was approximately 5 km/h. As the beacon was moving during the mentioned time period, it was necessary to find the real location of the beacon at each desired moment in this stage. This was done using the RTK system, introduced earlier in the present chapter. This system provided the possibility of recording the accurate real location data at every second, presenting the geographic Eastings and Northings of the spots. The RTK system was synchronized with the four signal scanners, as they were all connected to GPS.

The second research assistant carried the RTK system, walking beside the first assistant who carried the beacon during the 45 min of the second stage, so that the RTK device recorded the real location of the beacon at every second (Figure 4.9). At the end of this stage, the geographic coordinates of each of the 40 stations were also recorded for comparison and determining the stations at the desired moments when analyzing the data.

Figure 4.9 Data collection in the second stage of the experiment on a moving beacon.

The time interval between the signal detections by the scanners was approximately 5 to 7 s. In order to be able to apply KNN algorithm for positioning in the third stage at a certain moment, there should be simultaneous detections by all the four signal scanners at that moment in the second stage. The reason was that the beacon was moving and might not be detected by all the four scanners at all the points because of the mentioned signal detection intervals.

To find the moments at which all the four signal scanners detected the signals, transmitted by the moving beacon, a MATLAB code was written. This code was able to specify the moments at which signals were detected by the four scanners, with a difference of less than 1000 milliseconds (1 s) between each two of them. The moments in the second stage, which met this criterion were identified as matching moments and the corresponding

RSSI values detected by each of the four scanners were specified. The corresponding sets of RSSI values detected by the four scanners at the matching moments formed test vectors with four components.

In the third stage, the test vectors were compared with the calibration vectors by KNN algorithm in order to find the nearest vectors among the calibration vectors, resulting in determination of the estimated locations. Real locations at the matching moments were also extracted from the RTK data. The real geographical coordinates at these moments were compared with the geographical coordinates of the 40 stations and the closest stations to each of the real locations were assigned to the matching moments as the real locations. Having the estimated locations and real locations at each of the matching moments, the distance between them was calculated as the error of positioning for a moving beacon.

4.5.4 RSSI Filtering

RSSI values usually involve some fluctuations and outliers which pollute the data. In order to improve the accuracy of the positioning technique, effort was made to smooth the RSSI data sets, identify their outliers and remove them from the data. This may be done for the time periods the beacon is stationary, because multiple signals are collected from the same position during these periods. The outliers may be specified comparing the corresponding RSSI values with each other. In this study, filters were applied on the data collected in the calibration and test data collection stages of the experiments on stationary beacon; also, on the data collected in the calibration stage of the experiment on moving beacon.

Five filtering and smoothing algorithms including Savitzky-Golay, Rlowess, Center, Linear and Standard Deviation were selected for this purpose. The algorithms were selected

considering the low number of RSSI values in each station which were around 10 per minute. The developed positioning technique was followed by applying the five mentioned algorithms and the results were compared with each other to introduce the most appropriate one. MATLAB codes were used for applying the first four filters on the data. Standard Deviation filter was applied in Excel.

Savitzky-Golay Filter: It may be considered a generalized moving average and is also known as least-squares or polynomial smoothing filter. A moving average filter smooths the data replacing each data point with the average of its adjacent data points, located in a defined span:

$$x_s(i) = \frac{1}{2n+1}\big(x(i+n) + x(i+n-1) + \ldots + x(i-n)\big) \qquad (4.5)$$

in which:

$x\,(i)$ is the i^{th} data point,

$x_s\,(i)$ is the smoothed value of the i^{th} data point,

n is the number of the adjacent data points on either side of $x_s(i)$ in the span,

$2n+1$ is the span length.

Savitzky-Golay filter aims at enhancing the smoothness and precision of the data without shifting the signals trend. The filter coefficients are determined by an unweighted linear least-squares regression and a polynomial model of a given degree. Higher degrees of polynomial result in higher smoothing levels while maintaining the data features. It is necessary to meet the following rules when applying this filter:

- The span length must be odd.
- The span length must be greater than the polynomial degree.
- Uniform spacing is not necessary for the data points (Mathworks.com, 2021).

A span length of 3 and a polynomial degree of 1 were used for this filter. These values were selected considering the sizes of data sets and the mentioned rules.

Rlowess Filter: It is a smoothing algorithm and a robust version of Lowess filter. The name of Lowess is derived from "locally weighted scatter plot smooth". To smooth the data, Lowess filter utilizes locally weighted linear regression. A weighted process is used, and a regression weight function is defined for the span data points with an odd or even length. The regression uses a first-degree polynomial. Similar to moving average method, each data point is smoothed considering its adjacent data points located in a span. Outliers in the data set cause distortion of the smoothed values; hence they may not reflect the trend of the adjacent data points. This problem may be addressed utilizing RLowess filter, the robust version of Lowess. Rlowess uses a robust weight function, resistant to outliers. Residuals are calculated from the smoothing procedure first. For each data point in the span, robust weights are then calculated. The data are smoothed again using the robust weights in an iterative process (Mathworks.com, 2021). To apply this filter, the span length was selected equal to 5 considering the sizes of data sets.

Center Filter: It finds outliers in the data set and replaces them with the center value of the set. The center value is the median of the data. Outliers in this method are the values more than three scaled median absolute deviations away from the data set median. For a random data set X made up of $X_1, X_2, \ldots, X_n$, median absolute deviation (MAD) is a measure of dispersion. It is defined as the median of the absolute deviations of the data points from the median of the data set:

$$\text{for } i = 1,2,\ldots,n: MAD = \text{median}\left(\left|X_i - \text{median}\,(X)\right|\right) \qquad (4.6)$$

Scaled MAD is defined as:

$$\mathrm{c} \times MAD \qquad (4.7)$$

in which c may be considered equal to 1.48 (Mathworks.com, 2021).

Linear Filter: This filtering algorithm finds outliers in the data set and replaces them by linear interpolation of the adjacent non-outlier values. Similar to Center filter, outliers in this method are the values more than three scaled median absolute deviations away from the median of the data set (Mathworks.com, 2021).

Standard Deviation Filter: In this method, the values more than certain coefficients of data set standard deviation away from the mean are considered as outliers and removed. In this study, removal of the data points more than one standard deviation away from the mean will be examined.

4.6 Results

4.6.1 Part 1: Stationary Beacon

Table 4.1 involves the detailed results for each of the stations on the grids in Experiment 1, obtained using the developed technique as an example of the calculations in the conducted experiments. The table consists of the IDs of each of the stations according to Figure 4.5, their corresponding (x, y) coordinates measured from the imaginary x and y axes passing from the intersection center, the components of the calibration vectors for each station (the average of the RSSI values, corresponding to that station in the calibration stage collected by each signal scanner), the components of the test vectors collected in the second stage, and the nearest estimated location for each of the test points, obtained in the third stage. The distance between the estimated nearest location and the real location in each case was also calculated to specify the error of the method.

Table 4.1 Positioning using KNN algorithm, stationary beacon, Experiment 1.

Real location				Calibration stage				Test data collection stage				Positioning stage (estimated location)				
#	ID	x	y	RSSI by Scanner 1	RSSI by Scanner 2	RSSI by Scanner 3	RSSI by Scanner 4	RSSI by Scanner 1	RSSI by Scanner 2	RSSI by Scanner 3	RSSI by Scanner 4	#	ID	x	y	Error (m)
1	SO8	-1.5	-25.5	-74.0	-83.0	-71.6	-69.5	-73.2	-72.0	-68.5	-69.3	3	SO6	-1.5	-19.5	6.0
2	SO7	-1.5	-22.5	-77.6	-70.5	-73.0	-66.2	-73.2	-53.0	-73.3	-68.5	26	NO1	1.5	4.5	27.2
3	SO6	-1.5	-19.5	-75.6	-69.1	-69.1	-65.7	-77.5	-71.3	-68.5	-65.4	4	SO5	-1.5	-16.5	3.0
4	SO5	-1.5	-16.5	-79.2	-69.4	-67.7	-65.4	-79.0	-69.8	-67.0	-64.2	4	SO5	-1.5	-16.5	0.0
5	SO4	-1.5	-13.5	-76.5	-70.6	-65.6	-66.1	-78.4	-70.0	-65.6	-69.0	5	SO4	-1.5	-13.5	0.0
6	SO3	-1.5	-10.5	-72.3	-68.9	-63.2	-62.0	-72.0	-68.7	-63.5	-64.0	6	SO3	-1.5	-10.5	0.0
7	SO2	-1.5	-7.5	-72.4	-81.0	-64.5	-59.7	-72.8	-75.6	-66.5	-60.3	66	WI8	-25.5	-1.5	24.7
8	SO1	-1.5	-4.5	-62.4	-74.2	-65.2	-65.8	-64.6	-76.0	-68.0	-66.0	13	NI3	-1.5	10.5	15.0
9	ISW	-1.5	-1.5	-62.4	-75.0	-71.3	-72.5	-64.0	-78.5	-69.8	-69.3	9	ISW	-1.5	-1.5	0.0
10	INW	-1.5	1.5	-65.0	-61.0	-58.0	-60.6	-63.2	-61.0	-58.0	-61.8	10	INW	-1.5	1.5	0.0
11	NI1	-1.5	4.5	-65.2	-49.6	-60.4	-66.0	-65.5	-50.7	-64.3	-67.7	11	NI1	-1.5	4.5	0.0
12	NI2	-1.5	7.5	-65.5	-72.6	-73.4	-64.0	-69.6	-75.5	-71.0	-63.2	66	WI6	-19.5	-1.5	20.1
13	NI3	-1.5	10.5	-63.6	-76.4	-68.8	-63.3	-64.5	-76.7	-69.8	-63.6	13	NI3	-1.5	10.5	0.0
14	NI4	-1.5	13.5	-67.3	-68.3	-75.3	-67.6	-68.8	-65.0	-77.7	-67.3	63	WI3	-10.5	-1.5	17.5
15	NI5	-1.5	16.5	-73.6	-65.3	-74.0	-68.1	-73.3	-66.0	-76.5	-68.7	15	NI5	-1.5	16.5	0.0
16	NI6	-1.5	19.5	-76.8	-66.3	-74.8	-70.8	-75.7	-66.8	-74.0	-71.3	16	NI6	-1.5	19.5	0.0
17	NI7	-1.5	22.5	-80.2	-70.6	-74.6	-71.4	-80.0	-71.8	-77.0	-70.8	17	NI7	-1.5	22.5	0.0
18	NI8	-1.5	25.5	-75.6	-70.4	-77.1	-73.7	-78.1	-70.8	-76.4	-75.3	18	NI8	-1.5	25.5	0.0
19	NO8	1.5	25.5	-70.3	-64.4	-71.6	-64.8	-71.2	-64.8	-69.8	-64.5	19	NO8	1.5	25.5	0.0
20	NO7	1.5	22.5	-71.7	-65.7	-73.1	-66.9	-72.7	-66.3	-72.8	-67.8	20	NO7	1.5	22.5	0.0
21	NO6	1.5	19.5	-74.4	-66.4	-72.8	-67.6	-70.8	-67.3	-72.3	-68.8	63	WI3	-10.5	-1.5	24.2
22	NO5	1.5	16.5	-77.5	-67.2	-70.5	-65.3	-74.0	-65.8	-71.0	-65.8	54	EO7	22.5	-1.5	27.7
23	NO4	1.5	13.5	-69.1	-70.2	-67.5	-62.0	-67.9	-68.5	-65.8	-62.5	30	SI2	1.5	-7.5	21.0
24	NO3	1.5	10.5	-62.8	-61.3	-69.3	-59.5	-61.7	-61.0	-67.2	-59.8	24	NO3	1.5	10.5	0.0
25	NO2	1.5	7.5	-63.3	-65.5	-72.2	-61.8	-63.8	-63.0	-74.8	-65.0	45	EI1	4.5	1.5	6.7
26	NO1	1.5	4.5	-67.7	-59.0	-64.6	-68.3	-67.7	-56.0	-63.0	-69.0	26	NO1	1.5	4.5	0.0
27	INE	1.5	1.5	-58.6	-61.9	-61.7	-74.2	-60.3	-60.6	-61.8	-75.0	27	INE	1.5	1.5	0.0
28	ISE	1.5	-1.5	-60.6	-69.9	-68.1	-66.3	-60.5	-71.5	-67.4	-67.8	28	ISE	1.5	-1.5	0.0
29	SI1	1.5	-4.5	-54.3	-69.0	-72.8	-57.3	-54.8	-69.8	-69.5	-57.0	29	SI1	1.5	-4.5	0.0
30	SI2	1.5	-7.5	-69.6	-70.0	-65.4	-62.0	-70.2	-71.5	-65.5	-61.5	30	SI2	1.5	-7.5	0.0
31	SI3	1.5	-10.5	-72.6	-63.9	-62.1	-75.8	-70.7	-62.0	-61.0	-74.8	31	SI3	1.5	-10.5	0.0
32	SI4	1.5	-13.5	-70.3	-61.9	-62.0	-71.1	-71.2	-61.0	-61.8	-69.7	32	SI4	1.5	-13.5	0.0
33	SI5	1.5	-16.5	-70.0	-66.1	-63.0	-64.9	-70.5	-66.0	-62.7	-64.0	33	SI5	1.5	-16.5	0.0
34	SI6	1.5	-19.5	-64.3	-64.9	-65.2	-64.3	-66.0	-64.5	-64.8	-65.7	34	SI6	1.5	-19.5	0.0
35	SI7	1.5	-22.5	-62.4	-67.0	-67.2	-63.9	-63.5	-66.3	-64.7	-64.8	34	SI6	1.5	-19.5	3.0

(Continued)

(Continued)

Real location				Calibration stage				Test data collection stage				Positioning stage (estimated location)				
#	ID	x	y	RSSI by Scanner 1	RSSI by Scanner 2	RSSI by Scanner 3	RSSI by Scanner 4	RSSI by Scanner 1	RSSI by Scanner 2	RSSI by Scanner 3	RSSI by Scanner 4	#	ID	x	y	Error (m)
36	SI8	1.5	-25.5	-66.2	-72.6	-65.3	-65.4	-65.0	-68.7	-67.0	-65.9	47	EI3	10.5	1.5	28.5
37	WO8	-25.5	1.5	-75.6	-76.4	-71.5	-80.8	-75.2	-73.8	-70.8	-83.4	67	WI7	-22.5	-1.5	4.2
38	WO7	-22.5	1.5	-73.9	-71.6	-67.0	-80.9	-72.8	-71.0	-67.8	-80.8	38	WO7	-22.5	1.5	0.0
39	WO6	-19.5	1.5	-71.1	-67.4	-67.8	-75.8	-69.5	-67.4	-67.0	-74.5	39	WO6	-19.5	1.5	0.0
40	WO5	-16.5	1.5	-71.6	-64.0	-67.8	-73.6	-70.8	-64.0	-70.5	-72.4	40	WO5	-16.5	1.5	0.0
41	WO4	-13.5	1.5	-72.2	-66.4	-75.6	-72.9	-71.2	-66.7	-73.0	-72.8	52	EI8	25.5	1.5	39.0
42	WO3	-10.5	1.5	-72.8	-65.5	-71.8	-78.0	-75.6	-65.5	-67.6	-79.8	42	WO3	-10.5	1.5	0.0
43	WO2	-7.5	1.5	-74.2	-66.9	-61.9	-69.3	-77.4	-64.3	-62.5	-68.0	43	WO2	-7.5	1.5	0.0
44	WO1	-4.5	1.5	-74.4	-64.2	-56.5	-64.4	-77.2	-64.6	-57.4	-62.5	44	WO1	-4.5	1.5	0.0
45	EI1	4.5	1.5	-65.7	-63.8	-75.4	-65.5	-62.2	-62.7	-76.0	-66.4	45	EI1	4.5	1.5	0.0
46	EI2	7.5	1.5	-64.0	-69.2	-69.2	-61.7	-65.8	-68.6	-67.7	-61.6	47	EI3	10.5	1.5	3.0
47	EI3	10.5	1.5	-65.3	-68.7	-67.8	-62.7	-68.0	-70.3	-68.2	-62.8	23	NO4	1.5	13.5	15.0
48	EI4	13.5	1.5	-65.4	-77.3	-70.9	-63.5	-71.5	-73.7	-70.8	-63.8	66	WI6	-19.5	-1.5	33.1
49	EI5	16.5	1.5	-62.2	-68.0	-66.6	-64.0	-62.4	-69.2	-69.0	-63.8	46	EI2	7.5	1.5	9.0
50	EI6	19.5	1.5	-62.4	-65.8	-67.8	-64.1	-59.5	-65.0	-68.2	-64.2	50	EI6	19.5	1.5	0.0
51	EI7	22.5	1.5	-66.1	-67.0	-72.1	-70.0	-67.3	-66.0	-71.3	-69.8	51	EI7	22.5	1.5	0.0
52	EI8	25.5	1.5	-71.2	-67.7	-73.3	-71.9	-66.5	-66.2	-68.0	-73.5	64	WI4	-13.5	-1.5	39.1
53	EO8	25.5	-1.5	-77.1	-71.3	-75.9	-70.0	-75.5	-69.0	-73.3	-70.6	16	NI6	-1.5	19.5	34.2
54	EO7	22.5	-1.5	-72.6	-66.8	-71.4	-66.5	-72.2	-66.8	-66.4	-65.7	55	EO6	19.5	-1.5	3.0
55	EO6	19.5	-1.5	-71.1	-67.1	-66.8	-63.1	-75.4	-67.8	-65.7	-63.0	6	SO3	-1.5	-10.5	22.8
56	EO5	16.5	-1.5	-70.8	-70.3	-63.1	-60.4	-71.5	-70.8	-64.0	-60.7	56	EO5	16.5	-1.5	0.0
57	EO4	13.5	-1.5	-71.0	-80.0	-65.6	-64.6	-68.5	-79.3	-66.3	-63.7	57	EO4	13.5	-1.5	0.0
58	EO3	10.5	-1.5	-57.2	-81.6	-65.2	-60.4	-56.6	-74.7	-63.8	-58.0	58	EO3	10.5	-1.5	0.0
59	EO2	7.5	-1.5	-62.3	-68.0	-65.5	-59.1	-61.6	-68.0	-65.7	-60.5	59	EO2	7.5	-1.5	0.0
60	EO1	4.5	-1.5	-57.0	-61.6	-74.5	-67.2	-56.8	-60.6	-75.8	-69.8	60	EO1	4.5	-1.5	0.0
61	WI1	-4.5	-1.5	-73.4	-62.6	-57.4	-53.9	-76.2	-63.2	-57.3	-53.6	61	WI1	-4.5	-1.5	0.0
62	WI2	-7.5	-1.5	-67.3	-62.4	-68.1	-57.3	-66.8	-62.0	-68.0	-58.5	62	WI2	-7.5	-1.5	0.0
63	WI3	-10.5	-1.5	-70.6	-65.0	-71.0	-68.5	-70.0	-64.6	-69.0	-68.8	63	WI3	-10.5	-1.5	0.0
64	WI4	-13.5	-1.5	-67.8	-66.8	-69.7	-75.6	-67.2	-66.4	-69.0	-77.0	64	WI4	-13.5	-1.5	0.0
65	WI5	-16.5	-1.5	-70.1	-69.6	-71.0	-72.8	-68.8	-70.8	-67.8	-71.3	65	WI5	-16.5	-1.5	0.0
66	WI6	-19.5	-1.5	-72.8	-74.7	-71.5	-61.5	-72.0	-74.2	-72.6	-82.0	67	WI7	-22.5	-1.5	3.0
67	WI7	-22.5	-1.5	-74.0	-76.4	-72.5	-83.3	-73.7	-78.3	-73.2	-79.5	37	WO8	-25.5	1.5	4.2
68	WI8	-25.5	-1.5	-73.4	-72.9	-72.3	-79.0	-72.5	-72.0	-70.5	-76.8	68	WI8	-25.5	-1.5	0.0

Table 4.2 summarizes the results of Experiments 1–4 conducted on the stationary beacon. As observed in this table, by applying KNN algorithm on the vectors of Experiment 1, in 50 cases out of 68 test points (73.5%), the location was estimated with an

error equal to or less than 5 m ([0,5]). In this experiment, the positioning error was relatively high and more than 5 m in 18 cases out of 68 (26.5%). In Experiment 1, the distance between the stations was 3 m and the four signal scanners were placed at the corners in a symmetric arrangement.

Table 4.2 Comparison of the results in Experiments 1–4 for a stationary beacon.

	Stationary beacon			
	Experiment 1	Experiment 2	Experiment 3	Experiment 4
Number of the stations	68	36	40	40
0 ≤ Positioning error ≤ 5 m (number (percentage))	50 (73.5%)	29 (80.6%)	38 (95.0%)	36 (90.0%)
Positioning error > 5 m (number (percentage))	18 (26.5%)	7 (19.4%)	2 (5.0%)	4 (10.0%)
Error range for the errors of more than 5 m (m)	6.0–39.1	6.0–39.1	17.0–23.5	8.1–16.9
Average error for the errors of more than 5 m (m)	22.8	26.5	20.3	11.5

In Experiment 2, half of the stations on each intersection leg were eliminated in a zigzag pattern, but symmetric with respect to the intersection center; therefore, the distance between each of the two stations along the street lanes was increased to 6 m. There were still four stations in the middle of the intersection; hence, the total number of the stations was 36 in this experiment. The results of the second experiment indicate that among the 36 test points, in 29 cases, positioning was done with an error of [0,5] m (80.6%). In this experiment, positioning was done incorrectly with an error of more than 5 m in the other 7 cases (19.4%).

In Experiment 3, the number of the stations was 40 and the distance between each two of them on a lane was 5 m with a zigzag pattern on the adjacent lanes. There was also a mild asymmetry in the stations and scanners arrangement. In this experiment, in 38 cases out of 40 (95.0%), positioning was done with an error of [0,5] m, whereas the number of positionings with an error of more than 5 m was only 2 (5.0%).

In the fourth experiment, there were 40 stations; the distance between each two of them on a lane was 5 m with a zigzag pattern and the four scanners made an irregular quadrilateral shape with very different angles. The quality of the results in this experiment was high, similar to the results of the third experiment. In this experiment, among the 40 positionings, the technique estimated the location with an error of [0,5] m in 36 cases (90.0%). The positioning error in the other 4 cases (10.0%) was more than 5 m.

Figure 4.10 illustrates the fit linear trend lines of positioning error averages, calculated for all the test points (different from the average error for the errors of more than 5 m, in Table 4.2) to the distance from the intersection center in the four experiments. As observed in the chart, for all the four experiments, the average positioning error tends to increase as the distance from the intersection center (the point which is overall the closest to the four signal scanners) increases. This indicates that the accuracy of positioning has its highest level in the areas near the scanners and this level may decrease as the distance between the beacon and the scanners increases. Furthermore, Comparison of the trend line of Experiment 1 with the other experiments clearly indicates a reduction in the average errors and the positive effectiveness of the two types of changes made in the stations and scanners arrangements, that is, reducing the number of the stations considering the minimum required accuracy and making the system arrangement asymmetric.

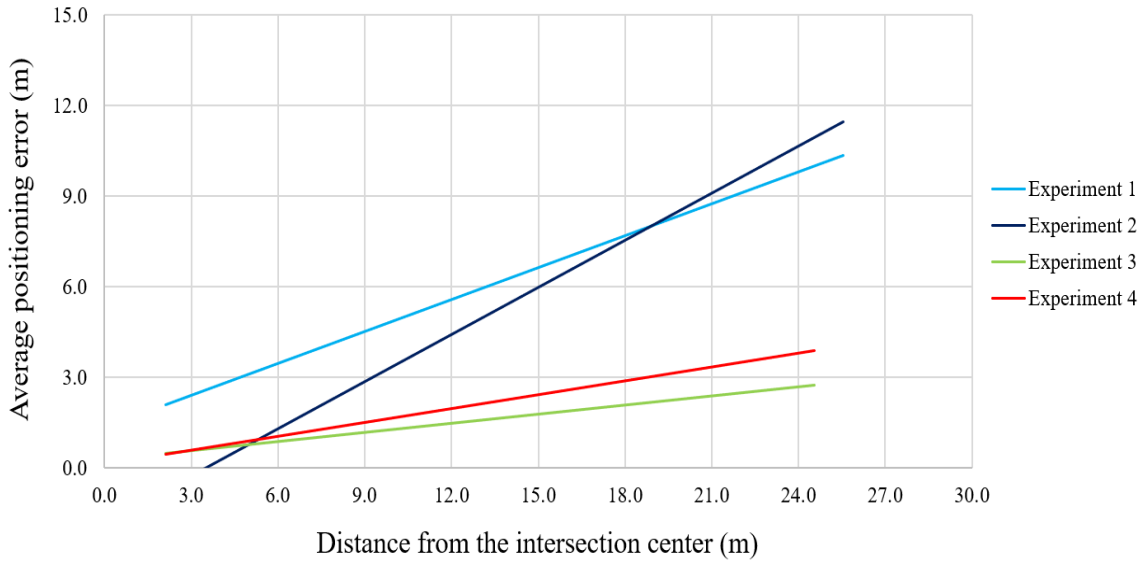

Figure 4.10 Average positioning error-distance from the intersection center chart for Experiments 1–4.

4.6.2 Part 2: Moving Beacon

The arrangement of the stations and scanners in this experiment was the same as Experiment 4 in the previous part. This set-up was selected because the results of the third and fourth experiments (asymmetric arrangements) were better compared with the results of the first and second experiments (symmetric arrangements). As described earlier, a MATLAB code was used to identify the moments at which the transmitted signals by the beacon were detected by all the four signal scanners. During the 45 min duration of data collection in the second stage, 18 moments were identified meeting the maximum time difference criterion (1 s). The corresponding RSSI values detected by each of the four signal scanners in each of these 18 moments were specified and test vectors were formed for them. KNN algorithm was applied on each of the test vectors in order to find their nearest calibration vectors. The corresponding points of the nearest calibration vectors indicated the most probable estimated locations at each of the matching moments. As mentioned earlier in the methodology, the real location of the beacon at each of the

matching moments of the second stage was obtained from the RTK data as well to be compared with the estimated locations. The results of this experiment are summarized in Table 4.3.

As observed in Table 4.3, among the 18 cases of matching moments, in 10 cases (55.6%), positioning was done with an error of [0,5] m. In this experiment, the positioning error was more than 5 m in the other 8 cases (44.4%).

Table 4.3 Summary of the results of the experiment conducted on a moving beacon.

	Moving beacon experiment
Number of the matching moments	18
0 ≤ Positioning error ≤ 5 m (number (percentage))	10 (55.6%)
Positioning error > 5 m (number (percentage))	8 (44.4%)
Error range for the errors of more than 5 m (m)	6.3–29.3
Average error for the errors of more than 5 m (m)	14.4

4.6.3 RSSI Filtering

Table 4.4 consists of RSSI values of a set of signals collected by a signal scanner from one of the stations during the 1 min data collection period in the calibration stage, as well as the filtered values using each of the five introduced filtering algorithms. As observed, Center filter, Linear filter and Standard Deviation filter identify outliers and remove them from the data. Center and Linear filters substitute the outliers with other

values in contrary to Standard Deviation filter in which the outliers are not replaced. Savitzky-Golay and Rlowess filters smooth the data set instead of removing the outliers.

Table 4.4 An example of RSSI data sets and the filtered values.

Original data set	Savitzky-Golay filter	Rlowess filter	Center filter	Linear filter	Standard Deviation filter
-77.0	-76.7	-76.9	-77.0	-77.0	-77.0
-76.0	-76.7	-76.3	-76.0	-76.0	-76.0
-77.0	-76.0	-75.5	-77.0	-77.0	-77.0
-75.0	-76.7	-75.0	-75.0	-75.0	-75.0
-78.0	-74.3	-75.0	-78.0	-78.0	-78.0
-70.0	-73.7	-73.0	-77.0	-75.5	-
-73.0	-74.0	-73.0	-73.0	-73.0	-
-79.0	-76.7	-75.5	-79.0	-79.0	-
-78.0	-78.0	-78.0	-78.0	-78.0	-78.0
-77.0	-77.0	-77.0	-77.0	-77.0	-77.0
-76.0	-76.0	-76.0	-76.0	-76.0	-76.0

Table 4.5 involves the summary of the positioning results after applying each of the five filtering algorithms on the data collected in the five conducted experiments.

Table 4.5 Summary of the positioning results after applying the filtering algorithms.

	Original data		Savitzky-Golay filter		Rlowess filter	
Experiment #	0 ≤ Positioning error ≤ 5 m (%)	Positioning error > 5 m (%)	0 ≤ Positioning error ≤ 5 m (%)	Positioning error > 5 m (%)	0 ≤ Positioning error ≤ 5 m (%)	Positioning error > 5 m (%)
Experiment 1	73.5	26.5	75.0	25.0	76.5	23.5
Experiment 2	80.6	19.4	75.0	25.0	80.6	19.4
Experiment 3	95.0	5.0	95.0	5.0	95.0	5.0
Experiment 4	90.0	10.0	90.0	10.0	87.5	12.5
Experiment 5 (moving beacon)	55.6	44.4	55.6	44.4	55.6	44.4
Average change relative to the original data (%)	-	-	-0.8	0.8	0.1	-0.1

	Center filter		Linear filter		Standard Deviation Filter	
Experiment #	0 ≤ Positioning error ≤ 5 m (%)	Positioning error > 5 m (%)	0 ≤ Positioning error ≤ 5 m (%)	Positioning error > 5 m (%)	0 ≤ Positioning error ≤ 5 m (%)	Positioning error > 5 m (%)
Experiment 1	73.5	26.5	75.0	25.0	73.5	26.5
Experiment 2	80.6	19.4	80.6	19.4	80.6	19.4
Experiment 3	95.0	5.0	95.0	5.0	95.0	5.0
Experiment 4	92.5	7.5	92.5	7.5	95.0	5.0
Experiment 5 (moving beacon)	61.1	38.9	61.1	38.9	61.1	38.9
Average change relative to the original data (%)	1.6	-1.6	1.9	-1.9	2.1	-2.1

Savitzky-Golay Filter: This filter increased the percentage of positionings with an error of [0,5] m in one experiment out of five and decreased it in another experiment. This percentage did not change in the other three experiments. Overall, this filter had a negative impact on the results, as it caused a reduction of 0.8% in the average percentage of positionings with an error of [0,5] m considering the five experiments together.

Rlowess Filter: Similar to Savitzky-golay filter, the percentage of positionings with an error of [0,5] m increased in one experiment out of five and decreased in another experiment. The average increase in the percentage of positionings with an error of [0,5] m was only 0.1 considering the five experiments.

Center Filter: This filter increased the percentage of positionings with an error of [0,5] m in two experiments, whereas it did not change this number in the other three experiments. The improvements were equal to 2.5 and 5.5% in Experiments 4 and 5 respectively. The average percentage of improvement considering the five experiments was 1.6.

Linear Filter: This filter improved the accuracy, increasing the percentage of positionings with an error of [0,5] m in three experiments, whereas this number did not change in the other two experiments. The improvements were 1.5, 2.5 and 5.5% in Experiments 1, 4 and 5 respectively. The average improvement in the five experiments was 1.9%.

Standard Deviation Filter: Applying Standard Deviation filter, the percentage of positionings with an error of [0,5] m increased in two experiments and did not change in the other three ones. The improvement was 5.0% in experiment 4, and 5.5% in Experiment

5. The average improvement in the percentage of positionings with an error of [0,5] m was 2.1% considering the five experiments together.

4.7 Discussion

The main difference between Experiment 1 and Experiment 2, conducted on a stationary beacon was the lower number of the stations in the same road segments in the second experiment compared with the first one. Comparing the results of these two experiments indicates a significant improvement in the percentage of positionings with an error of [0,5] m after reducing the number of the stations. This reduction along with meeting the minimum accuracy requirements, limits the number of the choices in the pool, from which the nearest point should be selected by KNN algorithm, and consequently results in reduction of the probability of mistakes by the algorithm. This increases the number of correct positionings and reduces the error magnitudes. By contrast, reducing the distances between the adjacent stations to the values less than the required accuracy by increasing the number of them may increase the probability of incorrect positioning. This is because of the similarity of the calibration vectors corresponding to the adjacent stations whose distances to the signal scanners are close to each other.

In Experiments 3 and 4, the arrangements were asymmetric. The results of these two experiments also indicate an improvement compared with Experiment 2, which confirms the hypothesis that introducing asymmetry to the system arrangement, and consequently the radio maps, improves the functionality of the algorithm. Probing the detailed results of the first and second experiments revealed a very probable type of errors in symmetric arrangements, which is the occurrence of folding errors. Symmetry of the stations on the radio maps (for example western and eastern stations) causes the RSSI values to be very

near each other, because of the similarity of the distances to the signal scanners. In addition, as the distance increases, the slopes of RSSI-distances curves gradually go to zero and RSSI values are very close to each other in long ranges. The result may be similar components in the calibration vectors of the symmetrical stations. Therefore, changing the locations of the scanners to an irregular and asymmetric pattern will produce differences in the distance between the stations and the scanners on different sides of the intersection. This results in different RSSI values, collected by the scanners, and reduces the error probability of KNN algorithm by decreasing the similarity among the points located on the radio maps and the calibration vectors. In fact, the increased distinction between the calibration vectors reduces the probability of the algorithm making mistakes.

It was also observed that the accuracy of positioning has its highest level in the areas near the signal scanners. This level tends to decrease as the distance between the beacon and the scanners increases and the incorrect positionings mostly occur for the points far from the scanners. This finding is reasonable according to the logarithmic pattern of RSSI-distance curves. The highest slopes in these curves are in short distances and as the distance increases, the slopes and consequently the distinction of RSSI values decrease. This is the reason for more similar calibration vectors in far distances from the signal scanners and increasing the error probability.

Although in proper stations and scanners arrangements, positioning of stationary beacons was done with an error of [0,5] m in 90.0% or more of the cases, the positioning accuracy of moving beacons had a lower level according to the results of the experiment conducted in Part 2. One reason could be the fact that the calibration vectors are normally created using average RSSI values in a time interval (1 min in this study) in order to

mitigate the impacts of RSSI fluctuations and outliers. By contrast, the test vectors for moving beacons have to be formed using single RSSI values at the matching moments. In Bluetooth mode, the signal scanner sends an enquiry to its nearby beacons in pre-set time intervals for scanning; the available beacons respond this enquiry, but the scanner only reports the first response during the mentioned period of time. Using single RSSI values for forming test vectors, increases the impacts of signal fluctuations and outliers, which causes the higher probability of incorrect positioning. It was also observed in the third chapter that motion of beacons generally increases RSSI variances. This may be another reason for lower achievable accuracy in positioning of moving beacons.

While Savitzky-golay and Rlowess filters could not improve the results, the other three algorithms, had a positive effect in increasing the accuracy of the positioning technique. Using Center, Linear and Standard Deviation filters, the average improvement in the percentage of positionings with an error of [0,5] m was 1.6, 1.9 and 2.1% respectively. The improvement in the results of the experiment on the moving beacon, obtained by these three filters was 5.5%.

The function of Savitzky-Golay and Rlowess filters is in the form of smoothing the data considering the data set members altogether. Hence, in these filters the outliers are not removed, and the average value of the data set members does not change significantly. This may be the reason these two filters were not successful in improving the results. By contrast, the other three filters identify and remove outliers from the data; therefore, by applying these filters, the average value varies more significantly compared with the first type of filters, in case outliers exist in the data set. Removing the outliers from the data mitigates the deviation of the data set average value from the standard average value,

corresponding to the distance between the beacon and signal scanner. This may result in improvement of the achievable accuracy of the wireless positioning technique.

The manufacturers of network modules are identifiable in MAC addresses (Gupta, 2016). As mentioned earlier in Chapter 3, there are some variations among the RSSI magnitudes of the signals transmitted from beacons produced by different manufacturers and in different environments. In order to have more reliable results in practice, it is recommended to create a database of reference data for different beacon manufacturers and environments. In addition, presence of obstacles in signal transmission paths may have negative impacts on the quality of the results. In these situations, attempt should be made to mitigate NLOS impacts, considering them in calibration of the models, and selecting proper installation locations for the signal scanners.

4.8 Summary

The purpose of this chapter was finding a solution for positioning of beacons transmitting wireless signals applicable in automated transportation data collection. The developed technique and the applied modifications in the set-ups and arrangements provide the possibility of locating smartphones in four-legged intersections and their surrounding areas as well as congested road segments in practice with numerous applications in traffic studies.

Bluetooth mode was used in development of the technique mainly because of the lower signal variances in this mode compared with Wi-Fi and BLE modes. The technique was based on the strength of Bluetooth signals, transmitted by beacons, creating radio maps, and applying KNN algorithm. Calibration, test data collection, and positioning were three stages of the technique.

The research was in the form of five field experiments on stationary and moving beacons. Four Bluetooth signal scanners and a beacon were used in the experiments conducted in an intersection and its approaches. The first four experiments were conducted on a stationary beacon. Attempt was made to improve the accuracy and functionality of the technique via modification of the system set-up and arrangement. Proper arrangements for the system were identified based on the results of the four experiments. The fifth experiment was conducted on a moving beacon considering the results of the experiments on the stationary beacon.

The results confirmed the functionality of the positioning technique. The modifications clearly indicated that [*i*] reducing the number of the reference stations along with meeting the minimum positioning accuracy requirements, and [*ii*] making the arrangement of the stations and signal scanners asymmetric can enhance the accuracy level of positioning. This is achieved via reducing the error probability of the algorithm and increasing the distinction level in the radio maps. By reducing the number of the reference stations via increasing the distance between them from 3 m to 5 m in each lane, and making the stations and scanners arrangement asymmetric in the first four experiments, the percentage of positionings with an error of [0,5] m, increased to 90.0–95.0% from the initial value of 73.5%.

It was observed that the positioning accuracy has its highest level in the areas near the signal scanners and this level tends to decrease as the distances between the beacon and signal scanners increase. The reason is the logarithmic pattern of RSSI-distance curves. In these curves, the highest slopes are in short distances and as the distance increases, the slopes and consequently the distinction of RSSI values gradually decrease. This results in

more similarity of the calibration vectors in longer distances from the scanners and increasing the probability of making mistakes by the algorithm.

The system arrangement in the fifth experiment which was conducted on a moving beacon was selected considering the results of the experiments on the stationary beacon. Although positioning of stationary beacons with an error of [0,5] m had a high precision in proper stations and scanners arrangements, the positioning of moving beacons was more challenging and had a lower accuracy level. The two identified reasons were using single RSSI values for forming test vectors and increase in the RSSI variances due to motion.

Different filtering algorithms were applied on the data sets in order to mitigate the impacts of signal fluctuations and outliers on the quality of the results. Five algorithms including Savitzky-Golay, Rlowess, Center, Linear and Standard Deviation filters were selected for this purpose. The developed positioning technique was followed by applying these algorithms on the data sets and the results were compared with each other to propose the most appropriate one.

The filters whose function was in the form of removing outliers from the data sets performed better compared with smoothing filters. Using the first type of filters including Center, Linear and Standard Deviation filters, the percentage of positionings with an error of [0,5] m in the experiment conducted on a moving beacon improved to 61.1% from the initial value of 55.6%.

Chapter 5: Development of a Technique for Determination of Turning Movements in Intersections Using Wireless Signals

5.1 Introduction

Traffic volumes and turning movements are among the fundamental data requirements of transportation agencies worldwide for assessment of the performance of transportation systems and their key elements such as roads and intersections. Collection of these data comes with considerable challenges requiring large resources. Traditional approaches such as manual counts and video recording are commonly used for collecting relevant data, but they suffer from critical shortcomings. They are not functional in all weather and illumination conditions and require clear line of sight between the sensor and the target vehicle. Utilization of wireless signals emitted by turning vehicles can complement video data and provide efficient coverage in adverse weather and illumination conditions. Moreover, sufficient prevalence of smart devices among road users via their smartphones or beacons enables turning movement detection for other types of road users who commonly carry these devices, *e.g.*, pedestrians and cyclists.

There have been several studies using this technology for determining travel time and OD trip distribution matrices on long road segments. However, a gap exists in applying this technology in development of suitable techniques for extracting microscopic traffic parameters such as turning movements within intersections located in dense urban areas. This is likely because of the limitation of accurate localization of road beacons as well as tracking the emission source.

This chapter builds on the outcomes of Chapter 3 and focuses on determination of turning movements in intersections. The purpose is to present the development of a method

applicable in dense urban areas, such as central business districts, in which the distances between the adjacent intersections are normally short. As elaborated in Section 1.4, in these situations, finding turning movements of road users based on the common MAC re-identification technique or determining the presence of beacons in the detection range of signal scanners solely is not practical and further information is required. The present chapter addressed this by developing a method which classifies turning movements based on signature points of RSSI-time profiles and their occurrence moments. The accuracy and functionality of the technique are examined in different conditions through extensive field experiments.

5.2 Research Equipment

Four wireless signal scanners equipped with BLE detectors and a BLE beacon were used in this research. The receiving sensitivity of the BLE detectors was −96 dBm and their transmission power was +4 dBm. Each signal detector had a 2.4 GHz, short-range, omnidirectional antenna with a gain of 0.5 dBi (Figure 5.1). The devices provided MAC address, signal mode, RSSI value and detection timestamp of the detected signals in a software platform. The beacon used in the experiments was a BLE 4.0/4.1 Signal transmitter.

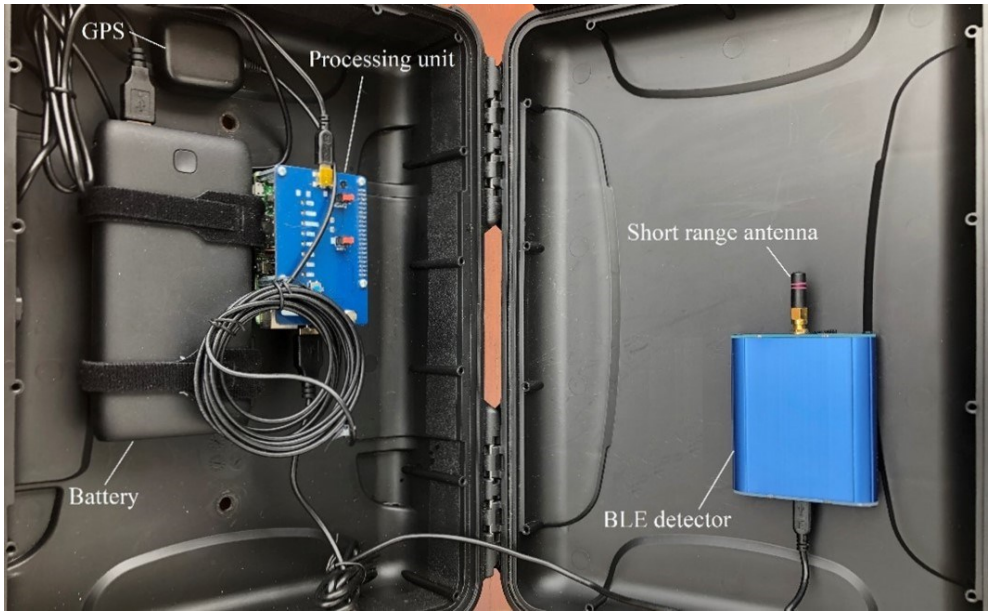

Figure 5.1 The components of a wireless signal scanner used in the experiments.

5.3 Experiments Location

The experiments of this chapter took place in a four-legged intersection located in National Capital Commission (NCC) tracks center for autonomous vehicle technologies, Ottawa, Canada (Figure 5.2). The streets leading to this intersection were two-way, two-lane. Through, right-turn and left-turn movements from the four streets were all permitted at the intersection, representing typical traffic utilization of a four-legged intersection (Figure 5.3). There were several buildings in the area, some utility poles around the intersection and outdoor Wi-Fi internet access available. Selection of this site provided the possibility of an extensive number of crossings in different situations, directions, and speeds.

(a)

(b)

Figure 5.2 (a) The location of the experiments; (b) and its aerial view (from Google Maps).

The vehicle used in the experiments was a passenger car. Although this was the only vehicle using the intersection during the experiments, the location was not isolated. There were some individuals in the vicinity and some activities taking place in there. During the experiments, the traffic lights of the intersection were deactivated. A video camera equipped with a clock recorded the experiments for reference.

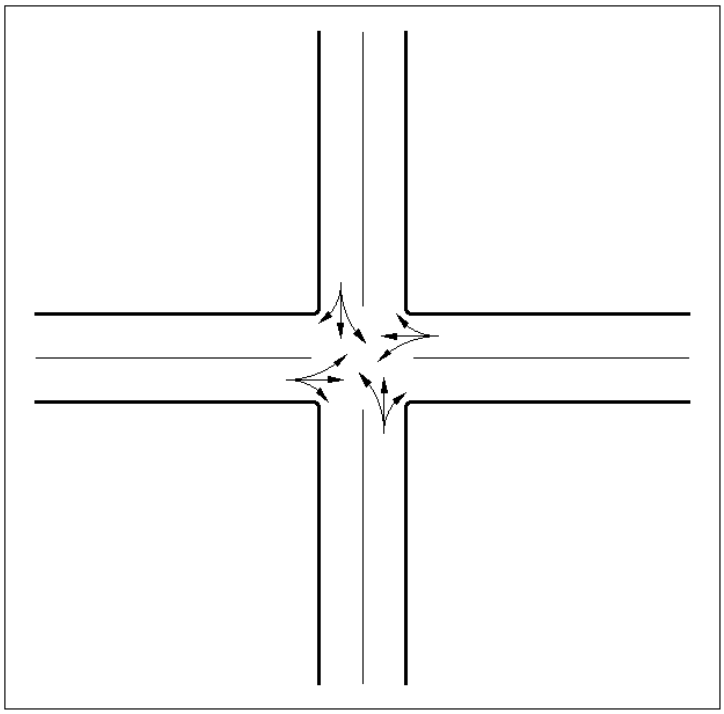

Figure 5.3 Permitted turning movements in the study site.

5.4 Analytical Preliminaries

The developed technique for determination of turning movements is on the basis of two observations in Chapter 3: [*i*] the characteristics of RSSI-distance curves in the range of 0 and around 10 m, [*ii*] a feature in BLE signal mode which is the capability of near-continuous signal transmission.

5.4.1 RSSI-Distance Curves Characteristics

It was observed in Chapter 3 that as the distance increases, average RSSI decreases logarithmically. This was true for the three studied signal modes including Wi-Fi, Bluetooth and BLE. A typical RSSI-distance curve based on the data collected by a signal scanner equipped with a short-range antenna with a detection range of around 60 m and the beacon used in the study may be observed in Figure 5.4. Although these curves always follow a logarithmic trend, some variations and fluctuations in the RSSI magnitudes are generally observed. Therefore, it is only possible to have an estimation of the distance between the beacon and the signal scanner based on these curves. According to this figure, the curve has its highest slopes when the distance between the beacon and the signal scanner is short and as the distance increases, the slope of the curve gradually decreases. As it is observed, in the range of 0 and around 10 m, the sensitivity of RSSI value to distance is relatively high and the RSSI values corresponding to this range are more distinct. The distinction of RSSI values in the mentioned range is one of the bases of the developed technique.

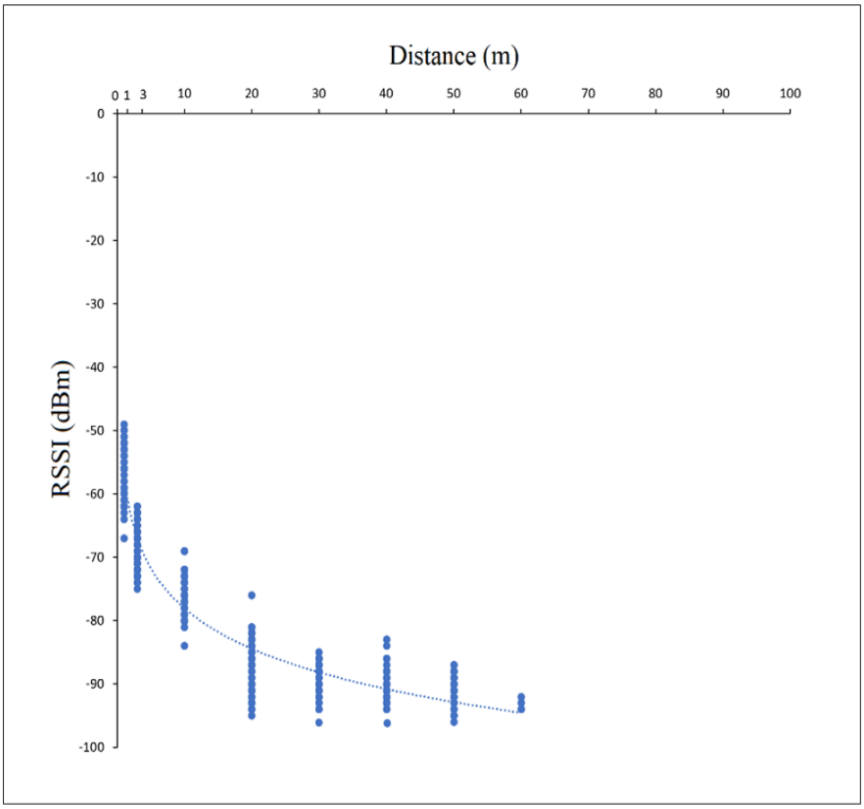

Figure 5.4 A typical RSSI-distance curve ($RSSI = -a \ln D - b$).

5.4.2 Signal Transmission Rate in BLE Mode

As observed in Chapter 3, signals in BLE mode may be transmitted by the beacon continuously (practically every second) and the signal scanners can detect them, especially when the distance is not close to the maximum detection range. It is noteworthy that based on extensive field observations, it is found that the number of the detected signals in a second is not always one and there may be multiple detections in some detection timestamps. This is unlike Wi-Fi and Bluetooth modes, in which there are several-second time intervals between the consecutive signals. This feature of BLE mode is the main reason for its selection as the applied wireless signal mode for the developed technique. It provides the possibility of detecting signals in the majority of the time period the beacon is in the detection range of a signal scanner. Having continuous signals when a beacon is

located in the detection range, is even more important for the signal scanners located on the origin and destination (origin and destination signal scanners). This makes it possible to have near-continuous RSSI-time profiles, involving signal strength values at the moments the beacon passes right in front of the origin and destination signal scanners.

5.5 Study Method

The goal is to develop a practical technique for determination of turning movements, applicable in intersections located in dense urban areas whose distances from their adjacent intersections are short. The method is based on [*i*] the characteristics of RSSI-distance curves in the range of 0 and around 10 m; [*ii*] a feature in BLE signal mode which is the capability of near-continuous signal transmission. Based on the collected data by the signal scanners, installed on the intersection legs, turning movements will be determined comparing RSSI-time profiles, created for the detected beacons.

In the location of the experiments, which was a four-legged intersection, four signal scanners were installed, one on each of the legs, on the road shoulder, close to its adjacent lane. The signal scanners were mounted at the height of 1.5 m on steel slotted angle posts with concrete bases. Short-range antennas with signal detection range of approximately 60 m in BLE mode were installed on the signal scanners, although long-range antennas with longer detection ranges were also available. This detection range means that if a beacon is detected by a signal scanner, its position is within a circle around the signal scanner with a radius of approximately 60 m at the detection moment, without any other information regarding its exact position or direction. The reason for selecting short-range antennas was minimizing the possible area of the beacon position when detected.

The first step in this technique is ensuring that a beacon is located within the intended intersection area; the traffic intersection and its legs. To determine this, the beacon should be simultaneously detected by all the four signal scanners installed on the four legs of the intersection (Figure 5.5). The distance from each of the signal scanners to its closest intersection corner was set to 17 m. The distance of 17 m was selected based on numerous field trials in order to provide a balance between two situations. If much longer distances were selected, the signal scanners would be too far from each other and would cover large areas of the adjacent intersections. In this case, it would be very probable that a beacon located in the intended intersection area is not detected by all of the signal scanners. If shorter distances were selected, adequate distinction between RSSI-time profiles of the origin and destination signal scanners and the other ones might not be provided.

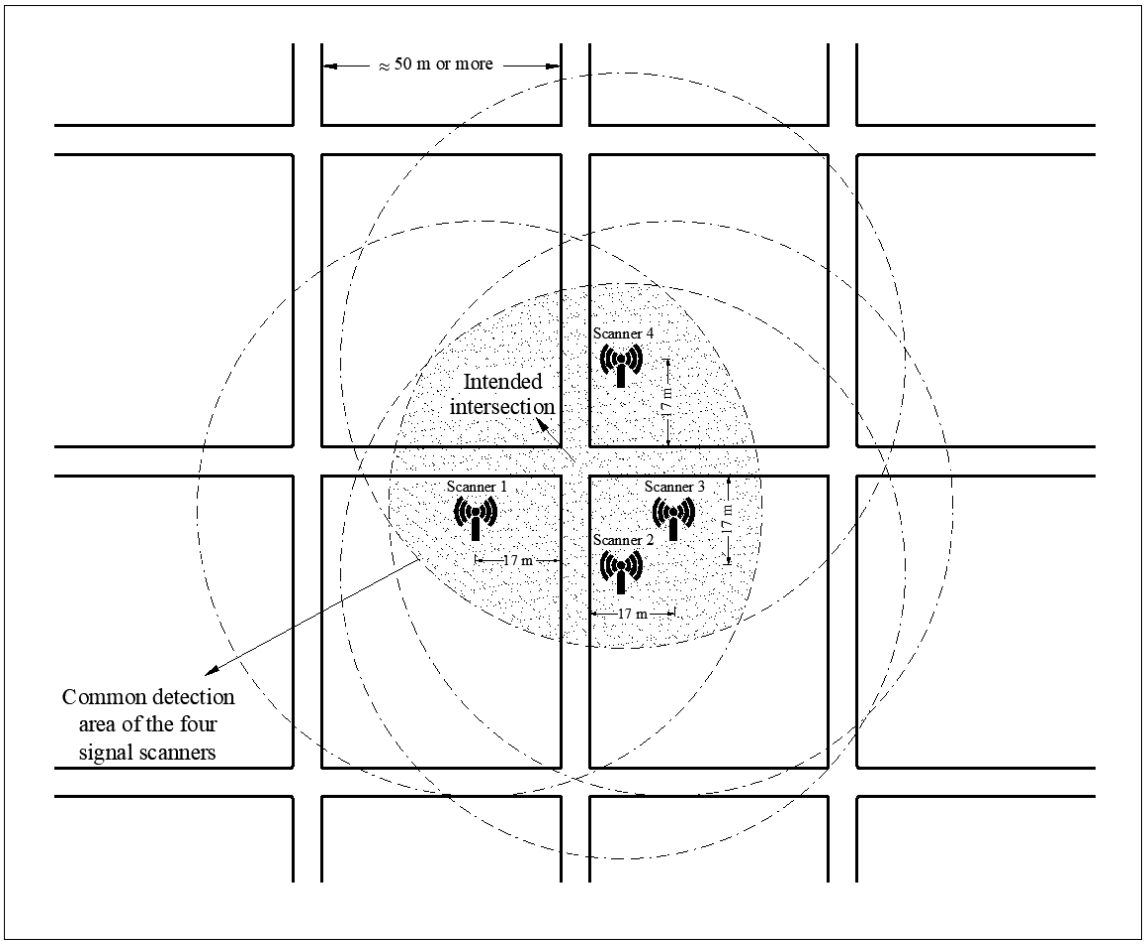

Figure 5.5 Determining the presence of a beacon in an intended intersection area. The common area of the coverage zones of the four signal scanners is the possible location of the beacon.

As the intersection was four-legged and the approaches were all two-way, there were four possible origins and four destinations. Because the through, right-turn and left-turn movements from the four streets were all permitted in the intersection, the number of the possible routes from the existing origins to the destinations was 12 (Figure 5.3). In an intersection area in which four signal scanners are installed on its legs, a beacon carried by a road user, may enter the detection zone of the origin signal scanner, cross the intersection, and exit the detection zone of the destination signal scanner. In order to provide this situation, a start and an end point were specified on each intersection leg, 80 m from the

signal scanner located on the same leg. The distance of 80 m was selected because it was longer enough than the 60-meter detection range of the signal scanners. Considering this, a route in the experiments was from the start point on an origin to an end point on a destination (Figure 5.6). A passenger car was used for carrying the beacon in the experiments. For travelling in a route, the vehicle started its motion from a start point, crossed the intersection, and ended it on an end point. Once the beacon carried by the vehicle entered the detection zone of a signal scanner, its transmitted signals were collected by the signal scanner. This continued until it exited the detection zone of the signal scanner.

The collected signals have different RSSI values, mostly depending on the distance between the beacon and the signal scanner at the detection moment. It is possible to illustrate the time-sequence of RSSI values, transmitted by the beacon and collected by the signal scanner at each detection moment during the time period the beacon was located inside the detection zone of the signal scanner in a graph. This graph is hereafter called RSSI-time profile.

There are two moments at which the vehicle travelling from an origin to a destination, passes in front of the signal scanners located on them. At each of these two moments, the distance between the beacon and the signal scanner in front of it is the shortest compared with its distance to the other signal scanners. This means that at each of these two moments, the RSSI value corresponding to the origin or destination signal scanner, should theoretically have the highest value, compared with the RSSI values of itself at the other times and also RSSI values of the other signal scanners at any time.

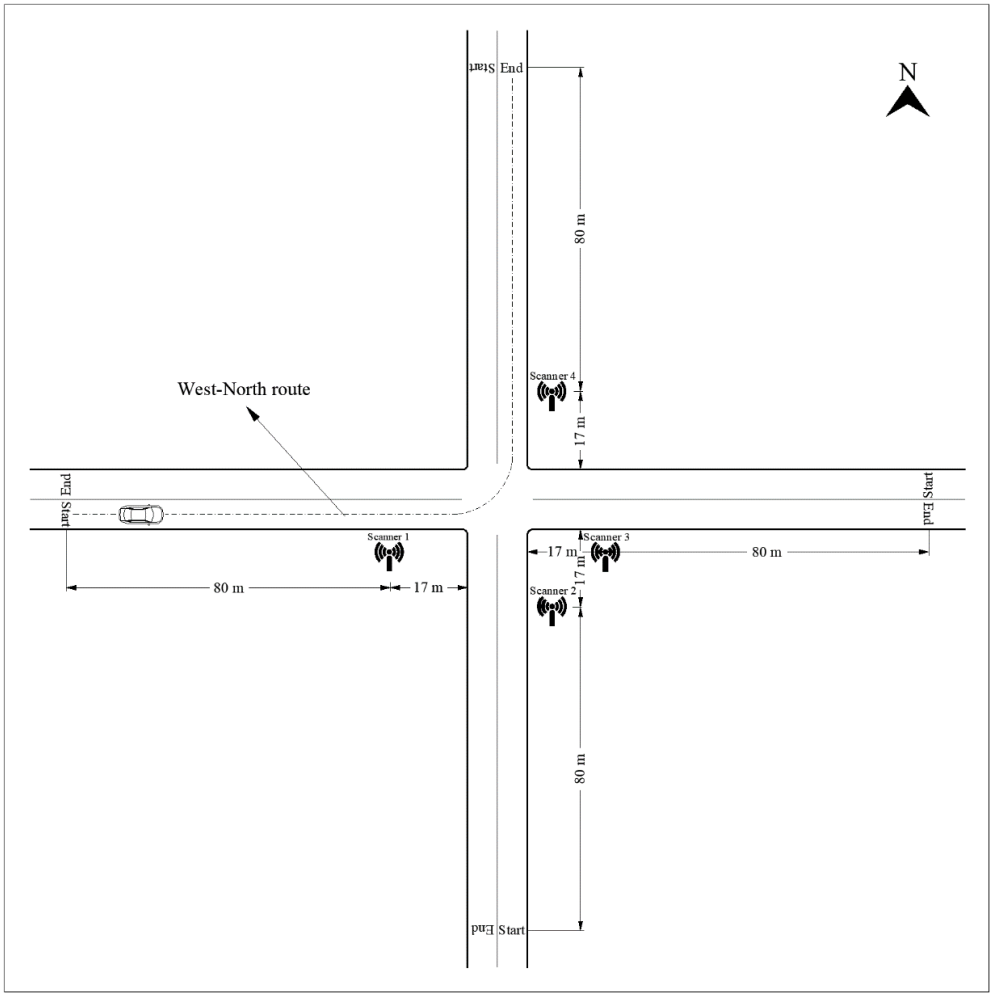

Figure 5.6 Signal scanners arrangement and start/end points of the routes (North direction is approximate.).

The intersection legs in this study were two-lane and the signal scanners were installed on the shoulders; close to their adjacent lanes. Therefore, the distance between the beacon and the origin or destination signal scanners was approximately between 1 and 7 m, when the beacon passed in front of them. This distance is in the mentioned range of 0 and around 10 m, in which RSSI-distance curves have high slopes and RSSI values are distinct compared with the RSSI values corresponding to the distances outside the range.

If RSSI-time profiles of the beacon are constructed for each of the four signal scanners, each profile will have a peak which should theoretically occur at the moment the distance between the beacon and the signal scanner is the shortest. For the signal scanners

located on the origin and destination of the route of the beacon, it will be very probable that the corresponding RSSI-time profiles have higher and distinct peak values compared with the other two profiles. The reason is that at the moment the beacon passes in front of the origin or destination signal scanners, the distance between the beacon and that signal scanner is approximately between 1 and 7 m. However, at this moment, the distance between the beacon and the other three signal scanners will be more than 24 m according to the geometry of the intersection and signal scanners arrangement. It was observed in Figure 5.4 that RSSI values in the first range are generally very distinct compared with the RSSI values in the second range.

5.5.1 Formal Procedure

Considering the above information, the procedure for finding turning movements in an intersection (four-legged intersection in this study) is presented as follows:

Input:

MAC address of a beacon, carried by a road user: (MAC)

Intersection approaches: ($Approach_n$), where $n \in \{1, \ldots, 4\}$

Output:

Origin and destination of the turning movement (O, D)

Procedure:

1. For n, find the number of times, MAC was detected by $Scanner_n$: (a_n)
2. For n, identify $RSSI$ values of MAC, detected by $Scanner_n$: ($RSSI_{n,b}$), where $b \in \{1, \ldots, a_n\}$
3. For n, identify detection timestamps corresponding to ($RSSI_{n,b}$) by $Scanner_n$,: ($t_{n,b}$)

4. Check that $\cap\{t_{n,b}\} \neq \emptyset$

   # Steps 1–4: It is required to ensure that the beacon is detected by all the four signal scanners installed on the four legs of the intersection simultaneously. If Step 4 is true, the beacon is located in the intended intersection area.

5. For n, assess $\{t_{n,b}\}$ to ensure that the timestamps are almost continuous around the moment(s) the beacon was detected by the four signal scanners simultaneously. If 4, 5 are true; then:

6. For n, create RSSI-time profile for $Scanner_n$: ($\lceil RSSI\text{-}time_n$)

   # Step 6: If the conditions, stated in Steps 4 and 5 are confirmed for a beacon, RSSI-time profiles of the beacon will be created for each of the four signal scanners during the time period, its transmitted signals have been detected by that signal scanner.

7. For n, find the peak *RSSI* of $\lceil RSSI\text{-}time_n$: ($PEAKRSSI_n$)

   # Step 7: For each of the four RSSI-time profiles, the peak *RSSI* value of the whole profile is specified. A profile may have multiple peaks with the same values.

8. Specify the two highest values among $PEAKRSSI_n$: ($RSSI_{peak,1}$, $RSSI_{peak,2}$)

   # Step 8: Among the four peak *RSSI* values of the four signal scanners, the two highest ones are determined. These two peaks may or may not be equal to each other. One of these two peak values will be corresponding to the origin signal scanner and the other peak will be corresponding to the destination signal scanner.

9. Specify the number of occurrences of $RSSI_{peak,1}$: (c)

10. Specify the number of occurrences of $RSSI_{peak,2}$: (d)
11. Specify the timestamps corresponding to $RSSI_{peak,1}$: ($t_{peak,1,e}$), where $e \in \{1, \ldots, c\}$
12. Specify the timestamps corresponding to $RSSI_{peak,2}$: ($t_{peak,2,f}$), where $f \in \{1, \ldots, d\}$

    # Steps 9–12: For the two highest peaks specified in Steps 9–10, the moments at which they occurred are specified. If there are multiple peaks with the same value in a profile, the corresponding occurrence moments of all of them are specified.

13. Specify the earliest of $t_{peak,1,e}$, $t_{peak,2,f}$: (t_{origin})
14. Specify the scanner corresponding to t_{origin}: ($Scanner_{origin}$)
15. Specify the intersection approach on which $Scanner_{origin}$ is located: (O)

    # Steps 13–15: Among the two highest peak values, determined in Step 8, the one with the earliest occurrence moment will be corresponding to the origin. This indicates that the RSSI-time profile involving this peak, belongs to the signal scanner located on the origin of the beacon route.

16. Specify the latest of $t_{peak,1,e}$, $t_{peak,2,f}$: ($t_{destination}$)
17. Specify the scanner corresponding to $t_{destination}$: ($Scanner_{destination}$)
18. Specify the intersection approach on which $Scanner_{destination}$ is located: (D)

    # Steps 16–18: Among the two highest peak values, the one with the latest occurrence moment will be corresponding to the destination. This means that the RSSI-time profile involving this peak, belongs to the signal scanner located on the destination of the beacon route.

In the above algorithm, t_{origin} and $t_{destination}$ indicate the two moments at which the beacon passed in front of the origin signal scanner and destination signal scanner

respectively. Knowing the distance between the locations of these two signal scanners, travel time and average speed of the road user carrying the beacon between the two points may also be determined.

5.5.2 Experiments

In the real word, a beacon may be in different conditions. The signals transmitted by the beacon may travel LOS or NLOS paths. Other than this, the road user carrying the beacon may have different speeds or may need to have frequent stops due to traffic conditions. Considering these factors, effort was made to simulate different situations in the form of six field experiments to examine the accuracy and robustness of the technique.

Experiment 1: In order to simulate the situations in which the speed is low and signals travel LOS paths, the intersection routes were travelled at a speed of 15 km/h, while the beacon was installed on the roof of the car. Each of the 12 possible routes in the intersection were traveled 5 times; therefore, the total number of crossings in this experiment was 60.

Experiment 2: To examine the technique in higher speeds and when the signal transmission paths are LOS, the routes were traveled at a speed of 30 km/h and the beacon was installed on the car roof. The speed of 30 km/h was the highest practical and safe speed in the experiment intersection considering its geometry. Each route was traveled 5 times in this experiment; therefore, the total number of crossings was 60, similar to the previous experiment.

Experiment 3: This experiment was designed to evaluate the robustness of the technique in conditions in which the road users have to stop behind a red light. The experiment was conducted in three situations according to the location of the stop point of

the vehicle. In the first situation, the location of the stop point (the front of the vehicle) was selected 10 m before the position of the origin signal scanner. In the second situation, the stop point was right in front of that signal scanner. In the third situation, the location of the stop point was considered 10 m after the origin signal scanner. The stop duration in each of these situations was 10 s. The speed was 15 km/h and the beacon was installed on the roof of the vehicle. Hence, in this experiment, the vehicle started its motion from the start point on an origin leg, reached the speed of 15 km/h and then kept it constant; once getting the stop point, stopped for 10 s and then started its motion again, reached the speed of 15 km/h and kept moving until got the end point of the route on a destination. Each route was travelled three times, one time dedicated to each of the three stop points. Therefore, the total number of crossings in this experiment was 36.

Experiment 4: This experiment was similar to Experiment 1, but with one difference. In order to examine the functionality of the technique in situations where signals travel in NLOS transmission paths, the beacon was placed inside the car on the dashboard, while the vehicle windows were closed. As a result, when the vehicle moved toward a signal scanner, there was at least a windscreen in the transmission path of the signals; while in the other directions, there were other obstacles such as the metal parts of the vehicle and two car occupants obstructing the path.

Experiment 5: This experiment was similar to Experiment 2. The only difference was that the beacon was placed on the dashboard inside the car while its windows were closed to change the signal transmission path to NLOS.

Experiment 6: This experiment was similar to Experiment 3, but to change the signal transmission path to NLOS, the beacon was placed on the car dashboard and the windows were closed.

5.6 Results

Determining each turning movement requires the identification of a pair of locations: origin and destination; hence, determination of a turning movement is considered correct, if the location of the beacon at the origin and destination, are both correctly identified.

For illustration, the RSSI-time profiles of the four signal scanners created for the beacon used in the study for one of the crossings of Experiment 4 may be observed in Figure 5.7. In this experiment, the speed was 15 km/h, and the beacon was placed inside the vehicle. The figure includes the peak RSSI and its occurrence moment for each of these four RSSI-time profiles. The peak RSSI values are −79, −68, −59 and −75, corresponding to the RSSI-time profiles of the signal scanners located on the west, south, east, and north intersection legs respectively. The two highest peaks among the four mentioned peaks are −68 and −59, corresponding to the south and east legs. At this point it may be concluded that south and east were the origin and destination of the turning movement, without knowing which one was the origin and which one was the destination. In Figure 5.7, it may be observed that the occurrence moment of −68, the peak of the RSSI-time profile of the south signal scanner is at 18:19:28 and the occurrence moment of −59, the peak of the RSSI-time profile of the east signal scanner is 18:19:17. It is obvious that the occurrence moment of the peak of the RSSI-time profile of the east signal scanner is before the south signal scanner; therefore it may be concluded that east was the origin of the turning movement and south was its destination.

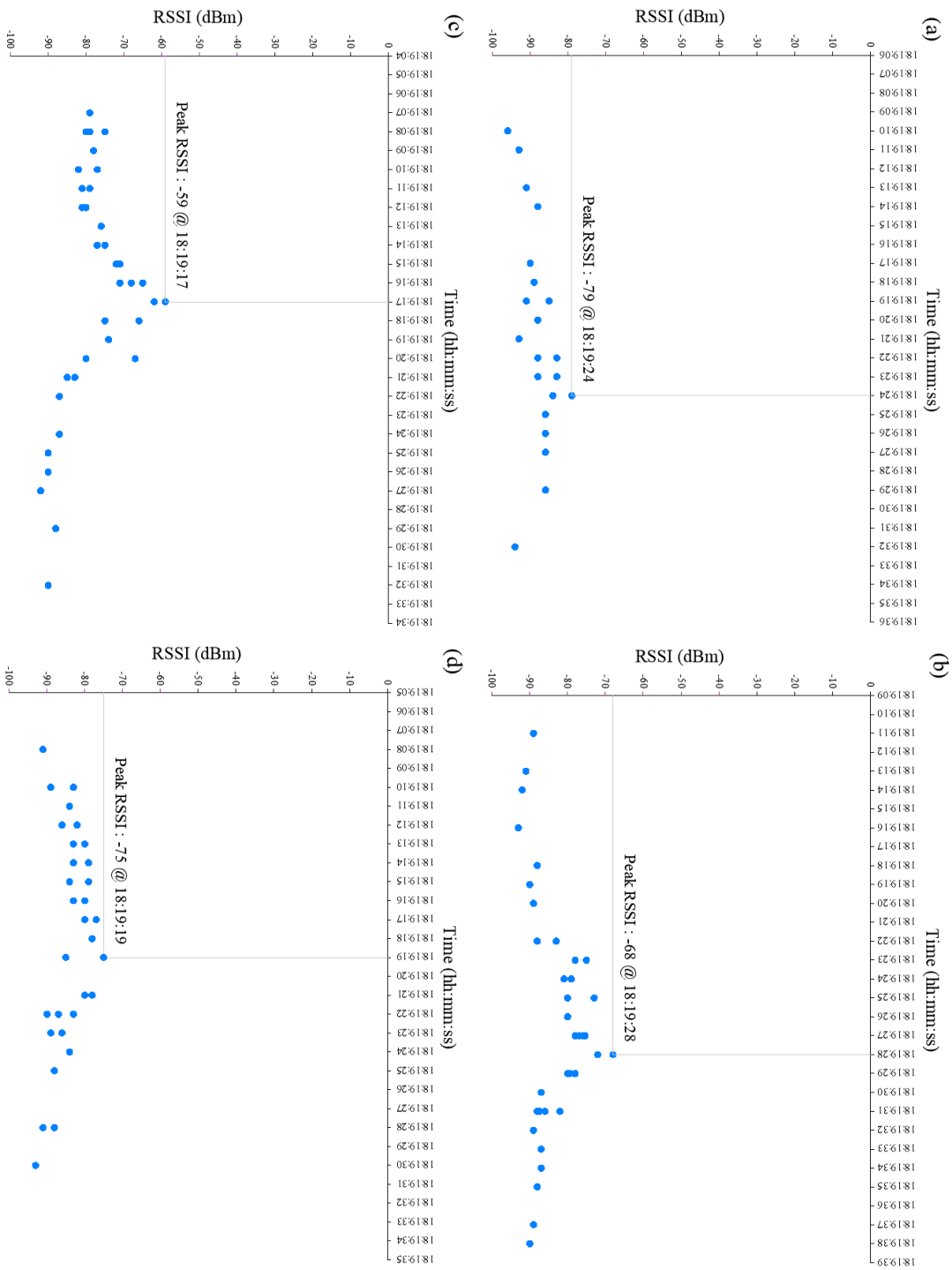

Figure 5.7 RSSI-time profiles of (a) west; (b) south; (c) east; (d) north signal scanners for a crossing in Experient 4.

The summary of the results of the six experiments conducted in this study is shown in Table 5.1. In the first three experiments, the beacon was installed on the roof of the vehicle to simulate the situations in which signals travel LOS paths. According to this table, in Experiment 1 in which the vehicle speed was 15 km/h, turning movements were determined correctly in 58 cases among the 60 crossings. This was equal to an accuracy of 96.7%. In Experiment 2, in which the speed of the vehicle was 30 km/h, turning movements were specified correctly in 56 cases out of 60 crossings, which was equal to an accuracy of 93.3%. In the third experiment in which motion-stop situations were tested at the speed of 15 km/h, the method performed correctly in 36 cases out of 36, equal to the accuracy of 100%.

Unlike the first three experiments, in Experiments 4, 5 and 6, the beacon was placed on the dashboard inside the vehicle with closed windows. Therefore, the signal transmission paths in these three experiments were NLOS. In Experiment 4, in which the vehicle speed was 15 km/h, in 56 cases out of 60 crossings, equal to 93.3%, the turning movements were determined correctly. In the fifth experiment conducted at the speed of 30 km/h, among 60 crossings, the results were correct in 55 cases, equal to 91.7%. In Experiment 6, conducted in motion-stop situations at the speed of 15 km/h, the method worked accurately in 33 crossings out of 36, which was equal to 91.7% of the cases.

Table 5.1 Summary of the results in determination of turning movements in a four-legged intersection using BLE signals.

Experiment #	Vehicle speed (km/h)	Motion type	Transmission path type	Number of crossings	Number of correct turning movement classifications	Percentage of correct turning movement classifications (%)
Experiment 1	15	Continuous	LOS	60	58	96.7
Experiment 2	30	Continuous	LOS	60	56	93.3
Experiment 3	15	Motion-stop	LOS	36	36	100.0
Experiment 4	15	Continuous	NOLS	60	56	93.3
Experiment 5	30	Continuous	NOLS	60	55	91.7
Experiment 6	15	Motion-stop	NOLS	36	33	91.7
Total				312	294	94.2

As stated earlier, since each turning movement involves an origin and a destination, in order to determine a turning movement, it is required to determine the location of the beacon two times. In the conducted experiments, in all the crossings for which the turning movement was not determined correctly, only one location among the origin and the destination was incorrectly specified; not both of them. If considering the origins and destinations separately, not as pairs, the number of the locations in each experiment will be twice the number of crossings in that experiment. Table 5.2 involves the summary of the results if the problem is turned into determining on which intersection leg the beacon is located, if it is in the intended intersection area. As observed, the accuracy in Experiments 1, 2 and 3 in which transmission paths were LOS was respectively 98.3, 96.7 and 100.0%. In Experiments 4, 5 and 6 with NLOS transmission paths, the technique determined the locations correctly in 96.7, 95.8 and 95.8 of the cases respectively. It is also observed that in all cases in which the location was determined incorrectly, the beacon was

located on the far lane of the road relative to the signal scanner at the positioning moment, not on the adjacent lane.

Table 5.2 Summary of the results in determination of origins and destinations separately in a four-legged intersection using BLE signals.

Experiment #	Vehicle speed (km/h)	Motion type	Transmission path type	Number of origins and destinations	Number of correct positionings	Correct positioning percentage (%)	Number of incorrect positionings on	
							Adjacent lane*	Far lane*
Experiment 1	15	Continuous	LOS	120	118	98.3	0	2
Experiment 2	30	Continuous	LOS	120	116	96.7	0	4
Experiment 3	15	Motion-stop	LOS	72	72	100.0	0	0
Experiment 4	15	Continuous	NOLS	120	116	96.7	0	4
Experiment 5	30	Continuous	NOLS	120	115	95.8	0	5
Experiment 6	15	Motion-stop	NOLS	72	69	95.8	0	3
Total				624	606	97.1	0	18

* Relative to the signal scanner

5.7 Discussion

The six experiments conducted in this study totally involved 312 crossings in a four-legged intersection. Turning movement was determined for each crossing among the 12 possible options. Considering the results of the six experiments altogether, the technique determined the turning movements correctly in 294 crossings out of 312, which is equal to an accuracy of 94.2%. In no cases among the 18 crossings for which the turning movement was not determined correctly, both the origin and destination were specified wrong. If considering the problem as determination of the origin and destination locations separately, the number of the cases in which the location was determined correctly was 606 out of 624, equal to 97.1% of the cases.

Wireless positioning approaches like trilateration and radio map, both require a calibration stage in which a reference for comparison of RSSI signals should be provided prior to specifying the location. This is done determining RSSI-distance formula in trilateration and forming calibration vectors in radio map technique, which are laborious and may need blockage of the positioning area. This stage may be done using beacon type, different from the one, positioning is conducted for. Additionally, the surrounding conditions in this stage may be different from the positioning conditions. These are two of the sources of the inaccuracies in the mentioned approaches, because of the variations of RSSI values for different beacon manufacturers and environmental conditions. The main reason for the high accuracy of the developed technique is that it does not require a calibration stage and a beacon is analyzed relative to itself in it, *i.e.*, only the data obtained from the target beacon in a short time period are used and compared with each other for finding a turning movement. The high percentages of correct determination of turning movements in the experiments demonstrate the accuracy and robustness of the developed technique. Nevertheless, there appear to be factors affecting the results.

Experiments 1, 2 and 3 were very similar to Experiments 4, 5 and 6 respectively, with only one difference. In the first three experiments, the beacon was installed on the roof of the vehicle to represent the situations in which signals travel LOS paths; while in the next three experiments, the beacon was placed inside the vehicle to simulate NLOS situations. Comparing the results in Experiment 1 with 4, Experiment 2 with 5, and Experiment 3 with 6 indicates a reduction in the accuracy of the results in NLOS situations which is slight.

The existence of obstructions in the transmission path of signals, causes attenuation in the strength of signals. The impacts of NLOS caused by a blocking vehicle as well as auto glass were investigated in Chapter 3 and a slight reduction around 1–3 dBm in the average RSSI values was observed compared with LOS situations in distances of less than 10 m. Although this factor seems to have some impacts on the results, the reduction in the accuracy of the technique is slight. One reason is that the reduction magnitudes in the strength of the signals passing through vehicle parts are not significant enough to severely vary the outcomes. The other reason is that in this method, the RSSI values obtained from a beacon in a short time period are compared with each other, not with other beacons in different conditions. Moreover, in this method, the peak RSSI values of RSSI-time profiles play the key role. The two highest peaks occur in the profiles of the signal scanners located on the origin and destination legs, when the beacon passes in front of them. Since in these two profiles, the peaks are the values which are important, reductions caused by obstacles such as buildings and vehicles located in the path, when the beacon is far from these two signal scanners, cannot have significant effects on the outcomes. The effect of these obstacles is in the form of reduction in the strength of the collected signals at moments other than the two moments, the beacon passes in front of the origin and destination signal scanners. Since at these two moments, the beacon is at the closest distance to the origin and destination signal scanners, the probability of the existence of large obstacles, completely blocking these signal scanners is low. An example of the situations in which the data may be spoiled is when a truck occupies some meters before and after the origin or destination signal scanners and completely blocks them.

The difference between Experiments 1 and 2 and also Experiments 4 and 5 was in the speed of the vehicle. The vehicle speed in Experiments 1 and 4 was relatively low and equal to 15 km/h, while the speed in Experiments 2 and 5 was 30 km/h, which was high for an intersection with two-lane legs. Comparing the results of each two experiments, it is observed that although there is a reduction in the accuracy at the speed of 30 km/h, it is not severe and the technique still performs well. As described earlier, in BLE mode, signals may be transmitted by the beacons and detected by the signal scanners in every second, especially in short distances. This is true when the beacon passes in front of the origin and destination signal scanners. The speed of 30 km/h is equal to 8.3 m/s; therefore, the maximum horizontal distance from which these two signal scanners may detect a signal, when the beacon passes in front of them is approximately 4.15 m (8.3 / 2). If the signal scanners are installed close to one of the lanes of a two-lane road, the maximum vertical distance between the signal scanner and the beacon carried by the vehicle will approximately be 7 m when the vehicle travels in the far lane of the road. Considering the horizontal distance of 4.15 and the vertical distance of 7 m, the maximum distance between the signal scanner and the beacon at the detection moment will be equal to the hypotenuse of the formed triangle and approximately 8.1 m. This distance is in the proper range of 0 and around 10 m in which RSSI values are distinct; hence, determination of turning movements in an intersection with two-lane legs can be done reliably, even for the vehicles traveling at the speed of 30 km/h or slightly above it, provided that the signal scanners are installed close enough to the road. This is relatively a high speed for an intersection with two-lane legs and located in dense urban areas.

It was observed in Table 5.2 that in all cases in which the origin or destination was determined incorrectly, the beacon was located on the far lane of the road relative to the location of the signal scanner at the positioning moment, not on the adjacent lane. This is because of the logarithmic pattern of the RSSI-distance curves, that is, the curve slope and the distinction of RSSI values gradually decrease as the distance increases, even in the range of 0 and 10 m. However, the impact of the increase in the distance between the beacon and signal scanner will be intensified in signal detection ranges longer than around 10 m. This range is exceeded in intersections whose legs have more than two lanes, if the signal scanners are installed outside the road. The result will be a significant reduction in the accuracy of the technique especially in determination of the turning movements for the vehicles moving on the far lanes. In intersections whose legs have three or four lanes, the maximum detection range of 10 m may be provided installing the signal scanners in the middle of the streets on the curbs if middle curbs are available or using warning signs before them due to the low speed of the vehicles in urban intersection areas.

Experiments 3 and 6 were conducted to examine the robustness of the technique in motion-stop situations. Comparing the results of these two experiments with the other four ones confirmed the robustness of the technique in these situations, as no significant difference was observed in the accuracy of the technique.

The experiments of this chapter were conducted to find the turning movements of a single vehicle. If the purpose is turning movement classification of traffic streams in an intersection, a few tasks in addition to the presented algorithm are required. The collected data may involve outliers and unwanted detections, *e.g.*, non-auto detections and stationary beacons. These detections should be removed from the data as they reduce the accuracy of

the classifications for the intended mode of travel. This may be done based on several factors such as [*i*] road user's travel time, [*ii*] the total time a beacon spends in the detection zone of the entire system including all the signal scanners and [*iii*] class of device which can be identified from the beacon MAC address. Moreover, since the collected data are samples of the actual volumes, they should be scaled up to the population using appropriate scale factors. The studies relevant to these tasks and the proposed solutions by the other researchers were cited in Chapter 2.

5.8 Summary

This chapter proposed a technique for detection and classification of turning movements, using wireless signals emitted from turning vehicles. The technique was developed and validated to be useful for small urban intersections as in such intersections, finding turning movements based on the common MAC re-identification technique is not possible. The distinction of RSSI-distance curves in the range of 0 and around 10 m and the capability of continuous signal transmission in BLE signal mode were two bases of the solution. The latter was also the main reason for selection of BLE as the applied wireless signal mode in development of the technique.

The technique utilized the time profiles of the RSSI values of the signals emitted by BLE beacons mounted on moving vehicles. The signals were collected by an array of signal scanners carefully located on the intersection approaches. Turning movements were determined comparing the peaks and their occurrence moments in the created RSSI-time profiles.

The technique was evaluated in six field experiments involving 312 crossings in a four-legged intersection with two lane legs, in which through, right-turn and left-turn

movements from the four legs were permitted. The practical feasibility and performance were examined in different situations including LOS and NLOS signal transmission paths, different relevant speeds for intersections located in congested urban areas, as well as motion-stop situations. Turning movement was determined for each crossing among the 12 possible options. The technique determined the turning movements correctly in 294 crossings out of 312. The achieved accuracy in the six experiments was between 91.7% and 100% with an overall average of 94.2%. In no cases among the 18 crossings for which the turning movement was not determined correctly, both the origin and destination were specified wrong. If considering the problem as determination of the origin and destination locations separately, the number of the cases in which the location was determined correctly was 606 out of 624, equal to 97.1% of the cases.

Comparison of the results for LOS and NLOS transmission paths indicated a reduction in the accuracy of the technique in NLOS situations, but this reduction was not large, and the performance was still well. One reason was the minor reductions in signal strengths which did not considerably affect the outcomes. The other reason was that in this method, the RSSI values obtained from a beacon in a short time period are compared with each other, not with other beacons in different conditions. Moreover, in this method, the peak RSSI values of RSSI-time profiles play the key role; conversely, the impact of presence of obstacles in the signal transmission path is in the form of reduction in RSSI values.

The effect of increasing the vehicle speed from 15 km/h to 30 km/h on the accuracy of the technique was similar to the effect of NLOS transmission path compared with LOS, *i.e.*, the reduction in the accuracy caused by the increase in speed was slight. The reason

was that due to the geometry of the intersection, speed of the vehicle and continues signal transmission feature of BLE signal mode, the maximum detection distance of the beacon passing in front of the origin and destination signal scanners was in the distinct range of 0 and 10 m in RSSI-distance curves.

The robustness of the technique was also confirmed in motion-stop situations, as these situations did not have considerable effects on the accuracy of the results. This confirms that this type of variations in the speed of the vehicles do not affect the results and the technique can be applied when the vehicles have to stop behind a red light or are in heavy traffic conditions.

Although the accuracy was slightly affected by the mentioned factors, the technique performed well in all the experiments. The achieved accuracy of the technique demonstrates its functionality and robustness in different situations. It may be applied as a practical solution for determination of turning movements in dense urban areas. The ideal situation for achieving the most satisfactory accuracy is where the installation location of the signal scanners, road geometry and the vehicle speeds provide the maximum signal detection distance of 10 m on the intersection approaches, when the vehicles pass in front of the scanners.

Chapter 6: Summary, Conclusions, Research Limitations and Recommendations for Future Research

6.1 Summary

This thesis was presented in six chapters. The subject was development of the applications of wireless signals in traffic studies. Effort was made to utilize wireless technology in automated transportation data collection.

In the first chapter, introduction, the most common types of traffic data collection which can be supported by wireless technology were overviewed. Wi-Fi, Bluetooth Classic (Bluetooth) and BLE, the three wireless signal modes utilized in this research were introduced. MAC re-identification technique, the basis for a significant part of wireless traffic data collection approaches, was explained. A number of shortcomings of those approaches were identified and the motivations for the present thesis were discussed. The objectives of the thesis were outlined, and the contributions were presented.

The second chapter was literature review. It provided an overview of the previous research relevant to the objectives of the thesis. This chapter was broadly divided into two parts. In the first part, the attributes of wireless signals with the potential to be applied in wireless signal positioning including RSSI, time of arrival, time difference of arrival and angle of arrival were overviewed. As the techniques proposed in this thesis were developed based on signal strengths, the focus was mostly on RSSI attribute of the signals. Several models developed for the relationship between RSSI and distance, as the foundation for RSSI-based positioning were introduced. Different studies on wireless signal positioning and the progress made in this area were also reviewed in the first part.

The second part of Chapter 2 covered past studies on the applications of wireless signal scanning in the field of transportation. These studies were classified into six major categories: [*i*] travel time and speed measurement, [*ii*] traffic flow and density, [*iii*] origin-destination, [*iv*] travel modes, [*v*] public transit, and [*vi*] safety applications. The first category had two subcategories due to the extent of the relevant studies: [*i*] outlier removal from travel time data and, [*ii*] travel time in alternative routes and vehicle trajectories. These are two important subjects, necessary for enhancing the quality and accuracy of travel time and speed measurements.

The third chapter investigated the characteristics of Wi-Fi, Bluetooth and BLE signals important in traffic studies which require the positional data of road users in the form of a comparative study. Considering the requirements of traffic studies, five factors including RSSI-distance relationship, precipitation effects on the signals, motion effects, NLOS effects, and signal transmission rates were selected for evaluation. The characteristics of the three signal modes were investigated and compared with each other based on the results of the experiments to find out which one provides better outcomes in terms of quality, accuracy, and convenience of traffic data collection.

The special case of integration of wireless technology in vehicle-pedestrian collision warning systems was discussed as an example of the applications of the comparative study. The effects of each of the five studied factors were probed considering the requirements of these systems to identify the most suitable signal mode for integration in them.

A technique for positioning of beacons based on their transmitted signals, applicable in transportation studies was developed in Chapter 4. This technique provides the possibility of positioning in intersections and their surrounding areas as well as congested

road segments. Bluetooth mode was selected for development of the technique mainly because of the lower signal variances in this mode compared with Wi-Fi and BLE modes. The technique was based on the strength of signals, transmitted by beacons, creating radio maps, and applying a mathematical algorithm called k-nearest neighbors (KNN). Calibration, test data collection, and positioning were three stages of the technique.

Five field experiments were conducted in a four-legged intersection. The first four experiments were on stationary beacons and the fifth one was on a moving beacon. In the experiments on the stationary beacon, attempt was made to optimize the procedure and improve the accuracy and functionality of the technique via modification of the system set-up and arrangement.

In order to further improve the accuracy of the technique, filtering algorithms were used to mitigate the impacts of signal fluctuations and outliers on the results. For this purpose, five filtering algorithms including Savitzky-Golay, Rlowess, Center, Linear and Standard Deviation were selected. The filters smoothed the data sets and removed the outliers from them. The algorithms were applied on the data sets and the results were compared with each other to propose the most appropriate ones.

Chapter 5 aimed at turning movement classification in intersections. A technique for finding turning movements based on wireless signals emitted by turning road users was developed. Effort was made to provide the solution applicable in dense urban areas such as central business districts in which the distances between the adjacent intersections are normally short.

BLE signal mode was used in development of the technique. The signals collected by the signal scanners, carefully located on the intersection approaches were used to create

RSSI-time profiles of moving beacons. Turning movements were determined comparing the peaks and their occurrence moments in the RSSI-time profiles. The accuracy and functionality of the technique was validated in six field experiments conducted in a four-legged intersection in which through, right-turn and left-turn movements from the four legs were permitted. LOS and NLOS signal transmission paths, different speeds, and motion-stop situations were covered in the experiments.

6.2 Conclusions

- Comparison of the fitness of RSSI-distance curves to the raw data and RSSI variances in the three signal modes indicated the superiority of Bluetooth and BLE modes. While the R-squared value was the highest in BLE mode, Bluetooth RSSI values had lower variances which increase the potential for more accurate distance estimation and positioning.
- Rainfall did not significantly affect the data in comparison with normal weather conditions in the three modes. This indicates that data collection stage in traffic studies may be conducted in rainy weather conditions.
- Beacon motion did not have severe impacts on the average RSSI values in any of the three modes. However, it increased RSSI variances, which may decrease the positioning accuracy of moving beacons. No considerable difference in the severity of the motion impacts on moving beacons was observed comparing the three modes with each other.
- Glass and vehicle obstacles caused a reduction in the number and strength of the signals. The obstacles did not have systematic impacts on RSSI variances. The reduction magnitudes in the number and strength of the signals were higher for the

vehicle obstacle especially at far distances. The changes in these parameters were not considerably different among the three modes.

- In Wi-Fi and Bluetooth modes, simultaneous detection rates of multiple signal scanners were very low. By contrast, the probability of having simultaneous detections was very high in BLE mode. Lower simultaneous detection rates in Wi-Fi and Bluetooth modes were mostly due to the lower signal transmission rates of beacons and higher detection intervals of signal scanners in these two modes in comparison with BLE mode. The outcome is that if applying Wi-Fi or Bluetooth scanning modes, the duration of traffic data collection for positioning of road users should be considered much longer compared with BLE mode.
- Overall consideration of the above factors indicates the superiority of Bluetooth and BLE modes over Wi-Fi in traffic studies, especially when positioning of road users is important. In case the accuracy of positioning has the highest priority, Bluetooth mode may be the most proper option. However, the time required for data collection in BLE mode is much shorter compared with Bluetooth mode which makes it a proper option when data collection time is limited. Wi-Fi mode is not recommended for these types of traffic studies.
- BLE mode is recommended as the most suitable signal mode for integration in vehicle-pedestrian collision warning systems. This is mainly because of the potential of this mode in providing the possibility of fast collision warnings thanks to its high signal transmission rates.

- The functionality of the wireless signal positioning technique developed based on the strengths of signals, creating radio maps, and applying KNN algorithm was confirmed through the conducted experiments.
- The modifications in the set-ups and arrangements for improving the accuracy of the positioning technique clearly indicated that [*i*] reducing the number of the reference stations along with meeting the minimum positioning accuracy requirements, and [*ii*] making the arrangement of the stations and signal scanners asymmetric can enhance the accuracy level of positioning. This is achieved via reducing the error probability of the algorithm and increasing the distinction level in the radio maps.
- The accuracy of positioning has its highest level in the areas near the signal scanners. This level tends to decrease as the distances between the beacon and the signal scanners increase. The reason is the higher similarity among the calibration vectors in longer distances from the signal scanners, due to the logarithmic pattern of RSSI-distance curves.
- While a high accuracy in positioning of stationary beacons was achieved by the developed technique via modification of the system set-up and arrangement, positioning of moving beacons was more challenging and had a lower level. The two identified reasons were using single RSSI values for forming test vectors of moving beacons and increase in the variances of RSSI values due to motion.
- The performance of the filters whose function was removing outliers from the data sets was better compared with the performance of smoothing filters. Linear, Center and Standard Deviation filters belonged to the first type, whereas Savitzky-golay and Rlowess filters were of the second type. Using smoothing filters, the outliers are not

removed, and the average value of the data set members does not change significantly. This may be the reason smoothing filters were not successful in improving the results. By contrast, applying the filters which identify and remove outliers from the data, the average value varies more significantly compared with smoothing filters, in case outliers exist in the data set. Removing the outliers from the data mitigates the deviation of the data set average value from the standard average value, corresponding to the distance between the beacon and signal scanner. This may result in improvement of the achievable accuracy by the wireless positioning technique.

- The accuracy, functionality, and robustness of the developed technique for turning movement classification based on RSSI-time profiles was confirmed according to the results of the experiments. The high accuracy of the technique in different situations indicated that it may be applied as a practical solution for determination of turning movements in dense urban areas.
- BLE mode was recommended to be used in development of the turning movement classification technique. The most important reason was the high signal transmission rate in this mode which provided the possibility of creating near-continuous RSSI-time profiles.
- A certain condition is required to achieve satisfactory accuracies in determination of turning movements by the proposed technique. The installation location of the signal scanners, road geometry and the vehicle speeds should provide the maximum signal detection distance of 10 m on the intersection approaches, when the vehicles pass in front of the scanners. This ensures that when the vehicles pass in front of the origin

and destination signal scanners, there are signals transmitted from the range in which RSSI values are distinct from the RSSI values corresponding to longer distances.

- The main reason for the high accuracy of the turning movement classification technique is that it does not require a calibration stage and a beacon is analyzed relative to itself in it, *i.e.*, only the data obtained from the target beacon in a short time period are used and compared with each other for finding a turning movement.
- NLOS signal transmission paths caused a reduction in the accuracy of turning movement classification technique in comparison with LOS paths, but this reduction was slight, and the technique still performed well in NLOS situations. One reason is the slightness of the reductions in the strength of the signals which do not considerably vary the outcomes; but the more important reason is that in in this technique, the peak RSSI values play the key role. By contrast, the impact of obstacles is in the form of reduction in RSSI values.
- The effect of increasing the vehicle speed from 15 km/h to 30 km/h on the results of the turning movement classification technique was a slight reduction in the accuracy. The reduction in the accuracy might not be slight if the maximum signal detection distance of 10 m on the origin and destination intersection legs was not observed when the vehicles passed in front of the signal scanners. Installation location of the signal scanners, speed of the vehicle and continues signal transmission feature in BLE mode provided the maximum detection distance of 10 m for the origin and destination signal scanners.
- Motion-stop situations did not have significant effects on the results. This confirms that this type of speed variations does not affect the results and the technique still

works when the vehicles have to stop behind a red light or are in heavy traffic conditions.

- The present research is one of the first studies which tried to apply RSSI in determination of traffic parameters, whereas the previous studies took only the advantage of MAC addresses and detection timestamps. Application of RSSI in transportation studies can enhance the accuracy level of the measurements and provide the possibility for determination of a wider range of parameters thanks to its potentials in providing the positional data of road users.
- Utilization of a traffic data collection technique by traffic practitioners is dependent on its cost-effectiveness and the affordability of the required equipment. Practical acceptance of wireless signal scanning systems may benefit from the long-lasting and low-cost availability of wireless technology in the market, the economic scalability of mass production and the advances in development of vehicular-specific amendments of wireless standards. Currently, wireless signal scanning systems are commercially available and widely used by traffic agencies. The supplement of this economic advantage is that today, most road users are carriers of different types of wireless signal transmitters thanks to their personal smart devices.

6.3 Research Limitations

- The purpose of the second experiment in Chapter 3 was investigating precipitation impacts on the signals. This experiment was conducted under moderate rainfall. Although the impacts were discussed, the test did not involve snowy and heavy rainy conditions.

- Experiment 3 in the third chapter was conducted to investigate the impacts of motion on the quality of signals; hence, it was necessary to keep the other factors, especially the distance between the beacon and the signal scanner constant. This was only possible by moving on a circle. The radius of the circle was selected equal to 10 m in order to be in the distinct range of RSSI-distance curves (between 0 and around 10 m). In this set-up, it was not possible to use a vehicle to test motion impacts in high speeds.
- Experiment 4 in the third chapter was conducted to investigate the impacts of NLOS signal transmission paths on wireless signals. In this experiment, the impacts of auto glass and vehicle blockage as two examples of the situations causing NLOS in traffic systems were evaluated. However, thorough study of NLOS impacts may require extensive research and lots of experiments. It should be mentioned that different materials exist in the real world and even in vehicles, which may cause more or less severe impacts on the signals compared with the obtained results.
- In the experiment conducted on a moving beacon in Chapter 4, the beacon was carried by a person walking at the speed of approximately 5 km/h. In this experiment, it was required to specify the position of the beacon at certain timestamps with an error of less than 1.5 m (half of the distance between the closest stations). Vehicles were not used in this experiment because of the limitation of the utilized RTK system in determining the position with the required accuracy. This device was able to specify the position in one-second time intervals. Even if a vehicle with the speed of 15 km/h (4.2 m/s) was used, it would move 4.2 m per second. Hence, the inaccuracy

of positioning would be more than 4.2 m considering the fact that the device itself had some inaccuracies as well.

- The experiments of the fifth chapter were conducted to find the turning movements of a single vehicle. If the purpose is turning movement classification of traffic streams in an intersection, a few tasks in addition to the presented algorithm are required. The collected data may include outliers and unwanted detections, *e.g.*, non-auto detections and stationary beacons. These detections should be filtered from the data as they reduce the accuracy of the classifications for the intended mode of travel. Furthermore, since the collected data are samples of the actual volumes, they should be scaled up to the population using appropriate scale factors. The studies relevant to these tasks and the proposed solutions by the other researchers were cited in the second chapter.
- The presented findings are specific to the experiments, equipment and setup procedures used in this study. The generality of the findings needs to be further examined.

6.4 Recommendations for Future Research

- There may be road users carrying more than one beacon. Current models for analysis of the signals detected by wireless signal scanners are not able to filter the signals transmitted by the extra beacons. Although this issue may be addressed setting suitable scale factors for finding traffic volumes, finding a solution for filtering this type of signals may improve the accuracy of traffic volume measurements.
- Development of a solution for finding queue length based on wireless signals is recommended.

- Using the potentials of wireless signal scanning systems in real-time determination of level of service is recommended.
- The accuracy of the proposed technique for positioning of moving beacons was lower than the accuracy for stationary beacons. Using time difference of arrival of signals may provide the possibility for positioning of moving beacons more accurately. However, it should be noted that this technique will require extremely precise instruments.
- Bluetooth 5 has been improved for measurement of angle of arrival and angle of departure. Utilizing Bluetooth 5 features is another recommendation for development of positioning techniques.
- The fifth generation of cellular networks (5G) provides the foundation for internet of things. Connecting vehicles can open the door for numerous applications of wireless technology in transportation systems. Utilizing 5G in design of dynamic traffic control and danger alert systems is recommended.

References

Abbas, M., Rajasekhar, L., Gharat, A. & Dunning, J. P., 2013. Microscopic Modeling of Control Delay at Signalized Intersections Based on Bluetooth Data. *Journal of Intelligent Transportation Systems,* Volume 17 (2), pp. 110-122.

Aimsun, 2021. *aimsun.com.* [Online] Available at: aimsun.com [Accessed 2021].

Alan, H. & Chi-Yu, H., 2010. *802.11 Wireless Networks: Security and Analysis.* London, UK: Springer.

Allström, A. et al., 2014. Calibration Framework based on Bluetooth Sensors for Traffic State Estimation Using a Velocity based Cell Transmission Model. *Transportation Research Procedia ,* Volume 3, pp. 972-981.

American Automobile Association Inc., 2019. *Automatic Emergency Braking with Pedestrian Detection,* s.l.: s.n.

Bachmann, C., Roorda, M. J., Abdulhai, B. & Moshiri, B., 2013. Fusing a Bluetooth Traffic Monitoring System With Loop Detector Data for Improved Freeway Traffic Speed Estimation. *Journal of Intelligent Transportation Systems,* pp. 152-164.

Barceló, J., Montero, L., Marqués, L. & Carmona, C., 2010. Travel Time Forecasting and Dynamic Origin–Destination Estimation for Freeways Based on Bluetooth Traffic Monitoring. *Transportation Research Record: Journal of the Transportation Research Board,* Volume 2175, pp. 19-27.

Bathaee, N. et al., 2018. A cluster analysis approach for differentiating transportation modes using Bluetooth sensor data. *Journal of Intelligent Transportation Systems,* Volume 22, NO. 4, pp. 353-364.

Bensky, A., 2016. *Wireless positioning technologies and applications.* 2nd ed. Boston: Artech House.

Bluetooth SIG, 2016. *Bluetooth Core Specification Version 5.0,* s.l.: Bluetooth SIG.

Bluetooth SIG, 2019. *Bluetooth Core Specification Version 5.1,* s.l.: Bluetooth SIG.

Bluetooth SIG, 2021. *Bluetooth Core Specification Version 5.3,* s.l.: Bluetooth SIG.

Bluetooth SIG, 2021. *Bluetooth SIG.* [Online] Available at: Bluetooth.com

Cao, H. et al., 2021. Fingerprint Positioning Method for Dual-Band Wi-Fi Based on Gaussian Process Regression and K-Nearest Neighbor. *International Journal of Geo-Information,* pp. 1-18.

Carpenter, C., Fowler, M. & Adler, T. J., 2012. Generating Route-Specific Origin–Destination Tables Using Bluetooth Technology. *Transportation Research Record: Journal of the Transportation Research Board,* Volume 2308, pp. 96-102.

Chen, M. & Chien, S. I. J., 2001. Determining the Number of Probe Vehicles for Freeway Travel Time Estimation by Microscopic Simulation. *Transportation Research Record,* Volume 1719, pp. 61-68.

Chen, Y. & Councill, I. G., 2003. *An Introduction to Support Vector Machines: A review,* s.l.: s.n.

Chitturi, M. V., Shaw, J. W., Campbell, J. R. & Noyce, D. A., 2014. Validation of Origin–Destination Data from Bluetooth Reidentification and Aerial Observation. *Transportation Research Record: Journal of the Transportation Research Board,* Volume No. 2430, Transportation Research Board of the National Academies, p. 116–123.

Cunche, M., 2014. I know your MAC address: targeted tracking of individual using Wi-Fi. *J Comput Virol Hack Tech,* pp. 219-227.

Dalal, U., 2015. *Wireless Communication and Networks.* New Delhi: Oxford University Press.

Devaki, C., Rainer, L. & Juho, P. eds., 2019. *5G for the Connected World.* New Jersey: John Wiley & Sons, Inc..

Dion, F. & Rakha, H., 2006. Estimating dynamic roadway travel times using automatic vehicle identification data for low sampling rates. *Transportation Research Part B,* Volume 40, pp. 745-766.

Dunlap, M., Li, Z., Henrickson, K. & Wang, Y., 2016. Estimation of Origin and Destination Information from Bluetooth and Wi-Fi Sensing for Transit. *Transportation Research Record: Journal of the Transportation Research Board,* Volume 2595, pp. 11-17.

Emami, A., Sarvi, M. & Asadi Bagloee, S., 2020. Short-term traffic flow prediction based on faded memory Kalman Filter fusing data from connected vehicles and Bluetooth sensors. *Simulation Modelling Practice and Theory,* Volume 102, pp. 1-17.

Farid, Z., Nordin, R. & Ismail, M., 2013. Recent Advances in Wireless Indoor Localization Techniques and System. *Journal of Computer Networks and Communications,* Volume 2013, pp. 1-12.

Florida Department of Transportation, 2021. *Manual on Uniform Traffic Studies.* Tallahassee, Florida: Traffic Engineering & Operations Office.

Friesen, M. et al., 2014. Vehicular Traffic Monitoring Using Bluetooth Scanning Over a Wireless Sensor Network. *Canadian Journal of Electrical and Computer Engineering,* Volume 37, No. 3, pp. 135-144.

Friesen, M. R. & McLeod, R. D., 2015. Bluetooth in Intelligent Transportation Systems: A Survey. *International Journal of Intelligent Transportation Systems Research,* Volume 13, pp. 143-153.

Garger, N. J. & Hoel, L., 2018. *Traffic and Highway Engineering.* Fifth ed. Boston: Cengage.

Garrido-Valenzuela, F., Raveau, S. & Herrera, J. C., 2022. Bayesian Route Choice Inference to Address Missed Bluetooth Detections. *IEEE Transaction on Intelligent Transportation Systems,* Volume 23, pp. 1865-1874.

Ghilani, C. D. & Wolf, P. R., 2012. *Elementary Surveying: An Introduction to Geomatics.* 13th ed. s.l.:Prentice Hall.

Gong, Y. & Abdel-Aty, M., 2021. Using Machine Learning to Estimate Pedestrian and Bicyclist Count of Intersection by Bluetooth Low Energy. *Journal of Transportation Engineering,* pp. 1-9.

Gong, Y., Abdel-Aty, M. & Park, J., 2019. Evaluation and augmentation of traffic data including Bluetooth detection system on arterials. *Journal of Intelligent Transportation Systems,* pp. 1-13.

Greatlearning, 2020. *mygreatlearning.com.* [Online] Available at: https://www.mygreatlearning.com/blog/support-vector-regression/

Gu, J. et al., 2021. Spatio-temporal trajectory estimation based on incomplete Wi-Fi probe data in urban rail transit network. *Knowledge-Based Systems,* Volume 211, pp. 1-13.

Gupta, N., 2016. *Inside Bluetooth Low Energy.* 2nd ed. Boston/London: Artech House.

Hainen, A. M. et al., 2011. Estimating Route Choice and Travel Time Reliability with Field Observations of Bluetooth Probe Vehicles. *Transportation Research Record: Journal of the Transportation Research Board,* Volume 2256, pp. 43-50.

Han, K. et al., 2019. Direct Positioning Method of Mixed Far-Field and Near-Field Based on 5G Massive MIMO System. *IEEE Access,* Volume 7, pp. 72170-72181.

Herrera, J. C. et al., 2010. Evaluation of traffic data obtained via GPS-enabled mobile phones: The mobile century field experiment. *Transportation research. Part C, Emerging technologies,* Volume 18 (4), pp. 568-583.

Hou, Y., Yang, X. & Abbasi, Q. H., 2018. Efficient AoA-Based Wireless Indoor Localization for Hospital Outpatients Using Mobile Devices. *Sensors,* Volume 3698, pp. 1-17.

Kuhn, M. & Johnson, K., 2013. *Applied Predictive Modeling.* 1st ed. s.l.:Springer Nature.

Kurkcu, A. & Ozbay, K., 2017. Estimating Pedestrian Densities, Wait Times, and Flows with Wi-Fi and Bluetooth Sensors. *Transportation Research Record: Journal of the Transportation Research Board,* Volume 2644, pp. 72-82.

Labiod, H., Afifi, H. & De Santis, C., 2007. *Wi-Fi, Bluetooth, ZigBee and WiMAX.* Dordrecht, The Netherlands: Springer.

Lee, J. G. et al., 2016. Accuracy Enhancement of RSSI-based Distance Estimation by Applying Gaussian Filter. *Indian Journal of Science and Technology,* Volume 9 (20), pp. 1-5.

Lee, J. K., Kim, Y., Lee, J.-H. & Kim, S.-C., 2014. An Efficient Three-Dimensional Localization Scheme Using Trilateration in Wireless Sensor Networks. *IEEE Communications Letters, Vol. 18, No. 9,* pp. 1591-1594.

Leica Geosystems, L. C., 2019. *Leica CS35.* [Online] Available at: file:///C:/Users/srrs2/Downloads/Leica_Captivate_DS_CS35-MK5_en.pdf

Leica Geosystems, L. G., 2019. *Leica GS15.* [Online] Available at: https://w3.leica-geosystems.com/downloads123/zz/gpsgis/viva%20gnss/brochures-datasheet/leica_viva_gnss_gs15_receiver_ds_en.pdf

Liu, H., Darabi, H., Banerjee, P. & Liu, J., 2007. Survey of Wireless Indoor Positioning Techniques and Systems. *IEEE Transactions on Systems, Man, and Cybernetics - Part C: Applications and Reviews,* Volume 37, pp. 1067-1080.

Maclookup.app, 2021. *maclookup.app.* [Online] Available at: maclookup.app [Accessed 2021].

Makki, A., Siddig, A., Saad, M. & Bleakley, C., 2015. Survey of WiFi positioning using time-based techniques. *Computer Networks, 88,* pp. 218-233.

Martin, J. et al., 2017. *A Study of MAC Address Randomization in Mobile Devices and When it Fails.* s.l., De Gruyter, pp. 365-383.

Mathworks.com, 2021. *mathworks.com.* [Online] Available at: https://www.mathworks.com/help/matlab/ref/filloutliers.html [Accessed 2021].

Mathworks.com, 2021. *mathworks.com.* [Online] Available at: https://www.mathworks.com/help/curvefit/smoothing-data.html [Accessed 2021].

Mercader, P. & Haddad, J., 2020. Automatic incident detection on freeways based on Bluetooth traffic monitoring. *Accident Analysis and Prevention,* Volume 146, pp. 1-12.

Namaki Araghi, B., Krishnan, R. & Lahrmann, H., 2016. Mode-Specific Travel Time Estimation Using Bluetooth Technology. *Journal of Intelligent Transportation Systems,* Volume 20(3), pp. 219-228.

National Highway Traffic Safety Administration , 2020. *Traffic Safety Facts, Overview of Motor Vehicle Crashes in 2019,* Washington, D.C.: U.S. Department of Transportation.

Novatel.com, 2021. *novatel.com.* [Online] Available at: https://novatel.com/an-introduction-to-gnss/chapter-5-resolving-errors/real-time-kinematic-rtk

Pande, A. & Wolshon, B., 2016. *Traffic Engineering Handbook,* Hoboken, New Jersey: John Wiley @ Sons.

Park, H., Noh, J. & Cho, S., 2016. Three-dimensional positioning system using Bluetooth low-energy beacons. *International Journal of Distributed Sensor Networks, Vol. 12(10),* pp. 1-11.

Ptvgroup, 2021. *ptvgroup.com.* [Online] Available at: ptvgroup.com [Accessed 2021].

Quayle, S. M., Koonce, P., DePencier, D. & Bullock, D. M., 2010. Arterial Performance Measures with Media Access Control Readers. *Transportation Research Record: Journal of the Transportation Research Board, No. 2192,* pp. 185-193.

Raeve, N. D. et al., 2020. A Bluetooth-Low-Energy-Based Detection and Warning System for Vulnerable Road Users in the Blind Spot of Vehicles. *Sensors,* Volume 20, 2727, pp. 2-18.

Raeve, N. D. et al., 2020. A Bluetooth-Low-Energy-Based Detection and Warning System for Vulnerable Road Users in the Blind Spot of Vehicles. *Sensors,* Volume 20, 2727, pp. 2-18.

Rappaport, T., 2002. *Wireless Communication Principles and Practice.* New Jersey: Prentice Hall PTR.

Retscher, G., 2017. Fusion of Location Fingerprinting and Trilateration Based on the Example of Differential Wi-Fi Positioning. *ISPRS Annals of the Photogrammetry, Remote Sensing and Spatial Information Sciences, 4,* pp. 377-384.

Salek Moghaddam, S. & Hellinga, B., 2013. Evaluating the Performance of Algorithms for the Detection of Travel Time Outliers. *Transportation Research Record: Journal of the Transportation Research Board,* Volume 2338, pp. 67-77.

Salek Moghaddam, S. & Hellinga, B., 2013. Quantifying Measurement Error in Arterial Travel Times Measured by Bluetooth Detectors. *Transportation Research Record: Journal of the Transportation Research Board, No. 2395,* pp. 111-122.

Sauter, M., 2011. *From GSM to LTE: an introduction to mobile networks and mobile broadband.* 1st ed. Chichester, West Sussex, U.K: Wiley.

Schneider, R., Patton, R., Toole, J. & Raborn, C., 2005. *Pedestrian and bicycle data collection in United States communities: quantifying use, surveying users, and documenting facility extent,* Washington DC: US Department of Transportation.

Schroeder, B. J. et al., 2010. *Manual of Transportation Engineering Studies.* 2nd ed. Washington, DC: Institute of Transportation Engineers (ITE).

Seo, T., Kusakabe, T. & Asakura, Y., 2015. Estimation of flow and density using probe vehicles with spacing measurement equipment. *Transportation Research Part C,* Volume 53, pp. 134-150.

Shi, K., Ma, Z. ,. Z. R., Hu, W. & Chen, H., 2015. Support Vector Regression Based Indoor Location in IEEE 802.11 Environments. *Hindawi Mobile Information Systems,* Volume 2015, pp. 1-14.

Spano, D. & Ricciato, F., 2017. Opportunistic Time-of-Arrival localization in fully asynchronous wireless networks. *Pervasive and Mobile Computing,* Volume 37, pp. 139-153.

Stallings, W., 2021. *5G Wireless: A Comprehensive Introduction.* s.l.:Addison-Wesley Professional.

Sung, Y., 2016. RSSI-Based Distance Estimation Framework Using a Kalman Filter for Sustainable Indoor Computing Environments. *Sustainability,* Volume 1136, pp. 1-9.

Svecko, J., Malajner, M. & Gleich, D., 2015. Distance estimation using RSSI and particle filter. *ISA Transactions,* Volume 55, pp. 275-285.

Tariq, Z. B., Cheema, D. M., Kamran, M. Z. & Naqvi, I. H., 2017. Non-GPS Positioning Systems: A Survey. *ACM Computing Surveys,* pp. 57:1-57:34.

Transport Canada, 2021. *Government of Canada.* [Online] Available at: https://tc.canada.ca/en/road-transportation/statistics-data/canadian-motor-vehicle-traffic-collision-statistics-2019 [Accessed 2021].

Turner, S. M., Eisele, W. L., Benz, R. J. & Holdener, D. J., 1998. *Travel Time Data Collection Handbook,* Texas: U.S. Department of Transportation, Texas Transportation Institute & Texas A&M University System.

Van Boxel, D., Schneider IV, W. H. & Bakula, C., 2011. Innovative Real-Time Methodology for Detecting Travel Time Outliers on Interstate Highways and Urban Arterials. *Transportation Research Record: Journal of the Transportation Research Board,* Volume 2256, pp. 60-67.

Vanhoef, M. et al., 2016. Why MAC Address Randomization is not Enough: An Analysis of Wi-Fi Network Discovery Mechanisms. *ASIA CCS '16,* pp. 413-424.

Walrand, J. & Parekh, S., 2018. *Communication Networks: A Concise Introduction.* 2nd ed. San Rafael, California: Morgan & Claypool .

Wang, B. et al., 2020. A Novel Weighted KNN Algorithm Based on RSS Similarity and Position Distance for Wi-Fi Fingerprint Positioning. *IEEE Access,* Volume 8, pp. 30591-30602.

Xu, J. et al., 2010. Distance Measurement Model Based on RSSI in WSN. *Wireless Sensor Network,* Volume 2, pp. 606-611.

Yang, S. & Wu, Y.-J., 2018. Travel mode identification using bluetooth technology. *Journal of Intelligent Transportation Systems,* Volume 22, p. 407–421.

Yildirimoglu, M., 2021. Joint estimation of paths and travel times from Bluetooth observations. *Transportmetrica B: Transport Dynamics,* Volume Vol. 9, No. 1, pp. 324-342.

Yuan, J. et al., 2018. Utilizing bluetooth and adaptive signal control data for real-time safety analysis on urban arterials. *Transportation Research Part C,* Volume 97, pp. 114-127.

Yu, W., Park, S., Kim, D. S. & Ko, S.-S., 2015. Arterial Road Incident Detection Based on Time-Moving Average Method in Bluetooth-Based Wireless Vehicle Reidentification System. *Journal of Transportation Engineering,* Volume 141(3), pp. 1-14.

Zarinbal Masouleh, A. & Hellinga, B., 2019. Simulation of the Bluetooth Inquiry Process for Application in Transportation Engineering. *IEEE Transactions Intelligent Transportation Systems, VOL. 20, NO. 3,* pp. 1020-1030.

Zhang, H. et al., 2020. A scalable indoor localization algorithm based on distance fitting and fingerprint mapping in Wi-Fi environments. *Neural Computing and Applications,* Volume 32, pp. 5131-5145.

Zhou, C., Yuan, J., Liu, H. & Qiu, J., 2017. Bluetooth Indoor Positioning Based on RSSI and Kalman Filter. *Springer Wireless Pers Commun,* Volume 96, pp. 4115-4130.

Appendices

Appendix A

Raw data of RSSI-Distance curves

1. Wi-Fi mode

MAC	Signal mode	RSSI	Timestamp	Timestamp	Distance (m)
c4438fd60469	2	-36	1524094682	7:38:02 PM	1
c4438fd60469	2	-31	1524094687	7:38:07 PM	1
c4438fd60469	2	-68	1524094693	7:38:13 PM	1
c4438fd60469	2	-31	1524094700	7:38:20 PM	1
c4438fd60469	2	-37	1524094706	7:38:26 PM	1
c4438fd60469	2	-35	1524094711	7:38:31 PM	1
c4438fd60469	2	-37	1524094716	7:38:36 PM	1
c4438fd60469	2	-34	1524094722	7:38:42 PM	1
c4438fd60469	2	-35	1524094729	7:38:49 PM	1
c4438fd60469	2	-36	1524094733	7:38:53 PM	1
c4438fd60469	2	-41	1524094739	7:38:59 PM	1
c4438fd60469	2	-48	1524094863	7:41:03 PM	3
c4438fd60469	2	-43	1524094869	7:41:09 PM	3
c4438fd60469	2	-39	1524094874	7:41:14 PM	3
c4438fd60469	2	-52	1524094880	7:41:20 PM	3
c4438fd60469	2	-52	1524094887	7:41:27 PM	3
c4438fd60469	2	-39	1524094893	7:41:33 PM	3
c4438fd60469	2	-52	1524094900	7:41:40 PM	3
c4438fd60469	2	-45	1524094905	7:41:45 PM	3
c4438fd60469	2	-46	1524094911	7:41:51 PM	3
c4438fd60469	2	-39	1524094919	7:41:59 PM	3
c4438fd60469	2	-55	1524095040	7:44:00 PM	10
c4438fd60469	2	-53	1524095047	7:44:07 PM	10
c4438fd60469	2	-57	1524095053	7:44:13 PM	10
c4438fd60469	2	-52	1524095058	7:44:18 PM	10
c4438fd60469	2	-70	1524095064	7:44:24 PM	10
c4438fd60469	2	-59	1524095069	7:44:29 PM	10
c4438fd60469	2	-60	1524095079	7:44:39 PM	10
c4438fd60469	2	-62	1524095085	7:44:45 PM	10
c4438fd60469	2	-62	1524095092	7:44:52 PM	10
c4438fd60469	2	-61	1524095097	7:44:57 PM	10

(Continued)

(Continued)

MAC	Signal mode	RSSI	Timestamp	Timestamp	Distance (m)
c4438fd60469	2	-68	1524095230	7:47:10 PM	20
c4438fd60469	2	-69	1524095235	7:47:15 PM	20
c4438fd60469	2	-79	1524095241	7:47:21 PM	20
c4438fd60469	2	-62	1524095246	7:47:26 PM	20
c4438fd60469	2	-62	1524095252	7:47:32 PM	20
c4438fd60469	2	-69	1524095257	7:47:37 PM	20
c4438fd60469	2	-69	1524095263	7:47:43 PM	20
c4438fd60469	2	-67	1524095268	7:47:48 PM	20
c4438fd60469	2	-79	1524095273	7:47:53 PM	20
c4438fd60469	2	-69	1524095279	7:47:59 PM	20
c4438fd60469	2	-77	1524095401	7:50:01 PM	30
c4438fd60469	2	-62	1524095407	7:50:07 PM	30
c4438fd60469	2	-67	1524095412	7:50:12 PM	30
c4438fd60469	2	-65	1524095418	7:50:18 PM	30
c4438fd60469	2	-63	1524095424	7:50:24 PM	30
c4438fd60469	2	-63	1524095430	7:50:30 PM	30
c4438fd60469	2	-63	1524095436	7:50:36 PM	30
c4438fd60469	2	-63	1524095442	7:50:42 PM	30
c4438fd60469	2	-63	1524095448	7:50:48 PM	30
c4438fd60469	2	-62	1524095453	7:50:53 PM	30
c4438fd60469	2	-61	1524095459	7:50:59 PM	30
c4438fd60469	2	-64	1524095585	7:53:05 PM	40
c4438fd60469	2	-65	1524095593	7:53:13 PM	40
c4438fd60469	2	-65	1524095599	7:53:19 PM	40
c4438fd60469	2	-78	1524095604	7:53:24 PM	40
c4438fd60469	2	-68	1524095610	7:53:30 PM	40
c4438fd60469	2	-78	1524095616	7:53:36 PM	40
c4438fd60469	2	-64	1524095623	7:53:43 PM	40
c4438fd60469	2	-78	1524095628	7:53:48 PM	40
c4438fd60469	2	-65	1524095639	7:53:59 PM	40
c4438fd60469	2	-65	1524095763	7:56:03 PM	50
c4438fd60469	2	-65	1524095769	7:56:09 PM	50
c4438fd60469	2	-63	1524095776	7:56:16 PM	50
c4438fd60469	2	-63	1524095782	7:56:22 PM	50
c4438fd60469	2	-65	1524095785	7:56:25 PM	50
c4438fd60469	2	-65	1524095796	7:56:36 PM	50
c4438fd60469	2	-63	1524095802	7:56:42 PM	50
c4438fd60469	2	-68	1524095808	7:56:48 PM	50
c4438fd60469	2	-69	1524095814	7:56:54 PM	50
c4438fd60469	2	-69	1524095818	7:56:58 PM	50

(Continued)

(Continued)

MAC	Signal mode	RSSI	Timestamp	Timestamp	Distance (m)
c4438fd60469	2	-73	1524095947	7:59:07 PM	60
c4438fd60469	2	-65	1524095953	7:59:13 PM	60
c4438fd60469	2	-73	1524095961	7:59:21 PM	60
c4438fd60469	2	-73	1524095966	7:59:26 PM	60
c4438fd60469	2	-69	1524095972	7:59:32 PM	60
c4438fd60469	2	-67	1524095978	7:59:38 PM	60
c4438fd60469	2	-73	1524095984	7:59:44 PM	60
c4438fd60469	2	-75	1524095989	7:59:49 PM	60
c4438fd60469	2	-73	1524095996	7:59:56 PM	60
c4438fd60469	2	-75	1524096123	8:02:03 PM	70
c4438fd60469	2	-75	1524096129	8:02:09 PM	70
c4438fd60469	2	-73	1524096134	8:02:14 PM	70
c4438fd60469	2	-73	1524096141	8:02:21 PM	70
c4438fd60469	2	-75	1524096146	8:02:26 PM	70
c4438fd60469	2	-71	1524096152	8:02:32 PM	70
c4438fd60469	2	-73	1524096157	8:02:37 PM	70
c4438fd60469	2	-73	1524096163	8:02:43 PM	70
c4438fd60469	2	-84	1524096169	8:02:49 PM	70
c4438fd60469	2	-84	1524096176	8:02:56 PM	70
c4438fd60469	2	-77	1524096302	8:05:02 PM	80
c4438fd60469	2	-86	1524096308	8:05:08 PM	80
c4438fd60469	2	-85	1524096313	8:05:13 PM	80
c4438fd60469	2	-85	1524096319	8:05:19 PM	80
c4438fd60469	2	-81	1524096324	8:05:24 PM	80
c4438fd60469	2	-86	1524096330	8:05:30 PM	80
c4438fd60469	2	-76	1524096337	8:05:37 PM	80
c4438fd60469	2	-85	1524096343	8:05:43 PM	80
c4438fd60469	2	-85	1524096348	8:05:48 PM	80
c4438fd60469	2	-81	1524096353	8:05:53 PM	80
c4438fd60469	2	-83	1524096359	8:05:59 PM	80
c4438fd60469	2	-79	1524096480	8:08:00 PM	90
c4438fd60469	2	-83	1524096486	8:08:06 PM	90
c4438fd60469	2	-77	1524096492	8:08:12 PM	90
c4438fd60469	2	-77	1524096499	8:08:19 PM	90
c4438fd60469	2	-79	1524096505	8:08:25 PM	90
c4438fd60469	2	-83	1524096518	8:08:38 PM	90
c4438fd60469	2	-79	1524096524	8:08:44 PM	90
c4438fd60469	2	-79	1524096529	8:08:49 PM	90
c4438fd60469	2	-75	1524096535	8:08:55 PM	90
c4438fd60469	2	-79	1524096661	8:11:01 PM	100

(Continued)

(Continued)

MAC	Signal mode	RSSI	Timestamp	Timestamp	Distance (m)
c4438fd60469	2	-81	1524096667	8:11:07 PM	100
c4438fd60469	2	-68	1524096673	8:11:13 PM	100
c4438fd60469	2	-75	1524096680	8:11:20 PM	100
c4438fd60469	2	-75	1524096686	8:11:26 PM	100
c4438fd60469	2	-75	1524096697	8:11:37 PM	100
c4438fd60469	2	-75	1524096704	8:11:44 PM	100
c4438fd60469	2	-75	1524096710	8:11:50 PM	100
c4438fd60469	2	-77	1524096719	8:11:59 PM	100

2. Bluetooth mode

MAC	Signal mode	RSSI	Timestamp	Timestamp	Distance (m)
30766f78abf1	0	-45	1521831724	3:02:04 PM	1
30766f78abf1	0	-48	1521831730	3:02:10 PM	1
30766f78abf1	0	-43	1521831737	3:02:17 PM	1
30766f78abf1	0	-47	1521831743	3:02:23 PM	1
30766f78abf1	0	-56	1521831749	3:02:29 PM	1
30766f78abf1	0	-43	1521831758	3:02:38 PM	1
30766f78abf1	0	-43	1521831764	3:02:44 PM	1
30766f78abf1	0	-49	1521831769	3:02:49 PM	1
30766f78abf1	0	-47	1521831776	3:02:56 PM	1
30766f78abf1	0	-54	1521831848	3:04:08 PM	3
30766f78abf1	0	-49	1521831856	3:04:16 PM	3
30766f78abf1	0	-49	1521831863	3:04:23 PM	3
30766f78abf1	0	-63	1521831868	3:04:28 PM	3
30766f78abf1	0	-60	1521831874	3:04:34 PM	3
30766f78abf1	0	-52	1521831879	3:04:39 PM	3
30766f78abf1	0	-54	1521831884	3:04:44 PM	3
30766f78abf1	0	-52	1521831889	3:04:49 PM	3
30766f78abf1	0	-54	1521831894	3:04:54 PM	3
30766f78abf1	0	-52	1521831899	3:04:59 PM	3
30766f78abf1	0	-64	1521831963	3:06:03 PM	10
30766f78abf1	0	-66	1521831970	3:06:10 PM	10
30766f78abf1	0	-58	1521831977	3:06:17 PM	10
30766f78abf1	0	-67	1521831982	3:06:22 PM	10
30766f78abf1	0	-66	1521831987	3:06:27 PM	10
30766f78abf1	0	-62	1521831992	3:06:32 PM	10
30766f78abf1	0	-64	1521831998	3:06:38 PM	10
30766f78abf1	0	-61	1521832003	3:06:43 PM	10
30766f78abf1	0	-61	1521832009	3:06:49 PM	10
30766f78abf1	0	-63	1521832014	3:06:54 PM	10
30766f78abf1	0	-64	1521832019	3:06:59 PM	10
30766f78abf1	0	-72	1521832082	3:08:02 PM	20
30766f78abf1	0	-65	1521832087	3:08:07 PM	20
30766f78abf1	0	-68	1521832099	3:08:19 PM	20
30766f78abf1	0	-62	1521832105	3:08:25 PM	20
30766f78abf1	0	-73	1521832112	3:08:32 PM	20
30766f78abf1	0	-72	1521832119	3:08:39 PM	20
30766f78abf1	0	-61	1521832124	3:08:44 PM	20
30766f78abf1	0	-64	1521832129	3:08:49 PM	20

(Continued)

(Continued)

MAC	Signal mode	RSSI	Timestamp	Timestamp	Distance (m)
30766f78abf1	0	-61	1521832137	3:08:57 PM	20
30766f78abf1	0	-66	1521832203	3:10:03 PM	30
30766f78abf1	0	-67	1521832209	3:10:09 PM	30
30766f78abf1	0	-66	1521832214	3:10:14 PM	30
30766f78abf1	0	-64	1521832221	3:10:21 PM	30
30766f78abf1	0	-65	1521832229	3:10:29 PM	30
30766f78abf1	0	-65	1521832237	3:10:37 PM	30
30766f78abf1	0	-66	1521832243	3:10:43 PM	30
30766f78abf1	0	-70	1521832248	3:10:48 PM	30
30766f78abf1	0	-76	1521832253	3:10:53 PM	30
30766f78abf1	0	-64	1521832259	3:10:59 PM	30
30766f78abf1	0	-66	1521832325	3:12:05 PM	40
30766f78abf1	0	-71	1521832331	3:12:11 PM	40
30766f78abf1	0	-67	1521832338	3:12:18 PM	40
30766f78abf1	0	-65	1521832343	3:12:23 PM	40
30766f78abf1	0	-72	1521832348	3:12:28 PM	40
30766f78abf1	0	-71	1521832354	3:12:34 PM	40
30766f78abf1	0	-67	1521832361	3:12:41 PM	40
30766f78abf1	0	-65	1521832369	3:12:49 PM	40
30766f78abf1	0	-71	1521832374	3:12:54 PM	40
30766f78abf1	0	-72	1521832379	3:12:59 PM	40
30766f78abf1	0	-70	1521832441	3:14:01 PM	50
30766f78abf1	0	-69	1521832448	3:14:08 PM	50
30766f78abf1	0	-76	1521832454	3:14:14 PM	50
30766f78abf1	0	-75	1521832460	3:14:20 PM	50
30766f78abf1	0	-77	1521832465	3:14:25 PM	50
30766f78abf1	0	-70	1521832471	3:14:31 PM	50
30766f78abf1	0	-73	1521832476	3:14:36 PM	50
30766f78abf1	0	-74	1521832482	3:14:42 PM	50
30766f78abf1	0	-78	1521832487	3:14:47 PM	50
30766f78abf1	0	-76	1521832560	3:16:00 PM	60
30766f78abf1	0	-75	1521832567	3:16:07 PM	60
30766f78abf1	0	-79	1521832574	3:16:14 PM	60
30766f78abf1	0	-79	1521832583	3:16:23 PM	60
30766f78abf1	0	-78	1521832588	3:16:28 PM	60
30766f78abf1	0	-84	1521832597	3:16:37 PM	60
30766f78abf1	0	-77	1521832604	3:16:44 PM	60
30766f78abf1	0	-81	1521832692	3:18:12 PM	70
30766f78abf1	0	-79	1521832709	3:18:29 PM	70
30766f78abf1	0	-81	1521832718	3:18:38 PM	70

(Continued)

(Continued)

MAC	Signal mode	RSSI	Timestamp	Timestamp	Distance (m)
30766f78abf1	0	-78	1521832723	3:18:43 PM	70
30766f78abf1	0	-83	1521832729	3:18:49 PM	70
30766f78abf1	0	-80	1521832734	3:18:54 PM	70
30766f78abf1	0	-84	1521832818	3:20:18 PM	80
30766f78abf1	0	-73	1521832827	3:20:27 PM	80
30766f78abf1	0	-83	1521832832	3:20:32 PM	80
30766f78abf1	0	-81	1521832852	3:20:52 PM	80
30766f78abf1	0	-80	1521832858	3:20:58 PM	80
30766f78abf1	0	-84	1521832941	3:22:21 PM	90
30766f78abf1	0	-85	1521832953	3:22:33 PM	90
30766f78abf1	0	-85	1521832966	3:22:46 PM	90
30766f78abf1	0	-88	1521833061	3:24:21 PM	100
30766f78abf1	0	-86	1521833082	3:24:42 PM	100
30766f78abf1	0	-88	1521833093	3:24:53 PM	100

3. BLE mode

MAC	Signal mode	RSSI	Timestamp	Timestamp	Distance (m)
d4e013a43b99	1	-61	1524085082	4:58:02 PM	1
d4e013a43b99	1	-61	1524085083	4:58:03 PM	1
d4e013a43b99	1	-51	1524085085	4:58:05 PM	1
d4e013a43b99	1	-53	1524085087	4:58:07 PM	1
d4e013a43b99	1	-56	1524085091	4:58:11 PM	1
d4e013a43b99	1	-51	1524085093	4:58:13 PM	1
d4e013a43b99	1	-50	1524085094	4:58:14 PM	1
d4e013a43b99	1	-50	1524085096	4:58:16 PM	1
d4e013a43b99	1	-47	1524085098	4:58:18 PM	1
d4e013a43b99	1	-46	1524085100	4:58:20 PM	1
d4e013a43b99	1	-47	1524085101	4:58:21 PM	1
d4e013a43b99	1	-50	1524085102	4:58:22 PM	1
d4e013a43b99	1	-58	1524085103	4:58:23 PM	1
d4e013a43b99	1	-52	1524085109	4:58:29 PM	1
d4e013a43b99	1	-49	1524085111	4:58:31 PM	1
d4e013a43b99	1	-53	1524085114	4:58:34 PM	1
d4e013a43b99	1	-50	1524085115	4:58:35 PM	1
d4e013a43b99	1	-50	1524085116	4:58:36 PM	1
d4e013a43b99	1	-48	1524085117	4:58:37 PM	1
d4e013a43b99	1	-48	1524085118	4:58:38 PM	1
d4e013a43b99	1	-47	1524085120	4:58:40 PM	1
d4e013a43b99	1	-48	1524085122	4:58:42 PM	1
d4e013a43b99	1	-49	1524085123	4:58:43 PM	1
d4e013a43b99	1	-54	1524085124	4:58:44 PM	1
d4e013a43b99	1	-49	1524085125	4:58:45 PM	1
d4e013a43b99	1	-50	1524085127	4:58:47 PM	1
d4e013a43b99	1	-48	1524085129	4:58:49 PM	1
d4e013a43b99	1	-49	1524085132	4:58:52 PM	1
d4e013a43b99	1	-54	1524085133	4:58:53 PM	1
d4e013a43b99	1	-49	1524085135	4:58:55 PM	1
d4e013a43b99	1	-50	1524085136	4:58:56 PM	1
d4e013a43b99	1	-48	1524085138	4:58:58 PM	1
d4e013a43b99	1	-59	1524085201	5:00:01 PM	3
d4e013a43b99	1	-62	1524085202	5:00:02 PM	3
d4e013a43b99	1	-61	1524085204	5:00:04 PM	3
d4e013a43b99	1	-65	1524085207	5:00:07 PM	3
d4e013a43b99	1	-61	1524085209	5:00:09 PM	3
d4e013a43b99	1	-61	1524085210	5:00:10 PM	3

(Continued)

(Continued)

MAC	Signal mode	RSSI	Timestamp	Timestamp	Distance (m)
d4e013a43b99	1	-61	1524085211	5:00:11 PM	3
d4e013a43b99	1	-61	1524085212	5:00:12 PM	3
d4e013a43b99	1	-62	1524085213	5:00:13 PM	3
d4e013a43b99	1	-62	1524085214	5:00:14 PM	3
d4e013a43b99	1	-59	1524085215	5:00:15 PM	3
d4e013a43b99	1	-60	1524085219	5:00:19 PM	3
d4e013a43b99	1	-59	1524085220	5:00:20 PM	3
d4e013a43b99	1	-56	1524085223	5:00:23 PM	3
d4e013a43b99	1	-54	1524085229	5:00:29 PM	3
d4e013a43b99	1	-67	1524085232	5:00:32 PM	3
d4e013a43b99	1	-61	1524085233	5:00:33 PM	3
d4e013a43b99	1	-56	1524085236	5:00:36 PM	3
d4e013a43b99	1	-56	1524085237	5:00:37 PM	3
d4e013a43b99	1	-56	1524085238	5:00:38 PM	3
d4e013a43b99	1	-64	1524085239	5:00:39 PM	3
d4e013a43b99	1	-67	1524085240	5:00:40 PM	3
d4e013a43b99	1	-70	1524085241	5:00:41 PM	3
d4e013a43b99	1	-74	1524085245	5:00:45 PM	3
d4e013a43b99	1	-74	1524085247	5:00:47 PM	3
d4e013a43b99	1	-72	1524085253	5:00:53 PM	3
d4e013a43b99	1	-66	1524085254	5:00:54 PM	3
d4e013a43b99	1	-67	1524085256	5:00:56 PM	3
d4e013a43b99	1	-71	1524085257	5:00:57 PM	3
d4e013a43b99	1	-72	1524085258	5:00:58 PM	3
d4e013a43b99	1	-74	1524085323	5:02:03 PM	10
d4e013a43b99	1	-70	1524085324	5:02:04 PM	10
d4e013a43b99	1	-64	1524085326	5:02:06 PM	10
d4e013a43b99	1	-70	1524085327	5:02:07 PM	10
d4e013a43b99	1	-75	1524085328	5:02:08 PM	10
d4e013a43b99	1	-75	1524085330	5:02:10 PM	10
d4e013a43b99	1	-72	1524085331	5:02:11 PM	10
d4e013a43b99	1	-72	1524085334	5:02:14 PM	10
d4e013a43b99	1	-73	1524085335	5:02:15 PM	10
d4e013a43b99	1	-77	1524085337	5:02:17 PM	10
d4e013a43b99	1	-75	1524085338	5:02:18 PM	10
d4e013a43b99	1	-78	1524085341	5:02:21 PM	10
d4e013a43b99	1	-81	1524085343	5:02:23 PM	10
d4e013a43b99	1	-81	1524085345	5:02:25 PM	10
d4e013a43b99	1	-73	1524085346	5:02:26 PM	10
d4e013a43b99	1	-71	1524085347	5:02:27 PM	10

(Continued)

(Continued)

MAC	Signal mode	RSSI	Timestamp	Timestamp	Distance (m)
d4e013a43b99	1	-64	1524085348	5:02:28 PM	10
d4e013a43b99	1	-70	1524085350	5:02:30 PM	10
d4e013a43b99	1	-75	1524085352	5:02:32 PM	10
d4e013a43b99	1	-74	1524085357	5:02:37 PM	10
d4e013a43b99	1	-75	1524085358	5:02:38 PM	10
d4e013a43b99	1	-73	1524085360	5:02:40 PM	10
d4e013a43b99	1	-72	1524085361	5:02:41 PM	10
d4e013a43b99	1	-75	1524085362	5:02:42 PM	10
d4e013a43b99	1	-77	1524085363	5:02:43 PM	10
d4e013a43b99	1	-72	1524085365	5:02:45 PM	10
d4e013a43b99	1	-72	1524085367	5:02:47 PM	10
d4e013a43b99	1	-75	1524085370	5:02:50 PM	10
d4e013a43b99	1	-80	1524085561	5:06:01 PM	20
d4e013a43b99	1	-73	1524085562	5:06:02 PM	20
d4e013a43b99	1	-81	1524085563	5:06:03 PM	20
d4e013a43b99	1	-77	1524085565	5:06:05 PM	20
d4e013a43b99	1	-77	1524085566	5:06:06 PM	20
d4e013a43b99	1	-72	1524085569	5:06:09 PM	20
d4e013a43b99	1	-71	1524085570	5:06:10 PM	20
d4e013a43b99	1	-70	1524085572	5:06:12 PM	20
d4e013a43b99	1	-76	1524085573	5:06:13 PM	20
d4e013a43b99	1	-70	1524085574	5:06:14 PM	20
d4e013a43b99	1	-69	1524085575	5:06:15 PM	20
d4e013a43b99	1	-70	1524085579	5:06:19 PM	20
d4e013a43b99	1	-70	1524085580	5:06:20 PM	20
d4e013a43b99	1	-69	1524085581	5:06:21 PM	20
d4e013a43b99	1	-70	1524085582	5:06:22 PM	20
d4e013a43b99	1	-74	1524085583	5:06:23 PM	20
d4e013a43b99	1	-79	1524085588	5:06:28 PM	20
d4e013a43b99	1	-88	1524085590	5:06:30 PM	20
d4e013a43b99	1	-88	1524085591	5:06:31 PM	20
d4e013a43b99	1	-77	1524085592	5:06:32 PM	20
d4e013a43b99	1	-72	1524085595	5:06:35 PM	20
d4e013a43b99	1	-75	1524085596	5:06:36 PM	20
d4e013a43b99	1	-68	1524085600	5:06:40 PM	20
d4e013a43b99	1	-71	1524085602	5:06:42 PM	20
d4e013a43b99	1	-69	1524085603	5:06:43 PM	20
d4e013a43b99	1	-70	1524085611	5:06:51 PM	20
d4e013a43b99	1	-69	1524085612	5:06:52 PM	20
d4e013a43b99	1	-74	1524085613	5:06:53 PM	20

(Continued)

(Continued)

MAC	Signal mode	RSSI	Timestamp	Timestamp	Distance (m)
d4e013a43b99	1	-75	1524085614	5:06:54 PM	20
d4e013a43b99	1	-78	1524085615	5:06:55 PM	20
d4e013a43b99	1	-79	1524085616	5:06:56 PM	20
d4e013a43b99	1	-83	1524085682	5:08:02 PM	30
d4e013a43b99	1	-78	1524085684	5:08:04 PM	30
d4e013a43b99	1	-78	1524085685	5:08:05 PM	30
d4e013a43b99	1	-80	1524085686	5:08:06 PM	30
d4e013a43b99	1	-76	1524085687	5:08:07 PM	30
d4e013a43b99	1	-74	1524085690	5:08:10 PM	30
d4e013a43b99	1	-77	1524085692	5:08:12 PM	30
d4e013a43b99	1	-79	1524085698	5:08:18 PM	30
d4e013a43b99	1	-78	1524085701	5:08:21 PM	30
d4e013a43b99	1	-80	1524085703	5:08:23 PM	30
d4e013a43b99	1	-86	1524085704	5:08:24 PM	30
d4e013a43b99	1	-82	1524085705	5:08:25 PM	30
d4e013a43b99	1	-81	1524085711	5:08:31 PM	30
d4e013a43b99	1	-84	1524085712	5:08:32 PM	30
d4e013a43b99	1	-81	1524085713	5:08:33 PM	30
d4e013a43b99	1	-76	1524085716	5:08:36 PM	30
d4e013a43b99	1	-78	1524085717	5:08:37 PM	30
d4e013a43b99	1	-77	1524085719	5:08:39 PM	30
d4e013a43b99	1	-80	1524085721	5:08:41 PM	30
d4e013a43b99	1	-82	1524085723	5:08:43 PM	30
d4e013a43b99	1	-75	1524085724	5:08:44 PM	30
d4e013a43b99	1	-79	1524085725	5:08:45 PM	30
d4e013a43b99	1	-80	1524085727	5:08:47 PM	30
d4e013a43b99	1	-73	1524085729	5:08:49 PM	30
d4e013a43b99	1	-74	1524085731	5:08:51 PM	30
d4e013a43b99	1	-78	1524085734	5:08:54 PM	30
d4e013a43b99	1	-79	1524085735	5:08:55 PM	30
d4e013a43b99	1	-86	1524085736	5:08:56 PM	30
d4e013a43b99	1	-77	1524085801	5:10:01 PM	40
d4e013a43b99	1	-81	1524085802	5:10:02 PM	40
d4e013a43b99	1	-80	1524085803	5:10:03 PM	40
d4e013a43b99	1	-81	1524085804	5:10:04 PM	40
d4e013a43b99	1	-81	1524085805	5:10:05 PM	40
d4e013a43b99	1	-78	1524085806	5:10:06 PM	40
d4e013a43b99	1	-76	1524085807	5:10:07 PM	40
d4e013a43b99	1	-76	1524085809	5:10:09 PM	40
d4e013a43b99	1	-78	1524085810	5:10:10 PM	40

(Continued)

(Continued)

MAC	Signal mode	RSSI	Timestamp	Timestamp	Distance (m)
d4e013a43b99	1	-82	1524085811	5:10:11 PM	40
d4e013a43b99	1	-75	1524085812	5:10:12 PM	40
d4e013a43b99	1	-78	1524085815	5:10:15 PM	40
d4e013a43b99	1	-81	1524085816	5:10:16 PM	40
d4e013a43b99	1	-81	1524085817	5:10:17 PM	40
d4e013a43b99	1	-75	1524085819	5:10:19 PM	40
d4e013a43b99	1	-72	1524085826	5:10:26 PM	40
d4e013a43b99	1	-81	1524085827	5:10:27 PM	40
d4e013a43b99	1	-87	1524085830	5:10:30 PM	40
d4e013a43b99	1	-85	1524085831	5:10:31 PM	40
d4e013a43b99	1	-80	1524085832	5:10:32 PM	40
d4e013a43b99	1	-81	1524085834	5:10:34 PM	40
d4e013a43b99	1	-77	1524085836	5:10:36 PM	40
d4e013a43b99	1	-77	1524085838	5:10:38 PM	40
d4e013a43b99	1	-77	1524085839	5:10:39 PM	40
d4e013a43b99	1	-79	1524085841	5:10:41 PM	40
d4e013a43b99	1	-81	1524085842	5:10:42 PM	40
d4e013a43b99	1	-84	1524085851	5:10:51 PM	40
d4e013a43b99	1	-80	1524085852	5:10:52 PM	40
d4e013a43b99	1	-81	1524085854	5:10:54 PM	40
d4e013a43b99	1	-85	1524085855	5:10:55 PM	40
d4e013a43b99	1	-84	1524085856	5:10:56 PM	40
d4e013a43b99	1	-80	1524085920	5:12:00 PM	50
d4e013a43b99	1	-77	1524085921	5:12:01 PM	50
d4e013a43b99	1	-84	1524085922	5:12:02 PM	50
d4e013a43b99	1	-86	1524085925	5:12:05 PM	50
d4e013a43b99	1	-88	1524085929	5:12:09 PM	50
d4e013a43b99	1	-87	1524085931	5:12:11 PM	50
d4e013a43b99	1	-81	1524085932	5:12:12 PM	50
d4e013a43b99	1	-85	1524085933	5:12:13 PM	50
d4e013a43b99	1	-79	1524085938	5:12:18 PM	50
d4e013a43b99	1	-82	1524085939	5:12:19 PM	50
d4e013a43b99	1	-84	1524085940	5:12:20 PM	50
d4e013a43b99	1	-86	1524085944	5:12:24 PM	50
d4e013a43b99	1	-84	1524085945	5:12:25 PM	50
d4e013a43b99	1	-79	1524085950	5:12:30 PM	50
d4e013a43b99	1	-86	1524085951	5:12:31 PM	50
d4e013a43b99	1	-83	1524085955	5:12:35 PM	50
d4e013a43b99	1	-82	1524085956	5:12:36 PM	50
d4e013a43b99	1	-79	1524085957	5:12:37 PM	50

(Continued)

`

(Continued)

MAC	Signal mode	RSSI	Timestamp	Timestamp	Distance (m)
d4e013a43b99	1	-77	1524085959	5:12:39 PM	50
d4e013a43b99	1	-78	1524085960	5:12:40 PM	50
d4e013a43b99	1	-79	1524085961	5:12:41 PM	50
d4e013a43b99	1	-79	1524085962	5:12:42 PM	50
d4e013a43b99	1	-80	1524085965	5:12:45 PM	50
d4e013a43b99	1	-79	1524085968	5:12:48 PM	50
d4e013a43b99	1	-78	1524085973	5:12:53 PM	50
d4e013a43b99	1	-78	1524085975	5:12:55 PM	50
d4e013a43b99	1	-79	1524085976	5:12:56 PM	50
d4e013a43b99	1	-81	1524086042	5:14:02 PM	60
d4e013a43b99	1	-83	1524086043	5:14:03 PM	60
d4e013a43b99	1	-83	1524086045	5:14:05 PM	60
d4e013a43b99	1	-86	1524086046	5:14:06 PM	60
d4e013a43b99	1	-83	1524086048	5:14:08 PM	60
d4e013a43b99	1	-87	1524086049	5:14:09 PM	60
d4e013a43b99	1	-86	1524086050	5:14:10 PM	60
d4e013a43b99	1	-91	1524086051	5:14:11 PM	60
d4e013a43b99	1	-83	1524086052	5:14:12 PM	60
d4e013a43b99	1	-80	1524086053	5:14:13 PM	60
d4e013a43b99	1	-81	1524086054	5:14:14 PM	60
d4e013a43b99	1	-81	1524086055	5:14:15 PM	60
d4e013a43b99	1	-82	1524086058	5:14:18 PM	60
d4e013a43b99	1	-84	1524086060	5:14:20 PM	60
d4e013a43b99	1	-86	1524086068	5:14:28 PM	60
d4e013a43b99	1	-87	1524086070	5:14:30 PM	60
d4e013a43b99	1	-89	1524086077	5:14:37 PM	60
d4e013a43b99	1	-85	1524086082	5:14:42 PM	60
d4e013a43b99	1	-84	1524086083	5:14:43 PM	60
d4e013a43b99	1	-83	1524086085	5:14:45 PM	60
d4e013a43b99	1	-85	1524086087	5:14:47 PM	60
d4e013a43b99	1	-85	1524086088	5:14:48 PM	60
d4e013a43b99	1	-85	1524086090	5:14:50 PM	60
d4e013a43b99	1	-84	1524086091	5:14:51 PM	60
d4e013a43b99	1	-83	1524086092	5:14:52 PM	60
d4e013a43b99	1	-88	1524086164	5:16:04 PM	70
d4e013a43b99	1	-80	1524086165	5:16:05 PM	70
d4e013a43b99	1	-80	1524086166	5:16:06 PM	70
d4e013a43b99	1	-83	1524086168	5:16:08 PM	70
d4e013a43b99	1	-84	1524086169	5:16:09 PM	70
d4e013a43b99	1	-85	1524086178	5:16:18 PM	70

(Continued)

(Continued)

MAC	Signal mode	RSSI	Timestamp	Timestamp	Distance (m)
d4e013a43b99	1	-90	1524086179	5:16:19 PM	70
d4e013a43b99	1	-86	1524086181	5:16:21 PM	70
d4e013a43b99	1	-82	1524086184	5:16:24 PM	70
d4e013a43b99	1	-82	1524086185	5:16:25 PM	70
d4e013a43b99	1	-82	1524086186	5:16:26 PM	70
d4e013a43b99	1	-82	1524086187	5:16:27 PM	70
d4e013a43b99	1	-86	1524086188	5:16:28 PM	70
d4e013a43b99	1	-86	1524086195	5:16:35 PM	70
d4e013a43b99	1	-88	1524086196	5:16:36 PM	70
d4e013a43b99	1	-85	1524086198	5:16:38 PM	70
d4e013a43b99	1	-83	1524086202	5:16:42 PM	70
d4e013a43b99	1	-78	1524086205	5:16:45 PM	70
d4e013a43b99	1	-77	1524086207	5:16:47 PM	70
d4e013a43b99	1	-77	1524086208	5:16:48 PM	70
d4e013a43b99	1	-85	1524086210	5:16:50 PM	70
d4e013a43b99	1	-79	1524086215	5:16:55 PM	70
d4e013a43b99	1	-79	1524086217	5:16:57 PM	70
d4e013a43b99	1	-79	1524086218	5:16:58 PM	70
d4e013a43b99	1	-85	1524863886	5:18:06 PM	80
d4e013a43b99	1	-89	1524863887	5:18:07 PM	80
d4e013a43b99	1	-85	1524863888	5:18:08 PM	80
d4e013a43b99	1	-88	1524863890	5:18:10 PM	80
d4e013a43b99	1	-88	1524863892	5:18:12 PM	80
d4e013a43b99	1	-88	1524863893	5:18:13 PM	80
d4e013a43b99	1	-90	1524863894	5:18:14 PM	80
d4e013a43b99	1	-89	1524863895	5:18:15 PM	80
d4e013a43b99	1	-88	1524863896	5:18:16 PM	80
d4e013a43b99	1	-89	1524863898	5:18:18 PM	80
d4e013a43b99	1	-89	1524863902	5:18:22 PM	80
d4e013a43b99	1	-84	1524863904	5:18:24 PM	80
d4e013a43b99	1	-86	1524863906	5:18:26 PM	80
d4e013a43b99	1	-85	1524863915	5:18:35 PM	80
d4e013a43b99	1	-87	1524863916	5:18:36 PM	80
d4e013a43b99	1	-88	1524863918	5:18:38 PM	80
d4e013a43b99	1	-89	1524863919	5:18:39 PM	80
d4e013a43b99	1	-85	1524863920	5:18:40 PM	80
d4e013a43b99	1	-84	1524863922	5:18:42 PM	80
d4e013a43b99	1	-89	1524863932	5:18:52 PM	80
d4e013a43b99	1	-84	1524863933	5:18:53 PM	80
d4e013a43b99	1	-85	1524863934	5:18:54 PM	80

(Continued)

(Continued)

MAC	Signal mode	RSSI	Timestamp	Timestamp	Distance (m)
d4e013a43b99	1	-84	1524863935	5:18:55 PM	80
d4e013a43b99	1	-84	1524863936	5:18:56 PM	80
d4e013a43b99	1	-82	1524863937	5:18:57 PM	80
d4e013a43b99	1	-87	1524864004	5:20:04 PM	90
d4e013a43b99	1	-86	1524864005	5:20:05 PM	90
d4e013a43b99	1	-89	1524864007	5:20:07 PM	90
d4e013a43b99	1	-88	1524864009	5:20:09 PM	90
d4e013a43b99	1	-88	1524864010	5:20:10 PM	90
d4e013a43b99	1	-86	1524864011	5:20:11 PM	90
d4e013a43b99	1	-85	1524864012	5:20:12 PM	90
d4e013a43b99	1	-86	1524864013	5:20:13 PM	90
d4e013a43b99	1	-87	1524864014	5:20:14 PM	90
d4e013a43b99	1	-84	1524864015	5:20:15 PM	90
d4e013a43b99	1	-83	1524864017	5:20:17 PM	90
d4e013a43b99	1	-86	1524864018	5:20:18 PM	90
d4e013a43b99	1	-86	1524864019	5:20:19 PM	90
d4e013a43b99	1	-84	1524864022	5:20:22 PM	90
d4e013a43b99	1	-85	1524864023	5:20:23 PM	90
d4e013a43b99	1	-86	1524864025	5:20:25 PM	90
d4e013a43b99	1	-88	1524864028	5:20:28 PM	90
d4e013a43b99	1	-85	1524864030	5:20:30 PM	90
d4e013a43b99	1	-88	1524864033	5:20:33 PM	90
d4e013a43b99	1	-87	1524864039	5:20:39 PM	90
d4e013a43b99	1	-87	1524864040	5:20:40 PM	90
d4e013a43b99	1	-88	1524864042	5:20:42 PM	90
d4e013a43b99	1	-85	1524864045	5:20:45 PM	90
d4e013a43b99	1	-87	1524864046	5:20:46 PM	90
d4e013a43b99	1	-88	1524864047	5:20:47 PM	90
d4e013a43b99	1	-89	1524864050	5:20:50 PM	90
d4e013a43b99	1	-91	1524864051	5:20:51 PM	90
d4e013a43b99	1	-93	1524864124	5:22:04 PM	100
d4e013a43b99	1	-85	1524864125	5:22:05 PM	100
d4e013a43b99	1	-86	1524864130	5:22:10 PM	100
d4e013a43b99	1	-84	1524864132	5:22:12 PM	100
d4e013a43b99	1	-87	1524864134	5:22:14 PM	100
d4e013a43b99	1	-88	1524864150	5:22:30 PM	100
d4e013a43b99	1	-92	1524864152	5:22:32 PM	100
d4e013a43b99	1	-95	1524864153	5:22:33 PM	100

Appendix B

Positioning using KNN algorithm

Table B.1 Positioning using KNN algorithm, stationary beacon, Experiment 1, original data.

Real location				Calibration stage				Test data collection stage				Positioning stage (estimated location)				
#	ID	x	y	RSSI by Scanner 1	RSSI by Scanner 2	RSSI by Scanner 3	RSSI by Scanner 4	RSSI by Scanner 1	RSSI by Scanner 2	RSSI by Scanner 3	RSSI by Scanner 4	#	ID	x	y	Error (m)
1	SO8	-1.5	-25.5	-74.0	-83.0	-71.6	-69.5	-73.2	-72.0	-68.5	-69.3	3	SO6	-1.5	-19.5	6.0
2	SO7	-1.5	-22.5	-77.6	-70.5	-73.0	-66.2	-73.2	-53.0	-73.3	-68.5	26	NO1	1.5	4.5	27.2
3	SO6	-1.5	-19.5	-75.6	-69.1	-69.1	-65.7	-77.5	-71.3	-68.5	-65.4	4	SO5	-1.5	-16.5	3.0
4	SO5	-1.5	-16.5	-79.2	-69.4	-67.7	-65.4	-79.0	-69.8	-67.0	-64.2	4	SO5	-1.5	-16.5	0.0
5	SO4	-1.5	-13.5	-76.5	-70.6	-65.6	-66.1	-78.4	-70.0	-65.6	-69.0	5	SO4	-1.5	-13.5	0.0
6	SO3	-1.5	-10.5	-72.3	-68.9	-63.2	-62.0	-72.0	-68.7	-63.5	-64.0	6	SO3	-1.5	-10.5	0.0
7	SO2	-1.5	-7.5	-72.4	-81.0	-64.5	-59.7	-72.8	-75.6	-66.5	-60.3	66	WI8	-25.5	-1.5	24.7
8	SO1	-1.5	-4.5	-62.4	-74.2	-65.2	-65.8	-64.6	-76.0	-68.0	-66.0	13	NI3	-1.5	10.5	15.0
9	ISW	-1.5	-1.5	-62.4	-75.0	-71.3	-72.5	-64.0	-78.5	-69.8	-69.3	9	ISW	-1.5	-1.5	0.0
10	INW	-1.5	1.5	-65.0	-61.0	-58.0	-60.6	-63.2	-61.0	-58.0	-61.8	10	INW	-1.5	1.5	0.0
11	NI1	-1.5	4.5	-65.2	-49.6	-60.4	-66.0	-65.5	-50.7	-64.3	-67.7	11	NI1	-1.5	4.5	0.0
12	NI2	-1.5	7.5	-65.5	-72.6	-73.4	-64.0	-69.6	-75.5	-71.0	-63.2	66	WI6	-19.5	-1.5	20.1
13	NI3	-1.5	10.5	-63.6	-76.4	-68.8	-63.3	-64.5	-76.7	-69.8	-63.6	13	NI3	-1.5	10.5	0.0
14	NI4	-1.5	13.5	-67.3	-68.3	-75.3	-67.6	-68.8	-65.0	-77.7	-67.3	63	WI3	-10.5	-1.5	17.5
15	NI5	-1.5	16.5	-73.6	-65.3	-74.0	-68.1	-73.3	-66.0	-76.5	-68.7	15	NI5	-1.5	16.5	0.0
16	NI6	-1.5	19.5	-76.8	-66.3	-74.8	-70.8	-75.7	-66.8	-74.0	-71.3	16	NI6	-1.5	19.5	0.0
17	NI7	-1.5	22.5	-80.2	-70.6	-74.6	-71.4	-80.0	-71.8	-77.0	-70.8	17	NI7	-1.5	22.5	0.0
18	NI8	-1.5	25.5	-75.6	-70.4	-77.1	-73.7	-78.1	-70.8	-76.4	-75.3	18	NI8	-1.5	25.5	0.0
19	NO8	1.5	25.5	-70.3	-64.4	-71.6	-64.8	-71.2	-64.8	-69.8	-64.5	19	NO8	1.5	25.5	0.0
20	NO7	1.5	22.5	-71.7	-65.7	-73.1	-66.9	-72.7	-66.3	-72.8	-67.8	20	NO7	1.5	22.5	0.0
21	NO6	1.5	19.5	-74.4	-66.4	-72.8	-67.6	-70.8	-67.3	-72.3	-68.8	63	WI3	-10.5	-1.5	24.2
22	NO5	1.5	16.5	-77.5	-67.2	-70.5	-65.3	-74.0	-65.8	-71.0	-65.8	54	EO7	22.5	-1.5	27.7
23	NO4	1.5	13.5	-69.1	-70.2	-67.5	-62.0	-67.9	-68.5	-65.8	-62.5	30	SI2	1.5	-7.5	21.0
24	NO3	1.5	10.5	-62.8	-61.3	-69.3	-59.5	-61.7	-61.0	-67.2	-59.8	24	NO3	1.5	10.5	0.0
25	NO2	1.5	7.5	-63.3	-65.5	-72.2	-61.8	-63.8	-63.0	-74.8	-65.0	45	EI1	4.5	1.5	6.7
26	NO1	1.5	4.5	-67.7	-59.0	-64.6	-68.3	-67.7	-56.0	-63.0	-69.0	26	NO1	1.5	4.5	0.0
27	INE	1.5	1.5	-58.6	-61.9	-61.7	-74.2	-60.3	-60.6	-61.8	-75.0	27	INE	1.5	1.5	0.0
28	ISE	1.5	-1.5	-60.6	-69.9	-68.1	-66.3	-60.5	-71.5	-67.4	-67.8	28	ISE	1.5	-1.5	0.0
29	SI1	1.5	-4.5	-54.3	-69.0	-72.8	-57.3	-54.8	-69.8	-69.5	-57.0	29	SI1	1.5	-4.5	0.0
30	SI2	1.5	-7.5	-69.6	-70.0	-65.4	-62.0	-70.2	-71.5	-65.5	-61.5	30	SI2	1.5	-7.5	0.0
31	SI3	1.5	-10.5	-72.6	-63.9	-62.1	-75.8	-70.7	-62.0	-61.0	-74.8	31	SI3	1.5	-10.5	0.0
32	SI4	1.5	-13.5	-70.3	-61.9	-62.0	-71.1	-71.2	-61.0	-61.8	-69.7	32	SI4	1.5	-13.5	0.0
33	SI5	1.5	-16.5	-70.0	-66.1	-63.0	-64.9	-70.5	-66.0	-62.7	-64.0	33	SI5	1.5	-16.5	0.0
34	SI6	1.5	-19.5	-64.3	-64.9	-65.2	-64.3	-66.0	-64.5	-64.8	-65.7	34	SI6	1.5	-19.5	0.0

(continued)

(continued)

Real location				Calibration stage				Test data collection stage				Positioning stage (estimated location)				
#	ID	x	y	RSSI by Scanner 1	RSSI by Scanner 2	RSSI by Scanner 3	RSSI by Scanner 4	RSSI by Scanner 1	RSSI by Scanner 2	RSSI by Scanner 3	RSSI by Scanner 4	#	ID	x	y	Error (m)
35	SI7	1.5	-22.5	-62.4	-67.0	-67.2	-63.9	-63.5	-66.3	-64.7	-64.8	34	SI6	1.5	-19.5	3.0
36	SI8	1.5	-25.5	-66.2	-72.6	-65.3	-65.4	-65.0	-68.7	-67.0	-65.9	47	EI3	10.5	1.5	28.5
37	WO8	-25.5	1.5	-75.6	-76.4	-71.5	-80.8	-75.2	-73.8	-70.8	-83.4	67	WI7	-22.5	-1.5	4.2
38	WO7	-22.5	1.5	-73.9	-71.6	-67.0	-80.9	-72.8	-71.0	-67.8	-80.8	38	WO7	-22.5	1.5	0.0
39	WO6	-19.5	1.5	-71.1	-67.4	-67.8	-75.8	-69.5	-67.4	-67.0	-74.5	39	WO6	-19.5	1.5	0.0
40	WO5	-16.5	1.5	-71.6	-64.0	-67.8	-73.6	-70.8	-64.0	-70.5	-72.4	40	WO5	-16.5	1.5	0.0
41	WO4	-13.5	1.5	-72.2	-66.4	-75.6	-72.9	-71.2	-66.7	-73.0	-72.8	52	EI8	25.5	1.5	39.0
42	WO3	-10.5	1.5	-72.8	-65.5	-71.8	-78.0	-75.6	-65.5	-67.6	-79.8	42	WO3	-10.5	1.5	0.0
43	WO2	-7.5	1.5	-74.2	-66.9	-61.9	-69.3	-77.4	-64.3	-62.5	-68.0	43	WO2	-7.5	1.5	0.0
44	WO1	-4.5	1.5	-74.4	-64.2	-56.5	-64.4	-77.2	-64.6	-57.4	-62.5	44	WO1	-4.5	1.5	0.0
45	EI1	4.5	1.5	-65.7	-63.8	-75.4	-65.5	-62.2	-62.7	-76.0	-66.4	45	EI1	4.5	1.5	0.0
46	EI2	7.5	1.5	-64.0	-69.2	-69.2	-61.7	-65.8	-68.6	-67.7	-61.6	47	EI3	10.5	1.5	3.0
47	EI3	10.5	1.5	-65.3	-68.7	-67.8	-62.7	-68.0	-70.3	-68.2	-62.8	23	NO4	1.5	13.5	15.0
48	EI4	13.5	1.5	-65.4	-77.3	-70.9	-63.5	-71.5	-73.7	-70.8	-63.8	66	WI6	-19.5	-1.5	33.1
49	EI5	16.5	1.5	-62.2	-68.0	-66.6	-64.0	-62.4	-69.2	-69.0	-63.8	46	EI2	7.5	1.5	9.0
50	EI6	19.5	1.5	-62.4	-65.8	-67.8	-64.1	-59.5	-65.0	-68.2	-64.2	50	EI6	19.5	1.5	0.0
51	EI7	22.5	1.5	-66.1	-67.0	-72.1	-70.0	-67.3	-66.0	-71.3	-69.8	51	EI7	22.5	1.5	0.0
52	EI8	25.5	1.5	-71.2	-67.7	-73.3	-71.9	-66.5	-66.2	-68.0	-73.5	64	WI4	-13.5	-1.5	39.1
53	EO8	25.5	-1.5	-77.1	-71.3	-75.9	-70.0	-75.5	-69.0	-73.3	-70.6	16	NI6	-1.5	19.5	34.2
54	EO7	22.5	-1.5	-72.6	-66.8	-71.4	-66.5	-72.2	-66.8	-66.4	-65.7	55	EO6	19.5	-1.5	3.0
55	EO6	19.5	-1.5	-71.1	-67.1	-66.8	-63.1	-75.4	-67.8	-65.7	-63.0	6	SO3	-1.5	-10.5	22.8
56	EO5	16.5	-1.5	-70.8	-70.3	-63.1	-60.4	-71.5	-70.8	-64.0	-60.7	56	EO5	16.5	-1.5	0.0
57	EO4	13.5	-1.5	-71.0	-80.0	-65.6	-64.6	-68.5	-79.3	-66.3	-63.7	57	EO4	13.5	-1.5	0.0
58	EO3	10.5	-1.5	-57.2	-81.6	-65.2	-60.4	-56.6	-74.7	-63.8	-58.0	58	EO3	10.5	-1.5	0.0
59	EO2	7.5	-1.5	-62.3	-68.0	-65.5	-59.1	-61.6	-68.0	-65.7	-60.5	59	EO2	7.5	-1.5	0.0
60	EO1	4.5	-1.5	-57.0	-61.6	-74.5	-67.2	-56.8	-60.6	-75.8	-69.8	60	EO1	4.5	-1.5	0.0
61	WI1	-4.5	-1.5	-73.4	-62.6	-57.4	-53.9	-76.2	-63.2	-57.3	-53.6	61	WI1	-4.5	-1.5	0.0
62	WI2	-7.5	-1.5	-67.3	-62.4	-68.1	-57.3	-66.8	-62.0	-68.0	-58.5	62	WI2	-7.5	-1.5	0.0
63	WI3	-10.5	-1.5	-70.6	-65.0	-71.0	-68.5	-70.0	-64.6	-69.0	-68.8	63	WI3	-10.5	-1.5	0.0
64	WI4	-13.5	-1.5	-67.8	-66.8	-69.7	-75.6	-67.2	-66.4	-69.0	-77.0	64	WI4	-13.5	-1.5	0.0
65	WI5	-16.5	-1.5	-70.1	-69.6	-71.0	-72.8	-68.8	-70.8	-67.8	-71.3	65	WI5	-16.5	-1.5	0.0
66	WI6	-19.5	-1.5	-72.8	-74.7	-71.5	-61.5	-72.0	-74.2	-72.6	-82.0	67	WI7	-22.5	-1.5	3.0
67	WI7	-22.5	-1.5	-74.0	-76.4	-72.5	-83.3	-73.7	-78.3	-73.2	-79.5	37	WO8	-25.5	1.5	4.2
68	WI8	-25.5	-1.5	-73.4	-72.9	-72.3	-79.0	-72.5	-72.0	-70.5	-76.8	68	WI8	-25.5	-1.5	0.0

Table B.2 Positioning using KNN algorithm, stationary beacon, Experiment 1, Savitzky-golay filter applied.

Real location				Calibration stage				Test data collection stage				Positioning stage (estimated location)				
#	ID	x	y	RSSI by Scanner 1	RSSI by Scanner 2	RSSI by Scanner 3	RSSI by Scanner 4	RSSI by Scanner 1	RSSI by Scanner 2	RSSI by Scanner 3	RSSI by Scanner 4	#	ID	x	y	Error (m)
1	SO8	-1.5	-25.5	-74.0	-83.0	-71.7	-69.6	-73.6	-72.0	-68.6	-69.3	3	SO6	-1.5	-19.5	6.0
2	SO7	-1.5	-22.5	-77.6	-70.9	-72.8	-66.5	-73.2	-53.0	-73.3	-68.6	26	NO1	1.5	4.5	27.2
3	SO6	-1.5	-19.5	-75.5	-69.0	-69.1	-65.7	-77.4	-71.5	-68.4	-65.5	4	SO5	-1.5	-16.5	3.0
4	SO5	-1.5	-16.5	-79.3	-69.3	-67.7	-65.3	-78.9	-69.8	-67.0	-64.5	4	SO5	-1.5	-16.5	0.0
5	SO4	-1.5	-13.5	-76.6	-70.6	-65.6	-66.0	-79.0	-70.0	-65.5	-69.0	5	SO4	-1.5	-13.5	0.0
6	SO3	-1.5	-10.5	-72.3	-68.9	-63.3	-61.9	-72.3	-68.7	-63.4	-64.0	6	SO3	-1.5	-10.5	0.0
7	SO2	-1.5	-7.5	-72.5	-81.0	-64.5	-59.6	-73.0	-75.4	-66.6	-60.3	7	SO2	-1.5	-7.5	0.0
8	SO1	-1.5	-4.5	-62.3	-73.8	-65.3	-65.8	-65.2	-76.0	-67.8	-66.2	13	NI3	-1.5	10.5	15.0
9	ISW	-1.5	-1.5	-62.3	-75.1	-71.4	-72.5	-64.0	-78.5	-70.2	-69.5	9	ISW	-1.5	-1.5	0.0
10	INW	-1.5	1.5	-65.1	-60.9	-58.1	-60.7	-63.5	-61.0	-58.0	-61.6	10	INW	-1.5	1.5	0.0
11	NI1	-1.5	4.5	-65.3	-49.6	-60.3	-65.9	-65.5	-50.7	-64.2	-68.0	11	NI1	-1.5	4.5	0.0
12	NI2	-1.5	7.5	-65.6	-72.6	-73.5	-64.1	-69.8	-75.2	-71.0	-63.4	48	EI4	13.5	1.5	16.2
13	NI3	-1.5	10.5	-63.5	-76.3	-68.6	-63.3	-63.9	-76.7	-69.5	-63.6	13	NI3	-1.5	10.5	0.0
14	NI4	-1.5	13.5	-67.2	-68.3	-75.4	-67.6	-68.6	-65.8	-77.7	-67.3	14	NI4	-1.5	13.5	0.0
15	NI5	-1.5	16.5	-73.5	-65.3	-73.9	-68.1	-73.1	-66.0	-76.6	-68.7	15	NI5	-1.5	16.5	0.0
16	NI6	-1.5	19.5	-76.6	-66.3	-74.7	-70.8	-75.6	-66.7	-74.0	-71.4	16	NI6	-1.5	19.5	0.0
17	NI7	-1.5	22.5	-80.0	-70.5	-74.5	-71.3	-80.0	-71.5	-77.0	-71.0	17	NI7	-1.5	22.5	0.0
18	NI8	-1.5	25.5	-75.8	-70.5	-77.1	-73.7	-78.2	-70.7	-76.5	-75.0	18	NI8	-1.5	25.5	0.0
19	NO8	1.5	25.5	-70.3	-64.3	-71.5	-64.9	-71.1	-65.0	-69.3	-64.5	19	NO8	1.5	25.5	0.0
20	NO7	1.5	22.5	-71.7	-65.7	-73.1	-66.9	-72.7	-66.3	-73.0	-67.8	20	NO7	1.5	22.5	0.0
21	NO6	1.5	19.5	-74.5	-66.4	-72.7	-67.7	-71.3	-67.4	-72.4	-68.6	20	NO7	1.5	22.5	3.0
22	NO5	1.5	16.5	-77.6	-67.3	-70.6	-65.3	-74.1	-66.3	-71.1	-65.5	54	EO7	22.5	-1.5	27.7
23	NO4	1.5	13.5	-69.1	-70.3	-67.5	-62.0	-67.6	-68.5	-65.8	-62.5	30	SI2	1.5	-7.5	21.0
24	NO3	1.5	10.5	-62.9	-61.2	-69.5	-59.6	-61.6	-61.1	-66.3	-59.9	24	NO3	1.5	10.5	0.0
25	NO2	1.5	7.5	-63.3	-65.3	-72.1	-61.5	-63.8	-63.3	-74.7	-65.0	45	EI1	4.5	1.5	6.7
26	NO1	1.5	4.5	-68.7	-58.9	-64.6	-68.3	-67.6	-55.8	-62.9	-69.2	26	NO1	1.5	4.5	0.0
27	INE	1.5	1.5	-58.7	-61.7	-61.8	-74.3	-61.2	-60.5	-61.7	-75.0	27	INE	1.5	1.5	0.0
28	ISE	1.5	-1.5	-60.7	-69.7	-68.1	-66.3	-58.3	-71.6	-67.4	-68.0	28	ISE	1.5	-1.5	0.0
29	SI1	1.5	-4.5	-54.3	-68.8	-72.8	-57.3	-54.7	-69.8	-69.5	-57.1	29	SI1	1.5	-4.5	0.0
30	SI2	1.5	-7.5	-69.6	-69.9	-65.4	-62.0	-69.9	-71.6	-65.5	-61.7	30	SI2	1.5	-7.5	0.0
31	SI3	1.5	-10.5	-72.7	-63.9	-62.1	-75.9	-71.2	-62.1	-61.0	-74.8	31	SI3	1.5	-10.5	0.0
32	SI4	1.5	-13.5	-70.2	-61.8	-62.0	-71.0	-71.2	-61.0	-61.8	-69.7	32	SI4	1.5	-13.5	0.0
33	SI5	1.5	-16.5	-70.0	-66.1	-63.0	-64.9	-70.6	-66.0	-62.7	-64.0	33	SI5	1.5	-16.5	0.0
34	SI6	1.5	-19.5	-64.4	-64.9	-65.2	-64.3	-66.0	-64.4	-64.8	-65.7	34	SI6	1.5	-19.5	0.0

(continued)

(continued)

Real location				Calibration stage				Test data collection stage				Positioning stage (estimated location)				
#	ID	x	y	RSSI by Scanner 1	RSSI by Scanner 2	RSSI by Scanner 3	RSSI by Scanner 4	RSSI by Scanner 1	RSSI by Scanner 2	RSSI by Scanner 3	RSSI by Scanner 4	#	ID	x	y	Error (m)
35	SI7	1.5	-22.5	-62.4	-67.0	-67.2	-63.9	-63.5	-66.3	-64.4	-64.8	34	SI6	1.5	-19.5	3.0
36	SI8	1.5	-25.5	-66.2	-72.7	-65.3	-65.5	-65.0	-68.7	-67.0	-69.0	28	ISE	1.5	-1.5	24.0
37	WO8	-25.5	1.5	-75.6	-76.4	-71.5	-80.5	-75.1	-74.0	-70.8	-83.5	66	WI6	-19.5	-1.5	6.7
38	WO7	-22.5	1.5	-74.0	-71.5	-67.4	-81.0	-72.7	-71.0	-67.8	-80.7	38	WO7	-22.5	1.5	0.0
39	WO6	-19.5	1.5	-71.1	-67.3	-67.7	-75.8	-69.6	-67.4	-67.1	-74.6	39	WO6	-19.5	1.5	0.0
40	WO5	-16.5	1.5	-71.5	-64.1	-67.6	-73.3	-70.9	-64.0	-70.5	-72.2	40	WO5	-16.5	1.5	0.0
41	WO4	-13.5	1.5	-72.3	-66.6	-75.7	-72.9	-71.3	-66.7	-72.9	-72.8	52	EI8	25.5	1.5	39.0
42	WO3	-10.5	1.5	-77.1	-65.5	-72.1	-78.0	-75.4	-65.6	-67.5	-79.8	42	WO3	-10.5	1.5	0.0
43	WO2	-7.5	1.5	-74.3	-66.8	-62.0	-69.4	-77.2	-64.3	-62.6	-68.0	43	WO2	-7.5	1.5	0.0
44	WO1	-4.5	1.5	-74.5	-64.2	-56.5	-64.5	-77.3	-64.7	-57.0	-62.3	44	WO1	-4.5	1.5	0.0
45	EI1	4.5	1.5	-65.7	-64.0	-75.3	-65.5	-61.8	-62.7	-76.4	-66.4	45	EI1	4.5	1.5	0.0
46	EI2	7.5	1.5	-64.1	-69.3	-69.3	-61.7	-65.7	-68.5	-67.7	-61.6	47	EI3	10.5	1.5	3.0
47	EI3	10.5	1.5	-65.1	-68.6	-67.9	-62.7	-68.1	-70.0	-68.3	-62.7	23	NO4	1.5	13.5	15.0
48	EI4	13.5	1.5	-65.5	-77.1	-70.9	-63.6	-71.5	-73.7	-71.0	-63.7	23	NO4	1.5	13.5	17.0
49	EI5	16.5	1.5	-62.1	-68.1	-66.8	-64.0	-62.5	-69.3	-69.1	-63.9	49	EI5	16.5	1.5	0.0
50	EI6	19.5	1.5	-61.2	-65.9	-67.8	-64.3	-59.1	-64.8	-68.1	-64.2	50	EI6	19.5	1.5	0.0
51	EI7	22.5	1.5	-63.2	-67.0	-72.0	-70.0	-70.0	-66.2	-71.2	-69.7	63	WI3	-10.5	-1.5	33.1
52	EI8	25.5	1.5	-71.0	-67.7	-73.2	-71.9	-69.5	-66.2	-68.0	-73.4	40	WO5	-16.5	1.5	42.0
53	EO8	25.5	-1.5	-77.2	-71.2	-76.0	-70.1	-75.6	-69.0	-73.1	-70.6	16	NI6	-1.5	19.5	34.2
54	EO7	22.5	-1.5	-72.6	-66.7	-71.4	-66.6	-72.1	-67.1	-65.9	-65.6	55	EO6	19.5	-1.5	3.0
55	EO6	19.5	-1.5	-71.1	-67.4	-66.9	-63.1	-75.8	-67.4	-65.6	-63.0	5	SO4	-1.5	-13.5	24.2
56	EO5	16.5	-1.5	-70.8	-70.2	-63.1	-60.4	-71.6	-70.5	-64.1	-60.7	56	EO5	16.5	-1.5	0.0
57	EO4	13.5	-1.5	-71.1	-80.1	-65.6	-64.6	-68.4	-79.3	-66.2	-63.7	57	EO4	13.5	-1.5	0.0
58	EO3	10.5	-1.5	-57.2	-81.4	-65.1	-60.4	-56.6	-74.7	-63.8	-58.1	58	EO3	10.5	-1.5	0.0
59	EO2	7.5	-1.5	-62.3	-68.3	-65.6	-59.0	-61.7	-68.4	-65.6	-60.8	59	EO2	7.5	-1.5	0.0
60	EO1	4.5	-1.5	-57.2	-61.4	-74.5	-67.6	-56.9	-60.5	-75.9	-69.9	60	EO1	4.5	-1.5	0.0
61	WI1	-4.5	-1.5	-73.4	-62.6	-57.3	-53.9	-76.6	-63.3	-57.4	-53.5	61	WI1	-4.5	-1.5	0.0
62	WI2	-7.5	-1.5	-67.3	-62.5	-68.4	-57.4	-66.9	-62.0	-67.9	-58.5	62	WI2	-7.5	-1.5	0.0
63	WI3	-10.5	-1.5	-70.6	-65.0	-70.9	-68.5	-70.1	-64.8	-68.9	-68.5	63	WI3	-10.5	-1.5	0.0
64	WI4	-13.5	-1.5	-67.8	-66.9	-69.8	-75.6	-67.2	-66.3	-68.9	-76.6	64	WI4	-13.5	-1.5	0.0
65	WI5	-16.5	-1.5	-70.1	-69.6	-71.0	-72.8	-68.8	-70.8	-67.5	-71.3	65	WI5	-16.5	-1.5	0.0
66	WI6	-19.5	-1.5	-72.8	-74.7	-71.5	-81.6	-72.1	-74.3	-73.0	-82.0	66	WI6	-19.5	-1.5	0.0
67	WI7	-22.5	-1.5	-74.0	-76.5	-72.4	-83.1	-73.4	-78.3	-73.2	-79.5	37	WO8	-25.5	1.5	4.2
68	WI8	-25.5	-1.5	-73.5	-72.7	-72.3	-79.6	-72.2	-72.0	-71.2	-68.0	3	SO6	-1.5	-19.5	30.0

Table B.3 Positioning using KNN algorithm, stationary beacon, Experiment 1, Rlowess filter applied.

Real location				Calibration stage				Test data collection stage				Positioning stage (estimated location)				
#	ID	x	y	RSSI by Scanner 1	RSSI by Scanner 2	RSSI by Scanner 3	RSSI by Scanner 4	RSSI by Scanner 1	RSSI by Scanner 2	RSSI by Scanner 3	RSSI by Scanner 4	#	ID	x	y	Error (m)
1	SO8	-1.5	-25.5	-74.0	-83.0	-72.3	-69.6	-69.5	-72.0	-68.6	-69.3	65	WI5	-16.5	-1.5	28.3
2	SO7	-1.5	-22.5	-77.3	-71.7	-76.3	-67.8	-73.3	-53.0	-73.3	-68.6	26	NO1	1.5	4.5	27.2
3	SO6	-1.5	-19.5	-75.5	-69.0	-68.3	-65.6	-77.3	-71.6	-68.3	-65.8	3	SO6	-1.5	-19.5	0.0
4	SO5	-1.5	-16.5	-81.3	-69.4	-67.6	-65.4	-78.9	-69.9	-67.0	-64.7	4	SO5	-1.5	-16.5	0.0
5	SO4	-1.5	-13.5	-76.2	-70.0	-65.5	-68.5	-78.8	-70.0	-65.5	-69.0	5	SO4	-1.5	-13.5	0.0
6	SO3	-1.5	-10.5	-72.0	-68.9	-63.3	-60.6	-73.3	-68.7	-63.1	-64.0	6	SO3	-1.5	-10.5	0.0
7	SO2	-1.5	-7.5	-73.0	-81.0	-65.7	-59.7	-73.7	-75.6	-66.9	-60.3	7	SO2	-1.5	-7.5	0.0
8	SO1	-1.5	-4.5	-62.1	-73.9	-65.3	-66.1	-66.0	-76.0	-67.9	-66.4	13	NI3	-1.5	10.5	15.0
9	ISW	-1.5	-1.5	-62.1	-74.8	-71.3	-70.8	-64.0	-78.5	-70.1	-70.4	9	ISW	-1.5	-1.5	0.0
10	INW	-1.5	1.5	-65.5	-61.0	-58.0	-63.1	-64.0	-61.0	-57.9	-61.6	10	INW	-1.5	1.5	0.0
11	NI1	-1.5	4.5	-65.7	-49.6	-60.8	-65.9	-65.5	-50.7	-64.2	-68.4	11	NI1	-1.5	4.5	0.0
12	NI2	-1.5	7.5	-67.3	-70.6	-73.4	-64.1	-69.7	-74.8	-71.0	-63.7	12	NI2	-1.5	7.5	0.0
13	NI3	-1.5	10.5	-65.3	-75.4	-67.8	-63.4	-63.3	-76.7	-68.8	-63.6	48	EI4	13.5	1.5	17.5
14	NI4	-1.5	13.5	-67.3	-67.8	-75.7	-68.9	-68.6	-68.9	-77.7	-67.3	14	NI4	-1.5	13.5	0.0
15	NI5	-1.5	16.5	-73.7	-65.1	-74.5	-68.1	-73.1	-66.0	-76.7	-68.7	15	NI5	-1.5	16.5	0.0
16	NI6	-1.5	19.5	-76.6	-66.4	-74.7	-70.9	-75.8	-66.6	-74.0	-71.6	16	NI6	-1.5	19.5	0.0
17	NI7	-1.5	22.5	-79.2	-70.5	-74.4	-70.9	-80.3	-70.8	-77.0	-71.0	17	NI7	-1.5	22.5	0.0
18	NI8	-1.5	25.5	-75.5	-70.3	-76.5	-72.8	-78.2	-70.7	-76.4	-74.7	18	NI8	-1.5	25.5	0.0
19	NO8	1.5	25.5	-70.1	-64.3	-70.9	-65.4	-70.9	-65.1	-68.4	-64.5	55	EO6	19.5	-1.5	32.4
20	NO7	1.5	22.5	-73.0	-65.6	-73.1	-67.4	-72.7	-66.3	-73.0	-67.9	20	NO7	1.5	22.5	0.0
21	NO6	1.5	19.5	-74.9	-66.4	-72.7	-67.7	-71.7	-67.4	-72.8	-68.4	20	NO7	1.5	22.5	3.0
22	NO5	1.5	16.5	-77.4	-67.2	-70.9	-65.3	-74.1	-67.1	-71.5	-65.0	54	EO7	22.5	-1.5	27.7
23	NO4	1.5	13.5	-69.1	-70.9	-67.6	-61.8	-67.5	-68.5	-65.9	-62.2	47	EI3	10.5	1.5	15.0
24	NO3	1.5	10.5	-62.9	-61.3	-69.7	-59.5	-61.5	-61.1	-66.4	-59.9	24	NO3	1.5	10.5	0.0
25	NO2	1.5	7.5	-63.3	-68.0	-72.3	-63.6	-63.7	-63.7	-74.7	-65.0	45	EI1	4.5	1.5	6.7
26	NO1	1.5	4.5	-67.3	-58.3	-64.6	-68.3	-67.4	-55.9	-62.8	-69.2	26	NO1	1.5	4.5	0.0
27	INE	1.5	1.5	-58.4	-61.9	-61.7	-73.8	-60.8	-61.3	-61.6	-75.0	27	INE	1.5	1.5	0.0
28	ISE	1.5	-1.5	-60.6	-69.0	-67.5	-66.3	-58.0	-71.6	-67.1	-68.4	28	ISE	1.5	-1.5	0.0
29	SI1	1.5	-4.5	-54.3	-68.6	-72.6	-57.4	-54.6	-69.8	-69.5	-57.1	29	SI1	1.5	-4.5	0.0
30	SI2	1.5	-7.5	-70.2	-70.4	-65.0	-62.6	-68.8	-71.5	-65.5	-61.9	30	SI2	1.5	-7.5	0.0
31	SI3	1.5	-10.5	-72.3	-64.0	-61.6	-75.8	-71.2	-62.1	-60.9	-74.7	31	SI3	1.5	-10.5	0.0
32	SI4	1.5	-13.5	-70.1	-61.8	-62.3	-71.0	-71.2	-61.0	-61.4	-69.7	32	SI4	1.5	-13.5	0.0
33	SI5	1.5	-16.5	-69.6	-66.2	-62.7	-64.9	-70.0	-66.0	-62.6	-64.0	33	SI5	1.5	-16.5	0.0
34	SI6	1.5	-19.5	-64.4	-64.9	-65.1	-64.5	-66.0	-64.1	-64.8	-65.7	34	SI6	1.5	-19.5	0.0

(continued)

(continued)

Real location				Calibration stage				Test data collection stage				Positioning stage (estimated location)				
#	ID	x	y	RSSI by Scanner 1	RSSI by Scanner 2	RSSI by Scanner 3	RSSI by Scanner 4	RSSI by Scanner 1	RSSI by Scanner 2	RSSI by Scanner 3	RSSI by Scanner 4	#	ID	x	y	Error (m)
35	SI7	1.5	-22.5	-62.3	-67.1	-66.5	-63.5	-63.2	-66.3	-65.8	-64.8	35	SI7	1.5	-22.5	0.0
36	SI8	1.5	-25.5	-66.3	-72.6	-64.9	-65.4	-65.0	-68.7	-67.0	-69.0	28	ISE	1.5	-1.5	24.0
37	WO8	-25.5	1.5	-75.7	-76.3	-71.7	-80.3	-75.5	-74.0	-70.8	-83.5	67	WI7	-22.5	-1.5	4.2
38	WO7	-22.5	1.5	-74.6	-71.4	-69.6	-81.0	-73.0	-71.2	-67.7	-80.7	38	WO7	-22.5	1.5	0.0
39	WO6	-19.5	1.5	-71.1	-67.3	-67.7	-74.5	-70.3	-67.4	-67.3	-74.8	39	WO6	-19.5	1.5	0.0
40	WO5	-16.5	1.5	-71.4	-64.1	-68.9	-73.3	-71.7	-64.0	-70.5	-72.3	40	WO5	-16.5	1.5	0.0
41	WO4	-13.5	1.5	-71.8	-66.5	-75.2	-71.6	-71.6	-66.7	-72.9	-72.9	41	WO4	-13.5	1.5	0.0
42	WO3	-10.5	1.5	-77.1	-65.5	-72.9	-78.0	-75.4	-65.7	-67.3	-79.8	42	WO3	-10.5	1.5	0.0
43	WO2	-7.5	1.5	-73.6	-66.8	-62.9	-69.2	-77.6	-64.3	-62.7	-68.0	43	WO2	-7.5	1.5	0.0
44	WO1	-4.5	1.5	-73.9	-64.6	-56.4	-64.1	-77.3	-64.7	-56.2	-61.9	44	WO1	-4.5	1.5	0.0
45	EI1	4.5	1.5	-65.6	-63.8	-74.9	-65.5	-61.7	-62.7	-76.8	-66.3	45	EI1	4.5	1.5	0.0
46	EI2	7.5	1.5	-63.6	-69.2	-69.3	-61.7	-65.8	-69.0	-69.1	-61.6	46	EI2	7.5	1.5	0.0
47	EI3	10.5	1.5	-64.8	-68.6	-67.4	-62.7	-68.3	-70.0	-68.2	-62.6	23	NO4	1.5	13.5	15.0
48	EI4	13.5	1.5	-63.9	-77.1	-70.6	-63.8	-71.5	-73.7	-71.4	-63.8	12	NI2	-1.5	7.5	16.2
49	EI5	16.5	1.5	-61.6	-68.4	-66.6	-64.1	-62.6	-68.4	-69.2	-64.0	50	EI6	19.5	1.5	3.0
50	EI6	19.5	1.5	-61.4	-67.1	-68.6	-64.5	-58.1	-64.6	-69.5	-66.3	50	EI6	19.5	1.5	0.0
51	EI7	22.5	1.5	-63.8	-67.0	-72.0	-70.0	-70.1	-66.4	-71.2	-69.7	63	WI3	-10.5	-1.5	33.1
52	EI8	25.5	1.5	-68.9	-68.1	-72.9	-73.0	-69.0	-66.1	-68.0	-72.3	39	WO6	-19.5	1.5	45.0
53	EO8	25.5	-1.5	-77.2	-72.0	-75.9	-70.5	-76.0	-69.0	-73.0	-70.7	16	NI6	-1.5	19.5	34.2
54	EO7	22.5	-1.5	-72.4	-66.7	-71.1	-66.3	-72.1	-67.0	-71.7	-65.7	54	EO7	22.5	-1.5	0.0
55	EO6	19.5	-1.5	-71.1	-65.6	-67.1	-63.2	-76.2	-66.8	-65.5	-63.0	3	SO6	-1.5	-19.5	27.7
56	EO5	16.5	-1.5	-70.9	-70.3	-63.1	-60.3	-71.4	-69.9	-64.1	-60.7	56	EO5	16.5	-1.5	0.0
57	EO4	13.5	-1.5	-71.0	-80.8	-65.7	-64.4	-68.1	-79.3	-66.2	-63.7	57	EO4	13.5	-1.5	0.0
58	EO3	10.5	-1.5	-57.2	-82.9	-64.0	-60.6	-56.6	-74.7	-63.7	-58.2	58	EO3	10.5	-1.5	0.0
59	EO2	7.5	-1.5	-62.3	-68.4	-65.6	-59.1	-61.0	-68.5	-65.8	-61.3	59	EO2	7.5	-1.5	0.0
60	EO1	4.5	-1.5	-56.8	-61.3	-73.3	-69.9	-56.8	-60.5	-76.1	-70.2	60	EO1	4.5	-1.5	0.0
61	WI1	-4.5	-1.5	-73.2	-62.7	-57.6	-53.7	-74.0	-63.3	-57.4	-53.6	61	WI1	-4.5	-1.5	0.0
62	WI2	-7.5	-1.5	-67.1	-62.0	-68.3	-57.6	-66.9	-62.0	-67.9	-58.5	62	WI2	-7.5	-1.5	0.0
63	WI3	-10.5	-1.5	-70.5	-65.0	-70.6	-68.5	-70.0	-64.8	-68.9	-68.5	63	WI3	-10.5	-1.5	0.0
64	WI4	-13.5	-1.5	-67.8	-66.4	-70.1	-75.7	-67.2	-66.3	-70.4	-75.1	64	WI4	-13.5	-1.5	0.0
65	WI5	-16.5	-1.5	-69.8	-70.4	-71.1	-72.8	-68.5	-69.5	-69.5	-71.3	65	WI5	-16.5	-1.5	0.0
66	WI6	-19.5	-1.5	-72.4	-74.7	-71.8	-80.5	-72.1	-73.1	-70.0	-82.0	66	WI6	-19.5	-1.5	0.0
67	WI7	-22.5	-1.5	-73.5	-76.5	-71.7	-83.0	-73.4	-78.3	-73.0	-79.5	37	WO8	-25.5	1.5	4.2
68	WI8	-25.5	-1.5	-73.5	-72.2	-71.7	-80.0	-71.4	-72.0	-73.9	-68.0	12	NI2	-1.5	7.5	25.6

Table B.4 Positioning using KNN algorithm, stationary beacon, Experiment 1, Center filter applied.

Real location				Calibration stage				Test data collection stage				Positioning stage (estimated location)				
#	ID	x	y	RSSI by Scanner 1	RSSI by Scanner 2	RSSI by Scanner 3	RSSI by Scanner 4	RSSI by Scanner 1	RSSI by Scanner 2	RSSI by Scanner 3	RSSI by Scanner 4	#	ID	x	y	Error (m)
1	SO8	-1.5	-25.5	-71.4	-83.0	-72.3	-69.5	-70.4	-72.0	-68.5	-69.3	65	WI5	-16.5	-1.5	28.3
2	SO7	-1.5	-22.5	-77.6	-70.7	-75.5	-68.2	-73.2	-53.0	-69.7	-68.5	26	NO1	1.5	4.5	27.2
3	SO6	-1.5	-19.5	-75.6	-69.1	-69.1	-65.7	-77.5	-71.3	-68.5	-65.4	3	SO6	-1.5	-19.5	0.0
4	SO5	-1.5	-16.5	-80.8	-69.4	-67.0	-65.4	-79.0	-69.8	-67.0	-64.2	4	SO5	-1.5	-16.5	0.0
5	SO4	-1.5	-13.5	-76.5	-69.9	-65.6	-67.4	-78.4	-70.0	-65.6	-69.0	5	SO4	-1.5	-13.5	0.0
6	SO3	-1.5	-10.5	-71.7	-68.9	-63.2	-60.9	-70.5	-69.0	-63.0	-64.0	30	SI2	1.5	-7.5	4.2
7	SO2	-1.5	-7.5	-72.4	-81.0	-65.5	-60.0	-72.8	-75.6	-66.5	-60.3	7	SO2	-1.5	-7.5	0.0
8	SO1	-1.5	-4.5	-62.4	-73.2	-67.2	-65.8	-64.6	-76.0	-68.0	-65.4	13	NI3	-1.5	10.5	15.0
9	ISW	-1.5	-1.5	-62.4	-75.0	-71.8	-73.5	-64.0	-78.5	-69.8	-67.3	48	EI4	13.5	1.5	15.3
10	INW	-1.5	1.5	-65.0	-61.0	-58.0	-63.0	-63.2	-61.0	-58.0	-61.8	10	INW	-1.5	1.5	0.0
11	NI1	-1.5	4.5	-65.2	-49.6	-61.1	-66.0	-65.5	-50.7	-64.3	-65.5	11	NI1	-1.5	4.5	0.0
12	NI2	-1.5	7.5	-67.2	-72.6	-73.4	-64.0	-69.6	-75.5	-71.0	-63.2	12	NI2	-1.5	7.5	0.0
13	NI3	-1.5	10.5	-64.8	-75.7	-68.8	-63.3	-66.8	-76.7	-69.8	-64.0	48	EI4	13.5	1.5	17.5
14	NI4	-1.5	13.5	-67.3	-68.3	-75.3	-67.6	-68.8	-69.0	-79.3	-67.3	14	NI4	-1.5	13.5	0.0
15	NI5	-1.5	16.5	-73.1	-65.3	-74.0	-68.0	-73.3	-66.0	-76.5	-68.7	15	NI5	-1.5	16.5	0.0
16	NI6	-1.5	19.5	-77.4	-66.0	-74.8	-70.8	-75.7	-67.0	-74.0	-71.3	16	NI6	-1.5	19.5	0.0
17	NI7	-1.5	22.5	-81.7	-70.6	-74.3	-71.4	-81.0	-70.8	-77.0	-70.0	17	NI7	-1.5	22.5	0.0
18	NI8	-1.5	25.5	-75.5	-70.4	-76.7	-73.7	-78.1	-70.8	-76.4	-74.0	18	NI8	-1.5	25.5	0.0
19	NO8	1.5	25.5	-69.1	-64.4	-71.6	-64.8	-71.2	-65.0	-72.6	-64.5	19	NO8	1.5	25.5	0.0
20	NO7	1.5	22.5	-73.3	-65.7	-73.1	-66.9	-73.0	-66.0	-72.8	-68.0	20	NO7	1.5	22.5	0.0
21	NO6	1.5	19.5	-74.4	-66.4	-72.8	-67.6	-70.8	-67.3	-72.3	-68.8	63	WI3	-10.5	-1.5	24.2
22	NO5	1.5	16.5	-77.5	-67.2	-71.0	-65.3	-74.0	-69.0	-71.0	-65.8	3	SO6	-1.5	-19.5	36.1
23	NO4	1.5	13.5	-69.1	-70.2	-67.5	-62.0	-67.9	-68.5	-66.0	-62.0	30	SI2	1.5	-7.5	21.0
24	NO3	1.5	10.5	-62.8	-61.3	-68.4	-59.5	-61.7	-60.4	-69.8	-59.8	24	NO3	1.5	10.5	0.0
25	NO2	1.5	7.5	-63.9	-65.5	-72.2	-63.6	-63.8	-63.0	-74.8	-65.0	45	EI1	4.5	1.5	6.7
26	NO1	1.5	4.5	-68.0	-58.2	-64.6	-68.3	-67.7	-58.0	-62.0	-69.0	26	NO1	1.5	4.5	0.0
27	INE	1.5	1.5	-59.0	-61.9	-61.0	-74.2	-60.0	-60.6	-62.0	-75.0	27	INE	1.5	1.5	0.0
28	ISE	1.5	-1.5	-60.6	-69.9	-68.1	-66.3	-59.0	-71.5	-66.0	-67.8	28	ISE	1.5	-1.5	0.0
29	SI1	1.5	-4.5	-54.3	-69.0	-72.3	-57.3	-55.0	-69.8	-69.5	-57.4	29	SI1	1.5	-4.5	0.0
30	SI2	1.5	-7.5	-69.6	-70.0	-65.0	-62.6	-70.2	-71.5	-65.5	-61.5	30	SI2	1.5	-7.5	0.0
31	SI3	1.5	-10.5	-72.5	-63.9	-62.1	-73.3	-68.2	-62.0	-61.0	-74.0	32	SI4	1.5	-13.5	3.0
32	SI4	1.5	-13.5	-70.3	-61.9	-62.0	-71.1	-71.2	-61.0	-61.8	-69.7	32	SI4	1.5	-13.5	0.0
33	SI5	1.5	-16.5	-69.2	-66.5	-63.0	-64.9	-70.5	-66.0	-62.0	-64.0	33	SI5	1.5	-16.5	0.0
34	SI6	1.5	-19.5	-64.3	-64.9	-65.2	-63.4	-66.0	-65.3	-64.8	-66.0	34	SI6	1.5	-19.5	0.0

(continued)

(continued)

Real location				Calibration stage				Test data collection stage				Positioning stage (estimated location)				
#	ID	x	y	RSSI by Scanner 1	RSSI by Scanner 2	RSSI by Scanner 3	RSSI by Scanner 4	RSSI by Scanner 1	RSSI by Scanner 2	RSSI by Scanner 3	RSSI by Scanner 4	#	ID	x	y	Error (m)
35	SI7	1.5	-22.5	-62.4	-67.0	-66.7	-63.6	-64.0	-67.0	-65.7	-64.8	35	SI7	1.5	-22.5	0.0
36	SI8	1.5	-25.5	-66.2	-72.6	-65.3	-65.4	-65.0	-68.7	-67.0	-69.0	28	ISE	1.5	-1.5	24.0
37	WO8	-25.5	1.5	-75.6	-76.4	-71.0	-80.8	-75.2	-72.8	-70.8	-83.4	68	WI8	-25.5	-1.5	3.0
38	WO7	-22.5	1.5	-73.9	-71.6	-69.8	-80.9	-72.8	-70.0	-67.0	-79.2	38	WO7	-22.5	1.5	0.0
39	WO6	-19.5	1.5	-71.1	-67.8	-67.8	-74.7	-70.3	-67.4	-67.0	-74.0	39	WO6	-19.5	1.5	0.0
40	WO5	-16.5	1.5	-72.1	-64.0	-69.2	-73.6	-71.6	-63.0	-70.5	-72.4	40	WO5	-16.5	1.5	0.0
41	WO4	-13.5	1.5	-71.3	-66.0	-75.6	-71.4	-71.2	-68.0	-73.0	-74.0	52	EI8	25.5	1.5	39.0
42	WO3	-10.5	1.5	-77.3	-65.5	-71.8	-78.0	-73.0	-66.0	-68.0	-79.8	39	WO6	-19.5	1.5	9.0
43	WO2	-7.5	1.5	-74.2	-66.9	-62.9	-69.3	-77.4	-69.0	-63.0	-68.0	5	SO4	-1.5	-13.5	16.2
44	WO1	-4.5	1.5	-74.4	-64.2	-56.5	-64.4	-77.2	-64.6	-56.0	-63.6	44	WO1	-4.5	1.5	0.0
45	EI1	4.5	1.5	-65.3	-62.4	-75.4	-65.5	-64.2	-62.7	-76.0	-66.0	45	EI1	4.5	1.5	0.0
46	EI2	7.5	1.5	-62.9	-69.2	-69.2	-61.7	-65.8	-69.0	-67.7	-62.0	47	EI3	10.5	1.5	3.0
47	EI3	10.5	1.5	-64.6	-68.7	-67.3	-63.0	-68.0	-70.3	-68.2	-62.8	23	NO4	1.5	13.5	15.0
48	EI4	13.5	1.5	-65.3	-77.3	-70.9	-65.1	-71.5	-71.7	-70.8	-63.8	23	NO4	1.5	13.5	17.0
49	EI5	16.5	1.5	-62.2	-69.6	-68.2	-64.0	-63.0	-69.2	-68.6	-64.0	49	EI5	16.5	1.5	0.0
50	EI6	19.5	1.5	-61.0	-66.6	-67.8	-64.1	-59.5	-65.6	-68.2	-65.7	50	EI6	19.5	1.5	0.0
51	EI7	22.5	1.5	-62.0	-67.0	-71.4	-69.8	-70.0	-67.0	-71.8	-69.8	63	WI3	-10.5	-1.5	33.1
52	EI8	25.5	1.5	-70.0	-67.7	-74.0	-72.9	-69.0	-66.2	-73.3	-72.5	52	EI8	25.5	1.5	0.0
53	EO8	25.5	-1.5	-77.1	-72.0	-75.9	-70.0	-76.0	-69.0	-72.1	-71.0	16	NI6	-1.5	19.5	34.2
54	EO7	22.5	-1.5	-72.3	-66.8	-71.4	-66.1	-72.2	-66.8	-70.8	-65.7	54	EO7	22.5	-1.5	0.0
55	EO6	19.5	-1.5	-71.1	-65.6	-66.8	-63.1	-72.8	-66.8	-65.7	-63.0	55	EO6	19.5	-1.5	0.0
56	EO5	16.5	-1.5	-70.8	-70.3	-63.1	-60.4	-70.7	-71.9	-64.0	-61.0	56	EO5	16.5	-1.5	0.0
57	EO4	13.5	-1.5	-71.0	-82.2	-65.6	-64.6	-67.1	-82.3	-66.3	-64.0	57	EO4	13.5	-1.5	0.0
58	EO3	10.5	-1.5	-57.2	-81.6	-65.2	-60.4	-57.0	-74.7	-63.8	-58.0	58	EO3	10.5	-1.5	0.0
59	EO2	7.5	-1.5	-61.8	-68.0	-65.5	-59.1	-61.6	-68.0	-65.7	-60.5	59	EO2	7.5	-1.5	0.0
60	EO1	4.5	-1.5	-57.0	-62.6	-72.0	-69.3	-56.8	-60.6	-74.3	-69.8	60	EO1	4.5	-1.5	0.0
61	WI1	-4.5	-1.5	-72.5	-62.6	-57.4	-53.9	-76.2	-63.3	-57.8	-54.0	61	WI1	-4.5	-1.5	0.0
62	WI2	-7.5	-1.5	-66.5	-62.0	-67.0	-58.3	-66.4	-62.0	-68.0	-58.8	62	WI2	-7.5	-1.5	0.0
63	WI3	-10.5	-1.5	-70.5	-65.0	-70.4	-68.5	-70.0	-64.6	-69.0	-68.8	63	WI3	-10.5	-1.5	0.0
64	WI4	-13.5	-1.5	-67.8	-66.3	-70.5	-75.6	-67.2	-66.4	-69.0	-77.0	64	WI4	-13.5	-1.5	0.0
65	WI5	-16.5	-1.5	-70.1	-70.3	-71.5	-72.8	-68.8	-69.9	-70.8	-72.0	65	WI5	-16.5	-1.5	0.0
66	WI6	-19.5	-1.5	-72.8	-74.7	-71.5	-81.5	-72.0	-74.2	-72.6	-82.0	66	WI6	-19.5	-1.5	0.0
67	WI7	-22.5	-1.5	-74.0	-74.9	-71.6	-83.3	-73.6	-78.3	-72.0	-79.5	37	WO8	-25.5	1.5	4.2
68	WI8	-25.5	-1.5	-73.4	-72.0	-71.3	-83.4	-75.1	-72.0	-70.5	-68.0	3	SO6	-1.5	-19.5	30.0

Table B.5 Positioning using KNN algorithm, stationary beacon, Experiment 1, Linear filter applied.

Real location				Calibration stage				Test data collection stage				Positioning stage (estimated location)				
#	ID	x	y	RSSI by Scanner 1	RSSI by Scanner 2	RSSI by Scanner 3	RSSI by Scanner 4	RSSI by Scanner 1	RSSI by Scanner 2	RSSI by Scanner 3	RSSI by Scanner 4	#	ID	x	y	Error (m)
1	SO8	-1.5	-25.5	-70.5	-83.0	-70.9	-69.5	-69.5	-72.0	-68.5	-69.3	65	WI5	-16.5	-1.5	28.3
2	SO7	-1.5	-22.5	-77.6	-70.5	-76.1	-68.4	-73.2	-53.0	-69.0	-68.5	26	NO1	1.5	4.5	27.2
3	SO6	-1.5	-19.5	-75.6	-69.1	-69.1	-65.7	-77.5	-71.3	-68.5	-65.4	3	SO6	-1.5	-19.5	0.0
4	SO5	-1.5	-16.5	-80.8	-69.4	-66.9	-65.4	-79.0	-69.8	-67.0	-64.2	4	SO5	-1.5	-16.5	0.0
5	SO4	-1.5	-13.5	-76.5	-69.8	-65.6	-68.0	-78.4	-70.0	-65.6	-69.0	5	SO4	-1.5	-13.5	0.0
6	SO3	-1.5	-10.5	-71.6	-68.9	-63.2	-60.9	-69.5	-69.0	-63.1	-64.0	30	SI2	1.5	-7.5	4.2
7	SO2	-1.5	-7.5	-72.4	-81.0	-65.8	-60.0	-72.8	-75.6	-66.5	-60.3	7	SO2	-1.5	-7.5	0.0
8	SO1	-1.5	-4.5	-62.4	-73.5	-67.4	-65.8	-64.6	-76.0	-68.0	-65.3	13	NI3	-1.5	10.5	15.0
9	ISW	-1.5	-1.5	-62.4	-75.0	-71.7	-74.0	-64.0	-78.5	-69.8	-66.0	48	EI4	13.5	1.5	15.3
10	INW	-1.5	1.5	-65.0	-61.0	-58.0	-63.0	-63.2	-61.0	-58.0	-61.8	10	INW	-1.5	1.5	0.0
11	NI1	-1.5	4.5	-65.2	-49.6	-61.1	-66.0	-65.5	-52.0	-64.3	-67.8	11	NI1	-1.5	4.5	0.0
12	NI2	-1.5	7.5	-67.2	-72.6	-73.4	-64.0	-69.6	-75.5	-71.0	-63.2	12	NI2	-1.5	7.5	0.0
13	NI3	-1.5	10.5	-65.2	-75.6	-68.8	-63.3	-66.5	-76.7	-69.8	-64.0	13	NI3	-1.5	10.5	0.0
14	NI4	-1.5	13.5	-67.3	-68.3	-75.3	-67.6	-68.8	-69.0	-79.5	-67.3	14	NI4	-1.5	13.5	0.0
15	NI5	-1.5	16.5	-73.1	-65.3	-74.0	-68.0	-73.3	-66.0	-76.5	-68.7	15	NI5	-1.5	16.5	0.0
16	NI6	-1.5	19.5	-77.0	-66.0	-74.8	-70.8	-75.7	-67.0	-74.0	-71.3	16	NI6	-1.5	19.5	0.0
17	NI7	-1.5	22.5	-82.0	-70.6	-74.3	-71.4	-81.0	-70.8	-77.0	-70.0	17	NI7	-1.5	22.5	0.0
18	NI8	-1.5	25.5	-75.5	-70.4	-76.6	-73.7	-78.1	-70.8	-76.4	-74.0	18	NI8	-1.5	25.5	0.0
19	NO8	1.5	25.5	-69.4	-64.4	-71.6	-64.8	-71.2	-64.8	-72.3	-64.5	19	NO8	1.5	25.5	0.0
20	NO7	1.5	22.5	-73.2	-65.7	-73.1	-66.9	-73.0	-66.0	-72.8	-68.0	20	NO7	1.5	22.5	0.0
21	NO6	1.5	19.5	-74.4	-66.4	-72.8	-67.6	-70.8	-67.3	-72.3	-68.8	63	WI3	-10.5	-1.5	24.2
22	NO5	1.5	16.5	-77.5	-67.2	-70.9	-65.3	-74.0	-69.0	-71.0	-65.8	3	SO6	-1.5	-19.5	36.1
23	NO4	1.5	13.5	-69.1	-70.2	-67.5	-62.0	-67.9	-68.5	-66.0	-62.0	30	SI2	1.5	-7.5	21.0
24	NO3	1.5	10.5	-62.8	-61.3	-68.3	-59.5	-61.7	-60.8	-69.8	-59.8	24	NO3	1.5	10.5	0.0
25	NO2	1.5	7.5	-63.7	-65.5	-72.2	-63.3	-63.8	-63.0	-74.8	-65.0	45	EI1	4.5	1.5	6.7
26	NO1	1.5	4.5	-68.0	-58.1	-64.6	-68.3	-67.7	-58.0	-62.0	-69.0	26	NO1	1.5	4.5	0.0
27	INE	1.5	1.5	-59.0	-61.9	-61.0	-74.2	-60.0	-60.6	-62.0	-75.0	27	INE	1.5	1.5	0.0
28	ISE	1.5	-1.5	-60.6	-69.9	-68.1	-66.3	-59.0	-71.5	-66.0	-67.8	28	ISE	1.5	-1.5	0.0
29	SI1	1.5	-4.5	-54.3	-69.0	-72.6	-57.3	-55.0	-69.8	-69.5	-57.3	29	SI1	1.5	-4.5	0.0
30	SI2	1.5	-7.5	-69.6	-70.0	-65.0	-62.6	-70.2	-71.5	-65.5	-61.5	30	SI2	1.5	-7.5	0.0
31	SI3	1.5	-10.5	-72.5	-63.9	-62.1	-73.2	-68.0	-62.0	-61.0	-74.0	32	SI4	1.5	-13.5	3.0
32	SI4	1.5	-13.5	-70.3	-61.9	-62.0	-71.1	-71.2	-61.0	-61.8	-69.7	32	SI4	1.5	-13.5	0.0
33	SI5	1.5	-16.5	-69.1	-66.5	-63.0	-64.9	-70.5	-66.0	-62.0	-64.0	33	SI5	1.5	-16.5	0.0
34	SI6	1.5	-19.5	-64.3	-64.9	-65.2	-63.1	-66.0	-65.3	-64.8	-66.0	34	SI6	1.5	-19.5	0.0

(continued)

(continued)

Real location				Calibration stage				Test data collection stage				Positioning stage (estimated location)				
#	ID	x	y	RSSI by Scanner 1	RSSI by Scanner 2	RSSI by Scanner 3	RSSI by Scanner 4	RSSI by Scanner 1	RSSI by Scanner 2	RSSI by Scanner 3	RSSI by Scanner 4	#	ID	x	y	Error (m)
35	SI7	1.5	-22.5	-62.4	-67.0	-66.7	-63.6	-64.0	-67.0	-65.8	-64.8	35	SI7	1.5	-22.5	0.0
36	SI8	1.5	-25.5	-66.2	-72.6	-65.3	-65.4	-65.0	-68.7	-67.0	-69.0	28	ISE	1.5	-1.5	24.0
37	WO8	-25.5	1.5	-75.6	-76.4	-71.0	-80.8	-75.2	-73.0	-70.8	-83.4	68	WI8	-25.5	-1.5	3.0
38	WO7	-22.5	1.5	-73.9	-71.6	-69.9	-80.9	-72.8	-70.0	-67.0	-78.9	38	WO7	-22.5	1.5	0.0
39	WO6	-19.5	1.5	-71.1	-67.8	-67.8	-74.6	-70.4	-67.4	-67.0	-74.0	39	WO6	-19.5	1.5	0.0
40	WO5	-16.5	1.5	-71.6	-64.0	-69.3	-73.6	-71.7	-63.0	-70.5	-72.4	40	WO5	-16.5	1.5	0.0
41	WO4	-13.5	1.5	-71.5	-66.0	-75.6	-71.4	-71.2	-68.0	-73.0	-74.0	52	EI8	25.5	1.5	39.0
42	WO3	-10.5	1.5	-77.3	-65.5	-71.8	-78.0	-73.0	-66.0	-68.0	-79.8	39	WO6	-19.5	1.5	9.0
43	WO2	-7.5	1.5	-74.2	-66.9	-63.0	-69.3	-77.4	-69.5	-63.0	-68.0	5	SO4	-1.5	-13.5	16.2
44	WO1	-4.5	1.5	-74.4	-64.2	-56.5	-64.4	-77.2	-64.6	-56.0	-63.8	44	WO1	-4.5	1.5	0.0
45	EI1	4.5	1.5	-65.3	-62.3	-75.4	-65.5	-64.0	-62.7	-76.0	-66.0	45	EI1	4.5	1.5	0.0
46	EI2	7.5	1.5	-61.6	-69.2	-69.2	-61.7	-65.8	-69.0	-67.7	-62.0	47	EI3	10.5	1.5	3.0
47	EI3	10.5	1.5	-64.7	-68.7	-67.3	-63.0	-68.0	-70.3	-68.2	-62.8	23	NO4	1.5	13.5	15.0
48	EI4	13.5	1.5	-65.3	-77.3	-70.9	-65.5	-71.5	-71.0	-70.8	-63.8	23	NO4	1.5	13.5	17.0
49	EI5	16.5	1.5	-62.2	-69.6	-68.2	-64.0	-63.0	-69.2	-68.3	-64.0	49	EI5	16.5	1.5	0.0
50	EI6	19.5	1.5	-61.0	-66.8	-67.8	-64.1	-59.5	-65.8	-69.0	-66.1	50	EI6	19.5	1.5	0.0
51	EI7	22.5	1.5	-62.0	-67.0	-71.6	-69.7	-70.0	-67.0	-71.7	-69.8	63	WI3	-10.5	-1.5	33.1
52	EI8	25.5	1.5	-70.0	-67.7	-74.0	-72.8	-69.0	-66.2	-74.0	-72.3	52	EI8	25.5	1.5	0.0
53	EO8	25.5	-1.5	-77.1	-72.1	-75.9	-70.0	-76.0	-69.0	-71.9	-71.0	16	NI6	-1.5	19.5	34.2
54	EO7	22.5	-1.5	-72.3	-66.8	-71.4	-66.1	-72.2	-66.8	-71.6	-65.7	54	EO7	22.5	-1.5	0.0
55	EO6	19.5	-1.5	-71.1	-65.4	-66.8	-63.1	-73.6	-66.9	-65.7	-63.0	55	EO6	19.5	-1.5	0.0
56	EO5	16.5	-1.5	-70.8	-70.3	-63.1	-60.4	-70.7	-72.5	-64.0	-61.0	56	EO5	16.5	-1.5	0.0
57	EO4	13.5	-1.5	-71.0	-82.1	-65.6	-64.6	-67.1	-82.0	-66.3	-64.0	57	EO4	13.5	-1.5	0.0
58	EO3	10.5	-1.5	-57.2	-81.6	-65.2	-60.4	-57.0	-74.7	-63.8	-58.0	58	EO3	10.5	-1.5	0.0
59	EO2	7.5	-1.5	-61.9	-68.0	-65.5	-59.1	-61.6	-68.0	-65.7	-60.5	59	EO2	7.5	-1.5	0.0
60	EO1	4.5	-1.5	-57.0	-63.0	-72.0	-69.2	-56.8	-60.6	-74.2	-69.8	60	EO1	4.5	-1.5	0.0
61	WI1	-4.5	-1.5	-73.0	-62.6	-57.4	-53.9	-76.2	-63.3	-57.8	-54.0	61	WI1	-4.5	-1.5	0.0
62	WI2	-7.5	-1.5	-66.5	-62.0	-67.3	-58.1	-66.5	-62.0	-68.0	-58.8	62	WI2	-7.5	-1.5	0.0
63	WI3	-10.5	-1.5	-70.5	-65.0	-70.3	-68.5	-70.0	-64.6	-69.0	-68.8	63	WI3	-10.5	-1.5	0.0
64	WI4	-13.5	-1.5	-67.8	-66.4	-70.5	-75.6	-67.2	-66.4	-69.0	-77.0	64	WI4	-13.5	-1.5	0.0
65	WI5	-16.5	-1.5	-70.1	-70.3	-71.5	-72.8	-68.8	-69.6	-71.1	-72.0	65	WI5	-16.5	-1.5	0.0
66	WI6	-19.5	-1.5	-72.8	-74.7	-71.5	-81.5	-72.0	-74.2	-72.6	-82.0	66	WI6	-19.5	-1.5	0.0
67	WI7	-22.5	-1.5	-74.0	-75.4	-71.7	-83.3	-73.6	-78.3	-72.0	-79.5	37	WO8	-25.5	1.5	4.2
68	WI8	-25.5	-1.5	-73.4	-72.1	-71.3	-84.0	-76.3	-72.0	-70.5	-68.0	3	SO6	-1.5	-19.5	30.0

Table B.6 Positioning using KNN algorithm, stationary beacon, Experiment 1, Standard deviation filter applied.

Real location				Calibration stage				Test data collection stage				Positioning stage (estimated location)				
#	ID	x	y	RSSI by Scanner 1	RSSI by Scanner 2	RSSI by Scanner 3	RSSI by Scanner 4	RSSI by Scanner 1	RSSI by Scanner 2	RSSI by Scanner 3	RSSI by Scanner 4	#	ID	x	y	Error (m)
1	SO8	-1.5	-25.5	-71.6	-83.0	-72.1	-69.8	-71.7	-72.0	-69.0	-69.0	65	WI5	-16.5	-1.5	28.3
2	SO7	-1.5	-22.5	-77.9	-70.8	-74.8	-68.2	-73.0	-53.0	-69.5	-68.5	26	NO1	1.5	4.5	27.2
3	SO6	-1.5	-19.5	-76	-68.9	-69.2	-65.7	-76.7	-70.0	-68.5	-64.3	3	SO6	-1.5	-19.5	0.0
4	SO5	-1.5	-16.5	-80.3	-68.3	-67.7	-64.5	-77.7	-69.3	-67.0	-64.3	4	SO5	-1.5	-16.5	0.0
5	SO4	-1.5	-13.5	-75.3	-70.8	-66.0	-67.0	-80.5	-70.0	-66.3	-69.0	4	SO5	-1.5	-16.5	3.0
6	SO3	-1.5	-10.5	-71.6	-69.0	-63.5	-61.4	-70.3	-69.0	-63.3	-62.5	6	SO3	-1.5	-10.5	0.0
7	SO2	-1.5	-7.5	-69.3	-82.5	-65.2	-60.0	-70.0	-76.5	-66.5	-60.7	23	NO4	1.5	13.5	21.2
8	SO1	-1.5	-4.5	-62.1	-73.3	-66.8	-65.7	-63.7	-76.0	-68.0	-65.3	13	NI3	-1.5	10.5	15.0
9	ISW	-1.5	-1.5	-62.3	-75.7	-71.8	-73.7	-64.0	-78.5	-68.5	-68.3	48	EI4	13.5	1.5	15.3
10	INW	-1.5	1.5	-65.4	-61.2	-58.0	-63.0	-64.0	-61.0	-58.5	-62.0	10	INW	-1.5	1.5	0.0
11	NI1	-1.5	4.5	-64.9	-49.4	-60.8	-66.1	-65.5	-52.0	-64.0	-65.6	11	NI1	-1.5	4.5	0.0
12	NI2	-1.5	7.5	-66.7	-73.0	-72.6	-63.7	-70.0	-74.8	-71.0	-63.3	12	NI2	-1.5	7.5	0.0
13	NI3	-1.5	10.5	-64.4	-75.6	-67.8	-63.7	-66.8	-77.0	-68.7	-64.0	13	NI3	-1.5	10.5	0.0
14	NI4	-1.5	13.5	-68	-68.3	-75.2	-68.1	-70.3	-69.3	-79.5	-67.3	14	NI4	-1.5	13.5	0.0
15	NI5	-1.5	16.5	-73.3	-66.3	-74.3	-68.0	-72.7	-66.0	-75.3	-68.8	15	NI5	-1.5	16.5	0.0
16	NI6	-1.5	19.5	-76.5	-66.0	-74.3	-70.9	-75.5	-67.0	-74.0	-71.7	16	NI6	-1.5	19.5	0.0
17	NI7	-1.5	22.5	-81.7	-70.7	-74.4	-71.5	-81.0	-70.7	-75.5	-70.4	17	NI7	-1.5	22.5	0.0
18	NI8	-1.5	25.5	-76.4	-70.5	-76.7	-73.8	-77.3	-71.3	-76.3	-74.0	18	NI8	-1.5	25.5	0.0
19	NO8	1.5	25.5	-69.5	-64.5	-71.4	-65.0	-69.0	-64.0	-72.6	-64.5	19	NO8	1.5	25.5	0.0
20	NO7	1.5	22.5	-72.8	-65.6	-72.4	-67.5	-73.0	-66.0	-72.7	-68.0	20	NO7	1.5	22.5	0.0
21	NO6	1.5	19.5	-74.4	-66.8	-73.1	-67.4	-70.0	-68.0	-73.0	-68.7	14	NI4	-1.5	13.5	6.7
22	NO5	1.5	16.5	-75.9	-67.3	-70.7	-64.8	-75.7	-69.0	-71.0	-66.0	3	SO6	-1.5	-19.5	36.1
23	NO4	1.5	13.5	-70	-71.2	-67.7	-62.0	-69.3	-68.5	-66.0	-62.2	30	SI2	1.5	-7.5	21.0
24	NO3	1.5	10.5	-62.8	-61.0	-68.6	-59.5	-61.8	-60.3	-71.0	-60.0	24	NO3	1.5	10.5	0.0
25	NO2	1.5	7.5	-64.5	-63.6	-73.4	-63.5	-63.0	-62.7	-74.5	-65.0	25	NO2	1.5	7.5	0.0
26	NO1	1.5	4.5	-68	-58.1	-64.7	-67.6	-67.8	-58.0	-62.4	-69.0	26	NO1	1.5	4.5	0.0
27	INE	1.5	1.5	-59	-61.4	-61.2	-72.4	-60.0	-61.0	-62.0	-75.0	27	INE	1.5	1.5	0.0
28	ISE	1.5	-1.5	-60.5	-70.4	-68.2	-66.6	-59.0	-72.0	-66.3	-67.5	28	ISE	1.5	-1.5	0.0
29	SI1	1.5	-4.5	-54.1	-68.3	-72.4	-57.5	-55.0	-68.7	-69.5	-57.4	29	SI1	1.5	-4.5	0.0
30	SI2	1.5	-7.5	-70.2	-69.8	-65.1	-62.6	-71.0	-70.7	-65.5	-61.5	30	SI2	1.5	-7.5	0.0
31	SI3	1.5	-10.5	-71.8	-63.7	-62.1	-74.3	-68.2	-62.0	-60.5	-74.3	31	SI3	1.5	-10.5	0.0
32	SI4	1.5	-13.5	-70.4	-61.8	-61.6	-70.3	-71.0	-61.0	-62.0	-69.0	32	SI4	1.5	-13.5	0.0
33	SI5	1.5	-16.5	-69.5	-65.9	-63.0	-64.6	-71.0	-66.0	-62.0	-64.0	33	SI5	1.5	-16.5	0.0
34	SI6	1.5	-19.5	-64.6	-64.5	-64.9	-63.4	-66.0	-65.3	-65.0	-66.0	34	SI6	1.5	-19.5	0.0

(continued)

(continued)

Real location				Calibration stage				Test data collection stage				Positioning stage (estimated location)				
#	ID	x	y	RSSI by Scanner 1	RSSI by Scanner 2	RSSI by Scanner 3	RSSI by Scanner 4	RSSI by Scanner 1	RSSI by Scanner 2	RSSI by Scanner 3	RSSI by Scanner 4	#	ID	x	y	Error (m)
35	SI7	1.5	-22.5	-62.3	-67.0	-66.9	-63.6	-63.8	-67.0	-65.8	-64.3	35	SI7	1.5	-22.5	0.0
36	SI8	1.5	-25.5	-66.4	-72.0	-65.0	-65.4	-65.0	-67.5	-67.0	-69.0	51	EI7	22.5	1.5	34.2
37	WO8	-25.5	1.5	-76	-76.6	-71.3	-81.0	-76.0	-72.7	-70.3	-82.0	38	WO7	-22.5	1.5	3.0
38	WO7	-22.5	1.5	-73.8	-71.5	-69.8	-80.8	-72.3	-70.5	-67.3	-79.3	38	WO7	-22.5	1.5	0.0
39	WO6	-19.5	1.5	-71.5	-67.8	-67.4	-74.7	-70.0	-66.8	-66.7	-74.0	39	WO6	-19.5	1.5	0.0
40	WO5	-16.5	1.5	-71.8	-63.3	-68.7	-74.0	-71.3	-63.0	-70.5	-72.3	40	WO5	-16.5	1.5	0.0
41	WO4	-13.5	1.5	-71.6	-65.8	-75.7	-71.8	-70.7	-68.0	-72.0	-74.0	52	EI8	25.5	1.5	39.0
42	WO3	-10.5	1.5	-77.9	-65.5	-71.1	-79.0	-73.8	-66.0	-68.0	-79.5	42	WO3	-10.5	1.5	0.0
43	WO2	-7.5	1.5	-73.4	-67.2	-62.9	-68.8	-77.7	-69.5	-63.0	-68.0	5	SO4	-1.5	-13.5	16.2
44	WO1	-4.5	1.5	-74.2	-63.6	-56.3	-64.4	-76.5	-64.7	-56.3	-63.7	44	WO1	-4.5	1.5	0.0
45	EI1	4.5	1.5	-66.1	-62.6	-75.6	-65.5	-64.3	-63.0	-76.3	-66.0	45	EI1	4.5	1.5	0.0
46	EI2	7.5	1.5	-63.7	-69.0	-69.0	-61.5	-67.7	-69.0	-69.2	-62.0	23	NO4	1.5	13.5	13.4
47	EI3	10.5	1.5	-64.5	-68.6	-67.4	-62.7	-69.0	-70.5	-67.5	-63.3	23	NO4	1.5	13.5	15.0
48	EI4	13.5	1.5	-65.2	-75.4	-70.8	-65.1	-71.5	-71.5	-71.3	-64.5	23	NO4	1.5	13.5	17.0
49	EI5	16.5	1.5	-62	-68.6	-68.2	-64.0	-62.8	-69.3	-68.6	-64.0	49	EI5	16.5	1.5	0.0
50	EI6	19.5	1.5	-61	-66.3	-67.3	-64.1	-62.3	-65.7	-68.3	-65.8	50	EI6	19.5	1.5	0.0
51	EI7	22.5	1.5	-62	-67.0	-71.5	-70.8	-70.0	-67.0	-71.5	-69.7	63	WI3	-10.5	-1.5	33.1
52	EI8	25.5	1.5	-70.7	-67.8	-73.7	-72.9	-69.0	-66.3	-73.5	-72.4	52	EI8	25.5	1.5	0.0
53	EO8	25.5	-1.5	-78.5	-72.4	-74.3	-70.3	-75.8	-69.0	-72.0	-71.0	16	NI6	-1.5	19.5	34.2
54	EO7	22.5	-1.5	-72.2	-66.8	-71.7	-66.1	-72.0	-68.0	-68.7	-66.6	54	EO7	22.5	-1.5	0.0
55	EO6	19.5	-1.5	-71	-65.5	-67.0	-63.4	-72.8	-66.8	-65.8	-63.0	55	EO6	19.5	-1.5	0.0
56	EO5	16.5	-1.5	-71.3	-69.3	-63.0	-60.6	-71.0	-72.0	-64.0	-61.0	56	EO5	16.5	-1.5	0.0
57	EO4	13.5	-1.5	-70.3	-81.0	-66.1	-64.2	-65.8	-82.5	-65.7	-64.0	57	EO4	13.5	-1.5	0.0
58	EO3	10.5	-1.5	-57	-82.3	-64.7	-60.4	-57.0	-75.0	-63.8	-58.0	59	EO2	7.5	-1.5	3.0
59	EO2	7.5	-1.5	-61.8	-69.7	-65.9	-58.6	-61.7	-66.3	-65.3	-60.5	35	SI7	1.5	-22.5	21.8
60	EO1	4.5	-1.5	-56.5	-62.3	-72.9	-69.3	-56.7	-60.3	-75.0	-70.7	60	EO1	4.5	-1.5	0.0
61	WI1	-4.5	-1.5	-71.5	-62.5	-57.4	-53.5	-76.7	-63.0	-57.0	-54.0	61	WI1	-4.5	-1.5	0.0
62	WI2	-7.5	-1.5	-66.5	-62.1	-67.3	-56.7	-66.4	-62.0	-66.7	-59.3	62	WI2	-7.5	-1.5	0.0
63	WI3	-10.5	-1.5	-69.8	-64.5	-71.3	-68.2	-69.8	-63.8	-69.0	-69.3	63	WI3	-10.5	-1.5	0.0
64	WI4	-13.5	-1.5	-68.1	-66.3	-70.2	-74.3	-66.7	-67.3	-70.5	-77.0	64	WI4	-13.5	-1.5	0.0
65	WI5	-16.5	-1.5	-70.5	-70.4	-71.6	-72.3	-69.0	-70.3	-71.0	-72.0	65	WI5	-16.5	-1.5	0.0
66	WI6	-19.5	-1.5	-72.5	-75.5	-72.0	-81.0	-72.0	-74.0	-71.5	-82.0	66	WI6	-19.5	-1.5	0.0
67	WI7	-22.5	-1.5	-73.4	-75.1	-71.9	-83.0	-74.0	-77.0	-72.3	-79.5	66	WI6	-19.5	-1.5	3.0
68	WI8	-25.5	-1.5	-73.5	-72.0	-72.0	-83.7	-75.3	-72.0	-72.0	-68.0	2	SO7	-1.5	-22.5	31.9

Appendix C

Sample raw data of turning movement classification

A crossing in Experiment 4: Speed of 15 km/h, NLOS signal transmission path

East-South movement

BLE Mode - Scanner 1 - West approach

MAC	Signal mode	RSSI (dBm)	Timestamp	Timestamp
fc4aac8fa25f	1	-96	1603923550	6:19:10 PM
fc4aac8fa25f	1	-93	1603923551	6:19:11 PM
fc4aac8fa25f	1	-93	1603923551	6:19:11 PM
fc4aac8fa25f	1	-91	1603923553	6:19:13 PM
fc4aac8fa25f	1	-88	1603923554	6:19:14 PM
fc4aac8fa25f	1	-90	1603923557	6:19:17 PM
fc4aac8fa25f	1	-89	1603923558	6:19:18 PM
fc4aac8fa25f	1	-85	1603923559	6:19:19 PM
fc4aac8fa25f	1	-91	1603923559	6:19:19 PM
fc4aac8fa25f	1	-88	1603923560	6:19:20 PM
fc4aac8fa25f	1	-93	1603923561	6:19:21 PM
fc4aac8fa25f	1	-83	1603923562	6:19:22 PM
fc4aac8fa25f	1	-88	1603923562	6:19:22 PM
fc4aac8fa25f	1	-83	1603923563	6:19:23 PM
fc4aac8fa25f	1	-88	1603923563	6:19:23 PM
fc4aac8fa25f	1	-79	1603923564	6:19:24 PM
fc4aac8fa25f	1	-84	1603923564	6:19:24 PM
fc4aac8fa25f	1	-86	1603923565	6:19:25 PM
fc4aac8fa25f	1	-86	1603923566	6:19:26 PM
fc4aac8fa25f	1	-86	1603923567	6:19:27 PM
fc4aac8fa25f	1	-86	1603923569	6:19:29 PM
fc4aac8fa25f	1	-94	1603923572	6:19:32 PM

BLE Mode - Scanner 2 - South approach

MAC	Signal mode	RSSI (dBm)	Timestamp	Timestamp
fc4aac8fa25f	1	-89	1603923551	6:19:11 PM
fc4aac8fa25f	1	-91	1603923553	6:19:13 PM
fc4aac8fa25f	1	-92	1603923554	6:19:14 PM
fc4aac8fa25f	1	-93	1603923556	6:19:16 PM
fc4aac8fa25f	1	-93	1603923556	6:19:16 PM
fc4aac8fa25f	1	-88	1603923558	6:19:18 PM
fc4aac8fa25f	1	-90	1603923559	6:19:19 PM
fc4aac8fa25f	1	-89	1603923560	6:19:20 PM
fc4aac8fa25f	1	-88	1603923562	6:19:22 PM
fc4aac8fa25f	1	-83	1603923562	6:19:22 PM
fc4aac8fa25f	1	-78	1603923563	6:19:23 PM
fc4aac8fa25f	1	-75	1603923563	6:19:23 PM
fc4aac8fa25f	1	-79	1603923564	6:19:24 PM
fc4aac8fa25f	1	-81	1603923564	6:19:24 PM
fc4aac8fa25f	1	-80	1603923565	6:19:25 PM
fc4aac8fa25f	1	-73	1603923565	6:19:25 PM
fc4aac8fa25f	1	-80	1603923566	6:19:26 PM
fc4aac8fa25f	1	-77	1603923567	6:19:27 PM
fc4aac8fa25f	1	-75	1603923567	6:19:27 PM
fc4aac8fa25f	1	-76	1603923567	6:19:27 PM
fc4aac8fa25f	1	-78	1603923567	6:19:27 PM
fc4aac8fa25f	1	-68	1603923568	6:19:28 PM
fc4aac8fa25f	1	-72	1603923568	6:19:28 PM
fc4aac8fa25f	1	-78	1603923569	6:19:29 PM
fc4aac8fa25f	1	-80	1603923569	6:19:29 PM
fc4aac8fa25f	1	-76	1603923569	6:19:29 PM
fc4aac8fa25f	1	-87	1603923570	6:19:30 PM
fc4aac8fa25f	1	-82	1603923571	6:19:31 PM
fc4aac8fa25f	1	-86	1603923571	6:19:31 PM
fc4aac8fa25f	1	-88	1603923571	6:19:31 PM
fc4aac8fa25f	1	-87	1603923571	6:19:31 PM
fc4aac8fa25f	1	-89	1603923572	6:19:32 PM
fc4aac8fa25f	1	-87	1603923573	6:19:33 PM

(Continued)

(Continued)

BLE Mode - Scanner 2 - South approach

MAC	Signal mode	RSSI (dBm)	Timestamp	Timestamp
fc4aac8fa25f	1	-87	1603923574	6:19:34 PM
fc4aac8fa25f	1	-88	1603923575	6:19:35 PM
fc4aac8fa25f	1	-89	1603923577	6:19:37 PM
fc4aac8fa25f	1	-90	1603923578	6:19:38 PM

BLE Mode - Scanner 3 - East approach

MAC	Signal mode	RSSI (dBm)	Timestamp	Timestamp
fc4aac8fa25f	1	-79	1603923547	6:19:07 PM
fc4aac8fa25f	1	-80	1603923548	6:19:08 PM
fc4aac8fa25f	1	-79	1603923548	6:19:08 PM
fc4aac8fa25f	1	-76	1603923548	6:19:08 PM
fc4aac8fa25f	1	-78	1603923549	6:19:09 PM
fc4aac8fa25f	1	-78	1603923549	6:19:09 PM
fc4aac8fa25f	1	-78	1603923549	6:19:09 PM
fc4aac8fa25f	1	-82	1603923550	6:19:10 PM
fc4aac8fa25f	1	-77	1603923550	6:19:10 PM
fc4aac8fa25f	1	-81	1603923551	6:19:11 PM
fc4aac8fa25f	1	-79	1603923551	6:19:11 PM
fc4aac8fa25f	1	-81	1603923551	6:19:11 PM
fc4aac8fa25f	1	-81	1603923552	6:19:12 PM
fc4aac8fa25f	1	-80	1603923552	6:19:12 PM
fc4aac8fa25f	1	-76	1603923553	6:19:13 PM
fc4aac8fa25f	1	-77	1603923554	6:19:14 PM
fc4aac8fa25f	1	-75	1603923554	6:19:14 PM
fc4aac8fa25f	1	-71	1603923555	6:19:15 PM
fc4aac8fa25f	1	-72	1603923555	6:19:15 PM
fc4aac8fa25f	1	-65	1603923556	6:19:16 PM
fc4aac8fa25f	1	-68	1603923556	6:19:16 PM
fc4aac8fa25f	1	-71	1603923556	6:19:16 PM
fc4aac8fa25f	1	-62	1603923557	6:19:17 PM
fc4aac8fa25f	1	-59	1603923557	6:19:17 PM
fc4aac8fa25f	1	-66	1603923558	6:19:18 PM
fc4aac8fa25f	1	-75	1603923558	6:19:18 PM
fc4aac8fa25f	1	-74	1603923559	6:19:19 PM
fc4aac8fa25f	1	-80	1603923560	6:19:20 PM
fc4aac8fa25f	1	-67	1603923560	6:19:20 PM
fc4aac8fa25f	1	-71	1603923560	6:19:20 PM
fc4aac8fa25f	1	-83	1603923561	6:19:21 PM
fc4aac8fa25f	1	-85	1603923561	6:19:21 PM
fc4aac8fa25f	1	-87	1603923562	6:19:22 PM

(Continued)

(Continued)

BLE Mode - Scanner 3 - East approach

MAC	Signal mode	RSSI (dBm)	Timestamp	Timestamp
fc4aac8fa25f	1	-87	1603923562	6:19:22 PM
fc4aac8fa25f	1	-87	1603923564	6:19:24 PM
fc4aac8fa25f	1	-90	1603923565	6:19:25 PM
fc4aac8fa25f	1	-90	1603923566	6:19:26 PM
fc4aac8fa25f	1	-92	1603923567	6:19:27 PM
fc4aac8fa25f	1	-88	1603923569	6:19:29 PM
fc4aac8fa25f	1	-88	1603923569	6:19:29 PM
fc4aac8fa25f	1	-90	1603923572	6:19:32 PM

BLE Mode - Scanner 4 - North approach

MAC	Signal mode	RSSI (dBm)	Timestamp	Timestamp
fc4aac8fa25f	1	-91	1603923548	6:19:08 PM
fc4aac8fa25f	1	-89	1603923550	6:19:10 PM
fc4aac8fa25f	1	-83	1603923550	6:19:10 PM
fc4aac8fa25f	1	-84	1603923551	6:19:11 PM
fc4aac8fa25f	1	-82	1603923552	6:19:12 PM
fc4aac8fa25f	1	-86	1603923552	6:19:12 PM
fc4aac8fa25f	1	-82	1603923552	6:19:12 PM
fc4aac8fa25f	1	-83	1603923553	6:19:13 PM
fc4aac8fa25f	1	-80	1603923553	6:19:13 PM
fc4aac8fa25f	1	-83	1603923554	6:19:14 PM
fc4aac8fa25f	1	-79	1603923554	6:19:14 PM
fc4aac8fa25f	1	-79	1603923555	6:19:15 PM
fc4aac8fa25f	1	-84	1603923555	6:19:15 PM
fc4aac8fa25f	1	-83	1603923556	6:19:16 PM
fc4aac8fa25f	1	-80	1603923556	6:19:16 PM
fc4aac8fa25f	1	-80	1603923557	6:19:17 PM
fc4aac8fa25f	1	-77	1603923557	6:19:17 PM
fc4aac8fa25f	1	-78	1603923558	6:19:18 PM
fc4aac8fa25f	1	-78	1603923558	6:19:18 PM
fc4aac8fa25f	1	-78	1603923559	6:19:19 PM
fc4aac8fa25f	1	-85	1603923559	6:19:19 PM
fc4aac8fa25f	1	-75	1603923559	6:19:19 PM
fc4aac8fa25f	1	-80	1603923561	6:19:21 PM
fc4aac8fa25f	1	-78	1603923561	6:19:21 PM
fc4aac8fa25f	1	-83	1603923562	6:19:22 PM
fc4aac8fa25f	1	-87	1603923562	6:19:22 PM
fc4aac8fa25f	1	-90	1603923562	6:19:22 PM
fc4aac8fa25f	1	-89	1603923563	6:19:23 PM
fc4aac8fa25f	1	-86	1603923563	6:19:23 PM
fc4aac8fa25f	1	-84	1603923564	6:19:24 PM
fc4aac8fa25f	1	-88	1603923565	6:19:25 PM
fc4aac8fa25f	1	-88	1603923568	6:19:28 PM
fc4aac8fa25f	1	-91	1603923568	6:19:28 PM
fc4aac8fa25f	1	-93	1603923570	6:19:30 PM

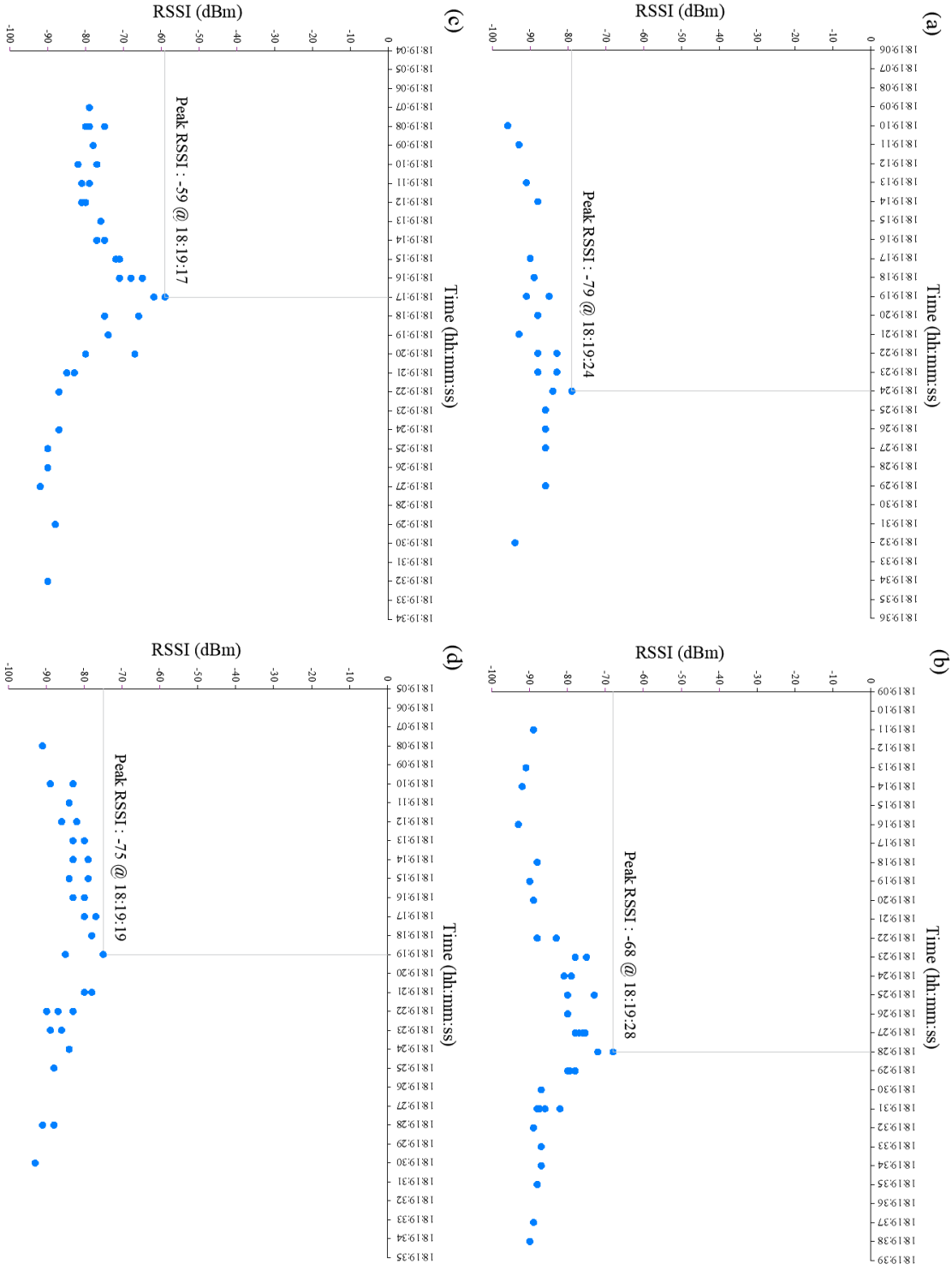

Figure C.1 RSSI-time profiles of (a) west; (b) south; (c) east; (d) north signal scanners for a crossing in Experient 4.

A crossing in Experiment 2: Speed of 30 km/h, LOS signal transmission path

South-West movement

BLE Mode - Scanner 1 - West approach

MAC	Signal mode	RSSI (dBm)	Timestamp	Timestamp
fc4aac8fa25f	1	-88	1603905654	1:20:54 PM
fc4aac8fa25f	1	-89	1603905654	1:20:54 PM
fc4aac8fa25f	1	-87	1603905655	1:20:55 PM
fc4aac8fa25f	1	-89	1603905655	1:20:55 PM
fc4aac8fa25f	1	-90	1603905655	1:20:55 PM
fc4aac8fa25f	1	-91	1603905656	1:20:56 PM
fc4aac8fa25f	1	-90	1603905659	1:20:59 PM
fc4aac8fa25f	1	-87	1603905660	1:21:00 PM
fc4aac8fa25f	1	-89	1603905660	1:21:00 PM
fc4aac8fa25f	1	-88	1603905661	1:21:01 PM
fc4aac8fa25f	1	-78	1603905661	1:21:01 PM
fc4aac8fa25f	1	-79	1603905661	1:21:01 PM
fc4aac8fa25f	1	-81	1603905662	1:21:02 PM
fc4aac8fa25f	1	-74	1603905662	1:21:02 PM
fc4aac8fa25f	1	-72	1603905663	1:21:03 PM
fc4aac8fa25f	1	-72	1603905663	1:21:03 PM
fc4aac8fa25f	1	-71	1603905663	1:21:03 PM
fc4aac8fa25f	1	-68	1603905664	1:21:04 PM
fc4aac8fa25f	1	-67	1603905664	1:21:04 PM
fc4aac8fa25f	1	-71	1603905665	1:21:05 PM
fc4aac8fa25f	1	-66	1603905665	1:21:05 PM
fc4aac8fa25f	1	-67	1603905665	1:21:05 PM
fc4aac8fa25f	1	-69	1603905666	1:21:06 PM
fc4aac8fa25f	1	-73	1603905666	1:21:06 PM
fc4aac8fa25f	1	-85	1603905669	1:21:09 PM
fc4aac8fa25f	1	-80	1603905669	1:21:09 PM
fc4aac8fa25f	1	-88	1603905670	1:21:10 PM
fc4aac8fa25f	1	-80	1603905670	1:21:10 PM
fc4aac8fa25f	1	-79	1603905671	1:21:11 PM
fc4aac8fa25f	1	-85	1603905671	1:21:11 PM
fc4aac8fa25f	1	-84	1603905671	1:21:11 PM

BLE Mode - Scanner 2 - South approach

MAC	Signal mode	RSSI (dBm)	Timestamp	Timestamp
fc4aac8fa25f	1	-87	1603905654	1:20:54 PM
fc4aac8fa25f	1	-85	1603905654	1:20:54 PM
fc4aac8fa25f	1	-84	1603905654	1:20:54 PM
fc4aac8fa25f	1	-86	1603905655	1:20:55 PM
fc4aac8fa25f	1	-86	1603905655	1:20:55 PM
fc4aac8fa25f	1	-85	1603905655	1:20:55 PM
fc4aac8fa25f	1	-87	1603905656	1:20:56 PM
fc4aac8fa25f	1	-88	1603905656	1:20:56 PM
fc4aac8fa25f	1	-87	1603905657	1:20:57 PM
fc4aac8fa25f	1	-77	1603905657	1:20:57 PM
fc4aac8fa25f	1	-80	1603905657	1:20:57 PM
fc4aac8fa25f	1	-80	1603905658	1:20:58 PM
fc4aac8fa25f	1	-79	1603905659	1:20:59 PM
fc4aac8fa25f	1	-67	1603905660	1:21:00 PM
fc4aac8fa25f	1	-64	1603905660	1:21:00 PM
fc4aac8fa25f	1	-67	1603905660	1:21:00 PM
fc4aac8fa25f	1	-66	1603905661	1:21:01 PM
fc4aac8fa25f	1	-66	1603905661	1:21:01 PM
fc4aac8fa25f	1	-70	1603905661	1:21:01 PM
fc4aac8fa25f	1	-69	1603905662	1:21:02 PM
fc4aac8fa25f	1	-76	1603905663	1:21:03 PM
fc4aac8fa25f	1	-73	1603905663	1:21:03 PM
fc4aac8fa25f	1	-73	1603905663	1:21:03 PM
fc4aac8fa25f	1	-77	1603905664	1:21:04 PM
fc4aac8fa25f	1	-82	1603905664	1:21:04 PM
fc4aac8fa25f	1	-82	1603905665	1:21:05 PM
fc4aac8fa25f	1	-86	1603905665	1:21:05 PM
fc4aac8fa25f	1	-88	1603905667	1:21:07 PM
fc4aac8fa25f	1	-87	1603905669	1:21:09 PM
fc4aac8fa25f	1	-91	1603905669	1:21:09 PM
fc4aac8fa25f	1	-87	1603905669	1:21:09 PM
fc4aac8fa25f	1	-90	1603905671	1:21:11 PM

BLE Mode - Scanner 3 - East approach

MAC	Signal mode	RSSI (dBm)	Timestamp	Timestamp
fc4aac8fa25f	1	-87	1603905659	1:20:59 PM
fc4aac8fa25f	1	-88	1603905660	1:21:00 PM
fc4aac8fa25f	1	-88	1603905660	1:21:00 PM
fc4aac8fa25f	1	-81	1603905661	1:21:01 PM
fc4aac8fa25f	1	-78	1603905662	1:21:02 PM
fc4aac8fa25f	1	-77	1603905663	1:21:03 PM
fc4aac8fa25f	1	-75	1603905663	1:21:03 PM
fc4aac8fa25f	1	-81	1603905664	1:21:04 PM
fc4aac8fa25f	1	-85	1603905664	1:21:04 PM
fc4aac8fa25f	1	-83	1603905665	1:21:05 PM
fc4aac8fa25f	1	-80	1603905665	1:21:05 PM
fc4aac8fa25f	1	-86	1603905665	1:21:05 PM
fc4aac8fa25f	1	-81	1603905665	1:21:05 PM
fc4aac8fa25f	1	-79	1603905666	1:21:06 PM
fc4aac8fa25f	1	-80	1603905666	1:21:06 PM
fc4aac8fa25f	1	-82	1603905667	1:21:07 PM
fc4aac8fa25f	1	-80	1603905667	1:21:07 PM
fc4aac8fa25f	1	-79	1603905667	1:21:07 PM
fc4aac8fa25f	1	-83	1603905668	1:21:08 PM
fc4aac8fa25f	1	-81	1603905670	1:21:10 PM
fc4aac8fa25f	1	-81	1603905670	1:21:10 PM
fc4aac8fa25f	1	-84	1603905671	1:21:11 PM
fc4aac8fa25f	1	-83	1603905671	1:21:11 PM
fc4aac8fa25f	1	-81	1603905671	1:21:11 PM

BLE Mode - Scanner 4 - North approach

MAC	Signal mode	RSSI (dBm)	Timestamp	Timestamp
fc4aac8fa25f	1	-86	1603905654	1:20:54 PM
fc4aac8fa25f	1	-87	1603905654	1:20:54 PM
fc4aac8fa25f	1	-87	1603905654	1:20:54 PM
fc4aac8fa25f	1	-86	1603905655	1:20:55 PM
fc4aac8fa25f	1	-86	1603905656	1:20:56 PM
fc4aac8fa25f	1	-94	1603905656	1:20:56 PM
fc4aac8fa25f	1	-83	1603905657	1:20:57 PM
fc4aac8fa25f	1	-84	1603905657	1:20:57 PM
fc4aac8fa25f	1	-81	1603905658	1:20:58 PM
fc4aac8fa25f	1	-82	1603905659	1:20:59 PM
fc4aac8fa25f	1	-87	1603905659	1:20:59 PM
fc4aac8fa25f	1	-86	1603905660	1:21:00 PM
fc4aac8fa25f	1	-81	1603905661	1:21:01 PM
fc4aac8fa25f	1	-86	1603905661	1:21:01 PM
fc4aac8fa25f	1	-80	1603905662	1:21:02 PM
fc4aac8fa25f	1	-77	1603905662	1:21:02 PM
fc4aac8fa25f	1	-76	1603905663	1:21:03 PM
fc4aac8fa25f	1	-80	1603905664	1:21:04 PM
fc4aac8fa25f	1	-82	1603905665	1:21:05 PM
fc4aac8fa25f	1	-89	1603905666	1:21:06 PM
fc4aac8fa25f	1	-85	1603905666	1:21:06 PM
fc4aac8fa25f	1	-83	1603905667	1:21:07 PM
fc4aac8fa25f	1	-87	1603905667	1:21:07 PM
fc4aac8fa25f	1	-85	1603905667	1:21:07 PM
fc4aac8fa25f	1	-90	1603905668	1:21:08 PM

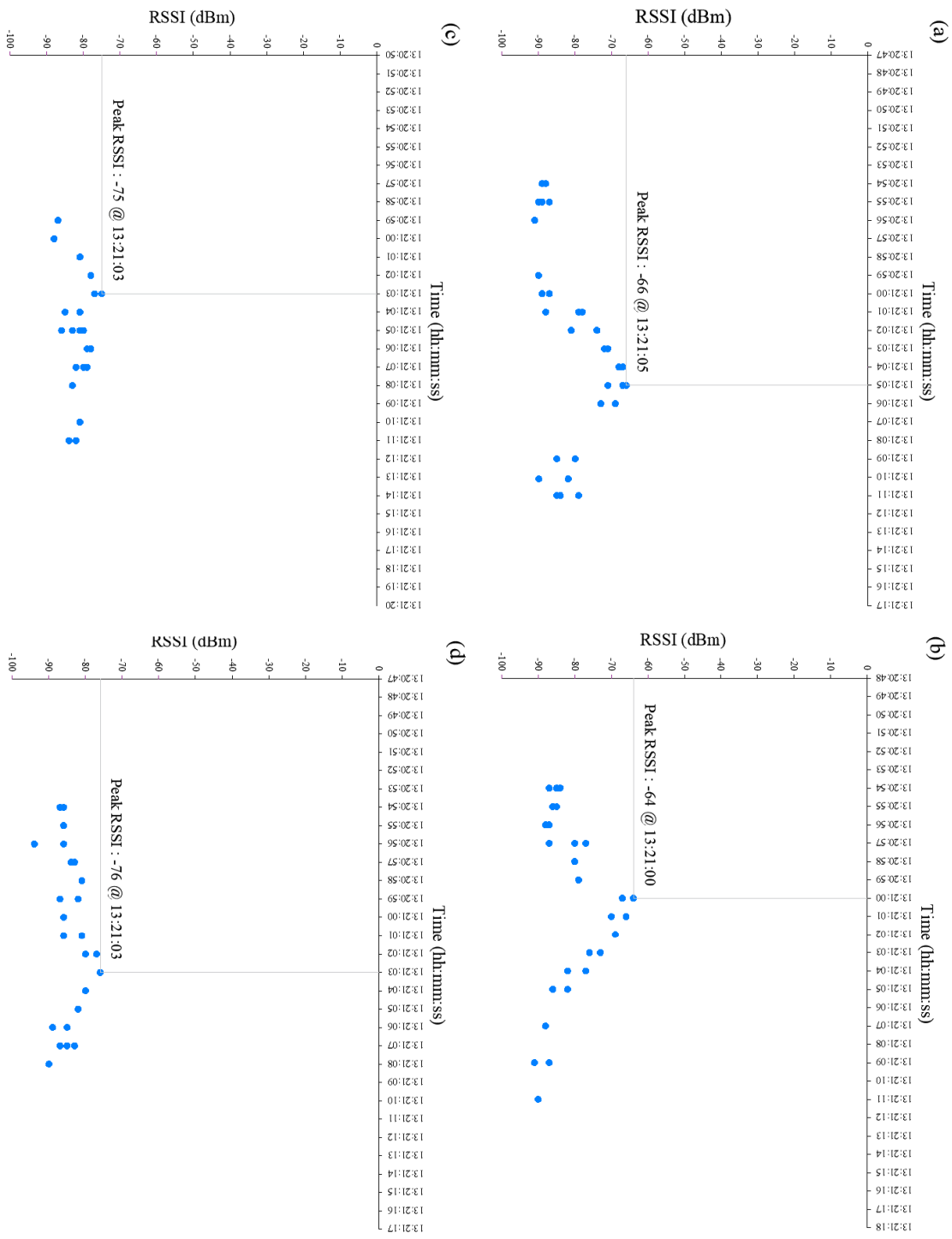

Figure C.2 RSSI-time profiles of (a) west; (b) south; (c) east; (d) north signal scanners for a crossing in Experient 2.

Appendix D

MATLAB codes

KNN algorithm for beacon positioning

```
localizer='knnalgorithm4scanners.xlsx';
localizer=xlsread(localizer);
x=localizer(:,1)
average_rssi_scanner_1=localizer(:,2);
average_rssi_scanner_2=localizer(:,3);
average_rssi_scanner_3=localizer(:,4);
average_rssi_scanner_4=localizer(:,5);
target_1=localizer(1,6);
target_2=localizer(1,7);
target_3=localizer(1,8);
target_4=localizer(1,9);
number_of_locations=length(x(~isnan(x)));
locations=[x];
rssi_matrix=[average_rssi_scanner_1 average_rssi_scanner_2
average_rssi_scanner_3 average_rssi_scanner_4];
target_matrix=[target_1 target_2 target_3 target_4];
three_k_nearest_location_number=knnsearch(rssi_matrix,targe
t_matrix,'K',3);
three_k_nearest_location_number=(three_k_nearest_location_n
umber)';
three_k_nearest_rssi=rssi_matrix(three_k_nearest_location_n
umber,:);
three_k_nearest_location=locations(three_k_nearest_location
_number,:);
```

Filtering algorithms including Savitzky-golay, Rlowess, Center and Linear

```
filter='rowdataforfilter.xlsx';
filter=xlsread(filter);
x=filter(:,1);
SGOLAY = sgolayfilt(x,1,3)
Rlowess = smoothdata(x,'rlowess',5);
LINEAR = filloutliers(x,'linear');
CENTER = filloutliers(x,'center');
```

Detection of matching moments by three signal scanners and the corresponding RSSI values

```
matchingmoments='matchingmoments3scanners.xlsx';
% Timestamps should be in milliseconds.
% First, the data of the signal scanner with the lowest number of detections.
% Third, the data of the signal scanner with the highest number of detections.
matchingmoments=xlsread(matchingmoments);
one_rssi_detections=matchingmoments(:,1);
one_detection_time=matchingmoments(:,2);
one_maximum_data_number=length(one_detection_time(~isnan(one_detection_time)));
one_detection_time=one_detection_time(~isnan(one_detection_time));
one_rssi_detections=one_rssi_detections(~isnan(one_rssi_detections));
one_maximum_time_difference=1000;
one_repeated_moments_id(1)=1;
for i=1:one_maximum_data_number-1;
    one_delta_time=one_detection_time(i+1)-one_detection_time(i);
    if one_delta_time>one_maximum_time_difference;

one_repeated_moments_id(i+1)=one_repeated_moments_id(i)+1;
    else

one_repeated_moments_id(i+1)=one_repeated_moments_id(i);
    end
end
one_repeated_moments_id=(one_repeated_moments_id)';
one_unrepeated_moments_id=unique(one_repeated_moments_id);
one_average_detection_time=accumarray(one_repeated_moments_id(:),one_detection_time(:),[],@mean);
one_mean_rssi_detections=accumarray(one_repeated_moments_id(:),one_rssi_detections(:),[],@mean);
one_number_of_unrepeated_moments=numel(one_unrepeated_moments_id);

two_rssi_detections=matchingmoments(:,3);
two_detection_time=matchingmoments(:,4);
two_maximum_data_number=length(two_detection_time(~isnan(two_detection_time)));
two_detection_time=two_detection_time(~isnan(two_detection_time));
```

```
two_rssi_detections=two_rssi_detections(~isnan(two_rssi_det
ections));
two_maximum_time_difference=1000;
two_repeated_moments_id(1)=1;
for m=1:two_maximum_data_number-1;
    two_delta_time=two_detection_time(m+1)-
two_detection_time(m);
    if two_delta_time>two_maximum_time_difference;

two_repeated_moments_id(m+1)=two_repeated_moments_id(m)+1;
    else

two_repeated_moments_id(m+1)=two_repeated_moments_id(m);
    end
end
two_repeated_moments_id=two_repeated_moments_id';
two_unrepeated_moments_id=unique(two_repeated_moments_id);
two_average_detection_time=accumarray(two_repeated_moments_
id(:),two_detection_time(:),[],@mean);
two_mean_rssi_detections=accumarray(two_repeated_moments_id
(:),two_rssi_detections(:),[],@mean);
two_number_of_unrepeated_moments=numel(two_unrepeated_momen
ts_id);

three_rssi_detections=matchingmoments(:,5);
three_detection_time=matchingmoments(:,6);
three_maximum_data_number=length(three_detection_time(~isna
n(three_detection_time)));
three_detection_time=three_detection_time(~isnan(three_dete
ction_time));
three_rssi_detections=three_rssi_detections(~isnan(three_rs
si_detections));
three_maximum_time_difference=1000;
three_repeated_moments_id(1)=1;
for u=1:three_maximum_data_number-1
    three_delta_time=three_detection_time(u+1)-
three_detection_time(u);
    if three_delta_time>three_maximum_time_difference;

three_repeated_moments_id(u+1)=three_repeated_moments_id(u)
+1;
    else

three_repeated_moments_id(u+1)=three_repeated_moments_id(u)
;
    end
end
```

```
three_repeated_moments_id=(three_repeated_moments_id)';
three_unrepeated_moments_id=unique(three_repeated_moments_i
d);
three_average_detection_time=accumarray(three_repeated_mome
nts_id(:),three_detection_time(:),[],@mean);
three_mean_rssi_detections=accumarray(three_repeated_moment
s_id(:),three_rssi_detections(:),[],@mean);
three_number_of_unrepeated_moments=numel(three_unrepeated_m
oments_id);

one_unrepeated_moments_id_number=numel(one_unrepeated_momen
ts_id);
two_unrepeated_moments_id_number=numel(two_unrepeated_momen
ts_id);
three_unrepeated_moments_id_number=numel(three_unrepeated_m
oments_id);

matching_moments(one_number_of_unrepeated_moments,1)=zeros;
matching_one_mean_rrsi_detections(one_number_of_unrepeated_
moments,1)=zeros;
matching_two_mean_rrsi_detections(two_number_of_unrepeated_
moments,1)=zeros;
matching_three_mean_rrsi_detections(three_number_of_unrepea
ted_moments,1)=zeros;


for k=1:one_unrepeated_moments_id_number;
      for p=1:two_unrepeated_moments_id_number;
          for w=1:three_unrepeated_moments_id_number;
          if and(and(one_average_detection_time(k)-
two_average_detection_time(p)<=1000 ,
one_average_detection_time(k)-
two_average_detection_time(p)>=-1000) , and
(one_average_detection_time(k)-
three_average_detection_time(w)<=1000 ,
one_average_detection_time(k)-
three_average_detection_time(w)>=-1000));

matching_moments(k)=one_average_detection_time(k);

matching_one_mean_rrsi_detections(k)=one_mean_rssi_detectio
ns(k);

matching_two_mean_rrsi_detections(p)=two_mean_rssi_detectio
ns(p);
```

```
matching_three_mean_rrsi_detections(w)=three_mean_rssi_dete
ctions(w);
          end
          end
      end
      end

matching_moments=nonzeros(matching_moments);
matching_one_mean_rrsi_detections=nonzeros(matching_one_mea
n_rrsi_detections);
matching_two_mean_rrsi_detections=nonzeros(matching_two_mea
n_rrsi_detections);
matching_three_mean_rrsi_detections=nonzeros(matching_three
_mean_rrsi_detections);
number_of_matching_detections=length(matching_moments);
```

Appendix E

Published papers and conference presentations

The following journal articles and conference presentation are based on the contents of this thesis:

1. Mohammadi, S., Ismail, K., 2022. Development of a Method for Determination of Turning Movements in Intersections Using Bluetooth Low Energy Signals. *Under Review.*
2. Mohammadi, S., Ismail, K. & Ghods, A. H., 2021. Investigating Wi-Fi, Bluetooth, and Bluetooth Low-Energy Signal Characteristics for Integration in Vehicle–Pedestrian Collision Warning Systems. *Sustainability*, 13,10823, pp. 1-20.
3. Mohammadi, S., Ismail, K. & Ghods, A. H., 2020. Development of a Positioning Technique for Traffic Data Collection Using Wireless Signal Scanners. *Transportation Research Record*, 2674(5), pp. 637-648.
4. Mohammadi, S., Ismail, K. & Ghods, A. H., 2019. Investigating Wi-Fi/Bluetooth Signal Characteristics for Positioning in Traffic Studies. *Proc., International Civil Engineering and Architecture Conference (ICEARC'19)*, Trabzon, Turkey.